POWER-OPTIMAL MIMO TWO-WAY RELAY NETWORKS

BY

Razgar Rahimi

A DISSERTATION SUBMITTED IN PARTIAL FULFILLMENT OF THE

REQUIREMENTS FOR THE DEGREE OF

DOCTOR OF PHILOSOPHY

IN

ELECTRICAL AND COMPUTER ENGINEERING

FACULTY OF ENGINEERING AND APPLIED SCIENCE

UNIVERSITY OF ONTARIO INSTITUTE OF TECHNOLOGY

OSHAWA, ONTARIO, CANADA

APRIL 2018

Contents

List of Figures

Abstract

In this dissertation, we study MIMO two-way relay networks consisting of single-antenna users which wish to exchange information with the help of multiple multi-antenna relays. The problem we aim to solve is to minimize the total transmit power consumed in the entire network while certain quality-of-service constraints are satisfied at the transceivers. To do so, we optimize jointly the relays' beamforming matrices and the transceivers' transmit powers. We assume that networks use the multiple access broadcast (MABC) relaying scheme where each round of information exchange between the transceivers takes place in two time-slots.

In Chapter 3, the network is assumed to be *synchronous* while in Chapter 4, we study *asynchronous* networks. In asynchronous networks, the data transmitted from transceivers will arrive with different delays at relays and the data forwarded from relays will arrive with different delays at each transceiver. In Chapter 5, we use a massive number of relay antennas in a two-way relay network with multiple peer-to-peer communications established with the help of multi-antenna relays.

We observe that under the assumption that the relay beamforming matrices are symmetric, the total power minimization problems in synchronous and asynchronous networks are amenable to semi-closed-form solutions. Considering asynchronous networks, we prove rigorously that at the optimum, only those relays corresponding to the power-optimal synchronous sub-network of relays must contribute to the data exchange between transceivers. Equipping relays in the multipair two-way relay networks with massive number of antennas, we study performance of linear relaying techniques such as the maximum ratio transmitting/combining (MRT/MRC) and the zero-forcing (ZF) schemes. Exploiting the approximate orthogonality among relay-transceiver channel vectors when number of relay antennas are very large, we show that the total power minimization problem for networks with a massive number of relay antennas will be amenable to a semi-closed form solution.

Acknowledgements

There are few words that could fully express my deep gratitude to my supervisor Prof. Shahram Shahbazpanahi for his steady and unwavering support, guidance, and insightful comments throughout the process of my PhD studies.

I am now and forever thankful to my family, whose genuine love and support always warm my heart to move forward.

My gratitude would not be complete without acknowledging my wife Farideh, for her unconditional love and consistent support. She was always patient and ready to support during the good and bad times I encountered throughout this long journey. Last but not least, I would like to acknowledge my son, Jiwan, the dearest blessing in my life.

Chapter 1

Introduction

1.1 Overview

Nowadays, wireless communication services are not just limited to occasional phone calls. These days, users' daily life and businesses are relying heavily on the services provided by wireless networks. For example, a significantly large portion of the entire world population currently have access to the Internet, which provides users in urban, rural, and remote areas with many social and economical benefits. This significant growth in the access to the Internet is largely because of wireless networks. Moreover, with the ever-increasing development of wireless networks, user demands are not remaining limited to the connectivity. Instead, user requirements are moving toward the quality-of-services being provided by the networks. To the contemporary users, anything but a seamless and ubiquitous access to the network is becoming inconvenient and unacceptable. Although, existing wireless networks relying on new technologies are becoming very dependable, but users are still asking for much better performances. Higher data-rates, lower latency, higher radio link reliability, higher connectivity, and higher mobility ranges are among the essential features users expect from future wireless networks [2, 3]. These ever-increasing user demands result in many challenges which prospective wireless networks have to overcome.

The users ever-growing demand for ubiquitous access to wireless networks with acceptable quality-of-service, drives researchers to unstoppably work on improving networks. Increasing the transmission power of the communication links can improve the network performance to some extents. However, increasing the transmission power can result in a significant growth in the network energy consumption which raises the concerns associated with the network running expenditures and maintenance costs. Aside from the energy costs, excessive usage of energy can also cause many environmental problems. These concerns emphasize on the need for methods considering the energy consumption efficiency. To address these issues, seeking the minimum energy consumption, many researchers are attracted to the areas focusing on optimizing different network design parameters. Recently, many studies have been aimed at minimizing the network energy/power consumption while certain constraints on the quality-of-service are guaranteed [4], and this is exactly what we aim to study in this dissertation.

In the remaining of this chapter, we first explain the main concepts that will be used in the forthcoming chapters. Next, we present motivations which encouraged us to conduct the research presented in this dissertation, and then, we describe objectives and methodology that will be employed in our work.

1.2 Relay-assisted Wireless Networks

Due to the broadcast nature of wireless communications, a signal being transmitted from a source node can travel through multiple paths before arriving at the destination. More specifically, a transmitted signal can be reflected or scattered by the surface of the objects in the propagation environment, causing various replicas of the transmitted signal to reach the destination. In such communication links, signals traveling through different paths can each arrive with distinct amplitude and delay at the destination. Indeed, the phase of a signal passing through a path is determined by the length of the path and by the positions of the source and destination nodes. A destination node equipped with a single antenna can only receive the superposition of the arriving signals, and as a result, cannot distinguish different replicas of the transmitted signal. The superposition of the received signals with different phases can be either constructive or destructive.

Aside from the effects of the signal arrival from multiple paths, the source and destination movements can cause the superposition of the signals arrived at the destination to fluctuate over time. The signal fluctuation caused by source and/or destination movements in the order of the signal wavelength is called the small-scale fading effect.

Furthermore, obstacles can block the signal traveling path, meaning that a signal originated from a source node may not reach some areas. The effect of the signal blockage caused by the obstacles in the propagation environment is known as shadowing. The signal strength in the coverage area can vary slowly from the points less affected by the blockage to the points that are completely blocked by the obstacles. That is, shadowing can be significant only when displacements of the source and/or the destination is in the order of the size of environmental obstacles. Signal fluctuations caused by the shadowing are known as the large-scale fading [5].

To summarize, movements in the order of the signal wavelength result in small-scale fading, while movements in the orders much larger than the signal wavelength can result in the large-scale fading [6, 7].

One of the methods widely being used to tackle the fading issue is to transmit signals conveying the same information through multiple statistically independent paths. Doing so, the receiver is provided with multiple replicas of the signal transmitted. Methods providing multiple statistically independent paths are known as diversity techniques. Diversity techniques are materialized by sending the same signal through different time-slots, through different frequency-bands, or through different spatial-directions. Combinations of these techniques can also be used to obtain multiple statistically independent paths.

In spatial diversity techniques, transmitter and/or receiver nodes are equipped with multiple antennas. Doing so, each link between a transmit antenna and a receive antenna can construct a signal path from the source to the destination [8, 9]. As a result, the probability of a complete signal blockage can decrease.

Equipping transmitter and receiver antennas with a number of antennas can also allow these nodes to employ *local beamforming* techniques. Using these techniques, transmitter and/or receiver can align their antenna beams such that signals arriving at the receiver combine in a constructive manner. Doing so, the communication range and the quality-of-signal at the receiver side can be improved.

Due to the terminal size limitation (particularly for handheld wireless devices), some network nodes cannot be equipped with a very large number of antennas. On the other hand, wireless nodes equipped with small number of antennas may not be able to afford the diversity gains expected. To achieve satisfactory diversity gains even with small number of antennas at source and destination, relay-assisted communication strategies have been proposed. In relay-assisted communications, multiple antennas are distributed among geographically separated network nodes called relays. Doing so, relays construct a virtual antenna array which can help with achieving spatial diversity gains required [8]. The technique of aligning the virtual beam of multiple single-antenna relays geographically distributed in the area between the source and the destination is known as the *network beamforming* technique.

Relay-assisted wireless networks can work as one-way relay networks transferring signals from source/s to destination/s, or as two-way relay networks exchanging signals between transceivers.

1.2.1 One-way Relay Networks

One-way relay networks are established to transfer information in one direction from source to a number relays and then to a destination. In one-way relay networks, transferring a signal from the source to the destination requires two time-slots. As can be seen in Fig. 1.1, in the first time-slot, signal is transmitted from the source to the relays. Then, each relay processes its received signal to produce the relay transmit signal. In the second time-slot, each relay transmits its transmit signal toward the destination.

Relays can use different schemes to process signals they receive. The *amplify-and-*

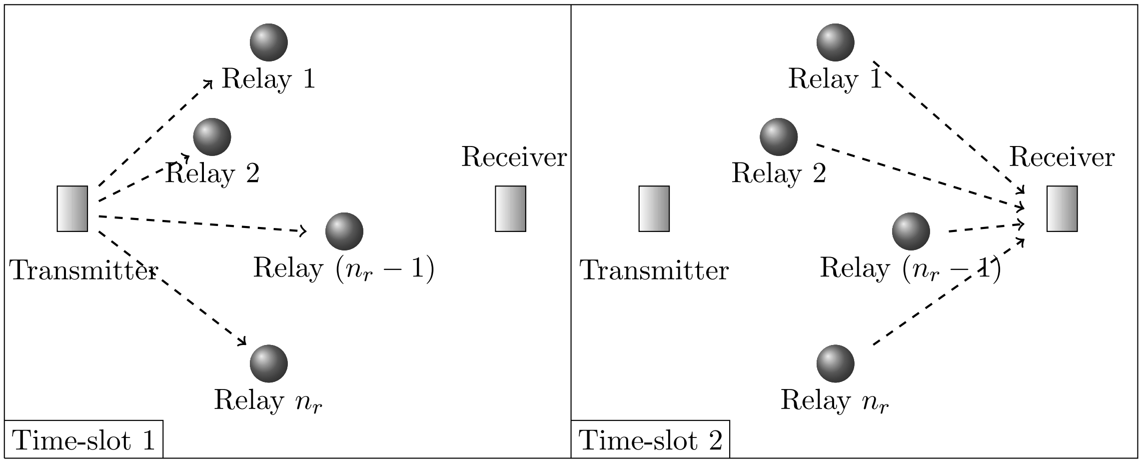

Figure 1.1: One-way relaying scheme with two time-slots (unidirectional from transmitter to receiver).

forward (AF) scheme is one of these signal processing techniques which is widely being studied in the literature. In AF relaying scheme, each relay multiplies its received signal by a complex valued weighting factor which amplifies the signal magnitude and adjusts the signal phase. Relays then forward the amplified signal toward the receiver. The AF relaying scheme imposes no significant processing delay to the signal transfer time. In AF relaying scheme, no extra information is broadcasted along with the processed signals. Hence, in terms of the security, networks which use AF relaying scheme are less vulnerable to the eavesdroppers [10]. Note that, under AF relaying scheme, summation of the received signal and noise at the relays is amplified. As a result, AF relaying scheme is mostly recommended for low-noise wireless communications [11, 12].

The *decode-and-forward* (DF) technique is another signal processing strategy which has been well studied in the literature. In the *decode-and-forward (DF)* technique, relays first decode the received signal to regenerate a replica of the original signal transmitted by the source. Relays then encode and forward the so-regenerated signal toward the destination [13]. In comparison to the AF scheme, the DF technique is more complicated. However, in some conditions, the DF relaying technique can perform very satisfying while AF relaying scheme may fail to do so. For example, consider a case where the noise power received at the relays is high. AF relaying scheme amplifies and forwards the high-power noise along with the intended signal. As a result, the quality of the signal reaching the destination is very poor. To the contrary, DF technique extracts the signal contaminated with the high-power noise. Doing so, DF relaying technique prevents high-power noise arrived at the relays to reach the destination. As a result, the quality of the signal arrived at the destination is expected to be satisfying.

Besides the AF and DF relaying techniques, compress-and-forward, estimate-and-forward, and filter-and-forward techniques have also been studied as relaying schemes. The *compress-and-forward* relaying scheme can be used when relays are unable to decode the signal sent by the source, but are able to transmit a compressed version of their observations to the destination [14, 15]. The compressed information transmitted by relays can help the receiver to decode the signal directly arriving from the source. The relays can employ different source coding techniques to compress the information they transmit to the destination [16, 17]. As another relaying scheme, the *compute-and-forward* technique can help with harnessing the interference in a wireless network. In compute-and-forward technique, relays provide the destination with the information they obtain through computing a linear combination of the signals they receive from the source. Employing the compute-and-forward technique, relays are not obliged to know or decode individual source signals [18].

In *estimate-and-forward* (EF) technique, relays use the received signal to obtain an estimated version of the transmitted signal. This estimate is then forwarded to the destination. In the EF technique, relays first use the received signal to estimate the original signal transmitted by the source. Relays then forward the so-obtained estimated signal toward the destination. The *filter-and-forward* (FF) technique is a relaying scheme being used in networks with frequency selective channel between each relay antenna and each transceiver antenna. In the FF technique, each relay is equipped with a finite impulse response (FIR) filter. Signals arriving at each relay are to pass through the relay FIR filter before being forwarded toward the destination.

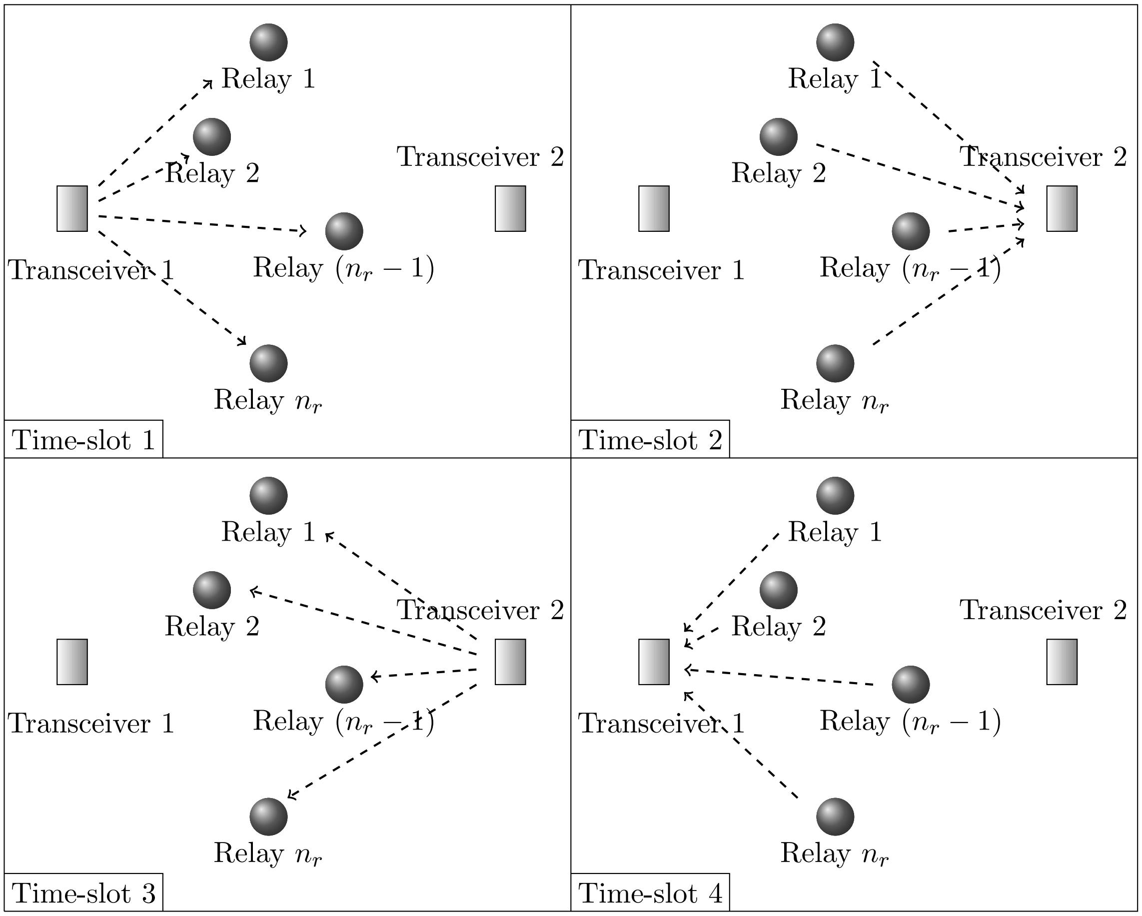

Figure 1.2: Conventional two-way relaying scheme with four time-slots.

The role of relay FIR filters is to compensate for the frequency selectivity of the relay-transceiver channels.

1.2.2 Two-way Relay Networks

Two-way relay networks are utilized to exchange information between transceivers in a bi-directional manner. That is, each node can both transmit and receive signal. In two-way relay networks, a round of information exchange between transceivers can take two, three, or four time-slots. Using Figs. 1.2, 1.3, and 1.4, we explain how information is exchanged between transceivers, when networks are employing different two-way relaying schemes. Note that, relay nodes in these figures can also be considered as base stations geographically distributed over a specific area in cellular networks.

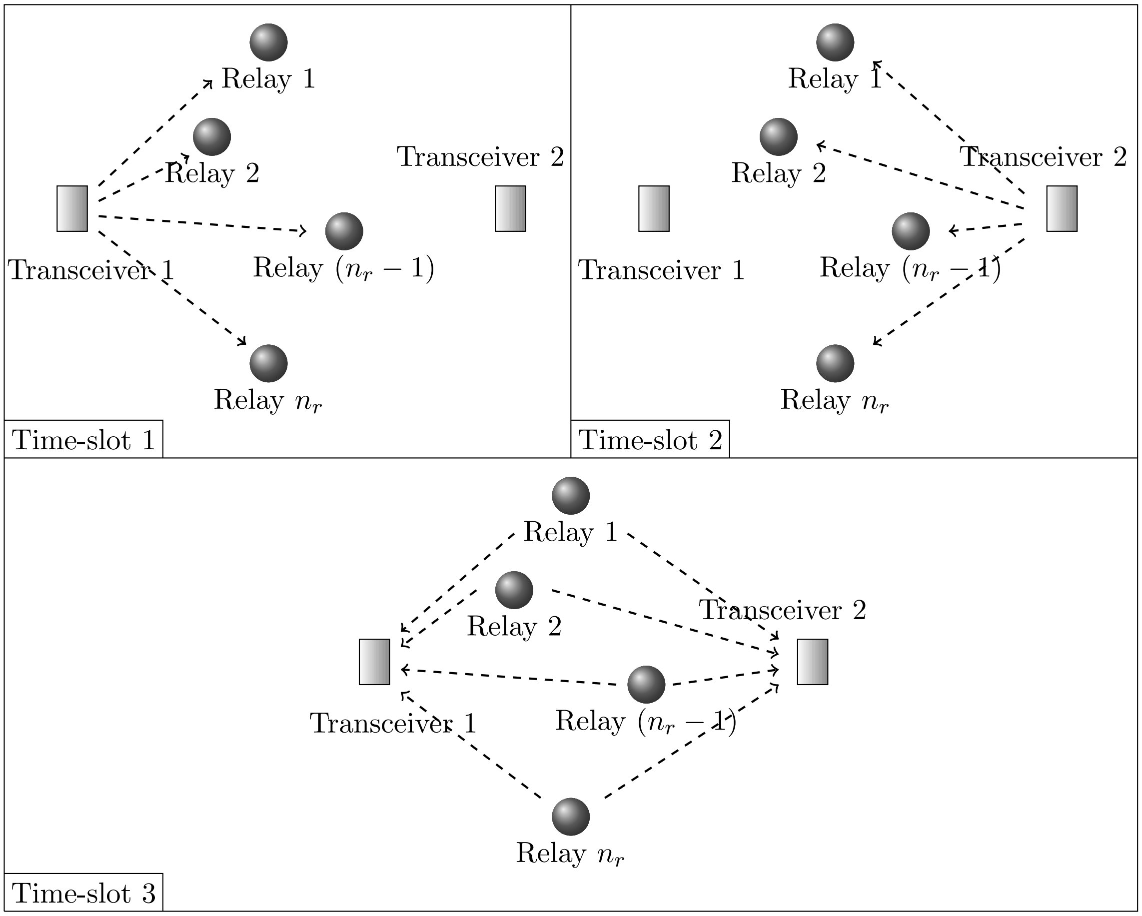

Figure 1.3: Time division broadcast (TDBC) relaying scheme.

Let us consider the *conventional relaying scheme*, shown in Fig. 1.2. This relaying scheme needs four time-slots for a complete round of information exchange between two transceivers. As Fig. 1.2 illustrates, in the first time-slot, Transceiver 1 transmits signal toward relays. Each relay then processes its received signal. In the second time-slot, relays transmit signals being processed toward Transceiver 2. In the third and fourth time-slots the signal transmission takes place in the opposite direction. That is, Transceiver 2 transmits its signal to the relays and then relays process and forward their received signals to Transceiver 1. In conventional two-way relaying scheme, signal transmission in each direction, from Transceiver 1 to Transceiver 2 or vice versa, can be viewed as a signal transmission in a one-way relay network. As a result, relays can use the same signal processing schemes being used in one-way relay

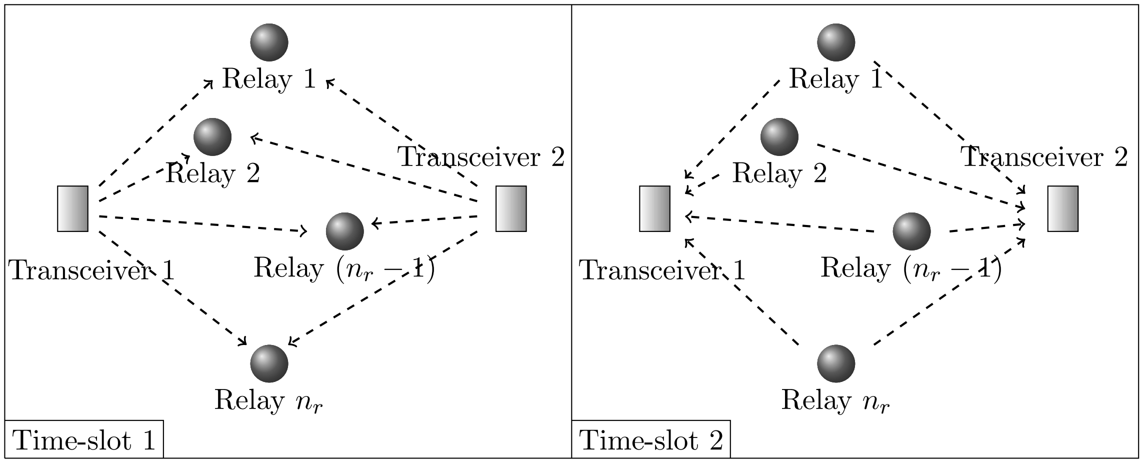

Figure 1.4: Multiple access broadcast (MABC) relaying scheme.

networks.

As can be seen from Fig. 1.3, the *time division broadcast* (TDBC) scheme needs three time-slots for a complete round of information exchange between two transceivers. Requiring three time-slots, the TDBC scheme can provide higher spectral efficiency in comparison to the simple relaying scheme with four time-slots. In the first time-slot of the TDBC scheme, one of the transceivers (e.g., Transceiver 1) transmits its signal toward the relays. In the second time-slot, the transceiver on the other side (i.e., Transceiver 2) transmits its signal toward relays. Then, each relay processes the signals received in the first and second time-slots. Doing so, in the third time-slot each relay broadcasts a combination of the signals arrived in the first two time-slots. Signal processing techniques such as AF relaying scheme, DF relaying scheme, etc. can also be used under the TDBC scheme. However, the way signal processing strategies are implemented is different from that for the one-way and conventional two-way relaying schemes. The difference in the signal processing strategies rises due to the fact that in TDBC scheme individual signals arrived from the transceiver are not relayed individually. Rather, at each relay a combination of the signals arrived in the first two time-slots are processed.

The *multiple access broadcast* (MABC) scheme proposed in [19], is a spectrally efficient relaying scheme. As Fig. 1.4 shows, the MABC scheme only needs two time-slots for a complete round of information exchange between two transceivers. More specifically, in the first time-slot, both transceivers transmit their signals toward the relays. In the second time-slot, relays broadcast a processed version of their received signals back to the transceivers.

1.2.3 Synchronous and Asynchronous Networks

Techniques being used to transmit a signal through multiple statistically independent paths can decrease the probability of complete signal blockage. Furthermore, these techniques can increase the communication range and also improve the quality of signal at the receivers. However, signals passing through different paths can arrive at the destination with different propagation delays. The propagation delay of different relaying paths can be different due to the fact that relays are geographically distributed at various locations. That is, different relaying paths can have different path lengths and fading conditions. Signal transmission over a relay network with significantly different propagation delays for different relaying paths resembles that of a multipath channel. In certain conditions, signal transmission over two-way relay networks can be presumed synchronous. For low data rate communications, when the difference between signal arrivals from different relaying paths are less than the symbol period of the transmitted signals, we can assume that the data transmission is synchronous. More specifically, in synchronous networks the difference between the maximum and the minimum propagation delays, known as the delay spread, is less than the length of one symbol period. Such networks with synchronous signal arrival are called *synchronous relay networks*. Note that when networks are not synchronous, overhead signals can be employed to compensate for the difference in the propagation delays and synchronize the data transmission. To do so, however, relays not only need to be equipped with extra memories, but also to execute more complex relaying processes.

Fig. 1.5 illustrates a synchronous networks in which symbols arrive with no timing misalignment at the receiver front-end of the transceivers. Indeed, this figure shows

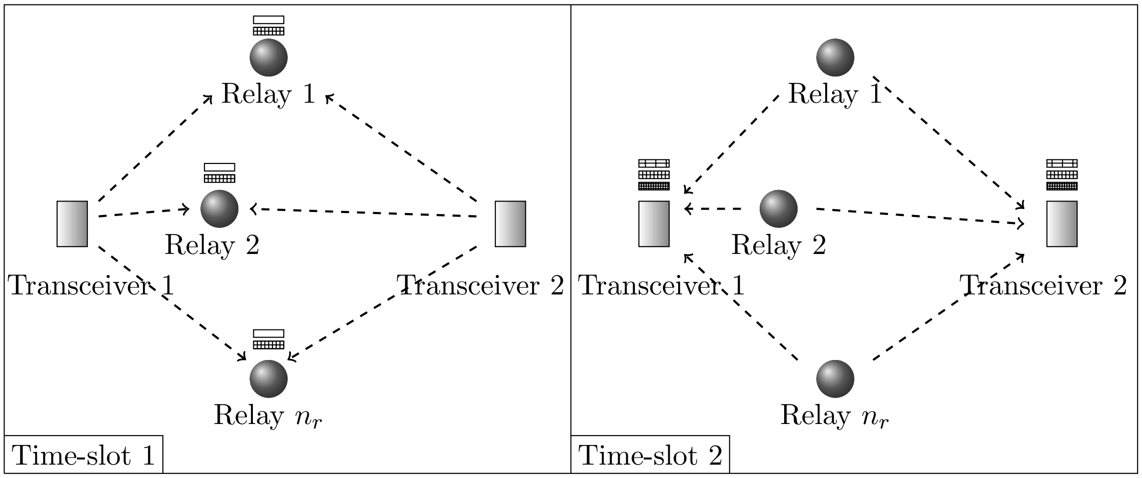

Figure 1.5: Synchronous two-way relay network with MABC relaying scheme.

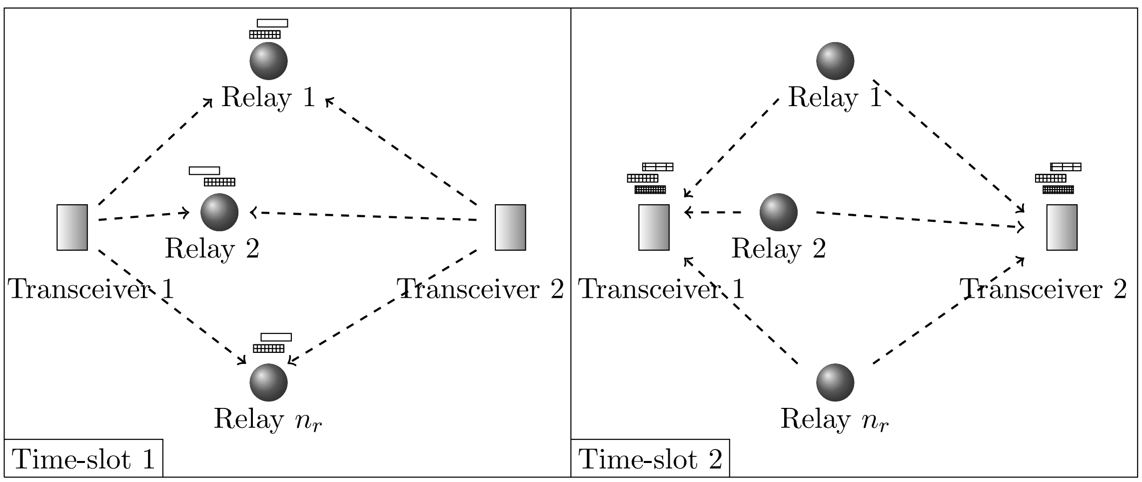

Figure 1.6: Asynchronous two-way relay network with MABC relaying scheme.

that replicas of the signal transmitted by each transceiver arrive at relays with the same delay and signals forwarded by the relays also arrive at each transceiver with the same delay.

Aiming to provide higher data rates, networks should reduce the length of symbol period. When symbol period length is smaller than the delay spread, the network is not synchronous. In such networks, the difference of the propagation delays for signals arriving from different relaying paths are greater than the length of the symbol period. These relay networks are called *asynchronous relay networks* (see Fig. 1.6). An asynchronous relay network resembles a multi-path channel. Receiving different replicas of the same signal with different delays can cause symbols to spread beyond the symbol period. As a result, each symbol can interfere with the preceding or succeeding transmitted symbols. This signal collision can cause inter-symbol interference (ISI) and intra-block interference. Moreover, in a sequential block transmission, the ISI can result in inter-block interference (IBI) between successive blocks.

1.3 Motivation

The ever-increasing user demands for access to wireless networks in remote, rural, and urban areas can be satisfied by increasing the number of cellular networks' base stations. However, utilizing more base stations, network providers require to deal with higher expenditures on network running and maintenance. Expanding networks causes the energy consumption to significantly soar. A significant growth in the energy consumption renders costs prohibitive. Besides, excessive energy consumption can also raise many environmental concerns. As a result, establishing wireless networks with the minimal energy consumption has attracted a significant amount of interest among researchers studying wireless network optimization [4]. From the environmental point of view, these studies will arrive at the the greenest design for wireless networks. Motivated by the demands for power optimal network designs, in this dissertation we aim to minimize the total transmit power consumed in the entire network while a certain set of quality-of-services, such as signal-to-noise-ratio or information exchange data-rate, are satisfied.

Synchronous two-way relay networks with multiple multi-antenna relays

The majority of the published work on two-way relay networks consider networks with single antenna nodes. On the other hand, the studies conducted on the two-way relay networks with multi-antenna nodes mainly consider networks including a single multi-antenna relay and two single-antenna transceivers. To the best of our knowledge, the published results on the two-way relay networks with multiple multi-antenna relays are scarce in the literature. The fact that networks with multiple multi-antenna relays are a generalized version of the formerly studied networks along with the fact that studies considering this setup are scarce, encouraged us to study such network setups. As such, we study two-way relay networks with *multiple multi-antenna relays*, a type of two-way relay network which has not been considered much in the literature.

The problems of relay beamforming and transceivers power allocation have been investigated in the literature for single-antenna multi-relay and multi-antenna single relay scenarios. However, to the best of our knowledge, the problem of total power minimization for multi-antenna multi-relay networks (where the beamforming matrices and transceivers power allocation are to be jointly considered) has not been studied. In the problem studied in Chapter 3, we aim to find the minimal power consumption in the entire network while guaranteeing two given quality-of-service thresholds at the receiver front-end of the two transceivers.

Asynchronous two-way relay networks with multiple multi-antenna relays

Considering the published results on asynchronous networks, a question worth answering is that for a single-carrier asynchronous two-way relay network, what is the minimal power consumption required to satisfy given data rate constraints at the two transceivers. While answering this question, one may not have any restriction on the type of the equalizers (i.e., linear or otherwise) or on where the equalizers are implemented (i.e., pre-channel equalization, post-channel equalization, or joint pre- and post-channel equalization). This question is answered for the case of two-way single-carrier asynchronous relay networks with single-antenna relays in [1]. Results presented in [1], motivated us to answer the same question for the case of two-way single-carrier asynchronous relay networks with multi-antenna relays. Solving this problem is not a trivial extension of the work in [1]. Indeed, as we show in Chapter 4, we have to optimize relay beamforming matrices while in [1] only one amplification factor per relay has to be optimized.

Multi-pair two-way networks with massive MIMO relays

A complete round of information exchange between two nodes, using one-way relaying scheme, takes four time-slots (channel uses) where signal transmission in each direction takes two time-slots. However, wireless networks employing two-way relaying schemes can provide higher spectral efficiency. The spectral efficiency of two-way relay networks can be even more improved via establishing peer-to-peer communications between more than a single pair of transceivers. This fact encouraged us to investigate two-way relay networks with multiple pairs of transceivers. Indeed, using the same amount of time and frequency resources, multipair two-way relay networks can transfer higher amount of data per channel use. However, in such networks, inter-pair interference (between transceivers belonging to different pairs) and intra-pair interference (users self-interference transferred back by relay(s)) raise new challenges.

The most recent approach being introduced to suppress interference is to equip relays with a very large number of antennas. Equipping relays with a massive number of antennas (often referred to as massive multiple input multiple output (MIMO) technique) can significantly improve the spectral and energy efficiencies in comparison to the traditional MIMO techniques. The massive MIMO technique can substantially suppress the intra- and inter-pair interferences. As such, when number of antennas are very large, the effects of noise and small-scale fading are asymptotically eliminated. Doing so, by employing simple signal processing techniques, networks can deal with the remaining channel effects such as path loss and large-scale fading. Moreover, as number of antennas are approaching infinity, the transmit power can be arbitrarily reduced without degrading the network performance.

The promising benefits of the massive MIMO technique along with the fact that published results on two-way network with massive MIMO relays are still scarce, encouraged us to adopt this technique in Chapter 5 and deal with the issues arising in multipair two-way relay networks.

Adopting the massive MIMO technique allows relays in multipair two-way relay networks to employ low-complexity relaying schemes such as linear signal processing techniques. The most common structures being used for the uplink and downlink beamforming matrices of two-way relay networks are constructed based on the MRT/MRC and the ZF techniques. As such, we have been motivated to use these techniques along with the massive MIMO concept to solve the total power minimization problem in multipair two-way relay networks.

1.4 Objective and Methodology

In this section, we provide an overview on the objective and methodology of the current dissertation.

1.4.1 Objective

In Chapter 3, we consider a two-way relay network consisting of two single-antenna transceivers communicating with the help of multiple multi-antenna relays. The network considered is assumed to be synchronous such that signals arriving at the receiver front-end of each transceiver via different relaying path are subjected to the same propagation delay. In the network studied in Chapter 3, relays are equipped with multiple antennas. Choosing the transceivers' transmit powers and the relay beamforming matrices as the design parameters, we aim to minimize the total transmit power consumed in the entire network while the signal-to-noise-ratios (SNRs) at the receiver front-end of transceivers are guaranteed to be greater than two given thresholds.

In Chapter 4, we consider a single-carrier asynchronous two-way relay network consisting of two single-antenna transceivers which wish to communicate with the help of multiple multi-antenna relays. Addressing the total transmit power minimization problem while the rates of the information exchange between transceivers are maintained above two given thresholds, we aim to jointly determine the relay beamforming matrices and the transceivers transmit powers.

In Chapter 5, we consider a two-way relay network consisting of multiple pairs of single-antenna transceivers which wish to communicate in a pair-wise manner. The information between transceiver pairs is exchanged with the help of multiple relays. Each relay is equipped with multiple antennas, where number of relay antennas is considered to be very large. Considering the relay beamforming matrices and the transceivers' transmit powers as design parameters, we aim to minimize the total power consumed in the entire network while signal-to-noise-ratio at the receiver front-end of the transceivers are maintained above a set of given thresholds. In this chapter, we study two different processing techniques at the relays. In the first technique, each relay uses a maximum ratio transmission/combining (MRT/MRC) method to obtain the relay's vector of transmitted signals from the relay's vector of received signals. In the second technique, a zero-forcing-based (ZF) method is used as relaying protocol.

1.4.2 Methodology

In this dissertation, we study three scenarios for two-way relay networks with multiple multi-antenna relays. Here below we present methods being developed for each each scenario.

First Scenario: ***Synchronous two-way relay networks with multiple multi-antenna relays***

In Chapter 3, assuming the relay beamforming matrices and the transceivers' transmit powers as design parameters, we study the total power minimization problem. This problem is considered for synchronous two-way relay networks consisting of two-transceivers and multiple multi-antenna relays. We first model the system and signals of such networks. We then show that the relay beamforming matrices have a special structure. Using this special structure, we reduce the dimensionality of the problem. The problem with reduced dimensionality is then studied under two different assumptions for the reduced size beamforming matrices.

In the first approach, we assume that the beamforming matrices are symmetric. We show that restricting matrices to be symmetric renders the total power minimization problem amenable to a semi-closed-form solution. That is, this problem can be solved efficiently.

In the second approach, we assume that the relay beamforming matrices are not restricted to be symmetric. We show that in this case, the total power minimization problem can be solved using a computationally prohibitive algorithm. This algorithm involves a 2-D search over a grid in the space of the transceivers' transmit powers along with a semi-definite programming at each vertex of this grid.

Using numerical examples, we compare the required power for maintaining SNRs at the receiver front-end of transceivers above two given thresholds, for both approaches with general and symmetric relay beamforming matrices.

Second Scenario: *Asynchronous two-way relay networks*

In Chapter 4, we study asynchronous two-way relay networks consisting of two single-antenna transceivers and a number of multi-antenna relays. We aim to minimize the total transmit power consumed in the entire network while data rate in each direction is maintained above a given threshold. The design parameters are assumed to be the relay beamforming matrices and the transceivers transmit powers. To provide a computationally affordable solution to this power minimization problem, we develop the following procedure:

We first model the system and signals of the asynchronous network under consideration. We then derive two expressions for data rates in terms of the design parameters. Exploiting the special structure of the beamforming matrices, similar to what is shown for synchronous networks in Chapter 3, we reduce the dimensionality of the problem. Next, to further simplify the problem, we assume that the beamforming matrices are symmetric. Doing so renders the total power minimization problem amenable to a closed-form solution. More specifically, we show that the asynchronous two-way relay network consists of several synchronous sub-networks. We rigorously prove that at the optimum, the end-to-end channel impulse response (CIR) only consists of a synchronous sub-network of relays. Indeed, at the optimum, only relays which contribute to the power-optimal sub-network will participate in relaying and the remainder of the relays have to be turned off. In other words, the total power minimization problem reduces down to finding the best synchronous sub-network which consumes the smallest total transmit power while satisfying the data rate constraints. Note that using the problem solved in Chapter 3, we can solve the total power minimization problem with signal-to-noise-ratio constraints (and similarly with data rate constraints) for synchronous networks. It is shown in Chapter 3 that this problem is amenable to a semi-closed-form solution. As a result, we arrive at the conclusion that the solution to the problem studied for asynchronous two-way relay networks consists of a number of problems each of which amenable to a semi-closed-form solution. The problem considered for asynchronous networks chooses the power-optimal solution of those obtained for a number of synchronous sub-networks. As such, the total power minimization for network is also amenable to a semi-closed-form.

Using numerical examples, we evaluate the performance of the asynchronous two-way relay networks with symmetric relay beamforming matrices.

Third Scenario: ***Multi-pair two-way networks with massive MIMO relays***

In Chapter 5, we study a synchronous two-way relay network consisting of several pairs of single-antenna transceivers and multiple relays each of which equipped with a massive number of antennas. We aim to minimize the total transmit power consumed in the entire network while the signal-to-noise-plus-interference at each transceiver is maintained above a given threshold. The design parameters are assumed to be the relay beamforming matrices and the transceivers transmit powers. To provide a computationally affordable solution to this power minimization problem, we develop the following procedure:

We consider two cases each of which employing a specific linear relaying scheme at relays. In the first case, we study the case where the maximum ratio transmit/

maximum ratio combining technique (MRT/MRC-based scheme) is employed at relays. In the second case, we study the case when the zero-forcing (ZF-based scheme) technique is used at the relays.

To this end, we first model the system and signals pertinent to each relaying scheme. We then use the fact that when the number of relay antennas is very large, the channel vectors between each relay and different transceivers are asymptotically orthogonal. Exploiting such asymptotical orthogonality, we show that the structure of the beamforming matrices for the two relaying schemes can be obtained from one another. As such, we proceed only with the MRT/MRC-based scheme, and formulate the total transmit power and signal-to-noise-ratio (SNRs) at the receiver front-end of users for this scheme. We then solve the problem for the MRT/MRC-based scheme. Next, we explain how the solution for the ZF–based technique is calculated from the solution obtained for the MRT/MRC-based scheme. We aim to minimize the total transmit power consumed in the entire network while certain SNR thresholds are satisfied at the receiver front-end of users. We show that under the assumption that channel vectors between each relay and transceivers are orthogonal, this problem boils down to a set of total power minimization problems each of which corresponding to a one-way relay network. We use the fact that each of these sub-problems are amenable to a semi-closed-form solution. Doing so, we show that the total power minimization problem for the network under consideration is also amenable to a semi-closed-form solution.

Using numerical examples, we evaluate the performance of the two-way relay networks with massive number of relay antennas. Numerical results are examined for the cases where the MRT/MRC- and the ZF–based signal processing schemes are employed at relays. We also compare the performance of networks when these two relaying schemes are being used.

1.5 Summary of Contributions

The main contributions of this dissertation are summarized as listed below:

- We model the signals and the system of synchronous two-way relay networks which employ multi-antenna relays. We obtain jointly optimal relay beamforming matrices as well as the optimal transceiver transmit powers for a synchronous network with multiple multi-antenna relays such that the total transmit power is minimized under two given SNR constraints at the transceivers. In order to guarantee the reciprocity of the end-to-end channel between the transceivers, we choose beamforming matrices to be symmetric. For this type of beamforming matrices, we prove that the power minimization problem has a unique semi-closed-form solution. That is, given a certain intermediate parameter, the symmetric beamforming matrices can be obtained in a closed-form. We prove that this parameter can be obtained using the efficient Newton-Raphson technique.

- We model the end-to-end channel for single-carrier asynchronous two-way relay networks which employ a number of multi-antenna relays. For the asynchronous networks with multiple multi-antenna relays, assuming the relay beamforming matrices as well as the transceivers transmit powers as the design parameters, we study the problem of total power minimization under two constraints which guarantee that the data rates at the two transceivers are above given thresholds. In order to obtain a computationally efficient solution to the power minimization problem, we assume that the relay beamforming matrices are symmetric. Using such an assumption, we develop a computationally efficient solution to the problem at hand.

- We model the signals and the system of two-way relay networks with multi-pair transceivers which employ relays with a massive number of antennas. We obtain jointly optimal relay beamforming matrices as well as the optimal transceiver transmit powers for these networks such that the total transmit power is minimized under given SNR constraints at the transceivers. We study cases where the MRT/MRC- and the ZF-based schemes are used as signal processing techniques at relays. We rigourously prove that the power minimization problem has a unique semi-closed-form solution. Using numerical examples we evaluate network performance for each of these two relaying schemes. We also examine how network performance is affected when the optimization parameters are calculated under the assumption that channel vectors between each relay and transceivers are orthogonal while they may not be completely orthogonal.

1.6 List of Publications

1. R. Rahimi, S. ShahbazPanahi,"Multi-pair two-way relay networks with massive MIMO relays," submitted to Transactions on Wireless Communications, 2018.

2. R. Rahimi, S. ShahbazPanahi,"Asynchronous two-way MIMO relaying: A multi-relay scenario," accepted to be published in Transactions on Wireless Communications, , 2018.

3. R. Rahimi, S. ShahbazPanahi, "Multiple peer-to-peer bidirectional cooperative communications using massive MIMO Relays," accepted in *2018 IEEE International Conference on Acoustics, Speech and Signal Processing (ICASSP 2018)*, Calgary, 2018.

4. R. Rahimi and S. Shahbazpanahi, "A two-way network beamforming approach based on total power minimization with symmetric relay beamforming matrices," in IEEE Access, vol. 5, pp. 12458-12474, 2017.

5. R. Rahimi and S. Shahbazpanahi, "Network beamforming for asynchronous MIMO two-way relay networks," *2017 IEEE 7th International Workshop on Computational Advances in Multi-Sensor Adaptive Processing (CAMSAP)*, Curacao, 2017, pp. 1-5.

6. R. Rahimi and S. Shahbazpanahi, "Symmetric beamforming for multi-antenna two-way relay networks," *2015 49th Asilomar Conference on Signals, Systems and Computers*, Pacific Grove, CA, 2015, pp. 802-806.

7. R. Rahimi and S. Shahbazpanahi, "Total power minimization for two-way networks with multi-antenna relays," *2015 IEEE 6th International Workshop on Computational Advances in Multi-Sensor Adaptive Processing (CAMSAP)*, Cancun, 2015, pp. 1-4.

1.7 Outline of Dissertation

The remainder of this dissertation is organized as follows. In Chapter 2, we first provide an overview on studies considering synchronous two-way relay networks. We then present a detailed review on several network setups being considered for two-way relay networks and discuss how modifications in setup can improve the network performance. In Chapter 2, we also look at the variety of criteria chosen as the measure of network performance. In the second section of Chapter 2, a survey on studies considering asynchronous two-way relay networks is presented. In the last section of Chapter 2, we provide an overview on studies extending single-pair two-way relay networks to networks with multiple pairs of users (i.e., multipair two-way relay networks). We then present a survey on studies incorporating the massive MIMO concept into the multipair two-way relay networks.

In Chapters 3, 4, and 5, we study two-way relay networks with multiple relay antennas in three different scenarios. Note that in these chapters parameters are denoted differently. As such, to avoid any confusion, we bring appendices of each chapter right at the end of that chapter.

In Chapter 3, we first model the system and signals corresponding to the two-way relay networks with multiple multi-antenna relays. We then provide the problem statement which is aimed at minimizing the total transmit power consumed in the entire network such that two SNR thresholds are satisfied at the receiver front-end of the transceivers. Next, we solve the power minimization problem under the assumption that the beamforming matrices are to be symmetric. We also solve the power minimization problem under the assumption that the beamforming matrices are not constrained to be symmetric. A discussion on the computational complexity of the proposed methods is presented as a remark in this chapter as well. In the last section of Chapter 3, we use numerical examples to evaluate the proposed methods with both symmetric and general beamforming matrices. At the end of Chapter 3, we provide the corresponding appendices.

In Chapter 4, we first model the signals and system for asynchronous two-way relay networks where relays employ multiple antennas. The problem we study in Chapter 4 is to minimize the total transmit power in an asynchronous two-way relay network while the data rates of the transceivers are maintained above two given thresholds. We then provide the problem statement and its solution along with the method being used to solve this problem. We next present an algorithm which summarizes how the proposed method must be implemented. In the last section of Chapter 4, we numerically evaluate the performance of the asynchronous two-way relay networks under consideration. At the end of Chapter 4, we provide the corresponding appendices.

In Chapter 5, we consider two-way relay networks with multiple massive MIMO relays helping to establish multiple bidirectional peer-to-peer communications. We assume that relays employ linear beamforming techniques such as the MRT/MRC and the ZF schemes to precess their received signals. Exploiting the approximate orthogonality of the channel vectors between each relay and transceivers, we provide a computationally efficient solution to the problem of minimizing the total transmit power when the transceivers signal-to-noise ratios (SNRs) are to be above certain thresholds.. At the end of Chapter 5, we provide the corresponding appendix.

Finally, we conclude the dissertation in Chapter 6 where observations and the results obtained are summarized. In this chapter, we also propose a number of ideas for future work which are based upon the results and observations obtained in the current dissertation.

1.8 Notations

Throughout this dissertation, we use small and capital boldface letters to denote vectors and matrices, respectively. The operators $(\cdot)^*$, $(\cdot)^T$, and $(\cdot)^H$ denote the complex conjugate, the transpose, and the Hermitian transpose, respectively. $[\mathbf{A}]_{i,j}$ (and $[\mathbf{A}]_{(i,j)}$) denotes the (i,j)-th entry of matrix $\mathbf{A}$, while $[\mathbf{a}]_i$ represents the i-th entry of vector $\mathbf{a}$. The operator $vec(\mathbf{A})$ represents a column vector obtained by stacking the columns of $\mathbf{A}$. The operator $\otimes$ denotes the Kronecker product. The operators $tr(\cdot)$ and $E\{\cdot\}$ denote the trace and the statistical expectation operators, respectively. We use $\mathbf{I}_r$ to represent an $r \times r$ identity matrix, $\mathbf{1}$ to denote a vector with all entries equal to 1, and $\mathbf{0}_{r\times s}$ to represent an $r \times s$ matrix with zero entries. $\|\cdot\|$ and $|\cdot|$ denote the Euclidean norm of a vector and the absolute value of a complex scalar, respectively. $\text{blkdiag}(\{\mathbf{E}_l\}_{l=1}^{L})$ is used to represent a block diagonal matrix whose l-th diagonal block is $\mathbf{E}_l$, for $l \in \{1, \cdots, L\}$. The cardinality of set $\mathcal{N}$ is denoted as $\text{card}(\mathcal{N})$.

Chapter 2

Background and Literature Review

In this chapter, we review recent studies on relay-assisted two-way relay networks. To begin with, we present an overview on studies investigating two-way relay networks in a basic form consisting of three single-antenna nodes, i.e., two transceivers and a relay node. We next review studies considering networks with extended numbers of relays or antennas. We then offer an overview of studies benefiting from both types of network extensions where multiple relays are employed and transceiver and/or relay(s) are equipped with multiple antennas. Reviewing various network setups, we discuss how each setup can affect the network performance. To do so, we provide a brief survey on the network performance measures chosen by different studies. We also review studies with various design parameters and constraints.

The rest of this chapter is organized as follows. In Section 2.1, we provide an overview on studies considering synchronous two-way relay networks. We present a detailed review on different network setups being considered for two-way relay networks and how setup modifications can improve the network performance. We then look at variety of criteria chosen by various studies as the measure of network performance. We also discuss the design parameters and constraints being considered in each study. A survey on studies considering asynchronous two-way relay networks is given in Section 2.2. In Section 2.3, we present a survey on studies incorporating the massive MIMO concept into the two-way relay networks. We also discuss how employing a massive number of relay antennas can improve the performance of two-way relay networks.

2.1 Synchronous Two-way Relay Networks

Networks providing a synchronous signal transmission over different relaying paths are called *synchronous relay networks*. In synchronous relay networks, signals traveling through different paths all arrive at the destination approximately with equal propagation delays. That is, the difference between the maximum and the minimum propagation delays, known as the delay spread, is less than the length of one symbol period. Note that when networks are not synchronous, overhead signals can be employed to compensate for the difference in the propagation delays and synchronize the data transmission. In this section, we survey studies which assume two-way relay networks are synchronous/synchronized.

2.1.1 Two-way Relying Strategies

In two-way relay networks, two transceivers exchange information symbols with the help of a number of relays. Different relaying strategies employed by the relays can take different number of time-slots for a complete round of information exchange between transceivers. For example, the traditional relaying strategy used for establishing a bidirectional communication between two transceivers, is implemented in four time-slots (see Fig. 1.2). In the first time-slot, signal is transmitted in one direction from one of the transceivers to the relay(s). In the second time-slot, each relay transmits a processed version of its received signal toward the transceiver on the other side. In the third and fourth time-slots, a similar communication link is established in the opposite direction. On the other hand, using the so-called time division broadcast (TDBC) strategy, one can reduce the number of required time-slots from four to three [20–23]. In the TDBC protocol (see Fig. 1.3), transceivers send their signals in two consecutive time-slots. Each relay then broadcasts a signal obtained via combining signals received at that relay in the first two time-slots. As another relaying strategy, the multiple access broadcast (MABC) scheme (see Fig. 1.4) can reduce the number of required time-slots to two time-slots [19,24–27]. In the first time-slot of the MABC scheme, transceivers transmit their signals simultaneously toward the relays. In the second time-slot, each relay transmits a processed version of its received signal toward transceivers. Doing so, a complete round of information exchange between two transceivers can take only two time-slots.

2.1.2 Network Setups

A two-way relay network in its simplest form consists of two single-antenna users assisted by a single-antenna relay. Increasing the number of relays can extend the coverage range, improve the spectral efficiency, and increase the link reliability [28]. Equipping a single relay with multiple antennas can also offer similar benefits [29–31]. Benefits provided by increasing either the number of relays or the number of antennas have driven researchers to investigate how combinations of these two techniques can improve the network performance [32–49]. Studies show that employing multiple multi-antenna relays can significantly boost the achievable advantages. The majority of the published results on two-way relay networks consider two-way relaying schemes with single antenna nodes, see [27] and references therein. The studies conducted on two-way relay networks with multi-antenna nodes mainly consider a two-way relay network including a single multi-antenna relay which assists the establishment of a link between two single-antenna transceivers [30, 50]. Compared to the volume of the results published on networks with single multi-antenna relay and on networks with multiple single-antenna relays, studies focusing on networks with multiple multi-antenna relays are scarce.

We here review some of the results on networks with multiple multi-antenna relays. In [51], the authors study a multi-pair two-way relay network where all the transceiver pairs communicate via one multi-antenna relay. Studies in [29, 52–56] focus on two-way relay networks with a single multi-antenna relay and multi-antenna transceivers. Two-way MIMO relay networks with multiple relays are considered in [39, 57]. In these networks, transceivers and relays are all equipped with multiple antennas. The setup of two-way relay networks is not limited just to single-hop relay networks. For example, a multi-hop two-way relay network is investigated in [58], where the authors assume that all the network nodes are equipped with multiple antennas. To investigate the two-way relay networks in a more practical setup, in [59], the authors look at a multi-pair two-way relay network. The network considered serves multiple pairs of single-antenna transceivers which wish to communicate in a pairwise manner, and each relay is equipped with multiple antennas.

2.1.3 Optimization Problems (Performance Measures, Design Parameters, and Problem Constraints)

We can categorize the results published on the two-way relay based on the chosen performance measure(s), design parameters, and problem constraints. In this section, we provide a brief review on the wide variety of the performance measures, design parameters, and problem constraints considered in the literature. Note that the studies we overview employ analytical methods to solve the optimization problems. However, to deal with challenging problems, studies can also examine heuristic methods as an alternative approach [20].

Transmit Power Minimization

The problem of minimizing the total transmit power in a relay-assisted network has been widely studied in the literature [27,60–66]. The motivation behind these studies is to arrive at the greenest design for the networks. The goal is to find the minimal power consumption in the entire network while the quality of signals at the receiver(s) front-end of users are maintained above certain thresholds. High energy consumption in networks can cause huge running expenditures and detrimental effects on the environment [67,68]. The problem of total transmit power minimization can be considered under various problem constraints. For example, in [66], the authors aim to maximize the smallest received SNR under a total transmit power budget. The goal in [27, 65] is to minimize the total transmit power such that SNR values at the transceivers are maintained above two given values. As another example, in [33], the authors formulated the optimization problem such that the transmission power and the network sum-rate are jointly optimized.

Sum-Rate Maximization

We here provide a brief overview on studies addressing the problem of sum-rate maximization along with the studies aimed at characterizing capacity region of two-way relay networks. The main focus of the studies in [29,30,39,56,57] is on maximizing the achievable sum-rate of two-way relay networks. Results in [69] show that two-way relay networks can achieve data rates higher than those provided by the one-way relay networks. The goal of studies in [70–72] is to allocate network resources such that the sum-rate of two-way relay networks is maximized for multi-carrier systems and OFDM techniques. In [19], the authors show that the MABC protocol can outperforms the TDBC (with three time-slots) and traditional relaying (with four time-slots) strategies, in terms of the achievable sum-rate achieved in two-way relay networks. In [22, 73, 74], the achievable sum-rate regions for two-way relay networks are characterized from an information theoretical point of view. Achievable rate regions for two-way relay networks with nodes operating in the full-duplex mode are derived in [75–77]. Note that, under the full-duplex mode, network nodes can transmit and receive signals at the same time. The maximum achievable rate region for single-antenna two-way relay networks is studied in [23], where the employed TDBC scheme is assumed to be implemented in time-slots with unequal durations.

Based on the studies conducted on end-to-end channels of two-way relay networks, achieving the capacity region is a challenging open problem. Equipping nodes with multiple antennas or employing multiple number of relays, only adds to the challenges of characterizing the capacity region of the network. In an effort to obtain the maximum data sum-rate, in [28] the authors study the achievable rate regions for two-way DF relay network with multiple single-antenna relays. On the other hand, in [29], the authors aim to achieve the capacity region of two-way relay network consisting of two single-antenna transceivers and a multi-antenna relay. In [40], the network weighted sum-rate is aimed to be maximized. Considering a two-way AF MIMO relay network, the authors of [30] derive two computationally affordable algorithms for the sum-rate maximization problem. Studies in [78] consider the data sum-rate maximization and the total mean-square error minimization problems given that certain individual signal-to-interference-plus-noise ratio (SINR) at the destinations are to be maintained above predefined thresholds. In a two-way relay network consisting of multi-antenna nodes, the achievable rate region and the optimal transmit strategies at both transceivers and at the relay are characterized by a weighted sum-rate maximization problem in [32]. In [79], a sum-rate maximization problem is considered where the data rate fairness between two opposite directions of a two-way relay network are to be satisfied.

Mean Square Error (MSE) Minimization

One of the interesting measures for two-way communication links is the mean square of the error (MSE) that may occur between the transmitted signals and the signals received/detected at the destinations. Employing multiple antennas either at transceivers or at relay(s) requires precoding/beamforming matrices to be designed at corresponding nodes. These matrices play the role of design parameters which can be set to minimize the mean square error between transmitted and received signals. In this subsection, we review studies dealing with the MSE minimization problem where precoding/beamforming matrices are designed such that some problem constraints (for example, in terms of power budget) are satisfied.

In [41], the focus is on minimizing the maximum value of MSE in two-way relay networks. An achievable rate region and the degradation related to the corresponding channel estimation error in a MIMO two-way relay channel is investigated in [80].

In [39], a scheme is proposed to design the source and relay precoding matrices (filters) to minimize the sum of the MSE in MIMO spatial multiplexing systems when multiple relays are employed for both one-way and two-way relay networks. In [43], the authors aim to jointly design precoders at both the transceivers and at the relays for MIMO two-way relaying, and the objective is to minimize the total MSE at transceivers. The main focus of [43] lies on minimizing the maximum of the signal estimation MSE among entire available data streams.

In [45], a joint beamforming scheme using MSE duality is proposed to maximize the sum-rate of an AF MIMO two-way relay system.

The network considered in [21] is a two-way relay network consisting of three multi-antenna nodes (two transceivers and one relay). Focusing on optimal joint source precoding and relay beamforming optimization, in [21] the authors derive the optimal structure of the source and relay precoding matrices via minimizing the mean squared error of the symbol estimates at the two transceivers.

2.1.4 Other Optimizations Problems

The antenna selection problem based on the max-min channel coefficients criterion in [50], the interference mitigation at the transceivers in [51], the diversity multiplexing tradeoff analysis of [58], the mean-square-error minimization approach of [54], and the energy efficiency maximization technique of [55] are other examples of studies conducted on the two-way relay networks. Moreover, a max-min fair criterion and weighted sum-rate are performance measures investigated in [19] and [10], respectively.

2.2 Asynchronous Two-way Relay Networks

In two-way relay networks, due to the fact that relays are geographically distributed at different locations, the propagation delays over various relaying paths can be different. A two-way relay network with significant difference between propagation delays for different relaying paths, resembles a multipath channel.

Most of the two-way relay-assisted networks studied in the literature are assumed to operate in a synchronous mode where different relaying paths cause (approximately) identical propagation delays. That is, symbols from different transceivers arrive simultaneously at each relay. Similarly, transceivers receive all the replicas of the relay forwarded signals at the same time. These networks are called synchronous networks. In wideband communications with high data-rate transmissions, network nodes are not guaranteed to operate synchronously and attempts for maintaining their synchronization can incur significant overhead. As a result, signals arrived from different paths experience different propagation delays. Hence, the end-to-end channel between transceivers can be viewed as a multi-path channel with multiple taps. These networks are known as asynchronous networks.

Due to the collision between the consecutively transmitted symbols in asynchronous networks, inter-symbol-interference (ISI) is produced at the receiver front-end of the transceivers. The studies on asynchronous relay networks can be categorized based on the approaches chosen either to avoid or to combat ISI. Addressing the frequency-selective nature of the time dispersed multi-path channel, one can avoid ISI via using the orthogonal frequency division multiplexing (OFDM) technique at the network nodes. Using the OFDM technique can partition the end-to-end channel into orthogonal frequency-flat sub-channels [81–84]. The two-way data transmission over these parallel narrowband sub-channels can then be presumed synchronous, provided that the length of the cyclic prefix is chosen to be equal to or greater than the end-to-end channel delay spread. As an alternative solution, distributed channel equalization techniques have been proposed in the literature. The filter-and-forward relaying scheme is used in [64, 85–87], where relays employ finite-impulse-response (FIR) filters to equalize the propagation delays of different paths such that ISI is minimized at the receiver front-end of the transceivers. Aiming to keep the signal processing at the relays simple, AF relaying scheme is used in [88], while the channel equalization is left to be implemented at two post-channel block equalizers used at the receiver front-end of the transceivers. As an alternative approach, the authors of [89] choose a pre-channel block equalization scheme to circumvent the ISI related issues in an asynchronous single-carrier two-way relay channel.

A question worth answering is that for a single-carrier asynchronous two-way relay network, what is the minimal power required to satisfy given data rate constraints at the two transceivers. While answering this question, one may not have any restriction on the type of the equalizers (i.e., linear or otherwise) or on where the equalizers are implemented (i.e., pre-channel equalization, post-channel equalization, or joint pre- and post-channel equalization). This question has been answered for the case of two-way single-carrier asynchronous relay networks with single-antenna relays [1]. In Chapter 4, we aim to answer the same question for the case of two-way single-carrier asynchronous relay networks with multi-antenna relays. Dealing with this problem is not a trivial extension of the work in [1]. Indeed, as we show in Chapter 4, we have to optimize relay beamforming matrices while in [1] only one amplification factor per relay has to be optimized.

A brief review on the published work on asynchronous networks shows interest in various design parameters and objectives. Resorting to the OFDM scheme, in [83] the authors aim to design the AF relay weights and the transceivers subcarrier powers such that the smallest subcarrier SNR at the receiver front-end of the transceivers is maximized while a total transmit power constraint is satisfied. In [88], the goal is to optimize the transceivers transmit powers, the relay amplification weights, and the post-channel block equalizing matrices in a way that the total MSE between the transmitted signals and the estimated received signals at the two transceivers is minimized while a total transmit power budget is guaranteed. Similar to [88], the objective in [89] is to minimize the total MSE under a total transmit power constraint. The network considered in [89] consists of two single-antenna transceivers which aim to communicate through multiple single-antenna relays. The authors of [90], characterize the achievable SNR region and equivalently the achievable rate region for an asynchronous multi-carrier two-way relay channel, with the restriction on the total available transmit power. In [91], a multi-carrier asynchronous two-way relay channel similar to that studied in [83] is considered. It is shown that the network sum-rate maximization problem with the total transmit power constraint results in a relay selection scheme suggested by the max-min SNR fair optimization problem in [83]. All the results published in [1, 64, 83, 85–93], focus on networks with single-antenna relays while studies in Chapters 3 and 4 of this dissertation consider two-way single-carrier relay networks with multi-antenna relays in synchronous and asynchronous, respectively . The single-carrier two-way relay networks we consider in Chapters 3 and 4, consist of two single-antenna transceivers which wish to communicate with the help of multiple multi-antenna relays. Addressing the total transmit power minimization problem while the SNRs or data rates of at two transceivers are maintained above two given thresholds, we aim to jointly determine the relay beamforming matrices and the transceivers transmit powers.

The problem of relay beamforming and transceiver power allocation has been investigated in the literature for single-antenna multi-relay networks, for multi-antenna single-relay scheme, and for multi-antenna multi-relay synchronous networks. However, the problem of total transmit power minimization for synchronous or asynchronous multi-antenna multi-relay networks, where the beamforming matrices and transceivers power allocation need to be jointly considered, has not been investigated. These two problems problems are exactly what we study in Chapters 3 and 4.

2.3 Massive MIMO Techniques and Multi-pair Two-way Relay Networks

The spectral efficiency of two-way relay networks can be improved via establishing peer-to-peer communications between more than a single pair of transceivers [63, 94–102]. Indeed, using the same amount of time and frequency resources, multipair two-way relay networks can transfer higher amount of data per channel use. However, in such multipair networks, inter-pair interference (between transceivers belonging to different pairs) and intra-pair interference (users self-interference transferred back by relay(s)) raise new challenges.

A simple method to avoid inter-pair interference is to establish peer-to-peer communications over orthogonal channels. Techniques such as code division multiple access (CDMA) [103] and orthogonal frequency division multiple access (OFDMA) [104] make the communication channels orthogonal. In [105], several low-complexity beamforming techniques are proposed which rely on the block-diagonalization concept. However, these techniques are not spectrally efficient in the sense that they do not allow multiple peer-to-peer communications to share the same channel (i.e., the same time and frequency resource). In [51, 106–110], the authors employ MIMO techniques to suppress interference while allow users share channel resources. The drawback of these techniques is their prohibitive computational complexity. Some of the other advanced techniques proposed to suppress the inter-pair interference are the dirty paper coding [111] and the interference alignment techniques [112]. The complexity burden of implementing these techniques is also significantly high.

The most recent approach being introduced to suppress interference is to equip relays with a very large number of antennas. Equipping relays with a massive number of antennas (often referred to as massive multiple input multiple output (MIMO) technique) can significantly improve the spectral and energy efficiencies in comparison to the traditional MIMO techniques [113–116]. The massive MIMO technique can substantially suppress the intra- and inter-pair interferences. As such, when number of antennas is very large, the effects of noise and small-scale fading are asymptotically eliminated [117]. Employing a massive number of antennas at the relays, allows network to deal with the remaining channel effects such as path loss and large-scale fading even using simple signal processing techniques. Moreover, as number of antennas are approaching infinity, the transmit power can be arbitrarily reduced without degrading the network performance [116, 118–120]. Due to these benefits, massive MIMO technique has been the center focus of a significant volume of studies in recent years. However, published results on two-way network with massive MIMO relays are still scarce.

In what follows, we describe how adopting massive MIMO technique can be of help with multipair two-way relay networks. The massive MIMO technique, allows relays in multipair two-way relay networks to employ low complexity relaying schemes such as linear signal processing techniques. Thanks to their simplicity in implementation, linear techniques have attracted a significant amount of interest in the literature. Among the linear techniques, AF relaying scheme is the most studied one. Indeed, adopting AF relaying scheme, relays do not require to decode their received signals. As a result, AF relaying scheme incurs low hardware and software complexity. Moreover, when AF relaying scheme is employed, the transmission delay due to the signal processing at relays is insignificant.

When AF relaying scheme is employed by two-way relay networks with multi-antenna relays, the vector of received signal at each relay is first multiplied by the uplink beamforming matrix and then by an amplification matrix. Next, the so-obtained vector is multiplied by the downlink beamforming matrix to be transmitted toward users. The most common structures being used for the uplink and downlink beamforming matrices of two-way relay networks are constructed based on the MRT/MRC [95, 96] and the ZF [97–99] techniques.

In Chapter 5, with massive number of antennas being used at the relays, we use two linear relaying schemes. We assume that relays employ linear beamforming techniques such as the MRT/MRC and the ZF schemes to process their received signals. Exploiting the approximate orthogonality among relay-transceiver channel vectors when number of relay antennas are very large, we aim to minimize the total transmit power while the transceivers signal-to-noise ratios are to be above given thresholds.

Chapter 3

Synchronous Two-way Networks with Multiple Multi-Antenna Relays

The focus of this chapter is on two-way relay networks consisting of two single-antenna transceivers and multiple multi-antenna relays. Assuming an MABC relaying scheme, our goal is to jointly obtain the optimal relay beamforming matrices as well as the optimal transceiver transmit powers which minimize the total transmit power under given signal-to-noise-ratio (SNR) constraints at the transceivers. To do so, we consider two different types of beamforming matrices. We first restrict the relay beamforming matrices to be symmetric, thereby rendering the end-to-end channel between the two transceivers reciprocal. Under such symmetry condition, we show that the aforementioned total power minimization yields a semi-closed form solution. We then solve the total power minimization problem for the case with general beamforming matrices (without assuming that these matrices are symmetric).

The organization of this chapter is as follows. In Section 3.1, we model the system and signals corresponding to the two-way relay networks with multiple multi-antenna relays. We also formulate the total transmit power and signal-to-noise-ratio (SNRs) at the receiver front-end of transceivers. In Section 3.2, we provide the problem statement, where we aim to minimize the total power consumed in the entire network while two SNR thresholds are satisfied at the receiver front-end of the transceivers.

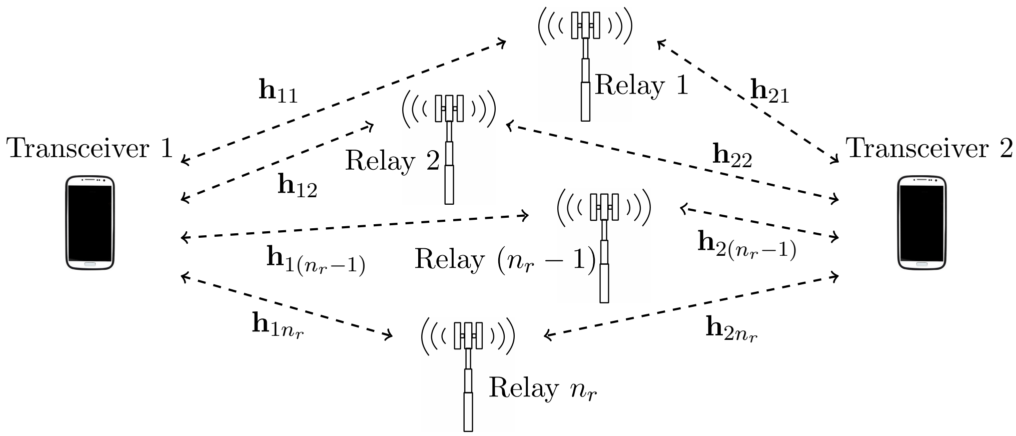

Figure 3.1: A two-way relay network with multiple multi-antenna relays.

In Section 3.3, we solve the power minimization problem under the assumption that the beamforming matrices are to be symmetric. In Section 3.4, we solve the power minimization problem under the assumption that the beamforming matrices are not constrained to be symmetric. A discussion on the computational complexity of the methods proposed and some other important remarks are provided in Section 3.5. In Section 3.6, we use numerical examples to evaluate the proposed methods with symmetric or general beamforming matrices.

3.1 System Model

As shown in Fig. 3.1, the two-way relay network we consider consists of two single-antenna transceivers which wish to communicate with the help of n_r multi-antenna relays. The scenario we are considering can be used in cellular communication systems, where user devices can use only a single antenna due to their size and weight limitations and the base stations act as relays. Indeed, our scheme can be viewed as a distributed MIMO system used for connecting two single-antenna user devices. Equipping the relays (base stations) with multiple antennas allows local beamforming at the relays while distributed beamforming is materialized by all base stations collectively.

Each relay transforms the vector of its received signals by multiplying it with a complex "beamforming" matrix. We refer to such a scheme as transform-and-forward (TF) relaying protocol. To determine the relay beamforming matrices and the transceivers' transmit powers, we aim to minimize the total transmit power consumed in the entire network while SNRs at the receiver front-ends of the transceivers are kept higher than or equal to two given thresholds. Assuming that each relay node is equipped with M antennas, we consider the two time-slot MABC relaying scheme, where in the first time-slot, the two transceivers transmit their signals simultaneously and in the second time-slot, each relay forwards a linearly transformed version of its received signal vector to the two transceivers. We assume that no direct link exists between the transceivers, i.e., all data transmissions go through the relay nodes.

For $j \in \{1, 2\}$, let s_j denote the unit-power scalar information symbol transmitted by Transceiver j with transmission power p_j. Assuming frequency-flat fading transceiver-relay channels, the $M \times 1$ vector $\mathbf{x}_i$ of the received baseband signals at relay i in the first time-slot is given as

$$\mathbf{x}_i = \sqrt{p_1}\mathbf{h}_{1i}s_1 + \sqrt{p_2}\mathbf{h}_{2i}s_2 + \mathbf{n}_i, \quad \text{for } i \in \{1, \ldots, n_r\}. \tag{3.1}$$

Here, $\mathbf{n}_i$ is the $M \times 1$ received noise vector at the i-th relay, while $\mathbf{h}_{1i}$ and $\mathbf{h}_{2i}$ are the $M \times 1$ complex vectors of the coefficients corresponding to the channels between the i-th relay and Transceivers 1 and 2, respectively. Denoting the beamforming matrix of the i-th relay as an $M \times M$ complex matrix $\mathbf{A}_i$, the $M \times 1$ vector of the signal transmitted by the i-th relay is denoted by $\mathbf{t}_i$ and can be expressed as

$$\mathbf{t}_i = \mathbf{A}_i\mathbf{x}_i. \tag{3.2}$$

Assuming that the relay-transceiver channels are reciprocal for uplink and downlink transmissions, the received signals $y_1 = \sum_{i=1}^{n_r} \mathbf{h}_{1i}^T\mathbf{t}_i + \eta_1$ and $y_2 = \sum_{i=1}^{n_r} \mathbf{h}_{2i}^T\mathbf{t}_i + \eta_2$ at Transceivers 1 and 2 are written, respectively, as

$$y_1 = \sum_{i=1}^{n_r} \sqrt{p_1}\mathbf{h}_{1i}^T\mathbf{A}_i\mathbf{h}_{1i}s_1 + \sum_{i=1}^{n_r} \sqrt{p_2}\mathbf{h}_{1i}^T\mathbf{A}_i\mathbf{h}_{2i}s_2 + \sum_{i=1}^{n_r} \mathbf{h}_{1i}^T\mathbf{A}_i\mathbf{n}_i + \eta_1 \tag{3.3}$$

$$y_2 = \sum_{i=1}^{n_r} \sqrt{p_1}\mathbf{h}_{2i}^T \mathbf{A}_i \mathbf{h}_{1i} s_1 + \sum_{i=1}^{n_r} \sqrt{p_2}\mathbf{h}_{2i}^T \mathbf{A}_i \mathbf{h}_{2i} s_2 + \sum_{i=1}^{n_r} \mathbf{h}_{2i}^T \mathbf{A}_i \mathbf{n}_i + \eta_2 \tag{3.4}$$

where η_j is the received noise at Transceiver j, for $j \in \{1, 2\}$. Since the two transceivers know their own transmitted signals and assuming that they have perfect knowledge of global channel state information (CSI), the first term in (3.3) and the second term in (3.4) (which are self-interference terms) can be subtracted from y_1 and y_2, respectively. The residual signals $\tilde{y}_1$ and $\tilde{y}_2$ are then given as

$$\tilde{y}_1 \triangleq \sum_{i=1}^{n_r} \sqrt{p_2}\mathbf{h}_{1i}^T \mathbf{A}_i \mathbf{h}_{2i} s_2 + \sum_{i=1}^{n_r} \mathbf{h}_{1i}^T \mathbf{A}_i \mathbf{n}_i + \eta_1 \tag{3.5}$$

$$\tilde{y}_2 \triangleq \sum_{i=1}^{n_r} \sqrt{p_1}\mathbf{h}_{2i}^T \mathbf{A}_i \mathbf{h}_{1i} s_1 + \sum_{i=1}^{n_r} \mathbf{h}_{2i}^T \mathbf{A}_i \mathbf{n}_i + \eta_2. \tag{3.6}$$

The noise processes at all nodes are assumed to be spatially white zero-mean complex Gaussian processes with variance σ^2. Therefore, we can write $E\{|\eta_1|^2\} = E\{|\eta_2|^2\} = \sigma^2$ and $E\{\mathbf{n}_i \mathbf{n}_i^H\} = \sigma^2 \mathbf{I}_M$. Hence, using (3.5) and (3.6), we can express the SNRs at Transceivers 1 and 2 as

$$\mathrm{SNR}_1 = \frac{p_2 \left| \sum_{i=1}^{n_r} \mathbf{h}_{1i}^T \mathbf{A}_i \mathbf{h}_{2i} \right|^2}{\sigma^2 (1 + \sum_{i=1}^{n_r} \|\mathbf{h}_{1i}^T \mathbf{A}_i\|^2)},$$

$$\mathrm{SNR}_2 = \frac{p_1 \left| \sum_{i=1}^{n_r} \mathbf{h}_{2i}^T \mathbf{A}_i \mathbf{h}_{1i} \right|^2}{\sigma^2 (1 + \sum_{i=1}^{n_r} \|\mathbf{h}_{2i}^T \mathbf{A}_i\|^2)}. \tag{3.7}$$

The total transmit power P_T in the network is the summation of the transceivers' transmit powers and the transmit power of all the relays, that is $P_T = p_1 + p_2 + P_r$, where

$$P_r \triangleq p_1 \sum_{i=1}^{n_r} \|\mathbf{A}_i \mathbf{h}_{1i}\|^2 + p_2 \sum_{i=1}^{n_r} \|\mathbf{A}_i \mathbf{h}_{2i}\|^2 + \sigma^2 \sum_{i=1}^{n_r} tr(\mathbf{A}_i \mathbf{A}_i^H) \tag{3.8}$$

is the total relay transmit power.

3.2 Power Minimization

In the current study, we aim to find the beamforming matrices and the transceivers' transmit powers such that the total transmit power P_T is minimized, while the SNRs at Transceivers 1 and 2 are maintained above given thresholds γ_1 and γ_2, respectively. This power minimization problem can be expressed as[1 2 3]

$$\min_{p_1,p_2,\{\mathbf{A}_i\}_{i=1}^{n_r}} P_T \qquad\qquad \text{subject to} \;\; \mathrm{SNR}_1 \geq \gamma_1, \;\; \mathrm{SNR}_2 \geq \gamma_2. \tag{3.9}$$

Using (3.7) and (3.8), we can recast the optimization problem as

$$\begin{aligned} \min_{p_1,p_2,\{\mathbf{A}_i\}_{i=1}^{n_r}} \;& p_1\left(1+\sum_{i=1}^{n_r}\|\mathbf{A}_i\mathbf{h}_{1i}\|^2\right)+p_2\left(1+\sum_{i=1}^{n_r}\|\mathbf{A}_i\mathbf{h}_{2i}\|^2\right)+\sigma^2\sum_{i=1}^{n_r}tr(\mathbf{A}_i\mathbf{A}_i^H) \\ \text{subject to} \;& \frac{p_2\left|\sum\limits_{i=1}^{n_r}\mathbf{h}_{1i}^T\mathbf{A}_i\;\mathbf{h}_{2i}\right|^2}{\sigma^2\left(1+\sum\limits_{i=1}^{n_r}\|\mathbf{h}_{1i}^T\mathbf{A}_i\|^2\right)} \geq \gamma_1, \\ & \frac{p_1\left|\sum\limits_{i=1}^{n_r}\mathbf{h}_{2i}^T\mathbf{A}_i\;\mathbf{h}_{1i}\right|^2}{\sigma^2\left(1+\sum\limits_{i=1}^{n_r}\|\mathbf{h}_{2i}^T\mathbf{A}_i\|^2\right)} \geq \gamma_2. \end{aligned} \tag{3.10}$$

We observe that at the optimum, the SNR inequality constraints in (3.10) are satisfied with equality, otherwise, if, at the optimum, any of these constraints is satisfied with inequality, then the corresponding optimal power can be reduced to satisfy this constraint with equality. This, in turn decreases the value of the objective

[1]It is worth mentioning that a total power minimization approach has been widely considered as a design technique for relay networks, see for example [27, 60–63, 66, 87, 121, 122]. The advantage of a total power minimization approach is to ensure the minimum amount of power is consumed in the entire network, thereby leading to the most power efficient design of the network.

[2]Note that the power consumption at each node is the sum of the node transmit power and the power consumed in the circuitry of the node. The latter power is the sum of the power consumption in the node circuitry, excluding the node power amplifier, which is constant, and the power consumed by the power amplifier and is a linear function of the node transmit power, see [123]. As such, minimizing the total transmit power will minimize the total power consumed in the network.

[3]Note that as shown in [29], the total power minimization problem in (3.9) can be used to solve a related problem, namely the weighted sum-rate maximization problem under a total power constraint. As shown in [29], the latter problem can be solved using a bisection type of algorithm along with an algorithm which solves the total power minimization problem. Interested readers are referred to [29] for more details on this approach.

function thereby contradicting the optimality. This observation implies that p_1 and p_2 can be respectively written as

$$p_1 = \frac{\sigma^2\gamma_2\left(1+\sum_{i=1}^{n_r}\|\mathbf{h}_{2i}^T\mathbf{A}_i\|^2\right)}{\left|\sum_{i=1}^{n_r}\mathbf{h}_{2i}^T\mathbf{A}_i\ \mathbf{h}_{1i}\right|^2}, \qquad p_2 = \frac{\sigma^2\gamma_1\left(1+\sum_{i=1}^{n_r}\|\mathbf{h}_{1i}^T\mathbf{A}_i\|^2\right)}{\left|\sum_{i=1}^{n_r}\mathbf{h}_{1i}^T\mathbf{A}_i\ \mathbf{h}_{2i}\right|^2}. \tag{3.11}$$

Using (3.11), we rewrite (3.10) as the following unconstrained optimization problem:

$$\begin{aligned}\min_{\{\mathbf{A}_i\}_{i=1}^{n_r}} & \frac{\gamma_2\sigma^2\left(1+\sum_{i=1}^{n_r}\|\mathbf{h}_{2i}^T\mathbf{A}_i\|^2\right)\left(1+\sum_{i=1}^{n_r}\|\mathbf{A}_i\mathbf{h}_{1i}\|^2\right)}{\left|\sum_{i=1}^{n_r}\mathbf{h}_{2i}^T\mathbf{A}_i\ \mathbf{h}_{1i}\right|^2} \\ & + \frac{\gamma_1\sigma^2\left(1+\sum_{i=1}^{n_r}\|\mathbf{h}_{1i}^T\mathbf{A}_i\|^2\right)\left(1+\sum_{i=1}^{n_r}\|\mathbf{A}_i\mathbf{h}_{2i}\|^2\right)}{\left|\sum_{i=1}^{n_r}\mathbf{h}_{1i}^T\mathbf{A}_i\ \mathbf{h}_{2i}\right|^2} + \sigma^2\sum_{i=1}^{n_r} tr(\mathbf{A}_i\mathbf{A}_i^H).\end{aligned} \tag{3.12}$$

Let us denote the $M \times 2$ matrix that spans the vector space of $\mathbf{h}_{1i}$ and $\mathbf{h}_{2i}$ as $\mathbf{U}_i$, where $\mathbf{U}_i^H\mathbf{U}_i = \mathbf{I}_2$. Following Theorem 3.1 of [29], we show in Appendix 3.A that the optimal value of matrix $\mathbf{A}_i$ can be written, without any loss of optimality, as

$$\mathbf{A}_i = \mathbf{U}_i^*\mathbf{B}_i\mathbf{U}_i^H. \tag{3.13}$$

Here, $\mathbf{B}_i$ is a 2×2 complex matrix which can be viewed, as shown in the sequel, as the effective beamforming matrix of the i-th relay. In light of (3.13), the beamforming matrix $\mathbf{A}_i$ is a cascade of three operations. The first operation is a receive beamforming matrix $\mathbf{U}_i^H$, which filters out the components of the relay received noise vector that do not reside in the signal subspace defined as the space spanned by $\mathbf{h}_{1i}$ and $\mathbf{h}_{2i}$. The second operation is denoted with $\mathbf{B}_i$ which transforms the output vector of the relay receive beamformer into a new vector. The third operation is a transmit beamforming operation represented by matrix $\mathbf{U}_i^*$ which guarantees that the transformed vector is transmitted only into the signal subspace. The matrices $\{\mathbf{B}_i\}_{i=1}^{n_r}$ are now determined such that the total transmit power is minimized subject to SNR constraints. That is, instead of finding the optimal values $\{\mathbf{A}_i\}_{i=1}^{n_r}$, without loss of optimality, we can obtain the optimal values of $\{\mathbf{B}_i\}_{i=1}^{n_r}$.

Let us define $\mathbf{q}_{1i} \triangleq \mathbf{U}_i^H \mathbf{h}_{1i}$ and $\mathbf{q}_{2i} \triangleq \mathbf{U}_i^H \mathbf{h}_{2i}$ as the effective channel vectors between the i-th relay and Transceivers 1 and 2, respectively. Then, the unconstrained problem in (3.12) can be equivalently written as

$$\begin{aligned}\min_{\{\mathbf{B}_i\}_{i=1}^{n_r}} \; & \frac{\gamma_2\sigma^2 \left(1+\sum_{i=1}^{n_r} \|\mathbf{q}_{2i}^T\mathbf{B}_i\|^2\right)\left(1+\sum_{i=1}^{n_r} \|\mathbf{B}_i\mathbf{q}_{1i}\|^2\right)}{\left|\sum_{i=1}^{n_r} \mathbf{q}_{2i}^T\mathbf{B}_i \; \mathbf{q}_{1i}\right|^2} \\ & + \frac{\gamma_1\sigma^2 \left(1+\sum_{i=1}^{n_r} \|\mathbf{q}_{1i}^T\mathbf{B}_i\|^2\right)\left(1+\sum_{i=1}^{n_r} \|\mathbf{B}_i\mathbf{q}_{2i}\|^2\right)}{\left|\sum_{i=1}^{n_r} \mathbf{q}_{1i}^T\mathbf{B}_i \; \mathbf{q}_{2i}\right|^2} \\ & + \sigma^2 \sum_{i=1}^{n_r} tr(\mathbf{B}_i\mathbf{B}_i^H).\end{aligned} \tag{3.14}$$

where the effective beamforming matrices $\{\mathbf{B}_i\}_{i=1}^{n_r}$ are now the optimization variables.

3.3 Power Minimization with Symmetric Beamforming Matrices

3.3.1 Symmetric relay beamforming matrices

To ensure the end-to-end reciprocity between the transceivers, we choose $\mathbf{A}_i$ to be a symmetric matrix, i.e., $\mathbf{A}_i = \mathbf{A}_i^T$. Indeed, from (3.3) and (3.4), the end-to-end gains are $\mathbf{h}_{1i}^T\mathbf{A}_i\mathbf{h}_{2i}$ and $\mathbf{h}_{2i}^T\mathbf{A}_i\mathbf{h}_{1i}$ which will be equal if we choose $\mathbf{A}_i = \mathbf{A}_i^T$. Assuming a symmetric[4] beamforming matrix $\mathbf{A}_i$, leads to a symmetric matrix $\mathbf{B}_i$, i.e., $\mathbf{B}_i = \mathbf{B}_i^T$. It is thus observed that in this case, for minimizing total power, the optimal scheme needs to determine $3n_r$ unknown complex parameters as each of the n_r matrices $\{\mathbf{B}_i\}_{i=1}^{n_r}$ has only three unknown complex parameters, which are to be optimally determined. Using the symmetric beamforming matrices assumption, the

[4] In the next section, we consider the case of non-symmetric beamforming matrices.

optimization problem (3.14) can be rewritten as

$$\min_{\{\mathbf{B}_i\}_{i=1}^{n_r}} \frac{\sigma^2(\gamma_1+\gamma_2)\left(1+\sum_{i=1}^{n_r}\|\mathbf{q}_{2i}^T\mathbf{B}_i\|^2\right)\left(1+\sum_{i=1}^{n_r}\|\mathbf{B}_i\mathbf{q}_{1i}\|^2\right)}{\left|\sum_{i=1}^{n_r}\mathbf{q}_{2i}^T\mathbf{B}_i\mathbf{q}_{1i}\right|^2} + \sigma^2\sum_{i=1}^{n_r} tr(\mathbf{B}_i\mathbf{B}_i^H)$$
$$\text{subject to } \; [\mathbf{B}_i]_{(1,2)} = [\mathbf{B}_i]_{(2,1)}, \;\text{ for } \; i = 1,\, 2, \ldots, n_r \tag{3.15}$$

where the last set of constraints guarantees that $\{\mathbf{B}_i\}_{i=1}^{n_r}$ are symmetric. Assuming that the beamforming matrices are symmetric renders the end-to-end channel over each relaying path reciprocal, i.e., $\mathbf{q}_{1i}^T\mathbf{B}_i\mathbf{q}_{2i} = \mathbf{q}_{2i}^T\mathbf{B}_i\mathbf{q}_{1i}$, and also leads to the following equalities $\|\mathbf{q}_{1i}^T\mathbf{B}_i\| = \|\mathbf{B}_i\mathbf{q}_{1i}\|$ and $\|\mathbf{q}_{2i}^T\mathbf{B}_i\| = \|\mathbf{B}_i\mathbf{q}_{2i}\|$, and thus, allows us to write the optimization problem (3.14) as in (3.15). The latter optimization, as we show in the sequel, is amenable to a computationally affordable solution, which is globally optimal under the assumption of symmetric beamforming matrices. We now observe that the matrices $\{\mathbf{B}_i\}_{i=1}^{n_r}$ remain unchanged for different values of γ_1 and γ_2 as long as $\gamma_1+\gamma_2$ does not change[5]. Hence, in (3.10), if we replace γ_2 with $\gamma_1+\gamma_2$ and then set γ_1 to 0, the optimal values of $\{\mathbf{A}_i\}_{i=1}^{n_r}$ (or equivalently the optimal values of $\{\mathbf{B}_i\}_{i=1}^{n_r}$) will not change. Note that in (3.10), replacing γ_1 with 0, means that p_2 will be equal to 0. Therefore, *as long as the optimal values of* $\{\mathbf{B}_i\}_{i=1}^{n_r}$ *are concerned*, we can solve the following optimization problem:

$$\min_{\tilde{p}_1,\{\mathbf{B}_i\}_{i=1}^{n_r}} \quad \tilde{p}_1\left(1+\sum_{i=1}^{n_r}\|\mathbf{B}_i\mathbf{q}_{1i}\|^2\right) + \sigma^2\sum_{i=1}^{n_r} tr(\mathbf{B}_i\mathbf{B}_i^H)$$
$$\text{subject to} \quad \frac{\tilde{p}_1\left|\sum_{i=1}^{n_r}\mathbf{q}_{2i}^T\mathbf{B}_i\;\mathbf{q}_{1i}\right|^2}{\sigma^2\left(1+\sum_{i=1}^{n_r}\|\mathbf{q}_{2i}^T\mathbf{B}_i\|^2\right)} \geq \gamma_1+\gamma_2$$
$$[\mathbf{B}_i]_{(1,2)} = [\mathbf{B}_i]_{(2,1)}, \;\text{ for } \; i = 1, 2, \ldots, n_r. \tag{3.16}$$

Note that the optimal value for $\tilde{p}_1$ in (3.16) is not the same as the optimal value of p_1 in (3.10). In other words, the matrices $\{\mathbf{B}_i\}_{i=1}^{n_r}$ obtained by solving (3.10) are

[5]Note that in case of single-antenna relays, each relay beamforming matrices shrinks to a scalar, and thus, the symmetric property of relay beamforming weights is automatically satisfied. The case of single-antenna relays which was studied in [27,121] has indeed inspired us to resort to symmetric beamforming matrices.

identical to the matrices $\{\mathbf{B}_i\}_{i=1}^{n_r}$ obtained by solving (3.16). However, the value of $\tilde{p}_1$ obtained by solving (3.16) is not the same as the value of p_1 obtained by solving (3.10). To obtain the optimal values of p_1 and p_2 in (3.10), once the optimal values of $\{\mathbf{B}_i\}_{i=1}^{n_r}$ in (3.16) are obtained, we can use (3.13) to obtain the corresponding optimal values of $\{\mathbf{A}_i\}_{i=1}^{n_r}$. The so-obtained $\mathbf{A}_i$'s can then be used in (3.11) to calculate the optimal values of p_1 and p_2. Indeed, by solving (3.16), we aim to find the optimal values of $\{\mathbf{B}_i\}_{i=1}^{n_r}$ and the transmit power of Transceiver 1 in a *one-way relay-assisted communication* scheme, where the received SNR at Transceiver 2 is at least equal to $\gamma_1 + \gamma_2$. Using the following identities $tr(\mathbf{ABC}) = (vec(\mathbf{A}^T))^T (\mathbf{I} \otimes \mathbf{B})\, vec(\mathbf{C})$ and $tr(\mathbf{A}^T\mathbf{BCD}^T) = (vec(\mathbf{A}^T))^T (\mathbf{D} \otimes \mathbf{B})\, vec(\mathbf{C})$, defining $\mathbf{b}_i \triangleq (vec(\mathbf{B}_i^T))^*$ and $\mathbf{f}_i \triangleq vec(\mathbf{q}_{1i}\, \mathbf{q}_{2i}^T)$, and after some algebraic manipulation, we can rewrite the optimization problem in (3.16) as

$$\begin{aligned} \min_{\tilde{p}_1,\{\mathbf{b}_i\}_{i=1}^{n_r}} \quad & \tilde{p}_1\Big(1+\sum_{i=1}^{n_r}\mathbf{b}_i^H(\mathbf{I}_2 \otimes \mathbf{q}_{1i}\mathbf{q}_{1i}^H)\mathbf{b}_i\Big)+\sigma^2\sum_{i=1}^{n_r}\mathbf{b}_i^H\mathbf{b}_i \\ \text{subject to} \quad & \tilde{p}_1\left|\sum_{i=1}^{n_r}\mathbf{b}_i^H\mathbf{f}_i\right|^2 - \sigma^2(\gamma_1+\gamma_2)\left(1+\sum_{i=1}^{n_r}\mathbf{b}_i^H(\mathbf{q}_{2i}\mathbf{q}_{2i}^H \otimes \mathbf{I}_2)\mathbf{b}_i\right)\geq 0 \\ & [\mathbf{b}_i]_2 = [\mathbf{b}_i]_3, \quad \text{for } \ i = 1,\, 2, \ldots, n_r. \end{aligned} \tag{3.17}$$

We now define $\mathbf{b} \triangleq [\mathbf{b}_1^T, \mathbf{b}_2^T, \ldots, \mathbf{b}_{n_r}^T]^T$ and $\mathbf{f} \triangleq [\mathbf{f}_1^T, \mathbf{f}_2^T, \ldots, \mathbf{f}_{n_r}^T]^T$, and hence, can write $\left|\sum_{i=1}^{n_r}\mathbf{b}_i^H\mathbf{f}_i\right|^2 = |\mathbf{b}^H\mathbf{f}|^2 = \mathbf{b}^H\mathbf{f}\,\mathbf{f}^H\mathbf{b}$. Doing so, we can express the optimization problem in (3.17) as

$$\begin{aligned} \min_{\tilde{p}_1} \quad & \tilde{p}_1 + \min_{\mathbf{b}}\, \mathbf{b}^H\left(\tilde{p}_1\mathbf{E}_0 + \sigma^2\mathbf{I}_{4n_r}\right)\mathbf{b} \\ \text{subject to} \quad & \mathbf{b}^H\left(\tilde{p}_1\mathbf{E}_1 - \sigma^2(\gamma_1+\gamma_2)\mathbf{E}_2\right)\mathbf{b} \geq \sigma^2(\gamma_1+\gamma_2) \\ & [\mathbf{b}]_{(i-1)n_r+2} = [\mathbf{b}]_{(i-1)n_r+3} \ \text{ for } \ i = 1, 2, \cdots, n_r \end{aligned} \tag{3.18}$$

where $\mathbf{E}_0$, $\mathbf{E}_1$, and $\mathbf{E}_2$ are defined as

$$\mathbf{E}_0 \triangleq \text{blkdiag}\Big(\{\mathbf{I}_2 \otimes \mathbf{q}_{1i}\,\mathbf{q}_{1i}^H\}_{i=1}^{n_r}\Big), \tag{3.19}$$

$$\mathbf{E}_1 \triangleq \mathbf{f}\,\mathbf{f}^H, \tag{3.20}$$

$$\mathbf{E}_2 \triangleq \text{blkdiag}\Big(\{\mathbf{q}_{2i}\,\mathbf{q}_{2i}^H \otimes \mathbf{I}_2)\}_{i=1}^{n_r}\Big). \tag{3.21}$$

Here blkdiag($\cdot$) stands for a block diagonal matrix. To solve (3.18), we can first fix $\tilde{p}_1$ and solve the minimization over $\mathbf{b}$. This value of $\mathbf{b}$ will be a function of $\tilde{p}_1$. We plug this value of $\mathbf{b}$ into the objective function of (3.18), thereby turning this function into a function of $\tilde{p}_1$ only. We then deal with solving a single-variable optimization problem. To further elaborate on this approach, we now focus on the inner minimization in (3.18).

3.3.2 Inner minimization in (3.18)

For *any given feasible value* of $\tilde{p}_1$, we rewrite this minimization as

$$\begin{aligned} \min_{\mathbf{b}}.\ & \mathbf{b}^H\left(\tilde{p}_1\mathbf{E}_0 + \sigma^2\mathbf{I}_{4n_r}\right)\mathbf{b} \\ \text{subject to}\ & \mathbf{b}^H(\tilde{p}_1\,\mathbf{E}_1\, - \sigma^2(\gamma_1+\gamma_2)\mathbf{E}_2\,)\,\mathbf{b} \geq \sigma^2(\gamma_1+\gamma_2) \\ & [\mathbf{b}]_{(i-1)n_r+2} = [\mathbf{b}]_{(i-1)n_r+3}\ \text{ for }\ i = 1, 2, \ldots, n_r. \end{aligned} \tag{3.22}$$

Using the following definitions:

$$\mathbf{T} \triangleq \begin{bmatrix} 1 & 0 & 0 \\ 0 & 1 & 0 \\ 0 & 1 & 0 \\ 0 & 0 & 1 \end{bmatrix}, \qquad \mathbf{L} \triangleq \mathbf{I}_{n_r} \otimes \mathbf{T} \tag{3.23}$$

we can write $\mathbf{b}_i = \mathbf{T}\,\tilde{\mathbf{b}}_i$, where $\tilde{\mathbf{b}}_i = [\,[\mathbf{b}_i]_1\ [\mathbf{b}_i]_2\ [\mathbf{b}_i]_4\,]^T$ is the vector of the free parameters in $\mathbf{b}_i$. We can further write $\mathbf{b} = \mathbf{L}\,\tilde{\mathbf{b}}$, where $\tilde{\mathbf{b}} = [\tilde{\mathbf{b}}_1^T\ \tilde{\mathbf{b}}_2^T\ \ldots\ \tilde{\mathbf{b}}_{n_r}^T]^T$. These definitions enable us to rewrite (3.22) as

$$\begin{aligned} \min_{\tilde{\mathbf{b}}}.\ & \tilde{\mathbf{b}}^H(\tilde{p}_1\tilde{\mathbf{E}}_0 + \sigma^2\mathbf{L}^H\mathbf{L})\tilde{\mathbf{b}} \\ \text{subject to}\ & \tilde{\mathbf{b}}^H(\tilde{p}_1\tilde{\mathbf{E}}_1 - \sigma^2(\gamma_1+\gamma_2)\tilde{\mathbf{E}}_2)\tilde{\mathbf{b}} \geq \sigma^2(\gamma_1+\gamma_2) \end{aligned} \tag{3.24}$$

where we further define: $\tilde{\mathbf{E}}_0 \triangleq \mathbf{L}^H\,\mathbf{E}_0\,\mathbf{L}$, $\tilde{\mathbf{E}}_1 \triangleq \mathbf{L}^H\,\mathbf{E}_1\,\mathbf{L}$, and $\tilde{\mathbf{E}}_2 \triangleq \mathbf{L}^H\,\mathbf{E}_2\,\mathbf{L}$.

We show in Appendix 3.B that the problem in (3.24) is feasible if and only if

$$\tilde{p}_1 > \frac{\sigma^2(\gamma_1+\gamma_2)}{\mathbf{q}_1^H\mathbf{q}_1}. \tag{3.25}$$

We now aim to solve the minimization problem in (3.24) for any feasible value of $\tilde{p}_1$ which satisfies (3.25). We note that under the feasibility condition in (3.25), this problem is a quadratic programming problem. Based on the fact that for any feasible $\tilde{p}_1$ at the optimum, the inequality constraint in (3.24) is satisfied with equality, and thus, we can use the method of Lagrangian multipliers to solve (3.24). As a result, the solution to (3.24), denoted by $\tilde{\mathbf{b}}^{\text{opt}}(\tilde{p}_1)$, is obtained as[6]

$$\tilde{\mathbf{b}}^{\text{opt}}(\tilde{p}_1) = \alpha \mathbf{u}(\tilde{p}_1). \tag{3.26}$$

Here, $\mathbf{u}(\tilde{p}_1) = \mathcal{P}\{\mathbf{S}(\tilde{p}_1)\}$ is the normalized principal eigenvector of the matrix[7]

$$\mathbf{S}(\tilde{p}_1) = (\tilde{p}_1\tilde{\mathbf{E}}_0 + \sigma^2\mathbf{L}^H\mathbf{L})^{-1}(\tilde{p}_1\tilde{\mathbf{E}}_1 - \sigma^2(\gamma_1+\gamma_2)\tilde{\mathbf{E}}_2) \tag{3.27}$$

and α is a scalar factor which guarantees that the constraint in (3.24) is satisfied with equality and is given as

$$\alpha = \left(\frac{\sigma^2(\gamma_1+\gamma_2)}{\mathbf{u}^H(\tilde{p}_1)(\tilde{p}_1\,\tilde{\mathbf{E}}_1 \; - \sigma^2(\gamma_1+\gamma_2)\tilde{\mathbf{E}}_2\;)\,\mathbf{u}(\tilde{p}_1)}\right)^{1/2}. \tag{3.28}$$

In the next subsection, we address the problem of optimally obtaining the parameter $\tilde{p}_1$.

3.3.3 Optimizing $\tilde{p}_1$

We can now rewrite the main problem in (3.18) as

$$\min_{\tilde{p}_1}.\;\; \tilde{p}_1 + \frac{\sigma^2(\gamma_1+\gamma_2)}{\lambda(\tilde{p}_1)} \quad \text{subject to} \quad \tilde{p}_1 > \frac{\sigma^2(\gamma_1+\gamma_2)}{\mathbf{q}_1^H\mathbf{q}_1} \tag{3.29}$$

where $\lambda(\tilde{p}_1) = \lambda_{max}\{\mathbf{S}(\tilde{p}_1)\}$ represents the principal eigenvalue of the matrix $\mathbf{S}(\tilde{p}_1)$.

Lemma 1 *The objective function in (3.29) has a unique extremum point in the interval* $(\frac{\sigma^2(\gamma_1+\gamma_2)}{\mathbf{q}_1^H\mathbf{q}_1}, +\infty)$*, which is the global minimum of this objective function.*

---

[6]Indeed, the optimization problem (3.24) is a quadratic programming problem and has a closed-form solution as in (3.26).

[7]From (3.23), we obtain

$$\mathbf{T}^T\mathbf{T} = \begin{bmatrix} 1 & 0 & 0 \\ 0 & 2 & 0 \\ 0 & 0 & 1 \end{bmatrix}, \qquad \mathbf{L}^T\mathbf{L} = \mathbf{I}_{n_r} \otimes \mathbf{T}^T\mathbf{T}.$$

Note that $\mathbf{L}^T\mathbf{L}$ is a block diagonal matrix of full-rank matrices $\mathbf{T}^T\mathbf{T}$. Hence, $(\tilde{p}_1\tilde{\mathbf{E}}_0 + \sigma^2\mathbf{L}^T\,\mathbf{L})$ is a full-rank matrix and thus invertible.

Proof See Appendix 3.C. ■

The unique solution to (3.29) can be obtained by equating the derivative of the objective function in (3.29) to zero. Denoting the objective function in (3.29) as $\psi(\tilde{p}_1)$, we show in Appendix 3.D that derivative of $\psi(\tilde{p}_1)$ with respect to $\tilde{p}_1$ is given by

$$\begin{aligned} g(\tilde{p}_1) \triangleq \frac{\partial \psi(\tilde{p}_1)}{\partial \tilde{p}_1} &= 1 - \sigma^2(\gamma_1+\gamma_2)\frac{\frac{\partial}{\partial \tilde{p}_1}\lambda(\tilde{p}_1)}{\lambda^2(\tilde{p}_1)} \\ &= 1 - \sigma^2(\gamma_1+\gamma_2)\frac{\tilde{p}_1^{-2} - \lambda(\tilde{p}_1)\tilde{\mathbf{f}}^H\mathbf{A}^{-1}(\tilde{p}_1)\tilde{\mathbf{E}}_0\mathbf{A}^{-1}(\tilde{p}_1)\tilde{\mathbf{f}}}{\lambda^2(\tilde{p}_1)\tilde{\mathbf{f}}^H\mathbf{A}^{-1}(\tilde{p}_1)(\tilde{p}_1\tilde{\mathbf{E}}_0+\sigma^2\mathbf{L}^T\mathbf{L})\mathbf{A}^{-1}(\tilde{p}_1)\tilde{\mathbf{f}}}. \end{aligned} \tag{3.30}$$

Here, the following definitions are used:

$$\mathbf{A}(\tilde{p}_1) \triangleq \sigma^2(\gamma_1+\gamma_2)\tilde{\mathbf{E}}_2 + \lambda(\tilde{p}_1)(\tilde{p}_1\tilde{\mathbf{E}}_0 + \sigma^2\mathbf{L}^T\,\mathbf{L}) \tag{3.31}$$

$$\tilde{\mathbf{f}} \triangleq \mathbf{L}^H\mathbf{f}\,, \tag{3.32}$$

and $\lambda(\tilde{p}_1)$ is the *largest eigenvalue* of the matrix $\mathbf{S}(\tilde{p}_1)$, and can be obtained, for any feasible value of $\tilde{p}_1$, as the *provably unique positive solution* to the following equation:

$$\tilde{p}_1\tilde{\mathbf{f}}^H\Big(\sigma^2(\gamma_1+\gamma_2)\tilde{\mathbf{E}}_2+\lambda(\tilde{p}_1)(\tilde{p}_1\tilde{\mathbf{E}}_0+\sigma^2\mathbf{L}^T\mathbf{L})\Big)^{-1}\tilde{\mathbf{f}}=1. \tag{3.33}$$

This unique solution can be obtained using a simple Newton-Raphson method or a bisection method. Once $\lambda(\tilde{p}_1)$ is obtained, the corresponding value of $g(\tilde{p}_1)$ can be obtained and thus the equation $g(\tilde{p}_1) = 0$ can be solved using another bisection method, thereby the optimum value of $\tilde{p}_1$ can be obtained. Denoting the so-obtained optimal value of $\tilde{p}_1$ as $\tilde{p}_1^{\mathrm{o}}$, we can use (3.26) to obtain $\tilde{\mathbf{b}}^{\mathrm{opt}}(\tilde{p}_1^{\mathrm{o}})$. The optimal value of $\mathbf{b}$ can then be calculated as $\mathbf{b}^{\mathrm{opt}} = [\mathbf{b}_1^T\ \mathbf{b}_2^T\ \ldots\ \mathbf{b}_{n_r}^T]^T = \mathbf{L}\tilde{\mathbf{b}}^{\mathrm{opt}}(\tilde{p}_1^{\mathrm{o}})$. Reshaping $\mathbf{b}_i$ yields the optimal value of $\mathbf{B}_i$ and finally the optimal value of $\mathbf{A}_i$ can be obtained from $\mathbf{A}_i = \mathbf{U}_i^*\mathbf{B}_i\mathbf{U}_i^H$. One can then use the so-obtained $\mathbf{A}_i$ in (3.11) to obtain the transceivers' transmit powers in closed-forms.

The proposed technique is summarized as in Algorithm 3.3.3.

Algorithm 1 Based on bisection Method

1. Calculate $\mathbf{E}_0 = \text{blkdiag}\left(\{\mathbf{I}_2 \otimes \mathbf{q}_{1i}\mathbf{q}_{1i}^H\}_{i=1)}^{n_r}\right)$ and $\mathbf{E}_2 = \text{blkdiag}\left(\{\mathbf{q}_{2i}\,\mathbf{q}_{2i}^H \otimes \mathbf{I}_2\}_{i=1}^{n_r}\right)$ as well as $\mathbf{L} = \mathbf{I}_{n_r} \otimes \mathbf{T}$, where $\mathbf{T} = \begin{bmatrix} 1 & 0 & 0 \\ 0 & 1 & 0 \\ 0 & 1 & 0 \\ 0 & 0 & 1 \end{bmatrix}$.
   Then, calculate $\tilde{\mathbf{E}}_0 = \mathbf{L}^H\,\mathbf{E}_0\,\mathbf{L}$, $\tilde{\mathbf{E}}_2 = \mathbf{L}^H\,\mathbf{E}_2\,\mathbf{L}$, and $\tilde{\mathbf{f}} = \mathbf{L}^H\mathbf{f}$ where the vector $\mathbf{f}$ is obtained as

$$\mathbf{f} = [(vec(\mathbf{q}_{11}\mathbf{q}_{21}^T))^T \quad (vec(\mathbf{q}_{12}\mathbf{q}_{22}^T))^T \quad \cdots \quad (vec(\mathbf{q}_{1n_r}\mathbf{q}_{2n_r}^T))^T]^T.$$

2. For any value of $z \in (\frac{\sigma^2(\gamma_1+\gamma_2)}{\mathbf{q}_1^H\mathbf{q}_1}, +\infty)$, define function $g(\cdot)$ as

$$g(z) = 1 - \sigma^2(\gamma_1+\gamma_2)\frac{z^{-2} - \lambda(z)\mathbf{u}^H(z)\tilde{\mathbf{E}}_0\mathbf{u}(z)}{\lambda^2(z)\mathbf{u}^H(z)(z\tilde{\mathbf{E}}_0 + \sigma^2\mathbf{L}^T\,\mathbf{L})\mathbf{u}(z)}.$$

   Here, for any value of $z \in (\frac{\sigma^2(\gamma_1+\gamma_2)}{\mathbf{q}_1^H\mathbf{q}_1}, +\infty)$, the value of $\lambda(z)$ is obtained, using a bisection method, as the provably unique positive solution to the following non-linear equation:

$$z\mathbf{f}^H(\sigma^2(\gamma_1+\gamma_2)\tilde{\mathbf{E}}_2 + \lambda(z)(z\tilde{\mathbf{E}}_0 + \sigma^2\mathbf{L}^H\mathbf{L}))^{-1}\mathbf{f} - 1 = 0$$

   and for any value of z, the $3n_r \times 1$ vector $\mathbf{u}(z)$ is obtained as

$$\mathbf{u}(z) = (\sigma^2(\gamma_1+\gamma_2)\tilde{\mathbf{E}}_2 + \lambda(z)(z\tilde{\mathbf{E}}_0 + \sigma^2\mathbf{L}^T\mathbf{L}))^{-1}\tilde{\mathbf{f}}$$

3. To solve $g(z) = 0$ in the interval $z \in (\frac{\sigma^2(\gamma_1+\gamma_2)}{\mathbf{q}_1^H\mathbf{q}_1}, +\infty)$, using a bisection method, choose z_l as

$$z_l = \frac{\sigma^2(\gamma_1+\gamma_2)}{\mathbf{q}_1^H\mathbf{q}_1} + \epsilon_1$$

   where ϵ_1 is an arbitrarily small positive number such that $g(z_l) < 0$. Also, choose z_u large enough such that $g(z_u) > 0$.

4. Choose ϵ_2 to be an arbitrarily small positive number.

5. Choose $z = (z_l + z_u)/2$.

6. If $|g(z)| < \epsilon_2$, go to Step 7. If $g(z) < -\epsilon_2$, then $z_l = z$. If $g(z) > \epsilon_2$, then $z_u = z$. Go to Step 5.

7. Set $\tilde{p}_1^{\text{o}}$ equal to z and use a bisection technique to obtain the optimal value of λ, denoted as λ^{o}, as the unique positive solution to the following non-linear equation:

$$\tilde{p}_1^{\text{o}}\tilde{\mathbf{f}}^H(\sigma^2(\gamma_1+\gamma_2)\tilde{\mathbf{E}}_2+\lambda(\tilde{p}_1^{\text{o}}\tilde{\mathbf{E}}_0+\sigma^2\mathbf{L}^H\mathbf{L}))^{-1}\tilde{\mathbf{f}}-1=0.$$

8. Calculate the total transmitter power, denoted as P_T, consumed in the entire network as

$$P_T=\tilde{p}_1^{\text{o}}+\frac{\sigma^2(\gamma_1+\gamma_2)}{\lambda^{\text{o}}}$$

9. Obtain $\tilde{\mathbf{b}}^{\text{opt}}(\tilde{p}_1)=[\tilde{\mathbf{b}}_1^T\ \ \tilde{\mathbf{b}}_2^T\ \ \cdots\ \ \tilde{\mathbf{b}}_{n_r}^T]^T$ as

$$\tilde{\mathbf{b}}^{\text{opt}}(\tilde{p}_1)=\kappa\ \underbrace{(\sigma^2(\gamma_1+\gamma_2)\tilde{\mathbf{E}}_2+\lambda^{\text{o}}(\tilde{p}_1^{\text{o}}\tilde{\mathbf{E}}_0+\sigma^2\mathbf{L}^H\mathbf{L}))^{-1}\tilde{\mathbf{f}}}_{\mathbf{u}(\tilde{p}_1)}$$

where κ is obtained as

$$\kappa=\sqrt{\frac{\sigma^2(\gamma_1+\gamma_2)}{\lambda^{\text{o}}\mathbf{u}^H(\tilde{p}_1)(\tilde{p}_1\tilde{\mathbf{E}}_1+\sigma^2\mathbf{L}^H\mathbf{L})\mathbf{u}(\tilde{p}_1)}}\,.$$

10. Calculate $\mathbf{b}^{\text{opt}}=[\mathbf{b}_1^T\ \mathbf{b}_2^T\ ...\ \mathbf{b}_{n_r}^T]^T=\mathbf{L}\tilde{\mathbf{b}}^{\text{opt}}(\tilde{p}_1^{\text{o}})$.

11. Reshape $\mathbf{b}_i$ to obtain the optimal value of the effective beamforming matrix $\mathbf{B}_i$ of the i-th relay, and finally, obtain the optimal value of the beamforming matrix of the i-th relay as $\mathbf{A}_i=\mathbf{U}_i^*\mathbf{B}_i\mathbf{U}_i^H$.

12. Use the so-obtained beamforming matrices to obtain the optimal values of the transceivers transmit powers in closed-forms as:

$$p_1=\frac{\sigma^2\gamma_2\left(1+\sum_{i=1}^{n_r}\|\mathbf{h}_{2i}^T\mathbf{A}_i\|^2\right)}{\left|\sum_{i=1}^{n_r}\mathbf{h}_{2i}^T\mathbf{A}_i\ \mathbf{h}_{1i}\right|^2},\qquad p_2=\frac{\sigma^2\gamma_1\left(1+\sum_{i=1}^{n_r}\|\mathbf{h}_{1i}^T\mathbf{A}_l\|^2\right)}{\left|\sum_{i=1}^{n_r}\mathbf{h}_{1i}^T\mathbf{A}_i\ \mathbf{h}_{2i}\right|^2}.$$

3.4 Power Minimization with General Beamforming Matrices

In this section, we present the solution to the power minimization problem for the case when the beamforming matrices are not constrained to be symmetric. The solution to this case can then be used to evaluate the performance of the power minimization problem with symmetric beamforming matrices. To develop the solution to the case of general beamforming matrices, we rely on the pioneer results of [29], which considers a three-node two-way relay network and minimizes the transmit power consumed in a single multi-antenna relay subject to SNR constraints at two single-antenna transceivers. Note however that the authors of [29] assume that the transceivers' transmit powers are fixed, while in our work, these powers are part of the design parameters. Nevertheless, the technique of [29] can be combined with a two-dimensional search over the plane of (p_1, p_2) to find the optimal values of transceivers' transmit powers. In this section, we briefly review the technique of [29], while extending this technique to allow the optimization of transceivers' transmit powers.

Using (3.13), we can write the optimization problem (3.10) as

$$\begin{aligned} &\min_{p_1,p_2,\{\mathbf{B}_i\}_{i=1}^{n_r}} \sum_{j=1}^{2} p_j \left(1 + \sum_{i=1}^{n_r} \|\mathbf{B}_i \mathbf{q}_{ji}\|^2\right) + \sigma^2 \sum_{i=1}^{n_r} tr(\mathbf{B}_i \mathbf{B}_i^H) \\ &\text{subject to} \quad \frac{p_j \left| \sum_{i=1}^{n_r} \mathbf{q}_{\bar{j}i}^T \mathbf{B}_i \ \mathbf{q}_{ji} \right|^2}{\sigma^2 \left(1 + \sum_{i=1}^{n_r} \|\mathbf{q}_{\bar{j}i}^T \mathbf{B}_i\|^2\right)} \geq \gamma_{\bar{j}}, \quad j \in \{1, 2\} \end{aligned} \tag{3.34}$$

where $\mathbf{q}_{1i} = \mathbf{U}_i^H \mathbf{h}_{1i}$ and $\mathbf{q}_{2i} = \mathbf{U}_i^H \mathbf{h}_{2i}$ are defined as the effective channels between the i-th relay and Transceivers 1 and 2, respectively. Also we can rewrite the norms in problem (3.34) as $\|\mathbf{B}_i \, \mathbf{q}_{ji}\|^2 = \mathbf{b}_i^H (\mathbf{I}_2 \otimes (\mathbf{q}_{ji}^* \, \mathbf{q}_{ji}^T)) \mathbf{b}_i$, $\|\mathbf{q}_{\bar{j}i}^T \mathbf{B}_i\|^2 = \mathbf{b}_i^H ((\mathbf{q}_{\bar{j}i}^* \, \mathbf{q}_{\bar{j}i}^T) \otimes \mathbf{I}_2) \mathbf{b}_i$, and $tr(\mathbf{B}_i \mathbf{B}_i^H) = \mathbf{b}_i^H \mathbf{b}_i$, where we use the following definition: $\mathbf{b}_i \triangleq (vec(\mathbf{B}_i^T))^*$. Further, defining

$$\breve{\mathbf{f}} \triangleq [vec^T(\mathbf{q}_{21} \, \mathbf{q}_{11}^T) \cdots vec^T(\mathbf{q}_{2n_r} \, \mathbf{q}_{1n_r}^T)]^T$$

we can write

$$\left|\sum_{i=1}^{n_r} \mathbf{q}_{1i}^T \mathbf{B}_i \, \mathbf{q}_{2i}\right|^2 = \mathbf{b}^H \breve{\mathbf{f}} \breve{\mathbf{f}}^H \mathbf{b}.$$

The optimization problem (3.34) can now be recast as

$$\begin{aligned}
\min_{p_1, p_2, \mathbf{b}} \quad & p_1 + p_2 + \mathbf{b}^H \left(p_1 \mathbf{E}_0 + p_2 \breve{\mathbf{E}}_0 + \sigma^2 \mathbf{I}_{4n_r} \right) \mathbf{b} \\
\text{subject to} \quad & \mathbf{b}^H \left(p_2 \, \breve{\mathbf{E}}_1 \, - \sigma^2 \gamma_1 \breve{\mathbf{E}}_2 \, \right) \mathbf{b} \geq \sigma^2 \gamma_1 \\
& \mathbf{b}^H \left(p_1 \, \mathbf{E}_1 \, - \sigma^2 \gamma_2 \mathbf{E}_2 \, \right) \mathbf{b} \geq \sigma^2 \gamma_2
\end{aligned} \tag{3.35}$$

where the following definitions are used:

$$\breve{\mathbf{E}}_0 \triangleq \text{blkdiag}\Big(\{ \mathbf{I}_4 \otimes \mathbf{q}_{2i} \mathbf{q}_{2i}^H \}_{i=1}^{n_r} \Big),$$

$$\breve{\mathbf{E}}_1 \triangleq \breve{\mathbf{f}} \breve{\mathbf{f}}^H,$$

$$\breve{\mathbf{E}}_2 \triangleq \text{blkdiag}\Big(\{ \mathbf{q}_{1i} \, \mathbf{q}_{1i}^H \otimes \mathbf{I}_4 \}_{i=1}^{n_r} \Big).$$

The optimization problem (3.35) does not seem to be amenable to a closed-form solution. We can solve the problem by finding the optimal value for $\mathbf{b}$ for any given transceiver powers, p_1 and p_2, and then find the optimal values for p_1 and p_2 by finding those values of p_1 and p_2 which yield the smallest value for the objective function. For given values of p_1 and p_2, the minimization over $\mathbf{b}$ can be written as a quadratically constrained quadratic problem (QCQP). If the feasible region in (p_1, p_2) plane is quantized into a sufficiently fine grid, we can obtain the optimal value of $\mathbf{b}$ corresponding to each vertex of this grid. We then choose, as the solution to the problem, the values of p_1, p_2, and the corresponding value of $\mathbf{b}$, which lead to the minimum value of the objective function.

To solve the minimization over $\mathbf{b}$ for any given pair of p_1 and p_2, we need to determine the set of feasible values of p_1 and p_2. One can see from the constraint in (3.35) that for those values of p_1 that make the matrix $(p_1 \, \mathbf{E}_1 \, - \sigma^2 \gamma_2 \mathbf{E}_2)$ negative semi-definite, the problem becomes infeasible. Similar condition holds true for p_2 in matrix $(p_2 \, \breve{\mathbf{E}}_1 \, - \sigma^2 \gamma_2 \breve{\mathbf{E}}_2)$. Hence, the infeasibility conditions can be written as

$$p_1 \mathbf{E}_1 - \sigma^2 \gamma_2 \mathbf{E}_2 \preccurlyeq 0, \qquad p_2 \breve{\mathbf{E}}_1 - \sigma^2 \gamma_1 \breve{\mathbf{E}}_2 \preccurlyeq 0, \tag{3.36}$$

where the notation $\mathbf{Z} \preccurlyeq 0$ means that matrix $\mathbf{Z}$ is negative semi-definite. These conditions mean that the minimum values of p_1 and p_2 that make the problem feasible are those for which the largest eigenvalues of the matrices in (3.36) are greater than zero. It can be shown that the feasible values of p_1 and p_2 must satisfy

$$p_1 > \frac{\sigma^2\gamma_2}{\mathbf{q}_1^H\mathbf{q}_1}, \quad \text{and} \quad p_2 > \frac{\sigma^2\gamma_1}{\mathbf{q}_2^H\mathbf{q}_2}. \tag{3.37}$$

where $\mathbf{q}_1 \triangleq [\mathbf{q}_{11}^T, \mathbf{q}_{12}^T, ..., \mathbf{q}_{1n_r}^T]^T$, and $\mathbf{q}_2 \triangleq [\mathbf{q}_{21}^T, \mathbf{q}_{22}^T, ..., \mathbf{q}_{2n_r}^T]^T$. Hence, we need to start the exhaustive search over the values of p_1 and p_2 which satisfy (3.37) . Let us consider the inner part of the minimization problem in (3.35) as

$$\begin{aligned} \min_{\mathbf{b}}. \quad & \mathbf{b}^H \left(p_1\mathbf{E}_0 + p_2\breve{\mathbf{E}}_0 + \sigma^2\mathbf{I}_{4n_r}\right)\mathbf{b} \\ \text{subject to} \quad & \mathbf{b}^H \left(p_2\breve{\mathbf{E}}_1 - \sigma^2\gamma_1\breve{\mathbf{E}}_2\right)\mathbf{b} \geq \sigma^2\gamma_1 \\ & \mathbf{b}^H \left(p_1\mathbf{E}_1 - \sigma^2\gamma_2\mathbf{E}_2\right)\mathbf{b} \geq \sigma^2\gamma_2 \end{aligned} \tag{3.38}$$

Once a feasible pair of p_1 and p_2 is chosen, we can solve the minimization problem in (3.38), as explained in the sequel. Using the following definitions

$$\mathbf{G}_0 \triangleq (p_1\mathbf{E}_0 + p_2\breve{\mathbf{E}}_0 + \sigma^2\mathbf{I}_{4n_r}) \quad \mathbf{G}_1 \triangleq \frac{p_1}{\sigma^2\gamma_2}\mathbf{E}_1 - \mathbf{E}_2, \quad \mathbf{G}_2 \triangleq \frac{p_2}{\sigma^2\gamma_1}\breve{\mathbf{E}}_1 - \breve{\mathbf{E}}_2 \tag{3.39}$$

we can solve the problem using standard semi-definite program (SDP) tools [124]. Defining $\mathbf{X} \triangleq \mathbf{b}\mathbf{b}^H$, we can rewrite the problem in (3.38) as

$$\begin{aligned} \min_{\mathbf{X}}. \quad & tr(\mathbf{G}_0\mathbf{X}) \\ \text{subject to} \quad & tr(\mathbf{G}_1\mathbf{X}) \geq 1,\, tr(\mathbf{G}_2\mathbf{X}) \geq 1,\, \text{rank}(\mathbf{X}) = 1, \mathbf{X} \succcurlyeq 0 \end{aligned} \tag{3.40}$$

Due to the rank-one constraint, this problem is not convex but we can exploit a semi-definite relaxation (SDR) method to solve this problem [29]. Interestingly enough, despite the relaxation, a rank-one solution to (3.40) exists and it can be extracted from the relaxed problem (for detailed procedure, refer to [125–127]). This rank-one solution for $\mathbf{X}$ yields the optimal $\mathbf{b}$ for the problem in (3.38) for the chosen p_1 and p_2.

3.5 Remarks

The following remarks are in order.

Remark 1: In terms of computational complexity, the proposed symmetric beamforming technique involves finding the root of $g(\tilde{p}_1)$ using a simple bisection technique. In each iteration of this bisection technique, one has to find the unique positive root of (3.33) for a given value of $\tilde{p}_1$ using another simple bisection technique, thereby obtaining $\lambda(\tilde{p}_1)$. Both of these bisection methods converge very fast [128]. Considering that the number of iterations in these two bisection methods are insensitive to the problem size [128], the computational complexity of calculating $g(\tilde{p}_1)$ and $\lambda(\tilde{p}_1)$ is $\mathcal{O}(n_r)$. On the other hand, the general beamforming matrix based method involves solving an SDP problem at each vertex of the grid which covers the (p_1, p_2) plane. The computational complexity of solving an SDP problem at each of these vertices is $\mathcal{O}(n_r^6)$. Taking into account that the SDP problem has to be solved over all vertices, the computational complexity of the proposed algorithm is significantly lower than the SDP based solution. Indeed, the computational complexity of the combination of the SDP based technique and the exhaustive search method is prohibitively high, thereby justifying the use of the proposed method. In the next section, our numerical examples show that the performance loss caused by imposing symmetry on the relay beamforming matrices is negligible.

Remark 2: It is worth mentioning that the proposed scheme can be implemented in a distributed manner. To further explain this, the optimization problem (3.15) can be rewritten as

$$\begin{aligned} \min_{\mathbf{b}}. \quad & \frac{\sigma^2(\gamma_1+\gamma_2)\left(1+\mathbf{b}^H\mathbf{E}_2\mathbf{b}\right)\left(1+\mathbf{b}^H\mathbf{E}_0\mathbf{b}\right)}{\mathbf{b}^H\mathbf{f}\,\mathbf{f}^H\mathbf{b}} + \sigma^2\mathbf{b}^H\mathbf{b} \\ \text{subject to} \quad & [\mathbf{b}]_{(i-1)n_r+2} = [\mathbf{b}]_{(i-1)n_r+3}, \text{ for } i = 1, 2, \ldots, n_r. \end{aligned} \tag{3.41}$$

or, equivalently, as

$$\min_{\tilde{\mathbf{b}}}. \frac{\sigma^2(\gamma_1+\gamma_2)(1+\tilde{\mathbf{b}}^H\tilde{\mathbf{E}}_2\tilde{\mathbf{b}})(1+\tilde{\mathbf{b}}^H\tilde{\mathbf{E}}_0\tilde{\mathbf{b}})}{\tilde{\mathbf{b}}^H\tilde{\mathbf{f}}\,\tilde{\mathbf{f}}^H\tilde{\mathbf{b}}} + \sigma^2\tilde{\mathbf{b}}^H\mathbf{L}^H\mathbf{L}\tilde{\mathbf{b}}. \tag{3.42}$$

Differentiating the objective function of (3.42) with respect to $\tilde{p}_1$ and equating it to zero yields

$$\frac{1}{(\tilde{\mathbf{b}}^H \tilde{\mathbf{f}})} \tilde{\mathbf{f}} = \mathbf{Q}(\tilde{\mathbf{b}})\, \tilde{\mathbf{b}} \tag{3.43}$$

where the following definition is used:

$$\mathbf{Q}(\tilde{\mathbf{b}}) \triangleq \frac{\tilde{\mathbf{E}}_2}{(1+\tilde{\mathbf{b}}^H\, \tilde{\mathbf{E}}_2\, \tilde{\mathbf{b}})} + \frac{\tilde{\mathbf{E}}_0}{(1+\tilde{\mathbf{b}}^H\, \tilde{\mathbf{E}}_0\, \tilde{\mathbf{b}})} + \frac{1}{(\gamma_1+\gamma_2)}\, \frac{\mathbf{L}^H\mathbf{L}\, (\tilde{\mathbf{b}}^H \tilde{\mathbf{f}}\, \tilde{\mathbf{f}}^H \tilde{\mathbf{b}})}{(1+\tilde{\mathbf{b}}^H\, \tilde{\mathbf{E}}_2\, \tilde{\mathbf{b}})(1+\tilde{\mathbf{b}}^H\, \tilde{\mathbf{E}}_0\, \tilde{\mathbf{b}})}. \tag{3.44}$$

Further, defining $\mu_0 \triangleq (1+\tilde{\mathbf{b}}^H\, \tilde{\mathbf{E}}_0\, \tilde{\mathbf{b}})$, $\mu_2 \triangleq (1+\tilde{\mathbf{b}}^H\, \tilde{\mathbf{E}}_2\, \tilde{\mathbf{b}})$, and $\mu_1 \triangleq \tilde{\mathbf{b}}^H \tilde{\mathbf{f}}$, we can rewrite (3.43) as

$$\mu_0\, \mu_2\, \tilde{\mathbf{f}} = \left(\mu_0 \tilde{\mathbf{E}}_2 + \mu_2 \tilde{\mathbf{E}}_0 + \frac{|\mu_1|^2}{(\gamma_1+\gamma_2)}\, \mathbf{L}^H\mathbf{L} \right) \mu_1 \tilde{\mathbf{b}}\,. \tag{3.45}$$

Since the matrix $\left(\mu_0 \tilde{\mathbf{E}}_2 + \mu_2 \tilde{\mathbf{E}}_0 + \frac{|\mu_1|^2}{(\gamma_1+\gamma_2)}\, \mathbf{L}^H\mathbf{L} \right)$ is invertible, we can obtain $\tilde{\mathbf{b}}$ as

$$\tilde{\mathbf{b}} = \frac{\mu_0\, \mu_2}{\mu_1} \left(\mu_0 \tilde{\mathbf{E}}_2 + \mu_2 \tilde{\mathbf{E}}_0 + \frac{|\mu_1|^2}{(\gamma_1+\gamma_2)}\, \mathbf{L}^H\mathbf{L} \right)^{-1} \tilde{\mathbf{f}}. \tag{3.46}$$

The fact that matrices $\tilde{\mathbf{E}}_0$, $\tilde{\mathbf{E}}_2$, and $\mathbf{L}^H\mathbf{L}$ are all block-diagonal matrices allows us to use (3.46) and write the optimal value of $\tilde{\mathbf{b}}_i$ for the i-th relay as

$$\tilde{\mathbf{b}}_i = \frac{\mu_0 \mu_2}{\mu_1} \left(\mu_0 (\tilde{\mathbf{E}}_2)_{(i)} + \mu_2 (\tilde{\mathbf{E}}_0)_{(i)} + \frac{|\mu_1|^2}{(\gamma_1+\gamma_2)} (\mathbf{L}^H\mathbf{L})_{(i)} \right)^{-1} \tilde{\mathbf{f}}_i \tag{3.47}$$

where $(\tilde{\mathbf{E}}_2)_{(i)}$, $(\tilde{\mathbf{E}}_0)_{(i)}$, and $(\mathbf{L}^H\mathbf{L})_{(i)}$ are the i-th diagonal blocks of $\tilde{\mathbf{E}}_2$, $\tilde{\mathbf{E}}_0$, and $\mathbf{L}^H\mathbf{L}$, respectively. If one of the two transceivers broadcasts the three parameters μ_0, μ_1, and μ_2, the i-th relay can then use (3.47) to obtain its $\tilde{\mathbf{b}}_i$ vector from its local CSI. Indeed, the matrices $(\tilde{\mathbf{E}}_2)_{(i)}$, $(\tilde{\mathbf{E}}_0)_{(i)}$, and $(\mathbf{L}^H\mathbf{L})_{(i)}$ depend only on the local CSI of the i-th relay.

In terms of CSI acquisition, two scenarios can be implemented: 1) Due to the bidirectional nature of the communication, each transceiver (user device) can obtain all the channel coefficients through training, see for example [129–138]. Both transceivers can then obtain the parameter $\tilde{p}_1$ and consequently, calculate the vectorized version of the beamforming matrices as in (3.26), and find the transceivers' transmit powers from (3.11). One of the transceivers can then calculate the parameters μ_0, μ_1, and μ_2 and broadcast these parameters to all relays. Each relay can use these three parameters along with its local CSI as in (3.47) to obtain the vectorized version of its effective beamforming matrix. 2) In the second scenario, all relays (base stations) provide their CSI (which can be acquired using traditional training procedures) to one of the relays (main relay or main base station) through a back haul link (for example through an optical fiber link). The main relay can then use the global CSI to calculate the parameter $\tilde{p}_1$, and consequently, the vectorized version of the beamforming matrices as in (3.26), as well as the parameters μ_0, μ_1, and μ_2, and broadcast these parameters to other relays. Each relay can then use these three parameters along with its local CSI as in (3.47) to obtain the vectorized version of its effective beamforming matrix.

Remark 3: Note that the total power minimization approach utilized in this study does not rely on individual per node power constraint. Adding such constraints can lead to the increase in the total power consumed in the entire network. As a result, it is recommended that the nodes hardware be designed to allow a relatively high amount of power consumption. Note also that it is reasonable to assume that the relay channel vectors are drawn from the same probability distribution function, and as a result, the long-term average transmit power of different relays will be the same. This is indeed what the numerical results of [27] showed for the case of two-way networks with multiple single-antenna relays.

Remark 4: It is also noteworthy that the relay beamforming matrices $\{\mathbf{A}_i\}_{i=1}^{n_r}$ can be written in terms of maximum ratio combining (MRC) and maximum ratio transmission (MRT) schemes. To show this, one can write $\mathbf{U}_i = [\mathbf{h}_{1i} \;\; \mathbf{h}_{2i}]\mathbf{W}_i$, where $\mathbf{W}_i$ is a 2×2 invertible matrix. As a result, using (3.13), the relay beamforming matrix can be written as $\mathbf{A}_i = [\mathbf{h}_{1i}^* \;\; \mathbf{h}_{2i}^*]\mathbf{W}_i^*\mathbf{B}_i\mathbf{W}_i^H[\mathbf{h}_{1i} \;\; \mathbf{h}_{2i}]^H$. Hence, the relay beamforming operation can be viewed as a cascade of an MRC operation, a multiplication of the MRC output with the matrix $\mathbf{W}_i^*\mathbf{B}_i\mathbf{W}_i^H$, and eventually an MRT scheme.

For very large M, i.e, in massive MIMO relaying schemes, where $\mathbf{h}_{1i}$ and $\mathbf{h}_{2i}$ are orthogonal, almost surely, one can easily show that at the optimum, matrix $\mathbf{C}_i \triangleq \mathbf{W}_i^* \mathbf{B}_i \mathbf{W}_i^H$ is anti-diagonal i.e., has zero diagonal entries. This means that self-interference will be zero. In this case, one still has to optimally obtain the two off-diagonal entries of matrix $\mathbf{C}_i$, To do so, one can show that we still need the same amount of CSI. The details of the derivations do not fit in the scope of this study and we leave these details to future studies.

Remark 5: In this study, we considered the network beamforming problem for a single-pair of transceivers. Designing network beamforming schemes to simultaneously establish communication between multiple pairs of transceivers in a peer-to-peer manner is yet another interesting problem. What we have done in this study can be useful when considering a multi-pair scneraio when the number of antennas at the relays is very large. The extension of results, here obtained for scenarios in this chapter, into a multi-pair scenario is studied in Chapter 5.

3.6 Simulation Results

In this section, we compare the performance of the proposed symmetric beamforming method, in terms of the total consumed power in the network, with the performance of the general beamforming method with no restriction on the beamforming matrices. We assume that the relays are randomly distributed between the two transceivers. Each transceiver-relay link is modeled as the product of three terms: a small-scale fading term (which is modeled as complex Gaussian random variables with zero mean and unit variance), a log-normal term with a standard deviation of 8 dB (which represents the shadowing effect), and a path loss component with a path loss exponent of 3.8. Also, the noise process in all nodes is assumed to be spatially white zero-mean Gaussian process with unit variance, i.e., $\sigma^2 = 1$.

Fig. 3.2 shows the average total transmit power, normalized to the noise power, versus equal SNR thresholds γ_1 for both the proposed symmetric beamforming

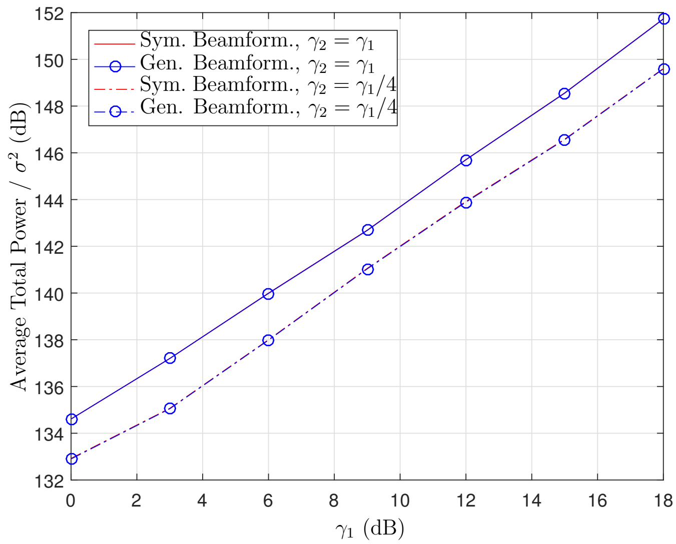

Figure 3.2: Average normalized total transmit power versus γ_1, for symmetric and general beamforming schemes, for $M = 4$ and $n_r = 4$.

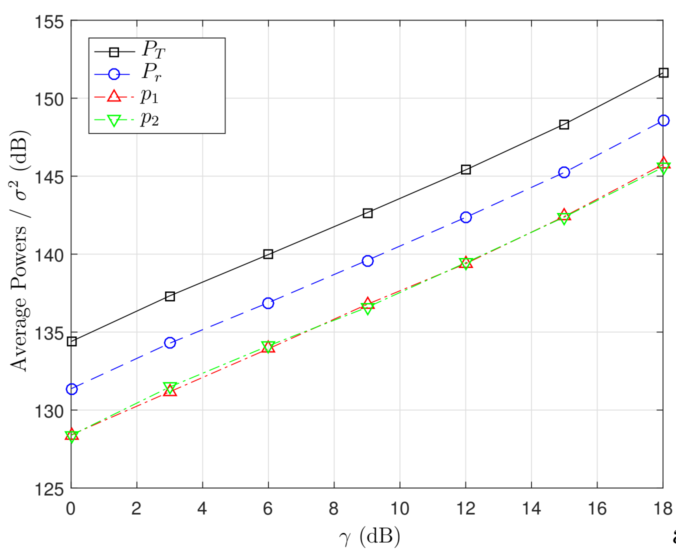

a

Figure 3.3: Average normalized total power, average normalized total relay power, and average normalized transceivers' transmit powers, versus $\gamma_1 = \gamma_2 = \gamma$, for $M = 4$ and $n_r = 4$.

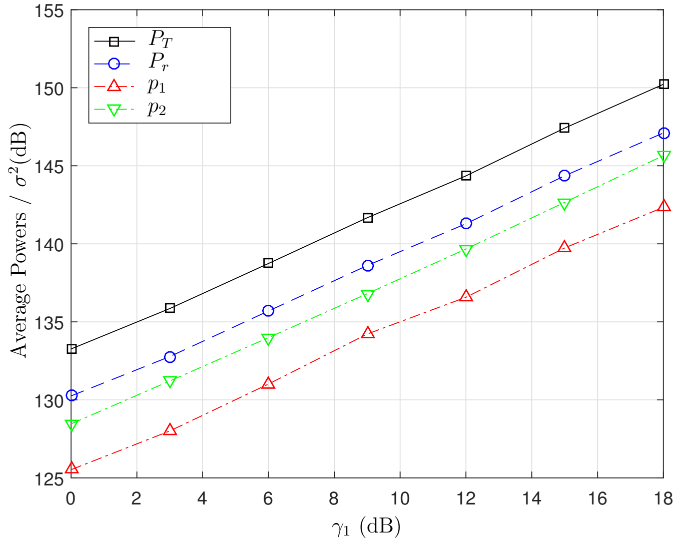

Figure 3.4: Average normalized total power, average normalized relay power, and average normalized transceivers' transmit powers, for non-equal SNR thresholds: $\gamma_2 = \gamma_1/2$, and for $M = 4$ and $n_r = 4$.

method and the general beamforming technique in two different scenarios, i) $\gamma_2 = \gamma_1$ and ii) $\gamma_2 = \gamma_1/4$. As can be seen from this figure, in both scenarios, the total power required for satisfying the SNR constraints in the network with symmetric beamforming matrices is very close to the total power for the same network with general beamforming matrices, while the computational complexity of the symmetric beamforming method is significantly lower than that of the general beamforming method. As a result, assuming symmetric beamforming matrices offers computational saving with negligible performance loss, compared to the case when the beamforming matrices are not restricted to be symmetric. In the remainder of our simulation results, we focus on the proposed symmetric beamforming method.

Fig. 3.3 illustrates the average normalized values of the total consumed power in the network, the average normalized total transmit power of the relays, and the average normalized transceivers' transmit powers, versus equal SNR thresholds, i.e., $\gamma_1 = \gamma_2 \triangleq \gamma$, for a network consisting two single-antenna transceivers and $n_r = 4$ relays each equipped with $M = 4$ antennas. As can be seen from this figure, the average total relay transmit power is 3 dB smaller than (i.e., half of) the average total transmit power consumed in the entire network. Although this figure shows averaged quantities, one can prove that *for any given set of channel realizations*, the total relay power is always half of the total transmit power consumed in the entire network, when $\gamma_1 = \gamma_2$. We can also observe from Fig. 3.3 that the average transmit power of each of the two transceivers are 6 dB lower than (or a quarter of) the average total transmit power. Note however that this observation is correct only for average quantities and it may not hold true for a given channel realizations.

Fig. 3.4 shows the same quantities as in Fig. 3.3 for the case when we choose $\gamma_2 = \gamma_1/2$. As can be observed from this figure, the average total relay transmit power is about half of the average total transmit power consumed in the entire network. Note however that this observation is true for average quantities and may not hold for all channel realizations.

Note that in this study, we did not consider per-node power constraints. Adding such constraints only shrinks the feasible set, and thus, increases the total power consumption. However, a guideline can be derived to choose the maximum average power consumption of each node. As shown in Fig. 3.3, under equal SNR thresholds, the power consumption of each of the two transceivers is $1/4$ of the total power consumed in the entire network. Also, as the total relay power is half of the total transmit power, if the relay-transceiver channels are drawn from the same probability distribution function, then each relay node consumes, in average, $1/(2n_r)$ of the total transmit power.

Fig. 3.5 illustrates the normalized average minimum total transmit power for different number of relays each of which is equipped with $M = 4$ antennas. Fig. 3.6 illustrates the normalized average minimum total transmit power when $n_r = 4$ relays are equipped with 4, 8, and 16 antennas. As can be seen from Fig. 3.5, doubling number of relays, while keeping the number of antennas per relays unchanged, reduces the average minimum total transmit power by 2.98 to 3.94 dB over the depicted range of γ. Fig. 3.6 shows that doubling the number of antennas per relays, while keeping the number of relays unchanged, will reduce the minimum total transmit power by 2.91

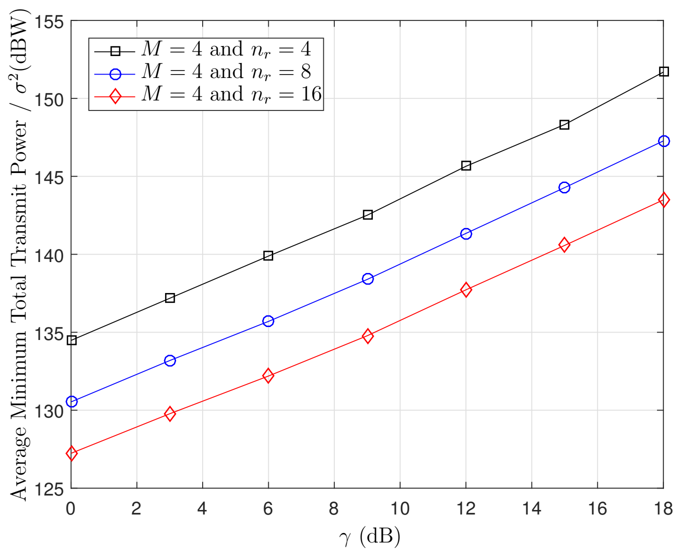

Figure 3.5: The average normalized total transmit power versus $\gamma_1 = \gamma_2 \triangleq \gamma$, for networks with different numbers of relays $n_r \in \{4, 8, 16\}$, and for $M = 4$.

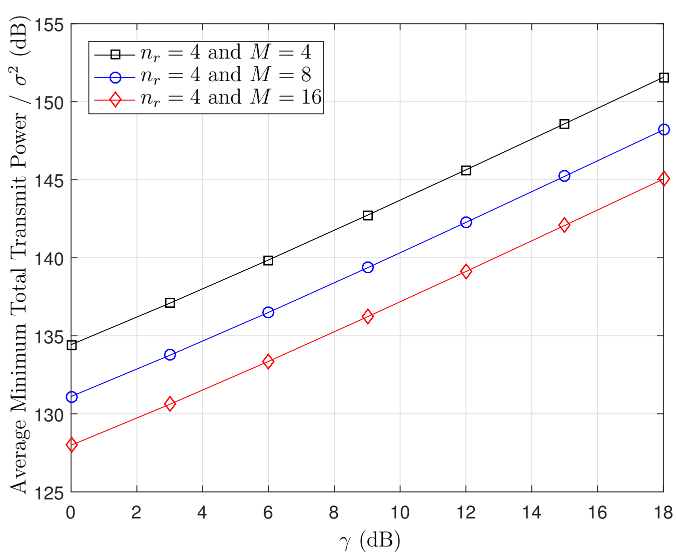

Figure 3.6: The normalized average minimum total transmit power, versus $\gamma_1 = \gamma_2 \triangleq \gamma$, for networks with $n_r = 4$, $M \in \{4, 8, 16\}$.

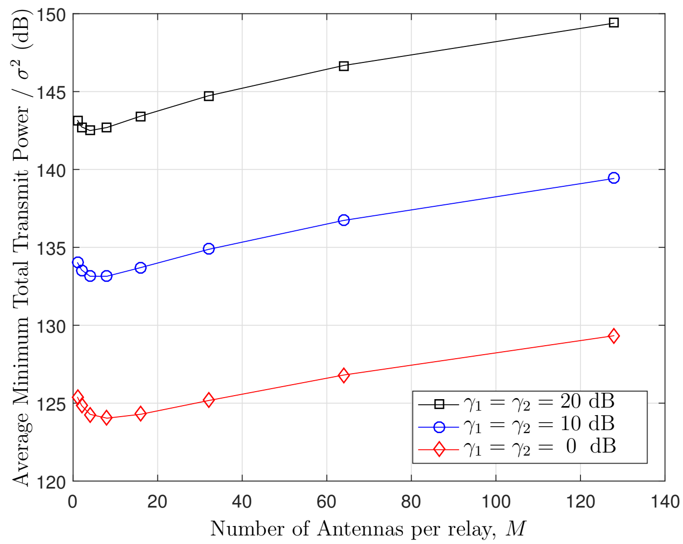

Figure 3.7: The normalized average minimum total transmit power versus number of antennas per relay M, for $Mn_r = 128$ and for different values of γ.

to 3.13 dB over the chosen range of γ.

In Fig. 3.7, we plot the normalized average minimum total transmit power versus M, when the total number of the relay antennas employed in the network is constant ($Mn_r = 128$), for different values of γ. Interestingly, we observe that when $\gamma = 0$ dB is chosen, the minimum power will be achieved when $n_r = 16$ relays, each with $M = 8$ are used. As γ is increased to 10 dB, the minimum power can still be achieved when $n_r = 16$ relays, each with $M = 8$ are employed, Further increasing γ to 20 dB shows that the scenario with $n_r = 32$ relays, each with $M = 4$ antennas results in the minimum power consumption. In other words, when the SNR requirements are more stringent, the network should become "more distributed". This observation shows that there exists a trade-off between local beamforming at the relays and network beamforming distributed in the entire network. For low SNR requirements, local beamforming appears to be power-optimal while for high SNR requirements, network beamforming tends to be power-efficient. The theoretical justification/analysis of this trade-off is certainly an interesting research direction but it does not fit in the scope of this study.

As shown in Fig. 3.5, for a *given number of antennas per relay*, increasing number of the relays consistently improves the performance of the proposed scheme. Also, Fig. 3.6 shows that *for a fixed number of relays*, increasing number of antennas per relay consistently improves the performance. However, *for a fixed number of total number of available antenna*, it appears from Fig. 3.7 that there exists an optimal number of antennas per relay, and thus an optimal number of relays, which lead to the best performance in terms of the total transmit power consumption. Finding the optimal number of relays and/or developing an optimal node selection strategy appears to be an interesting direction for future work on this topic.

Appendices

3.A Problem Dimensionality Reduction

Let us denote the $M \times 2$ unitary matrix that spans the vector space of $\mathbf{h}_{1i}$ and $\mathbf{h}_{2i}$ as $\mathbf{U}_i$, where $\mathbf{U}_i^H \mathbf{U}_i = \mathbf{I}_2$. Then, without loss of generality, we can write $\mathbf{A}_i$ as

$$\mathbf{A}_i = \left[\begin{array}{cc} \mathbf{U}_i^* & (\mathbf{U}_i^{\perp})^* \end{array} \right] \left[\begin{array}{cc} \mathbf{B}_i & \mathbf{C}_i \\ \mathbf{D}_i & \mathbf{E}_i \end{array} \right] \left[\begin{array}{cc} \mathbf{U}_i & \mathbf{U}_i^{\perp} \end{array} \right]^H \tag{3.A.1}$$

where $\mathbf{U}_i^{\perp}$ is an $M \times (M-2)$ matrix with orthonormal columns which span the null-space of matrix $\mathbf{U}_i$, i.e., $(\mathbf{U}_i^{\perp})^H \mathbf{U}_i^{\perp} = \mathbf{I}_{M-2}$ and $\mathbf{U}_i^H \mathbf{U}_i^{\perp} = \mathbf{0}$. Also, $\mathbf{B}_i$, $\mathbf{C}_i$, $\mathbf{D}_i$, and $\mathbf{E}_i$ are complex matrices of sizes 2×2, $2 \times (M-2)$, $(M-2) \times 2$, and $(M-2) \times (M-2)$, respectively. We show in Appendix C that the following identities hold true:

$$\left| \sum_{i=1}^{n_r} \mathbf{h}_{1i}^T \mathbf{A}_i \mathbf{h}_{2i} \right|^2 = \left| \sum_{i=1}^{n_r} \mathbf{h}_{1i}^T \mathbf{U}_i^* \mathbf{B}_i \mathbf{U}_i^H \mathbf{h}_{2i} \right|^2 \tag{3.A.2}$$

$$\left| \sum_{i=1}^{n_r} \mathbf{h}_{2i}^T \mathbf{A}_i \mathbf{h}_{1i} \right|^2 = \left| \sum_{i=1}^{n_r} \mathbf{h}_{2i}^T \mathbf{U}_i^* \mathbf{B}_i \mathbf{U}_i^H \mathbf{h}_{1i} \right|^2 \tag{3.A.3}$$

$$\|\mathbf{h}_{1i}^T \mathbf{A}_i\|^2 = \|\mathbf{h}_{1i}^T \mathbf{U}_i^* \mathbf{B}_i\|^2 + \|\mathbf{h}_{1i}^T \mathbf{U}_i^* \mathbf{C}_i\|^2 \tag{3.A.4}$$

$$\|\mathbf{h}_{2i}^T \mathbf{A}_i\|^2 = \|\mathbf{h}_{2i}^T \mathbf{U}_i^* \mathbf{B}_i\|^2 + \|\mathbf{h}_{2i}^T \mathbf{U}_i^* \mathbf{C}_i\|^2 \tag{3.A.5}$$

$$\|\mathbf{A}_i \mathbf{h}_{1i}\|^2 = \|\mathbf{B}_i \mathbf{U}_i^H \mathbf{h}_{1i}\|^2 + \|\mathbf{D}_i \mathbf{U}_i^H \mathbf{h}_{1i}\|^2 \tag{3.A.6}$$

$$\|\mathbf{A}_i \mathbf{h}_{2i}\|^2 = \|\mathbf{B}_i \mathbf{U}_i^H \mathbf{h}_{2i}\|^2 + \|\mathbf{D}_i \mathbf{U}_i^H \mathbf{h}_{2i}\|^2 \tag{3.A.7}$$

$$tr(\mathbf{A}_i\mathbf{A}_i^H) = tr\left\{\mathbf{U}_i^*(\mathbf{B}_i\mathbf{B}_i^H + \mathbf{C}_i\mathbf{C}_i^H)\mathbf{U}_i^T + (\mathbf{U}_i^\perp)^*(\mathbf{D}_i\mathbf{D}_i^H + \mathbf{E}_i\mathbf{E}_i^H)(\mathbf{U}_i^\perp)^T\right\}. \quad (3.A.8)$$

From (3.A.2) and (3.A.3), we observe that matrices $\mathbf{C}_i$, $\mathbf{D}_i$, and $\mathbf{E}_i$ do not contribute to the denominators of the fractions of the objective function in (3.12). Also, as $\|\mathbf{h}_{1i}^T\mathbf{U}_i^*\mathbf{C}_i\|^2 \geq 0$, $\|\mathbf{h}_{2i}^T\mathbf{U}_i^*\mathbf{C}_i\|^2 \geq 0$, and $tr\{\mathbf{U}_i^*(\mathbf{C}_i\mathbf{C}_i^H)(\mathbf{U}_i^T\} \geq 0$, we see from (3.A.4), (3.A.5), and (3.A.8) that any non-zero matrix $\mathbf{C}_i$ increases the values of the second terms in (3.A.4) and (3.A.5) (which contribute to the numerators of the fractions of the objective function in (3.12)) and the second terms in (3.A.8) (which contribute to the last term of the objective function). The same discussion holds true for matrix $\mathbf{D}_i$ with the corresponding terms in (3.A.6), (3.A.7), and (3.A.8). That is, any non-zero values for matrices $\mathbf{C}_i$ and $\mathbf{D}_i$ result in a value for the objective function which is larger than the case when these matrices are chosen to be zero. Since $tr\{(\mathbf{U}_i^\perp)^*(\mathbf{E}_i\mathbf{E}_i^H)(\mathbf{U}_i^\perp)^T\} \geq 0$ in (3.A.8), similar discussion holds true for any non-zero matrix $\mathbf{E}_i$. We conclude that at the optimum $\mathbf{C}_i$, $\mathbf{D}_i$, and $\mathbf{E}_i$ must be $\mathbf{0}$, for $i = 1, ..., n_r$, and thus, the minimum power is achieved by finding only the optimum values for matrices $\{\mathbf{B}_i\}_{i=1}^{n_r}$. Thus, we can define $\mathbf{B}_i \triangleq \mathbf{U}_i^T\mathbf{A}_i\mathbf{U}_i$ as the effective beamforming matrix for relay i.

3.B Deriving the feasibility condition (3.25)

We observe from the constraint in (3.24) that for values of $\tilde{p}_1$ for which the matrix $(\tilde{p}_1 \tilde{\mathbf{E}}_1 - \sigma^2(\gamma_1+\gamma_2)\tilde{\mathbf{E}}_2)$ is negative semi-definite, the problem becomes infeasible. Therefore, the infeasibility condition can be written as

$$\tilde{p}_1 \mathbf{L}^H \mathbf{f}\,\mathbf{f}^H \mathbf{L} - \sigma^2(\gamma_1+\gamma_2)\mathbf{L}^H \mathbf{F}\,\mathbf{F}^H \mathbf{L} \preccurlyeq 0. \tag{3.B.1}$$

Here, we used the definition of matrix $\mathbf{E}_1$ in (3.19) along with the fact that matrix $\mathbf{E}_2$ in (3.21) can be written as $\mathbf{E}_2 = \mathbf{F}\,\mathbf{F}^H$, where the following definitions are used: $\mathbf{F} \triangleq \text{blkdiag}\{\mathbf{F}_1, \mathbf{F}_2, ..., \mathbf{F}_{n_r}\}$, $\mathbf{F}_i \triangleq [\, r_{1i}\mathbf{I}_2,\, r_{2i}\mathbf{I}_2\,]^T$, $r_{1i} \triangleq [\mathbf{q}_{2i}]_1$, and $r_{2i} \triangleq [\mathbf{q}_{2i}]_2$. Using these definitions, we can also write $\mathbf{f} = \mathbf{F}\mathbf{q}_1$, where $\mathbf{q}_1 \triangleq [\mathbf{q}_{11}^T,\, \mathbf{q}_{12}^T, ..., \mathbf{q}_{1n_r}^T]^T$. Hence, the infeasibility condition in (3.B.1) can be written as

$$\tilde{p}_1 \mathbf{L}^H \mathbf{F}\, \mathbf{q}_1\, \mathbf{q}_1^H\, \mathbf{F}^H \mathbf{L} - \sigma^2(\gamma_1+\gamma_2)\mathbf{L}^H \mathbf{F}\,\mathbf{F}^H \mathbf{L} \preccurlyeq 0 \tag{3.B.2}$$

which is equivalent to the following condition on $\tilde{p}_1$:

$$\mathbf{L}^H \mathbf{F}\, \left(\tilde{p}_1\, \mathbf{q}_1\, \mathbf{q}_1^H - \sigma^2(\gamma_1+\gamma_2)\mathbf{I}_{2n_r}\right) \mathbf{F}^H \mathbf{L} \preccurlyeq 0\,. \tag{3.B.3}$$

We now argue that the condition in (3.B.3) is equivalent to the following condition:

$$\left(\tilde{p}_1\, \mathbf{q}_1\, \mathbf{q}_1^H - \sigma^2(\gamma_1+\gamma_2)\mathbf{I}_{2n_r}\right) \preccurlyeq 0\,. \tag{3.B.4}$$

It is obvious that if (3.B.4) holds true, then (3.B.3) also holds true. To show the reverse, we note that if (3.B.3) holds true, then for any $3n_r \times 1$ vector $\mathbf{z}$, we can write $\mathbf{z}^H \mathbf{L}^H \mathbf{F}\, \left(\tilde{p}_1\, \mathbf{q}_1\, \mathbf{q}_1^H - \sigma^2(\gamma_1+\gamma_2)\mathbf{I}_{2n_r}\right) \mathbf{F}^H \mathbf{L}\mathbf{z} < 0$. Since $\mathbf{F}^H\mathbf{L}$ is a fat matrix, the vector $\mathbf{F}^H\mathbf{L}\mathbf{z}$ can be any $2n_r \times 1$ vector. We hence conclude that the matrix $\tilde{p}_1\, \mathbf{q}_1\, \mathbf{q}_1^H - \sigma^2(\gamma_1+\gamma_2)\mathbf{I}_{2n_r}$ is negative semi-definite, i.e., (3.B.4) holds true. As a results, to find the feasible values of $\tilde{p}_1$, it is necessary and sufficient to find those values of $\tilde{p}_1$ which result in the largest eigenvalue of the matrix $\tilde{p}_1\, \mathbf{q}_1\, \mathbf{q}_1^H - \sigma^2(\gamma_1+\gamma_2)\mathbf{I}_{2n_r}$ being positive. The largest eigenvalue of this matrix is equal to $\tilde{p}_1\, \mathbf{q}_1^H \mathbf{q}_1 - \sigma^2(\gamma_1+\gamma_2)$. Hence, the problem in (3.24) is feasible if and only if

$$\tilde{p}_1 > \frac{\sigma^2(\gamma_1+\gamma_2)}{\mathbf{q}_1^H \mathbf{q}_1}. \tag{3.B.5}$$

The derivation of the feasibility condition is complete.

3.C Proof of Lemma 1

To prove that the objective function in (3.29), defined as $\psi(\tilde{p}_1) \triangleq \tilde{p}_1 + \frac{\sigma^2(\gamma_1+\gamma_2)}{\lambda(\tilde{p}_1)}$, has a unique extremum in the interval $(\frac{\sigma^2(\gamma_1+\gamma_2)}{\mathbf{q}_1^H\mathbf{q}_1}, +\infty)$, we first show that $\psi(\tilde{p}_1)$ approaches $+\infty$, either when $\tilde{p}_1 \to +\infty$ or when $\tilde{p}_1 \to \frac{\sigma^2(\gamma_1+\gamma_2)}{\mathbf{q}_1^H\mathbf{q}_1}$, and thus, $\psi(\tilde{p}_1)$ has at least one minimum in the interval $(\frac{\sigma^2(\gamma_1+\gamma_2)}{\mathbf{q}_1^H\mathbf{q}_1}, +\infty)$. We then show that this minimum is unique. Note that we can write

$$\begin{aligned}
\lim_{\tilde{p}_1 \to \frac{\sigma^2(\gamma_1+\gamma_2)}{\mathbf{q}_1^H\mathbf{q}_1}} \mathbf{S}(\tilde{p}_1) &= \left(\frac{\sigma^2(\gamma_1+\gamma_2)}{\mathbf{q}_1^H\mathbf{q}_1}\tilde{\mathbf{E}}_0 + \sigma^2\mathbf{L}^H\mathbf{L}\right)^{-1}\left(\frac{\sigma^2(\gamma_1+\gamma_2)}{\mathbf{q}_1^H\mathbf{q}_1}\tilde{\mathbf{E}}_1 - \sigma^2(\gamma_1+\gamma_2)\tilde{\mathbf{E}}_2\right) \\
&= \left(\frac{\sigma^2(\gamma_1+\gamma_2)}{\|\mathbf{q}_1\|^2}\tilde{\mathbf{E}}_0 + \sigma^2\mathbf{L}^H\mathbf{L}\right)^{-1}\left(\frac{\sigma^2(\gamma_1+\gamma_2)}{\|\mathbf{q}_1\|^2}\mathbf{L}^H\mathbf{F}\mathbf{q}_1\mathbf{q}_1^H\mathbf{F}^H\mathbf{L} - \sigma^2(\gamma_1+\gamma_2)\mathbf{L}^H\mathbf{F}\mathbf{F}^H\mathbf{L}\right) \\
&= \left(\frac{\sigma^2(\gamma_1+\gamma_2)}{\|\mathbf{q}_1\|^2}\tilde{\mathbf{E}}_0 + \sigma^2\mathbf{L}^H\mathbf{L}\right)^{-1}\left(\sigma^2(\gamma_1+\gamma_2)\mathbf{L}^H\mathbf{F}\left(\frac{1}{\|\mathbf{q}_1\|^2}\mathbf{q}_1\mathbf{q}_1^H - \mathbf{I}_{2n_r}\right)\mathbf{F}^H\mathbf{L}\right)
\end{aligned} \tag{3.C.1}$$

It is obvious that the largest eigenvalue of matrix $\frac{1}{\mathbf{q}_1^H\mathbf{q}_1}\mathbf{q}_1\mathbf{q}_1^H - \mathbf{I}_{2n_r}$ in (3.C.1) is equal to zero. Hence, when $\tilde{p}_1 \to \frac{\sigma^2(\gamma_1+\gamma_2)}{\mathbf{q}_1^H\mathbf{q}_1}$, the largest eigenvalue of $\mathbf{S}(\tilde{p}_1)$, i.e., $\lambda(\tilde{p}_1)$ approaches 0, and thus, $\psi(\tilde{p}_1)$ approaches $+\infty$. It is also obvious that as $\tilde{p}_1$ approaches $+\infty$, the objective function $\psi(\tilde{p}_1)$ also approaches $+\infty$. Hence, $\psi(\tilde{p}_1)$ has at least one minimum in the interval $(\frac{\sigma^2(\gamma_1+\gamma_2)}{\mathbf{q}_1^H\mathbf{q}_1}, +\infty)$. We now prove that this minimum is the only extremum $\psi(\tilde{p}_1)$ can have. To this end, note that $\psi(\tilde{p}_1)$ is the sum of a monotonically increasing function (i.e., $\tilde{p}_1$) and the function $\frac{\sigma^2(\gamma_1+\gamma_2)}{\lambda(\tilde{p}_1)}$. If we can prove that $\lambda(\tilde{p}_1)$ is monotonically increasing with respect to $\tilde{p}_1$, we can then conclude that $\psi(\tilde{p}_1)$ has a unique minimum and the proof is then complete. We now prove that when $\tilde{p}_1 \in (\frac{\sigma^2(\gamma_1+\gamma_2)}{\mathbf{q}_1^H\mathbf{q}_1}, +\infty)$, $\lambda(\tilde{p}_1)$ is a monotonically increasing function of $\tilde{p}_1$. To prove this, in this interval, the derivative of $\lambda(\tilde{p}_1)$ with respect to $\tilde{p}_1$ is positive.

The derivative of $\lambda(\tilde{p}_1)$ is obtained in Appendix 3.D as

$$\begin{aligned}
\frac{\partial\lambda(\tilde{p}_1)}{\partial\tilde{p}_1} &= \frac{\tilde{p}_1^{-2} - \lambda(\tilde{p}_1)\tilde{\mathbf{f}}^H\mathbf{A}^{-1}(\tilde{p}_1)\tilde{\mathbf{E}}_0\mathbf{A}^{-1}(\tilde{p}_1)\tilde{\mathbf{f}}}{\tilde{\mathbf{f}}^H\mathbf{A}^{-1}(\tilde{p}_1)(\tilde{p}_1\tilde{\mathbf{E}}_0 + \sigma^2\mathbf{L}^T\,\mathbf{L})\mathbf{A}^{-1}(\tilde{p}_1)\tilde{\mathbf{f}}} && \text{(3.C.2)}\\
&> \frac{\tilde{p}_1^{-2} - \lambda(\tilde{p}_1)\tilde{\mathbf{f}}^H\mathbf{A}^{-1}(\tilde{p}_1)(\tilde{\mathbf{E}}_0 + \frac{\sigma^2}{\tilde{p}_1}\mathbf{L}^T\mathbf{L})\mathbf{A}^{-1}(\tilde{p}_1)\tilde{\mathbf{f}}}{\tilde{\mathbf{f}}^H\mathbf{A}^{-1}(\tilde{p}_1)(\tilde{p}_1\tilde{\mathbf{E}}_0 + \sigma^2\mathbf{L}^T\,\mathbf{L})\mathbf{A}^{-1}(\tilde{p}_1)\tilde{\mathbf{f}}}\\
&= \frac{\tilde{p}_1^{-2}}{\tilde{\mathbf{f}}^H\mathbf{A}^{-1}(\tilde{p}_1)(\tilde{p}_1\tilde{\mathbf{E}}_0 + \sigma^2\mathbf{L}^T\mathbf{L})\mathbf{A}^{-1}(\tilde{p}_1)\tilde{\mathbf{f}}} - \frac{\lambda(\tilde{p}_1)}{\tilde{p}_1}\\
&= \frac{\lambda(\tilde{p}_1)}{\tilde{p}_1}\left(\frac{\tilde{p}_1^{-1}}{\tilde{\mathbf{f}}^H\mathbf{A}^{-1}(\tilde{p}_1)\lambda(\tilde{p}_1)(\tilde{p}_1\tilde{\mathbf{E}}_0 + \sigma^2\mathbf{L}^T\mathbf{L})\mathbf{A}^{-1}(\tilde{p}_1)\tilde{\mathbf{f}}} - 1\right)\\
&\geq \frac{\lambda(\tilde{p}_1)}{\tilde{p}_1}\left(\frac{\tilde{p}_1^{-1}}{\tilde{\mathbf{f}}^H\mathbf{A}^{-1}(\tilde{p}_1)\Big(\sigma^2(\gamma_1+\gamma_2)\tilde{\mathbf{E}}_2 + \lambda(\tilde{p}_1)(\tilde{p}_1\tilde{\mathbf{E}}_0 + \sigma^2\mathbf{L}^T\mathbf{L})\Big)\mathbf{A}^{-1}(\tilde{p}_1)\tilde{\mathbf{f}}} - 1\right)\\
&= \frac{\lambda(\tilde{p}_1)}{\tilde{p}_1}\left(\frac{\tilde{p}_1^{-1}}{\tilde{\mathbf{f}}^H\mathbf{A}^{-1}(\tilde{p}_1)\mathbf{A}(\tilde{p}_1)\mathbf{A}^{-1}(\tilde{p}_1)\tilde{\mathbf{f}}} - 1\right)\\
&= \frac{\lambda(\tilde{p}_1)}{\tilde{p}_1}\left(\frac{\tilde{p}_1^{-1}}{\tilde{\mathbf{f}}^H\mathbf{A}^{-1}(\tilde{p}_1)\tilde{\mathbf{f}}} - 1\right) = 0 && \text{(3.C.3)}
\end{aligned}$$

where, in the first inequality, we have used the fact that

$$\lambda(\tilde{p}_1)\tilde{\mathbf{f}}^H\mathbf{A}^{-1}(\tilde{p}_1)(\frac{\sigma^2}{\tilde{p}_1}\mathbf{L}^T\,\mathbf{L})\mathbf{A}^{-1}(\tilde{p}_1)\tilde{\mathbf{f}} > 0.$$

In the second inequality, we have used the fact that $\mathbf{E}_2$ is positive semi-definite, and in the last equality, we have used the fact that at optimum, as proven in Appendix 3.D, $\tilde{\mathbf{f}}^H\mathbf{A}^{-1}(\tilde{p}_1)\tilde{\mathbf{f}} = \frac{1}{\tilde{p}_1}$ holds true. Hence, we conclude that $\frac{\partial\lambda(\tilde{p}_1)}{\partial\tilde{p}_1} > 0$ is positive, implying that $\lambda(\tilde{p}_1)$ is a monotonically increasing function of $\tilde{p}_1$. This completes the proof.

3.D Deriving $\lambda(\tilde{p}_1)$ and its derivative

In what follows, we derive an expression for $\frac{\partial\lambda(\tilde{p}_1)}{\partial\tilde{p}_1}$. Since $\lambda(\tilde{p}_1)$ is the largest eigenvalue of the matrix $\mathbf{S}(\tilde{p}_1)$, we can write $(\mathbf{S}(\tilde{p}_1) - \lambda(\tilde{p}_1)\mathbf{I}_{3n_r})\,\mathbf{u}(\tilde{p}_1) = \mathbf{0}$ which is equivalent to

$$\Big((\tilde{p}_1\tilde{\mathbf{E}}_0+\sigma^2\mathbf{L}^T\mathbf{L})^{-1}\Big(\tilde{p}_1\tilde{\mathbf{E}}_1-\sigma^2(\gamma_1+\gamma_2)\tilde{\mathbf{E}}_2\Big)-\lambda(\tilde{p}_1)\mathbf{I}_{3n_r}\Big)\,\mathbf{u}(\tilde{p}_1) = \mathbf{0} \tag{3.D.1}$$

where we use the definition of $\mathbf{S}(\tilde{p}_1)$ in (3.27). It follows from (3.D.1) that the matrix $\mathbf{S}(\tilde{p}_1) - \lambda(\tilde{p}_1)\mathbf{I}_{3n_r}$ has at least one zero eigenvalue. Multiplying (3.D.1) from left by $(\tilde{p}_1\tilde{\mathbf{E}}_0 + \sigma^2\mathbf{L}^T\,\mathbf{L})$, we arrive at

$$\Big(\tilde{p}_1\,\tilde{\mathbf{E}}_1\; - \sigma^2(\gamma_1+\gamma_2)\tilde{\mathbf{E}}_2 - \lambda(\tilde{p}_1)(\tilde{p}_1\tilde{\mathbf{E}}_0 + \sigma^2\mathbf{L}^T\,\mathbf{L})\Big)\,\mathbf{u}(\tilde{p}_1) = \mathbf{0}. \tag{3.D.2}$$

Based on the fact that if $\tilde{p}_1 > \sigma^2(\gamma_1+\gamma_2)/\mathbf{q}_1^H\mathbf{q}_1$, then $\lambda(\tilde{p}_1) > 0$ holds true, and that the matrix $\mathbf{L}^T\,\mathbf{L}$ is full rank, we conclude that the matrix

$$\mathbf{A}(\tilde{p}_1) \triangleq \sigma^2(\gamma_1+\gamma_2)\tilde{\mathbf{E}}_2 + \lambda(\tilde{p}_1)(\tilde{p}_1\tilde{\mathbf{E}}_0 + \sigma^2\mathbf{L}^T\,\mathbf{L}) \tag{3.D.3}$$

is nonsingular, and hence, $\mathbf{A}^{-1}(\tilde{p}_1)$ exists. As a result, we can write (3.D.2) as

$$(\tilde{p}_1\mathbf{A}^{-1}(\tilde{p}_1)\tilde{\mathbf{E}}_1 - \mathbf{I}_{3n_r})\mathbf{u}(\tilde{p}_1) = \mathbf{0}. \tag{3.D.4}$$

In light of (3.D.4), we observe that the matrix $\tilde{p}_1\mathbf{A}^{-1}(\tilde{p}_1)\tilde{\mathbf{E}}_1 - \mathbf{I}_{3n_r}$ must have at least one zero eigenvalue. Defining $\tilde{\mathbf{f}} \triangleq \mathbf{L}^H\mathbf{f}$, we can write $\tilde{\mathbf{E}}_1 = \tilde{\mathbf{f}}\,\tilde{\mathbf{f}}^H$, which is a rank-one matrix. Hence the matrix $\mathbf{A}^{-1}(\tilde{p}_1)\tilde{\mathbf{E}}_1$ is also rank-one. Therefore, all the eigenvalues of the matrix $\tilde{p}_1\mathbf{A}^{-1}(\tilde{p}_1)\tilde{\mathbf{E}}_1 - \mathbf{I}_{3n_r}$ are equal to -1, except the largest eigenvalue which is given by $\tilde{p}_1\,\tilde{\mathbf{f}}^H\mathbf{A}^{-1}(\tilde{p}_1)\tilde{\mathbf{f}} - 1$. Thus, equating this largest eigenvalue to 0 yields

$$\tilde{\mathbf{f}}^H\mathbf{A}^{-1}(\tilde{p}_1)\tilde{\mathbf{f}} = \frac{1}{\tilde{p}_1}. \tag{3.D.5}$$

Differentiating both sides of (3.D.5) with respect to $\tilde{p}_1$ yields

$$\tilde{\mathbf{f}}^H\mathbf{A}^{-1}(\tilde{p}_1)\frac{\partial\mathbf{A}(\tilde{p}_1)}{\partial\tilde{p}_1}\mathbf{A}^{-1}(\tilde{p}_1)\tilde{\mathbf{f}} = \frac{1}{\tilde{p}_1^2}. \tag{3.D.6}$$

We now use the fact that

$$\frac{\partial \mathbf{A}^{-1}(\tilde{p}_1)}{\partial \tilde{p}_1} = -\mathbf{A}^{-1}(\tilde{p}_1)\frac{\partial \mathbf{A}(\tilde{p}_1)}{\partial \tilde{p}_1}\mathbf{A}^{-1}(\tilde{p}_1)$$

and that

$$\frac{\partial \mathbf{A}(\tilde{p}_1)}{\partial \tilde{p}_1} = \frac{\partial \lambda(\tilde{p}_1)}{\partial \tilde{p}_1}(\tilde{p}_1\tilde{\mathbf{E}}_0 + \sigma^2\mathbf{L}^T\mathbf{L}) + \lambda(\tilde{p}_1)\tilde{\mathbf{E}}_0$$

to rewrite (3.D.6) as

$$\frac{\partial \lambda(\tilde{p}_1)}{\partial \tilde{p}_1}\tilde{\mathbf{f}}^H\mathbf{A}^{-1}(\tilde{p}_1)(\tilde{p}_1\tilde{\mathbf{E}}_0 + \sigma^2\mathbf{L}^T\mathbf{L})\mathbf{A}^{-1}(\tilde{p}_1)\tilde{\mathbf{f}} + \lambda(\tilde{p}_1)\tilde{\mathbf{f}}^H\mathbf{A}^{-1}(\tilde{p}_1)\tilde{\mathbf{E}}_0\mathbf{A}^{-1}(\tilde{p}_1)\tilde{\mathbf{f}} = \frac{1}{\tilde{p}_1^2}. \tag{3.D.7}$$

Therefore, we arrive at

$$\frac{\partial \lambda(\tilde{p}_1)}{\partial \tilde{p}_1} = \frac{\tilde{p}_1^{-2} - \lambda(\tilde{p}_1)\tilde{\mathbf{f}}^H\mathbf{A}^{-1}(\tilde{p}_1)\tilde{\mathbf{E}}_0\mathbf{A}^{-1}(\tilde{p}_1)\tilde{\mathbf{f}}}{\tilde{\mathbf{f}}^H\mathbf{A}^{-1}(\tilde{p}_1)(\tilde{p}_1\tilde{\mathbf{E}}_0 + \sigma^2\mathbf{L}^T\mathbf{L})\mathbf{A}^{-1}(\tilde{p}_1)\tilde{\mathbf{f}}}. \tag{3.D.8}$$

By substituting (3.D.8) in (3.30), we can write

$$g(\tilde{p}_1) = 1 - \sigma^2(\gamma_1 + \gamma_2)\frac{\tilde{p}_1^{-2} - \lambda(\tilde{p}_1)\tilde{\mathbf{f}}^H\mathbf{A}^{-1}(\tilde{p}_1)\tilde{\mathbf{E}}_0\mathbf{A}^{-1}(\tilde{p}_1)\tilde{\mathbf{f}}}{\lambda^2(\tilde{p}_1)\tilde{\mathbf{f}}^H\mathbf{A}^{-1}(\tilde{p}_1)(\tilde{p}_1\tilde{\mathbf{E}}_0+\sigma^2\mathbf{L}^T\mathbf{L})\mathbf{A}^{-1}(\tilde{p}_1)\tilde{\mathbf{f}}} \tag{3.D.9}$$

Equating $g(\tilde{p}_1)$ to 0 does not yield a closed-form solution when $n_r > 1$, or when $M > 1$. However, the solution to the equation $g(\tilde{p}_1) = 0$ can be obtained using a simple Newton-Raphson method or a bisection technique. Note that in order to calculate $g(\tilde{p}_1)$ as in (3.D.9), one needs to calculate $\lambda(\tilde{p}_1)$ for each value of $\tilde{p}_1$. To calculate $\lambda(\tilde{p}_1)$, we plug $\mathbf{A}(\tilde{p}_1)$ from (3.D.3) into (3.D.5) and arrive at the following equality:

$$\tilde{p}_1\tilde{\mathbf{f}}^H\Big(\sigma^2(\gamma_1+\gamma_2)\tilde{\mathbf{E}}_2+\lambda(\tilde{p}_1)(\tilde{p}_1\tilde{\mathbf{E}}_0+\sigma^2\mathbf{L}^T\mathbf{L})\Big)^{-1}\tilde{\mathbf{f}}=1. \tag{3.D.10}$$

which can be used to obtain $\lambda(\tilde{p}_1)$ for every feasible value of $\tilde{p}_1$. We now prove that (3.D.10) yields a unique value for $\lambda(\tilde{p}_1)$ for any given feasible value of $\tilde{p}_1$. To do so, we first observe that the function

$$\hbar(z) \triangleq \tilde{p}_1\tilde{\mathbf{f}}^H\Big(\sigma^2(\gamma_1+\gamma_2)\tilde{\mathbf{E}}_2+z(\tilde{p}_1\tilde{\mathbf{E}}_0+\sigma^2\mathbf{L}^T\mathbf{L})\Big)^{-1}\tilde{\mathbf{f}} \tag{3.D.11}$$

is monotonically decreasing in z, for any feasible value of $\tilde{p}_1$. We then observe that $\lim_{z\to+\infty} \hbar(z) = 0$. Hence, if we show that $\lim_{z\to 0} \hbar(z) \to +\infty$, for any feasible value of $\tilde{p}_1$, we can conclude that for any feasible value of $\tilde{p}_1$, the equation $\hbar(z) = 1$ has a unique solution, so does (3.D.10).

To do so, let us define $\mathbf{\Gamma}(z) \triangleq \sigma^2(\gamma_1 + \gamma_2)\tilde{\mathbf{E}}_2 + z(\tilde{p}_1\tilde{\mathbf{E}}_0 + \sigma^2\mathbf{L}^T\mathbf{L})$. Due to the fact that $\mathbf{L}^T\mathbf{L}$ is a positive definite matrix, $\tilde{p}_1 > 0$, and $\tilde{\mathbf{E}}_0$ is Hermitian, we arrive at the conclusion that $\mathbf{\Gamma}(z)$ is positive definite. Using the singular value decomposition method, we can write $\mathbf{\Gamma}(z)$ as

$$\mathbf{\Gamma}(z) = \mathbf{\Lambda}(z)\mathbf{\Sigma}(z)\mathbf{\Lambda}^H(z) \tag{3.D.12}$$

where $\mathbf{\Sigma}(z)$ and $\mathbf{\Lambda}(z)$ are $3n_r \times 3n_r$ matrices and $\mathbf{\Sigma}(z)$ is diagonal. Due to the fact that $\mathbf{\Gamma}(z)$ is positive definite, all entries of matrix $\mathbf{\Sigma}(z)$ are positive. We observe that when z approaches zero, matrix $\mathbf{\Gamma}(z)$ becomes more and more close to the matrix $\sigma^2(\gamma_1 + \gamma_2)\tilde{\mathbf{E}}_2$, which is not a full-rank matrix. That is, as z approaches zero, some of the diagonal entries of $\mathbf{\Sigma}(z)$ approach zero. In other words, since $\mathbf{\Gamma}(z)$ is positive definite all its eigenvalues are positive, however, as z approaches zero, some of the positive-valued eigenvalues of $\mathbf{\Gamma}(z)$ approach zero. As a result, the positive-valued determinant of $\mathbf{\Gamma}(z)$ becomes more and more close to zero. Since $\hbar(z) = p_1\tilde{\mathbf{f}}^H\mathbf{\Gamma}^{-1}(z)\tilde{\mathbf{f}}$ is inversely proportional to the determinant of $\mathbf{\Gamma}(z)$, as z approaches zero, the value of $\hbar(z)$ more and more approaches infinity. That is, $\lim_{z\to 0}\hbar(z) \to +\infty$, and hence, (3.D.10) has a unique solution in terms of $\lambda(\tilde{p}_1)$.

Chapter 4

Asynchronous Two-way Networks with Multiple Multi-Antenna Relays

The single-carrier asynchronous two-way relay network we consider in this chapter consists of two single-antenna transceivers which wish to communicate with the help of multiple multi-antenna relays. Addressing the total transmit power minimization problem while the rates of the information exchange between transceivers are maintained above two given thresholds, we aim to jointly determine the relay beamforming matrices and the transceivers' transmit powers.

The organization of this chapter is as follows. In Section 4.1, we model the signals and system for asynchronous two-way relay networks where relays employ multiple antennas. The problem we here study is to minimize the total transmit power in an asynchronous two-way relay network while the data rates of the transceivers are maintained above two given thresholds. In Section 4.2, the problem statement and its solution along with the method being used to solve the problem are provided. In Section 4.3, we provide an algorithm which summarizes how the proposed method must be implemented. In Section 4.4, we numerically evaluate the performance of the asynchronous two-way relay networks under consideration.

4.1 Signals and System Model

As shown in Fig. 4.1, we consider a network where L relay nodes collaborate to establish a two-way communication link between a pair of single-antenna transceivers. The l-th relay node is equipped with M_l antennas. It is assumed that the information symbols are transmitted sequentially, in blocks with length N_s, over the channels. The frequency-flat fading channels remain constant during an end-to-end block exchange between the two transceivers. In addition, the perfect channel state information (CSI) is assumed to be available at the transceivers. The employed relaying conforms to the multiple access broadcast (MABC) scheme, where a round of information exchange consists of two time-slots. In the first time-slot, relays receive a noisy superposition of the attenuated versions of the signals transmitted by the transceivers. Each relay then multiplies the $M_l \times 1$ signal vector arrived at its antennas by a complex beamforming matrix and broadcasts, in the second time-slot, the elements of the transformed vector over its antennas. The propagation delays over various relaying paths are different due to the fact that the relays are geographically distributed at different locations in the environment. The relay networks with significantly different propagation delays for different relaying paths are herein referred to as *asynchronous relay networks*. An asynchronous relay network resembles a multi-path channel with multiple taps. The multi-path characteristic of the asynchronous relay network can cause symbols to spread beyond the symbol period. As a result, each symbol can interfere with the preceding or succeeding transmitted symbols, thereby causing ISI, which in turn can lead to intra-block interference in each block of symbols. Moreover, in a sequential block transmission, the ISI can also result in inter-block interference (IBI) between successive blocks. Adding cyclic prefix to a block at the transmitter side provides a guard interval which eliminates IBI. The so-obtained IBI-free signal still contains intra-block interference. One can devise a relay synchronization scheme which entails adding extra hardware and more computations. To avoid such complexities at the relays, we herein assume no synchronization at the relays and rather

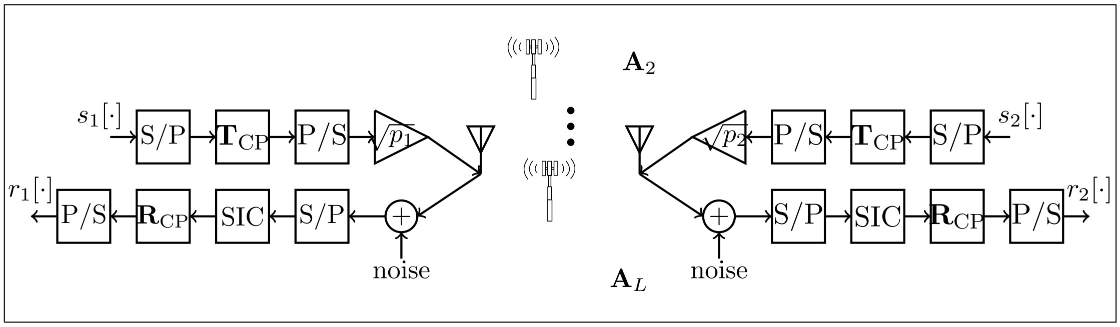

Figure 4.1: System block diagram.

aim to combat the intra-block interference while obtaining the network parameters. We aim to determine the relay beamforming matrices and the transceivers' transmit powers such that the total power consumed in the entire network is minimized while the data rates of the transceivers are maintained above two given thresholds. Since, intra-block interference significantly affects the information exchange data rate, to maintain the data rates above given thresholds, the optimal solution must tackle intra-block interference.

End-to-end channel model: Aiming to exchange information, the two transceivers simultaneously broadcast their signals toward the relays. Each relay transforms the vector of its received signals, by multiplying this vector with a beamforming matrix, into a vector whose entries are transmitted over different antennas. Each transceiver then receives a noisy superpositions of multiple attenuated replicas of two distinct signals, i.e., its own transmitted signal and the signal transmitted by the other transceiver. Any attenuated replica of the transmitted signal arrived at a transceiver experiences a distinct delay. Let us define the $M_l \times M_l$ complex matrix $\mathbf{A}_l$ as the beamforming matrix of the l-th relay, and denote $\mathbf{g}_{lq}$ as the $M_l \times 1$ complex vector of the coefficients associated with the channels between the l-th relay and Transceiver q. Then, the end-to-end attenuation/amplification factor of the l-th relaying path from Transceiver $\bar{q}$ to Transceiver q can be written as

$$\alpha_{l\bar{q}q} \triangleq \mathbf{g}_{lq}^T \mathbf{A}_l \mathbf{g}_{l\bar{q}}, \quad \text{for} \quad q, \bar{q} \in \{1, 2\},\ l \in \{1, 2, \ldots, L\}. \tag{4.1}$$

Here, we define $\bar{q} \triangleq 2$ when $q = 1$, and $\bar{q} \triangleq 1$ when $q = 2$. The aggregate end-to-end channel from Transceiver $\bar{q}$ to Transceiver q is characterized as a multi-path channel, whose impulse response is given as

$$\hbar_{\bar{q}q}(t) = \sum_{l=1}^{L} \alpha_{l\bar{q}q} \delta(t - \tau_l) \quad \text{for} \quad q, \bar{q} \in \{1, 2\} \tag{4.2}$$

where $\delta(t)$ is the Dirac delta function and τ_l denotes the propagation delay corresponding to the l-th relaying path. Employing a pulse shaping filter at the transmitter front-end of the transceivers produces a bandlimited signal associated with each generated symbol. Denoting the pulse shaping filter response as $\phi(t)$, we can express the signal transmitted by Transceiver q as

$$s_q(t) = \sum_{k=-\infty}^{\infty} s_q[k] \phi(t - kT_s), \quad q \in \{1, 2\} \tag{4.3}$$

where $s_q[k]$ is the k-th symbol transmitted by Transceiver q, and T_s is the symbol period. The received signal $r_q(t)$ at Transceiver $q \in \{1, 2\}$ is a superposition of the transmitted signals after going through the end-to-end channel, that is

$$r_q(t) = \sum_{\bar{q}=1}^{2} s_{\bar{q}}(t) * \hbar_{\bar{q}q}(t) = \sum_{\bar{q}=1}^{2} \sum_{k=-\infty}^{\infty} s_{\bar{q}}[k] \sum_{l=1}^{L} \alpha_{l\bar{q}q} \phi(t - kT_s - \tau_l) \tag{4.4}$$

where $*$ represents the continuous-time convolution operation. Sampling $r_q(t)$ at the symbol rate $1/T_s$, we can express the discrete-time received sequence $r_q[n]$ as

$$r_q[n] = r_q(t)\Big|_{t=nT_s} = \sum_{\bar{q}=1}^{2} \sum_{k=-\infty}^{\infty} s_{\bar{q}}[k] \sum_{l=1}^{L} \alpha_{l\bar{q}q} \phi((n-k)T_s - \tau_l) = \sum_{\bar{q}=1}^{2} s_{\bar{q}}[n] \star h_{\bar{q}q}[n] \tag{4.5}$$

where $\star$ denotes the discrete-time convolution operation, and

$$h_{\bar{q}q}[n] \triangleq \sum_{l=1}^{L} \alpha_{l\bar{q}q} \phi(nT_s - \tau_l) \tag{4.6}$$

serves as the equivalent discrete-time impulse response corresponding to the end-to-end channel from Transceiver $\bar{q}$ to Transceiver q. Assuming that $\phi(\cdot)$ is a rectangular pulse with duration T_s, we note that only when $0 < nT_s - \tau_l \leq T_s$ holds true for the l-th relay, the value of $\phi(nT_s - \tau_l)$ is non-zero, implying that the l-th relay contributes to the n-th tap of $h_{\bar{q}q}[\cdot]$. Let N denote the maximum delay spread of the end-to-end CIR $h_{\bar{q}q}[\cdot]$, i.e., $N = \max\limits_{1\leq l\leq L} \lceil \tau_l / T_s \rceil$. To represent the contribution of the l-th relay to the tap n of $h_{\bar{q}q}[\cdot]$, we introduce an $N \times 1$ vector $\mathbf{d}_l \triangleq [d_{l,0} \;\; d_{l,1} \;\; \cdots \;\; d_{l,(N-1)}]^T$, where the following definition is used:

$$d_{l,n} \triangleq \begin{cases} 1 & (n-1)T_s \leq \tau_l < nT_s \\ 0 & \text{otherwise} \end{cases}, \quad \text{for } n = 0, 1, 2, \cdots N-1. \tag{4.7}$$

We now use (4.1), (4.6), and (4.7) to write $h_{\bar{q}q}[n]$ as

$$h_{\bar{q}q}[n] = \sum_{l=1}^{L} d_{l,n}\, \mathbf{g}_{lq}^T \mathbf{A}_l \mathbf{g}_{l\bar{q}}. \tag{4.8}$$

Defining $\mathbf{h}_{\bar{q}q} \triangleq [h_{\bar{q}q}[0] \;\; h_{\bar{q}q}[1] \;\; \cdots \;\; h_{\bar{q}q}[N-1]]^T$ as the vector of the taps of end-to-end CIR $h_{\bar{q}q}[\cdot]$, and using (4.8), we can write

$$\mathbf{h}_{\bar{q}q} = \sum_{l=1}^{L} \mathbf{d}_l\, \mathbf{g}_{lq}^T \mathbf{A}_l \mathbf{g}_{l\bar{q}} \tag{4.9}$$

The channel model in (4.9) is essential in our forthcoming derivations.

Received noise model: Let $\gamma_{lm}(t)$ denotes the measurement noise at the m-th antenna of the l-th relay. This noise is assumed to be spatially and temporally white with variance σ^2. The noise processes received at the M_l antennas of the l-th relay form an $M_l \times 1$ noise vector $\boldsymbol{\gamma}_l(t) \triangleq [\gamma_{l1}(t) \quad \gamma_{l2}(t) \quad \cdots \quad \gamma_{lM_l}(t)]^T$. In the *transform-and-forward relaying* scheme, the vector of the signals received at the l-th relay is multiplied by the beamforming matrix $\mathbf{A}_l$. As a result, $\boldsymbol{\gamma}_l(t)$ is also multiplied by the same matrix. The transformed noise vector is transmitted along with the superposition of the transformed versions of the relay received signals. The attenuated version of the transformed noise vector arrives at Transceiver q with delay $\breve{\tau}_{lq}$, where $\breve{\tau}_{lq}$ represents the propagation delay between the l-th relay and Transceiver

q. The total discrete-time noise $\eta_q[n]$ received at Transceiver q is a combination of the noises forwarded by the relays and the additive noise at the receiver front-end of that transceiver and is given by

$$\eta_q[n] = \sum_{l=1}^{L} \boldsymbol{\gamma}_l^T((n - \breve{n}_{lq})T_s)\mathbf{A}_l^T \mathbf{g}_{lq} + \eta'_q[n], \quad \text{for} \quad q \in \{1, 2\} \tag{4.10}$$

where ${\eta'}_q[n]$ denotes the additive noise at Transceiver q. The integer parameter $\breve{n}_{l_q}$ is the discrete-time delay experienced by the transformed noise vector when these noise travels from the l-th relay to Transceiver q transformed noises are and satisfies $\frac{\breve{\tau}_{lq}}{T_s} < \breve{n}_{l_q} \leq \frac{\breve{\tau}_{lq}}{T_s} + 1$. The $N_t \times 1$ noise vector $\boldsymbol{\eta}_q[i]$, received at Transceiver q during the i-th N_t successive transmissions can be written as

$$\boldsymbol{\eta}_q[i] = \sum_{l=1}^{L} \boldsymbol{\Gamma}_l^T(i)\mathbf{A}_l^T \mathbf{g}_{lq} + \boldsymbol{\eta}'_q[i], \quad \text{for} \quad q \in \{1, 2\} \tag{4.11}$$

where the following definitions are used:

$$\boldsymbol{\eta}_q[i] \triangleq [\eta_q[(i-1)N_t] \;\; \eta_q[(i-1)N_t + 1] \;\; \cdots \;\; \eta_q[iN_t - 1]]^T,$$

$$\boldsymbol{\eta}'_q[i] \triangleq \left[\eta'_q[(i-1)N_t] \;\; \eta'_q[(i-1)N_t + 1] \;\; \cdots \;\; \eta'_q[iN_t - 1]\right]^T.$$

Moreover, $\boldsymbol{\Gamma}_l(i) \triangleq [\boldsymbol{\gamma}_l(((i-1)N_t - \breve{n}_{lq})T_s) \;\; \boldsymbol{\gamma}_l(((i-1)N_t + 1 - \breve{n}_{lq})T_s) \ldots \boldsymbol{\gamma}_l((i(N_t - 1) - \breve{n}_{lq})T_s)]$ is an $M_l \times N_t$ matrix whose m-th column is a sequence of noise processes which arrive at the m-th antenna of the l-th relay during N_t successive transmissions.

Received signal model: Let the vector $\mathbf{s}_q(i) = [s_q[iN_s] \;\; s_q[iN_s{+}1] \;\; \cdots \;\; s_q[iN_s + N_s - 1]]^T$ denote the i-th block of information symbols with length N_s transmitted by Transceiver q, for $q \in \{1, 2\}$, with transmission power p_q. Here, $s_q[k]$ represents the k-th symbol transmitted by Transceiver q.

The frequency selectivity of the end-to-end channel leads to inter-block-interference (IBI) between successive transmitted blocks. Hence, the signals received at Transceiver $\bar{q}$, corresponding to the i-th transmitted block, depend on the i-th and the $(i-1)$-th blocks transmitted by Transceiver q, i.e., $\mathbf{s}_q(i)$ and $\mathbf{s}_q(i-1)$. In order to eliminate IBI, a cyclic prefix is annexed to $\mathbf{s}_q(i)$ by pre-multiplying it with the matrix $\mathbf{T}_{\text{cp}} \triangleq [\tilde{\mathbf{I}}_{\text{cp}}^T \ \mathbf{I}_{N_s}^T]^T$, where $\tilde{\mathbf{I}}_{\text{cp}}$ is the matrix of the last N rows of the identity matrix, and N is the length of the vector of the equivalent discrete-time end-to-end CIR $h_{\bar{q}q}[\cdot]$ taps. After the cyclic prefix insertion, the corresponding i-th transmitted block $\bar{\mathbf{s}}_q(i)$ (with length $N_t \triangleq N_s + N$) can be written as

$$\begin{aligned}\bar{\mathbf{s}}_q(i) &\triangleq \mathbf{T}_{\text{cp}}\mathbf{s}_q(i)\\ &= [s_q[(i+1)N_s - N] \ldots s_q[(i+1)N_s - 1] \ s_q[iN_s] \ldots s_q[(i+1)N_s - 1]]^T\end{aligned} \tag{4.12}$$

These transmitted blocks can arrive at the relay nodes at different time instants due to the different propagation delays corresponding to different relay-transceiver links. Therefore, there can be a timing misalignment between the received versions of these signals. The i-th signal block at the output of the self-interference cancellation block at Transceiver q can be written as [139]

$$\bar{\mathbf{r}}_q(i) = \sqrt{p_{\bar{q}}}\,\mathbf{H}_0^{\bar{q}q}(\mathcal{A})\,\bar{\mathbf{s}}_{\bar{q}}(i) + \sqrt{p_{\bar{q}}}\,\mathbf{H}_1^{\bar{q}q}(\mathcal{A})\,\bar{\mathbf{s}}_{\bar{q}}(i-1) + \boldsymbol{\eta}_q(i) \tag{4.13}$$

where $\mathcal{A} \triangleq \{\mathbf{A}_l\}_{l=1}^L$ is the set of the relays' beamforming matrices. Furthermore, $p_{\bar{q}}$ is the transmit power of Transceiver $\bar{q}$, and matrices $\mathbf{H}_0^{\bar{q}q}(\mathcal{A})$ and $\mathbf{H}_1^{\bar{q}q}(\mathcal{A})$ are defined respectively as [139]

$$\mathbf{H}_0^{\bar{q}q}(\mathcal{A}) \triangleq \begin{bmatrix} h_{\bar{q}q}[0] & 0 & 0 & \cdots & 0 \\ \vdots & h_{\bar{q}q}[0] & 0 & \cdots & 0 \\ h_{\bar{q}q}[N-1] & \cdots & \ddots & \cdots & \vdots \\ \vdots & \ddots & \cdots & \ddots & 0 \\ 0 & \cdots & h_{\bar{q}q}[N-1] & \cdots & h_{\bar{q}q}[0] \end{bmatrix},$$

$$\mathbf{H}_1^{\bar{q}q}(\mathcal{A}) \triangleq \begin{bmatrix} 0 & \cdots & h_{\bar{q}q}[N-1] & \cdots & h_{\bar{q}q}[1] \\ \vdots & \ddots & 0 & \cdots & 0 \\ 0 & \cdots & \ddots & \cdots & h_{\bar{q}q}[N-1] \\ \vdots & \vdots & \vdots & \ddots & \vdots \\ 0 & \cdots & 0 & \cdots & 0 \end{bmatrix}. \tag{4.14}$$

The received signal vector $\bar{\mathbf{r}}_q(i)$ is multiplied by $\mathbf{R}_{\text{cp}} \triangleq [\mathbf{0}_{N_s\times N} \ \mathbf{I}_{N_s}]$, which is the cyclic prefix removal matrix, and thus, the first N entries of $\bar{\mathbf{r}}_q(i)$ are discarded. One can easily verify that $\mathbf{R}_{\text{cp}}\mathbf{H}_1^{\bar{q}q}(\mathcal{A}) = \mathbf{0}$, and hence, the IBI-inducing matrix $\mathbf{H}_1^{\bar{q}q}(\mathcal{A})$ is eliminated through the cyclic prefix removal operation. Therefore, using (4.13), we can write

$$\mathbf{r}_q(i) \triangleq \sqrt{p_{\bar{q}}}\,\tilde{\mathbf{H}}_{\bar{q}q}(\mathcal{A})\,\mathbf{s}_{\bar{q}}(i) + \tilde{\boldsymbol{\eta}}_q(i) \tag{4.15}$$

where we define $\tilde{\boldsymbol{\eta}}_q(i) \triangleq \mathbf{R}_{\rm cp}\boldsymbol{\eta}_q(i)$, while $\tilde{\mathbf{H}}_{\bar{q}q}(\mathcal{A}) = \mathbf{R}_{\rm cp}\mathbf{H}_0^{\bar{q}q}(\mathcal{A})\,\mathbf{T}_{\rm cp}$ is an $N_s \times N_s$ circulant matrix whose (k,l)-th entry is given by $\tilde{h}_{\bar{q}q}[(k-l) \bmod N_s]$, where we define $\tilde{h}_{\bar{q}q}[n] = h_{\bar{q}q}[n]$, for $0 \le n \le N-1$ and $\tilde{h}_{\bar{q}q}[n] = 0$, for $N \le n \le N_s - 1$. That is,

$$\tilde{\mathbf{H}}_0^{\bar{q}q}(\mathcal{A}) \triangleq \begin{bmatrix} \tilde{h}_{\bar{q}q}[0] & \tilde{h}_{\bar{q}q}[N_s-1] & \tilde{h}_{\bar{q}q}[N_s-2] & \cdots & \tilde{h}_{\bar{q}q}[1] \\ \tilde{h}_{\bar{q}q}[1] & \tilde{h}_{\bar{q}q}[0] & \tilde{h}_{\bar{q}q}[N_s-1] & \cdots & \tilde{h}_{\bar{q}q}[2] \\ \vdots & \vdots & \vdots & \ddots & \vdots \\ \tilde{h}_{\bar{q}q}[N_s-1] & \tilde{h}_{\bar{q}q}[N_s-2] & \tilde{h}_{\bar{q}q}[N_s-3] & \cdots & \tilde{h}_{\bar{q}q}[0] \end{bmatrix}. \tag{4.16}$$

Total transmit power: The $M_l \times N_t$ matrix $\mathbf{X}_l(i)$ of the blocks received at the l-th relay in the first time-slot is given as

$$\mathbf{X}_l(i) = \sqrt{p_1}\,\mathbf{g}_{l1}\bar{\mathbf{s}}_1^T(i) + \sqrt{p_2}\,\mathbf{g}_{l2}\bar{\mathbf{s}}_2^T(i) + \boldsymbol{\Gamma}_l(i), \quad \text{for } l \in \{1, 2, \ldots, L\}. \tag{4.17}$$

Here, the m-th row of the matrix $\mathbf{X}(i)$ is the signal block received at the m-th antenna of the l-th relay and $\boldsymbol{\Gamma}_l(i)$ is the $M_l \times N_t$ noise at the l-th relay. The $M_l \times N_t$ matrix of the signals transmitted by the l-th relay is represented by $\mathbf{T}_l(i)$ and can be expressed as $\mathbf{T}_l(i) = \mathbf{A}_l\mathbf{X}_l(i)$. Based on (4.17), the average transmit power of the l-th relay is obtained as (see Appendix 4.A)

$$P_l \triangleq \frac{1}{N_t}E\{\mathbf{1}^T\mathbf{T}_l^H(i)\mathbf{T}_l(i)\mathbf{1})\} = p_1\|\mathbf{A}_l\mathbf{g}_{l1}\|^2 + p_2\|\mathbf{A}_l\mathbf{g}_{l2}\|^2 + \sigma^2 tr(\mathbf{A}_l\mathbf{A}_l^H). \tag{4.18}$$

The total transmit power $P_{\rm T}$ in the network is the summation of the transceivers' transmit powers and the transmit power of all the relays, that is,

$$\begin{aligned} P_{\rm T} &= p_1 + p_2 + \sum_{l=1}^{L} P_l \\ &= p_1\left(1 + \sum_{l=1}^{L}\|\mathbf{A}_l\mathbf{g}_{l1}\|^2\right) + p_2\left(1 + \sum_{l=1}^{L}\|\mathbf{A}_l\mathbf{g}_{l2}\|^2\right) + \sigma^2\sum_{l=1}^{L} tr(\mathbf{A}_l\mathbf{A}_l^H). \end{aligned} \tag{4.19}$$

In the next section, we use the channel model in (4.9), the data model in (4.15), and the total power expression in (4.19) to optimally determine the transceivers' transmit powers p_1 and p_2 as well as the beamforming matrices $\{\mathbf{A}_l\}_{l=1}^{L}$ under the constraint that these matrices are symmetric. It is worth mentioning that without such symmetry constraints, the total power minimization problem does not appear to be amenable to a computationally efficient solution.

4.2 Total Power Minimization

To find the relay beamforming matrices as well as the transceivers' transmit powers, the total transmit power minimization problem, subject to two constraints which guarantee that the data rates at Transceivers 1 and 2 are maintained above two given thresholds b_1 and b_2, respectively, can be expressed as[1][2]

$$\min_{\mathcal{P},\mathcal{A}}. \; P_{\mathrm{T}} \quad \text{subject to} \quad R_1(\mathcal{A}, p_2) \geq b_1, \;\; R_2(\mathcal{A}, p_1) \geq b_2, \;\; p_1 \geq 0, \;\; p_2 \geq 0, \tag{4.20}$$

where $\mathcal{P} \triangleq \{p_q\}_{q=1}^{2}$, and $\mathcal{A} = \{\mathbf{A}_l\}_{l=1}^{L}$ are defined as the set of the transceivers' transmit powers and the set of the relays' beamforming matrices, respectively. The main contribution of this chapter is to solve the optimization problem (4.20) under the assumption that the beamforming matrices $\{\mathbf{A}_l\}_{l=1}^{L}$ are symmetric, i.e., $\mathbf{A}_l = \mathbf{A}_l^T$. Indeed, in the absence of such an assumption, the problem is not amenable to a computationally efficient solution[3]. To develop a computationally affordable solution to (4.20), we take the following steps:

- **Step 1:** We first derive two expressions for the data rates $R_1(\mathcal{A}, p_2)$ and $R_2(\mathcal{A}, p_1)$ in terms of the design parameters.

[1]The power minimization problem (4.20) is solved under the assumption that the relay network is asynchronous, meaning that the signal transmitted by any of the two transceivers arrives at different relays with different delays and signals transmitted by different relays arrive at any of the two transceivers with different delays. That is, this minimization is solved for the model presented for the end-to-end CIR in the previous section. This model and also the solution to this minimization have not appeared prior to this study.

[2]For now, we do not express the symmetric constraints on the relay beamforming matrices. We add these constraints later.

[3]As shown in [140], even for synchronous networks with multi-antenna relays, solving the total power minimization problem without the assumption of symmetric beamforming matrices is computationally prohibitive. Asynchronism only adds to the challenge that one has to overcome when solving the total power minimization problem.

- **Step 2:** Based on the expressions obtained in the first step, we use a change of variables to simplify the problem in (4.20).

- **Step 3:** We then exploit a special structure of the matrices ($\{\mathbf{A}_l\}_{l=1}^{L}$) (as proven in [29]) to reduce the dimensionality of the problem.

- **Step 4:** Next, we use the symmetric beamforming assumption to further simplify the problem. After this step, the optimality is only studied under the assumption that the relay beamforming matrices are symmetric.

- **Step 5:** In this step, we relax the problem by ignoring some of the constraints and solve the relaxed problem. Using the structure of the relaxed problem, we prove that the solution to the relaxed problem satisfies the original constraints being relaxed, and thus, this solution is optimal for the original problem with symmetric relay beamforming matrices.

- **Step 6:** We then solve the relaxed problem, thereby showing that this problem is amenable to a semi-closed-form solution. To develop this solution, we prove rigorously that at the optimum, the end-to-end CIR in (4.8) has only one non-zero tap. As a result, only those relays which contribute to the non-zero tap of the end-to-end CIR will participate in relaying and the remainder of the relays have to be turned off. Those relays which contribute to one tap of the end-to-end CIR constitute a synchronous sub-network. As a result, the problem reduces to finding the best synchronous sub-network which consumes the smallest total power while satisfying the rate constraints. For synchronous network, however, finding the solution to total power minimization problem under rate constraints is amenable to a semi-closed-form solution.

The rest of this section presents the details of the above steps. To ensure that the flow of the presentation is easy to follow, we bring the details of the derivations in the appendices. Readers interested only in implementation of the proposed algorithm are referred to the summary of the algorithm presented in Section 4.3.

Step1: Developing rate expressions

The data model in (4.15) can be viewed as a multi-input multi-output (MIMO) scheme. Hence, one can use the expression for the rate of a MIMO channel to obtain an expression for the data rate of the two transceivers. Indeed, based on the results of [7], the data rate corresponding to the MIMO data model in (4.15) can be written as[4]

$$R_q(\mathcal{A}, p_{\bar{q}}) = \log \det \left(\mathbf{I}_{N_s} + p_{\bar{q}} \mathbf{C}_q^{-\frac{1}{2}}(\mathcal{A})\, \tilde{\mathbf{H}}_{\bar{q}q}(\mathcal{A})\, \tilde{\mathbf{H}}_{\bar{q}q}^H(\mathcal{A})\, \mathbf{C}_q^{-\frac{1}{2}}(\mathcal{A}) \right) \tag{4.21}$$

where $\det(\cdot)$ denotes the determinant of a matrix and $\mathbf{C}_q(\mathcal{A})$ is the correlation matrix of the noise $\tilde{\boldsymbol{\eta}}_q(i)$ at Transceiver q and, as shown in Appendix 4.B, is given by

$$\mathbf{C}_q(\mathcal{A}) = \sigma^2 \left(\sum_{l=1}^{L} \|\mathbf{A}_l^T \mathbf{g}_{lq}\|^2 + 1 \right) \mathbf{I}_{N_s}. \tag{4.22}$$

Exploiting the fact that the matrix $\tilde{\mathbf{H}}_{\bar{q}q}(\mathcal{A})$ is circulant, we show in Appendix 4.C that (4.21) can be simplified as

$$R_q(\mathcal{A}, p_{\bar{q}}) = \log \prod_{k=1}^{N_s} \left(1 + \frac{p_{\bar{q}}\, |\psi_{\bar{q}q}^k(\mathcal{A})|^2}{\sigma^2 \left(\sum_{l=1}^{L} \|\mathbf{A}_l^T \mathbf{g}_{lq}\|^2 + 1 \right)} \right) \tag{4.23}$$

where the following definitions are used:

$$\psi_{\bar{q}q}^k(\mathcal{A}) = \sqrt{N_s}\, \boldsymbol{\phi}_k^H \tilde{\mathbf{h}}_{\bar{q}q} \tag{4.24}$$

$$\boldsymbol{\phi}_k \triangleq \frac{1}{\sqrt{N_s}} [1 \;\; e^{\frac{j2\pi(k-1)}{N_s}} \;\; \cdots \;\; e^{\frac{j2\pi(N_s-1)(k-1)}{N_s}}]^T, \qquad \text{for } k = 1, 2, \ldots, N_s \tag{4.25}$$

$$\tilde{\mathbf{h}}_{\bar{q}q} \triangleq [\mathbf{h}_{\bar{q}q}^T \;\; \mathbf{0}_{1\times(N_s-N)}^T]^T. \tag{4.26}$$

Indeed, $\tilde{\mathbf{h}}_{\bar{q}q} = [\mathbf{h}_{\bar{q}q}^T \;\; \mathbf{0}_{1\times(N_s-N)}^T]^T$ is the zero-padded version of the channel vector $\mathbf{h}_{\bar{q}q}$, the $N_s \times 1$ vector $\boldsymbol{\phi}_k$ is the k-th column of the matrix $\mathbf{F}^H$, for $k = 1, 2, \ldots, N_s$, and $\mathbf{F}$ is the DFT matrix, i.e., $[\mathbf{F}]_{k,k'} = \frac{1}{\sqrt{N_s}} e^{-j2\pi(k-1)(k'-1)/N_s}$, for $k, k' = 1, 2, \ldots, N_s$. As a result, $\psi_{\bar{q}q}^k(\mathcal{A})$ is the frequency response of the end-to-end CIR $h_{\bar{q}q}[\cdot]$ at the normalized frequency $\frac{k}{N_s}$.

[4]Note that we drop the factor $1/2(N_s + N)$, where $2(N_s + N)$ is the number of channel uses. As a result, the thresholds b_1 and b_2 are measured in bits.

By using (4.23) and (4.19), the optimization problem in (4.20) can be rewritten as

$$\begin{aligned}
\min_{\mathcal{P},\,\mathcal{A}}.\quad & \sum_{q=1}^{2} p_q \left(1+\sum_{l=1}^{L}\|\mathbf{A}_l\mathbf{g}_{lq}\|^2\right)+\sigma^2\sum_{l=1}^{L} tr(\mathbf{A}_l\mathbf{A}_l^H)\\
\text{subject to}\quad & \log\prod_{k=1}^{N_s}\left(1+\frac{p_{\bar{q}}\,|\psi_{\bar{q}q}^{k}(\mathcal{A})|^2}{\sigma^2\left(\sum_{l=1}^{L}\|\mathbf{A}_l^T\mathbf{g}_{lq}\|^2+1\right)}\right)\geq b_q,\quad \text{for}\quad q,\bar{q}\in\{1,2\}\\
& p_1\geq 0,\quad p_2\geq 0.
\end{aligned} \tag{4.27}$$

We observe that at the optimum, the first two inequality constraints in (4.27) are satisfied with equality. Otherwise, if at the optimum, any of these constraints is satisfied with inequality, the corresponding optimal power can be reduced to satisfy this constraint with equality. This, in turn, decreases the value of the objective function which contradicts the optimality. Hence, we have

$$\sum_{k=1}^{N_s}\log\left(1+\frac{p_{\bar{q}}\,|\psi_{\bar{q}q}^{k}(\mathcal{A})|^2}{\sigma^2\left(\sum_{l=1}^{L}\|\mathbf{A}_l^T\mathbf{g}_{lq}\|^2+1\right)}\right)=b_q. \tag{4.28}$$

Step 2: Change of variables

We now replace the optimization variables p_1 and p_2 with two new sets of optimization variables, *without any loss of optimality*. Let us define the new optimization variables $\{\beta_{\bar{q}q}^{k}\}_{k=1}^{N_s}$, for $q=1,2$, as

$$\beta_{\bar{q}q}^{k}\triangleq\frac{p_{\bar{q}}\,|\psi_{\bar{q}q}^{k}(\mathcal{A})|^2}{\sigma^2\left(\sum_{l=1}^{L}\|\mathbf{A}_l^T\mathbf{g}_{lq}\|^2+1\right)},\ \text{for } k=1,2,\ldots,N_s,\ \text{and } q=1,2. \tag{4.29}$$

Using (4.29), we can then express $p_{\bar{q}}$ as

$$p_{\bar{q}}=\frac{\sigma^2\beta_{\bar{q}q}^{k}}{|\psi_{\bar{q}q}^{k}(\mathcal{A})|^2}\left(\sum_{l=1}^{L}\|\mathbf{A}_l^T\mathbf{g}_{lq}\|^2+1\right),\quad \text{for } k=1,2,\ldots,N_s,\ \text{and } q=1,2 \tag{4.30}$$

It follows from (4.30) that

$$\frac{\beta_{\bar{q}q}^{k}}{|\psi_{\bar{q}q}^{k}(\mathcal{A})|^2}=\frac{\beta_{\bar{q}q}^{k'}}{|\psi_{\bar{q}q}^{k'}(\mathcal{A})|^2},\quad \text{for}\ \ q\in\{1,2\},\text{and } k,k'\in\{1,2,\ldots,N_s\}. \tag{4.31}$$

Using (4.31), we can rewrite (4.30) as

$$p_{\bar{q}}=\frac{\sigma^2}{N_s}\left(\sum_{k=1}^{N_s}\frac{\beta_{\bar{q}q}^{k}}{|\psi_{\bar{q}q}^{k}(\mathcal{A})|^2}\right)\left(\sum_{l=1}^{L}\|\mathbf{A}_l^T\mathbf{g}_{lq}\|^2+1\right),\ \text{for } q=1,2. \tag{4.32}$$

Using (4.28), (4.29), (4.31), and (4.32), we can now rewrite the power minimization problem in (4.27) as

$$
\begin{aligned}
\min_{\boldsymbol{\beta}_1,\boldsymbol{\beta}_2,\mathcal{A}} \ & \frac{\sigma^2}{N_s}\sum_{q=1}^{2}\left\{\left(\sum_{k=1}^{N_s}\frac{\beta_{\bar{q}q}^k}{|\psi_{\bar{q}q}^k(\mathcal{A})|^2}\right)\left(\sum_{l=1}^{L}\|\mathbf{A}_l^T\mathbf{g}_{lq}\|^2+1\right)\left(1+\sum_{l=1}^{L}\|\mathbf{A}_l\mathbf{g}_{l\bar{q}}\|^2\right)\right\} \\
& + \sigma^2\sum_{l=1}^{L} tr(\mathbf{A}_l\mathbf{A}_l^H) \\
\text{subject to} \ & \sum_{k=1}^{N_s}\log(1+\beta_{\bar{q}q}^k) = b_q, \qquad \text{for} \quad q\in\{1,2\} \\
& \frac{\beta_{\bar{q}q}^k}{|\psi_{\bar{q}q}^k(\mathcal{A})|^2} = \frac{\beta_{\bar{q}q}^{k'}}{|\psi_{\bar{q}q}^{k'}(\mathcal{A})|^2}, \qquad \text{for} \ \ q\in\{1,2\}, \ \text{and} \ k,k'\in\{1,2,\ldots,N_s\} \\
& \beta_{\bar{q}q}^k \geq 0, \qquad \text{for} \ k=1,2,\ldots,N_s, \ \text{and} \ q=1,2
\end{aligned} \tag{4.33}
$$

where

$$
\boldsymbol{\beta}_q \triangleq [\beta_{\bar{q}q}^1 \ \ \beta_{\bar{q}q}^2 \ \ \cdots \ \ \beta_{\bar{q}q}^{N_s}]^T, \ \text{for} \ \ q\in\{1,2\} \tag{4.34}
$$

are the two vectors of the new optimization variables.

Step 3: Dimensionality reduction

To reduce the dimensionality of the problem, we use the following lemma:

Lemma 2 *Let* $\mathbf{U}_l$ *be any* $M_l \times 2$ *matrix whose columns span the vector space spanned by* $\mathbf{g}_{l1}$ *and* $\mathbf{g}_{l2}$ *and* $\mathbf{U}_l^H\mathbf{U}_l = \mathbf{I}_2$*. Then, without loss of optimality, the beamforming matrix* $\mathbf{A}_l$ *can be written as*

$$
\mathbf{A}_l = \mathbf{U}_l^*\mathbf{B}_l\mathbf{U}_l^H, \tag{4.35}
$$

where $\mathbf{B}_l$ *is a* 2×2 *complex matrix.*

Proof The proof is similar to the proof of Theorem 3.1 in [29] and also the proof in [141]. ■

The structure of $\mathbf{A}_l$ given in (4.35) can be intuitively explained: According to (4.35), first the signal is multiplied with $\mathbf{U}_l^H$ whose columns span the two-dimensional signal space. Doing so yields a linear estimate for the 2×1 vector of the symbols transmitted by the two transceivers. The so-obtained linear estimate is then rotated via multiplication with $\mathbf{B}_l$, whose role is to ensure that each of the two elements of the linear estimate contains a sufficient amount of corresponding symbol of interest while interference from the other symbol is minimal, and at the same time, the total power is minimized. The matrix $\mathbf{U}_l^*$ guarantees that the so-obtained rotated linearly estimated vector is transmitted on the bases of the signal subspace, and hence, power is not wasted in transmitting over the noise subspace.

Let us define $\mathbf{q}_{l1} \triangleq \mathbf{U}_l^H \mathbf{g}_{l1}$ and $\mathbf{q}_{l2} \triangleq \mathbf{U}_l^H \mathbf{g}_{l2}$ as the effective channels between the l-th relay and Transceivers 1 and 2, respectively. Then, the optimization problem in (4.33) can be equivalently written as

$$\begin{aligned}
\min_{\boldsymbol{\beta}_1, \boldsymbol{\beta}_2, \mathcal{B}} \; & \frac{\sigma^2}{N_s} \sum_{q=1}^{2} \left\{ \left(\sum_{k=1}^{N_s} \frac{\beta_{\bar{q}q}^k}{|\zeta_{\bar{q}q}^k(\mathcal{B})|^2} \right) \left(\sum_{l=1}^{L} \|\mathbf{B}_l^T \mathbf{q}_{lq}\|^2 + 1 \right) \left(1 + \sum_{l=1}^{L} \|\mathbf{B}_l \mathbf{q}_{l\bar{q}}\|^2 \right) \right\} \\
& + \sigma^2 \sum_{l=1}^{L} tr(\mathbf{B}_l \mathbf{B}_l^H) \\
\text{subject to} \; & \sum_{k=1}^{N_s} \log(1 + \beta_{\bar{q}q}^k) = b_q, \qquad \text{for} \quad q \in \{1, 2\} \\
& \frac{\beta_{\bar{q}q}^k}{|\zeta_{\bar{q}q}^k(\mathcal{B})|^2} = \frac{\beta_{\bar{q}q}^{k'}}{|\zeta_{\bar{q}q}^{k'}(\mathcal{B})|^2}, \qquad \text{for} \;\; q \in \{1, 2\}, \text{ and } k, k' \in \{1, 2, \ldots, N_s\} \\
& \beta_{\bar{q}q}^k \geq 0, \qquad \text{for } k = 1, 2, \ldots, N_s, \text{ and } q = 1, 2
\end{aligned} \tag{4.36}$$

where $\mathcal{B} \triangleq \{\mathbf{B}_l\}_{l=1}^L$ is a set of effective beamforming matrices and as shown in Appendix 4.D, we can write

$$\begin{aligned}
\zeta_{\bar{q}q}^k(\mathcal{B}) &\triangleq \psi_{\bar{q}q}^k(\mathcal{A})\Big|_{\{\mathbf{A}_l = \mathbf{U}_l^* \mathbf{B}_l \mathbf{U}_l^H\}_{l=1}^L} \\
&= \sqrt{N_s} \boldsymbol{\phi}_k^H \tilde{\mathbf{h}}_{\bar{q}q}\Big|_{\{\mathbf{A}_l = \mathbf{U}_l^* \mathbf{B}_l \mathbf{U}_l^H\}_{l=1}^L} = \sqrt{N_s} \boldsymbol{\phi}_k^H \begin{bmatrix} \sum_{l=1}^L \mathbf{d}_l \, \mathbf{q}_{lq}^T \mathbf{B}_l \mathbf{q}_{l\bar{q}} \\ \\ \mathbf{0}_{(N_s - N)\times 1} \end{bmatrix}.
\end{aligned} \tag{4.37}$$

In the second equality above, we use (4.24), while in the third equality, we use (4.9) and (4.35) along with the following definition: $\tilde{\mathbf{h}}_{\bar{q}q} = [\mathbf{h}_{\bar{q}q}^T \;\; \mathbf{0}_{1\times(N_s - N)}^T]^T$ to write

$$\mathbf{h}_{\bar{q}q} = \begin{bmatrix} \sum_{l=1}^L \mathbf{d}_l \, \mathbf{q}_{lq}^T \mathbf{B}_l \mathbf{q}_{l\bar{q}} \\ \\ \mathbf{0}_{(N_s - N)\times 1} \end{bmatrix}. \tag{4.38}$$

Note that $\zeta_{\bar{q}q}^k(\mathcal{B})$ now represents the frequency response of the end-to-end CIR $h_{\bar{q}q}[\cdot]$ at the normalized frequency $\frac{k}{N_s}$. Compared to the optimization problem (4.33), the optimization problem (4.36) has a lower dimensionality as matrices $\{\mathbf{B}_l\}_{l=1}^L$ are 2×2, while in (4.33), matrices $\{\mathbf{A}_l\}_{l=1}^L$ are $M_l \times M_l$.

Step 4: Imposing symmetry on beamforming matrices

The optimization problem (4.36) does not appear to be amenable to a computationally efficient solution. To develop such a solution, we now impose the constraint that the beamforming matrices are symmetric, $\mathbf{A}_l^T = \mathbf{A}_l$, or equivalently, $\mathbf{B}_l^T = \mathbf{B}_l$. Hereafter, the optimality is claimed only under the assumption that the relay beamforming matrices are symmetric. Imposing such a constraint renders the end-to-end channel over each relaying path reciprocal, i.e., $\mathbf{q}_{l1}^T\mathbf{B}_l\mathbf{q}_{l2} = \mathbf{q}_{l2}^T\mathbf{B}_l\mathbf{q}_{l1}$, which in turn, in light of (4.37), leads to $\zeta_{12}^k(\mathcal{B}) = \zeta_{21}^k(\mathcal{B})$. Moreover, for such symmetric beamforming matrices, we can write $\|\mathbf{q}_{l1}^T\mathbf{B}_l\| = \|\mathbf{B}_l\mathbf{q}_{l1}\|$ and $\|\mathbf{q}_{l2}^T\mathbf{B}_l\| = \|\mathbf{B}_l\mathbf{q}_{l2}\|$. Defining $\zeta^k(\mathcal{B}) \triangleq \zeta_{12}^k(\mathcal{B}) = \zeta_{21}^k(\mathcal{B})$, we rewrite the optimization problem (4.36) as[5]

$$
\begin{aligned}
\min_{\boldsymbol{\beta}_1,\boldsymbol{\beta}_2,\mathcal{B}} \quad & \frac{\sigma^2}{N_s}\left(\sum_{k=1}^{N_s}\frac{\beta_{12}^k+\beta_{21}^k}{|\zeta^k(\mathcal{B})|^2}\right)\left(1+\sum_{l=1}^{L}\|\mathbf{B}_l\mathbf{q}_{l1}\|^2\right)\left(1+\sum_{l=1}^{L}\|\mathbf{B}_l\mathbf{q}_{l2}\|^2\right)\\
& +\sigma^2\sum_{l=1}^{L} tr(\mathbf{B}_l\mathbf{B}_l^H)\\
\text{subject to} \quad & \sum_{k=1}^{N_s}\log(1+\beta_{q\bar{q}}^k) = b_q, \qquad \text{for } q\in\{1,2\}\\
& \frac{\beta_{\bar{q}q}^k}{|\zeta^k(\mathcal{B})|^2} = \frac{\beta_{\bar{q}q}^k}{|\zeta^{k'}(\mathcal{B})|^2}, \qquad \text{for } q\in\{1,2\}, \text{ and } k,k'\in\{1,2,\ldots,N_s\}\\
& \beta_{\bar{q}q}^k \geq 0, \qquad \text{for } q\in\{1,2\}, \text{ and } k\in\{1,2,\ldots,N_s\}\\
& [\mathbf{B}_l]_{(1,2)} = [\mathbf{B}_l]_{(2,1)}, \qquad \text{for } l\in\{1,2,\ldots,L\}
\end{aligned} \tag{4.39}
$$

where the last set of the constraints emphasizes that the effective beamforming matrices $\{\mathbf{B}_l\}_{l=1}^L$ should be symmetric. Using the following identities: $tr(\mathbf{X}_1\mathbf{X}_2\mathbf{X}_3) = vec(\mathbf{X}_1{}^T)^T\,(\mathbf{I}\otimes\mathbf{X}_2)\,vec(\mathbf{X}_3)$, and $tr(\mathbf{X}_1{}^T\mathbf{X}_2\mathbf{X}_3\mathbf{X}_4{}^T) = vec(\mathbf{X}_1{}^T)^T\,(\mathbf{X}_4\otimes\mathbf{X}_2)\,vec(\mathbf{X}_3)$,

[5]Note also with $\mathbf{A}_l^T = \mathbf{A}_l$, it follows from (4.8) and (4.9), that $h_{12}[\cdot] = h_{21}[\cdot]$ and thus, $\mathbf{h}_{12} = \mathbf{h}_{21}$ holds true, implying that the end-to-end channel is reciprocal.

we can write

$$\|\mathbf{B}_l \mathbf{q}_{l1}\|^2 = \mathbf{b}_l^H (\mathbf{I}_2 \otimes \mathbf{q}_{l1}\mathbf{q}_{l1}^H)\mathbf{b}_l \tag{4.40}$$

$$\|\mathbf{q}_{l2}^T \mathbf{B}_l\|^2 = \mathbf{b}_l^H (\mathbf{q}_{l2}\mathbf{q}_{l2}^H \otimes \mathbf{I}_2)\mathbf{b}_l \tag{4.41}$$

$$tr(\mathbf{B}_l \mathbf{B}_l^H) = \mathbf{b}_l^H \mathbf{b}_l. \tag{4.42}$$

where the following definition is used: $\mathbf{b}_l \triangleq vec(\mathbf{B}_l^H)$, for $l = 1, 2, \ldots, L$. Using (4.40)-(4.42) and defining $\mathbf{b} \triangleq [\mathbf{b}_1^T \ \mathbf{b}_2^T \ ... \ \mathbf{b}_L^T]^T$, we can rewrite the optimization problem (4.39) as

$$\begin{aligned}
\min_{\boldsymbol{\beta}_1, \boldsymbol{\beta}_2, \mathbf{b}} \quad & \frac{\sigma^2}{N_s}\left(\sum_{k=1}^{N_s} \frac{\beta_{12}^k + \beta_{21}^k}{|\zeta^k(\mathbf{b})|^2}\right)\left(1 + \mathbf{b}^H \mathbf{E}_1 \mathbf{b}\right)\left(1 + \mathbf{b}^H \mathbf{E}_2 \mathbf{b}\right) + \sigma^2 \mathbf{b}^H \mathbf{b} \\
\text{subject to} \quad & \sum_{k=1}^{N_s} \log(1 + \beta_{\bar{q}q}^k) = b_q, \quad \text{for } q \in \{1, 2\} \\
& [\mathbf{b}]_{4(l-1)+2} = [\mathbf{b}]_{4(l-1)+3}, \quad \text{for } l \in \{1, 2, \ldots, L\} \\
& \frac{\beta_{\bar{q}q}^k}{|\zeta^k(\mathbf{b})|^2} = \frac{\beta_{\bar{q}q}^{k'}}{|\zeta^{k'}(\mathbf{b})|^2}, \quad \text{for } q \in \{1, 2\}, \text{ and } k, k' \in \{1, 2, \ldots, N_s\} \\
& \beta_{\bar{q}q}^k \geq 0, \quad \text{for } q \in \{1, 2\}, \text{ and } k \in \{1, 2, \ldots, N_s\}
\end{aligned} \tag{4.43}$$

where $\mathbf{E}_1$ and $\mathbf{E}_2$ are defined as

$$\mathbf{E}_1 \triangleq \text{blkdiag}\left(\{\mathbf{I}_2 \otimes \mathbf{q}_{l1}\mathbf{q}_{l1}^H\}_{l=1}^L\right), \quad \mathbf{E}_2 \triangleq \text{blkdiag}\left(\{\mathbf{q}_{l2}\,\mathbf{q}_{l2}^H \otimes \mathbf{I}_2\}_{l=1}^L\right). \tag{4.44}$$

Note that in (4.43), since vector $\mathbf{b}$ includes the vectorized version of matrices $\{\mathbf{B}_l\}_{l=1}^L$, with a small abuse of notation, we write $\zeta^k(\mathbf{b}) = \zeta^k(\mathcal{B})$. Indeed, $\zeta^k(\mathbf{b})$ now represents the frequency response of the end-to-end CIR $h_{\bar{q}q}[\cdot]$ at the normalized frequency $\frac{k}{N_s}$. Using the following definitions: $\mathbf{T} \triangleq \begin{bmatrix} 1 & 0 & 0 \\ 0 & 1 & 0 \\ 0 & 1 & 0 \\ 0 & 0 & 1 \end{bmatrix}$ and $\mathbf{L} \triangleq \mathbf{I}_L \otimes \mathbf{T}$, we can write $\mathbf{b}_l = \mathbf{T}\,\tilde{\mathbf{b}}_l$, where $\tilde{\mathbf{b}}_l = [\ [\mathbf{b}_l]_1 \ [\mathbf{b}_l]_2 \ [\mathbf{b}_l]_4\ ]^T$ is the vector of the free parameters in $\mathbf{b}_l$. Furthermore, $\mathbf{b}$ can be written as $\mathbf{b} = \mathbf{L}\,\tilde{\mathbf{b}}$, where $\tilde{\mathbf{b}} = [\tilde{\mathbf{b}}_1^T \ \tilde{\mathbf{b}}_2^T \ ... \ \tilde{\mathbf{b}}_L^T]^T$. Now, defining $\tilde{\mathbf{E}}_1 \triangleq \mathbf{L}^H\,\mathbf{E}_1\,\mathbf{L}$ and $\tilde{\mathbf{E}}_2 \triangleq \mathbf{L}^H\,\mathbf{E}_2\,\mathbf{L}$ results in the following identities

$$\mathbf{b}^H \mathbf{E}_q \mathbf{b} = \tilde{\mathbf{b}}^H \mathbf{L}^H \mathbf{E}_q \mathbf{L} \tilde{\mathbf{b}} = \tilde{\mathbf{b}}^H \tilde{\mathbf{E}}_q \tilde{\mathbf{b}}, \quad \text{for } q \in \{1, 2\}. \tag{4.45}$$

Identities in (4.45) enable us to rewrite (4.43) as

$$
\begin{aligned}
\min_{\boldsymbol{\beta}_1, \boldsymbol{\beta}_2, \tilde{\mathbf{b}}}. \quad & \frac{\sigma^2}{N_s} \left(\sum_{k=1}^{N_s} \frac{\beta_{12}^k + \beta_{21}^k}{|\zeta^k(\tilde{\mathbf{b}})|^2} \right) \left(1 + \tilde{\mathbf{b}}^H \tilde{\mathbf{E}}_1 \tilde{\mathbf{b}}\right) \left(1 + \tilde{\mathbf{b}}^H \tilde{\mathbf{E}}_2 \tilde{\mathbf{b}}\right) + \sigma^2 \tilde{\mathbf{b}}^H \mathbf{L}^H \mathbf{L} \tilde{\mathbf{b}} \\
\text{subject to} \quad & \sum_{k=1}^{N_s} \log(1 + \beta_{\bar{q}q}^k) = b_q, \quad \text{for } \ q \in \{1, 2\} \\
& \frac{\beta_{\bar{q}q}^k}{|\zeta^k(\tilde{\mathbf{b}})|^2} = \frac{\beta_{\bar{q}q}^{k'}}{|\zeta^{k'}(\tilde{\mathbf{b}})|^2}, \qquad \text{for } \ q \in \{1, 2\}, \text{ and } k, k' \in \{1, 2, \ldots, N_s\} \\
& \beta_{\bar{q}q}^k \geq 0, \qquad\qquad\qquad \text{for } \ q \in \{1, 2\}, \quad \text{ and } k \in \{1, 2, \ldots, N_s\}
\end{aligned} \tag{4.46}
$$

where once more with a small abuse of notation, we write $\zeta^k(\tilde{\mathbf{b}}) = \zeta^k(\mathbf{b})$. Indeed, by using the vectors of free parameters, i.e., $\tilde{\mathbf{b}}$ instead of $\mathbf{b}$, the second set of constraints in (4.43) is automatically satisfied.

Step 5: Relaxation

To solve (4.46), we relax the last two sets of constraints. Let us consider the problem in (4.46) with only the first set of constraints:

$$
\begin{aligned}
\min_{\boldsymbol{\beta}_1, \boldsymbol{\beta}_2, \tilde{\mathbf{b}}}. \quad & \frac{\sigma^2}{N_s} \left(\sum_{k=1}^{N_s} \frac{\beta_{12}^k + \beta_{21}^k}{|\zeta^k(\tilde{\mathbf{b}})|^2} \right) \left(1 + \tilde{\mathbf{b}}^H \tilde{\mathbf{E}}_1 \tilde{\mathbf{b}}\right) \left(1 + \tilde{\mathbf{b}}^H \tilde{\mathbf{E}}_2 \tilde{\mathbf{b}}\right) + \sigma^2 \tilde{\mathbf{b}}^H \mathbf{L}^H \mathbf{L} \tilde{\mathbf{b}} \\
\text{subject to} \quad & \sum_{k=1}^{N_s} \log(1 + \beta_{\bar{q}q}^k) = b_q, \qquad \text{for } \ q \in \{1, 2\}.
\end{aligned} \tag{4.47}
$$

We soon show that such a relaxation will not cause any loss of optimality. In other words, any solution to (4.47) will satisfy the relaxed constraints.

The following lemma enables us to solve (4.47).

Lemma 3 *At the optimum of* (4.47)*, the following equalities*

$$\beta_{12}^k = \beta_{12}^{k'} \qquad \textit{and} \qquad \beta_{21}^k = \beta_{21}^{k'} \tag{4.48}$$

$$|\zeta^k(\tilde{\mathbf{b}})| = |\zeta^{k'}(\tilde{\mathbf{b}})|\,, \quad \textit{for } k, k' \in \{1, 2, \ldots, N_s\}. \tag{4.49}$$

hold true.

Proof See Appendix 4.E. ∎

It follows from (4.48) and (4.49) that at the optimum of (4.47), the relaxed constraints in (4.46) are satisfied with equality. *Hence, any solution to the relaxed problem* (4.47) *is a solution to the original problem* (4.46).

Step 6: Solving the relaxed problem

To solve the relaxed problem, using (4.48) along with the rate constraints in (4.47), we observe that at optimum

$$\beta_{21}^{\mathrm{opt}} \triangleq \beta_{21}^{k} = \beta_{21}^{k'} = 2^{\frac{b_1}{N_s}} - 1 \quad \text{and} \quad \beta_{12}^{\mathrm{opt}} \triangleq \beta_{12}^{k} = \beta_{12}^{k'} = 2^{\frac{b_2}{N_s}} - 1 \tag{4.50}$$

hold true. Note also that as $\zeta(\tilde{\mathbf{b}}) \triangleq \zeta^k(\tilde{\mathbf{b}})$ represents the frequency response of the end-to-end CIR $h[\cdot]$ at the normalized frequency $\frac{k}{N_s}$, we infer from (4.49) that at the optimum, the CIR $h[\cdot]$ must be frequency flat. As this CIR has a finite length, it must have only one non-zero tap. Since each relay contributes only to one of the taps of $h[\cdot]$, we conclude that at the optimum only a *synchronous* subset of the relays (corresponding to the *best* tap) has to be selected and the remainder of the relays will not participate in the relaying (that is, their beamforming matrices are zero). If $\mathcal{C}_n$ stands for the set of the vectors $\tilde{\mathbf{b}}$ which result in the n-th tap of the end-to-end CIR being non-zero, then, based on the fact that no relay contributes to two different taps of the end-to-end CIR, $\mathcal{C}_n \bigcap \mathcal{C}_n' = \emptyset$ holds true for $n \neq n'$. Hence, defining $\mathcal{N} \triangleq \{n \big| 0 \leq n \leq N-1, C_n \neq \emptyset\}$ and using (4.49) and (4.50), the optimization problem (4.47) can be equivalently written as

$$\min_{n\in\mathcal{N}} \min_{\tilde{\mathbf{b}}\in\mathcal{C}_n} \frac{\sigma^2(\beta_{12}^{\mathrm{opt}}+\beta_{21}^{\mathrm{opt}})}{|\zeta(\tilde{\mathbf{b}})|^2}(1+\tilde{\mathbf{b}}^H\tilde{\mathbf{E}}_1\tilde{\mathbf{b}})(1+\tilde{\mathbf{b}}^H\tilde{\mathbf{E}}_2\tilde{\mathbf{b}}) + \sigma^2\tilde{\mathbf{b}}^H\mathbf{L}^H\mathbf{L}\tilde{\mathbf{b}}\,. \tag{4.51}$$

For any $n \in \mathcal{N}$, the inner minimization in (4.51) aims to find the optimal values of the compact version of the vectorized beamforming matrices, i.e., $\tilde{\mathbf{b}}$, while assuming that only relays contributing to the n-th tap of the end-to-end CIR are active. For any $n \in \mathcal{N}$, the value of the objective obtained by solving the inner minimization in (4.51) is the minimum amount of the total power consumed in the *synchronous sub-network* which consists of the relays that contribute to the n-th tap of the end-to-end CIR. The outer minimization aims to determine which of the card(N) synchronous sub-networks results in the least amount of the total power consumption. Note that if none of the relays contributes to the n-th tap of the end-to-end CIR, then $\mathcal{C}_n$ will be empty. Note also that when $\tilde{\mathbf{b}} = [\tilde{\mathbf{b}}_1^T \ \ \tilde{\mathbf{b}}_2^T \ \ \cdots \ \ \tilde{\mathbf{b}}_L^T]^T \in \mathcal{C}_n$, then $\tilde{\mathbf{b}}_l = \mathbf{0}$, if the l-th relay does not contribute to the n-th tap of the end-to-end CIR. For any $n \in \mathcal{N}$, let $\mathbf{a}_n$ be the vector of all $\tilde{\mathbf{b}}_l$'s which corresponds to those relays that contribute to the n-th tap of the end-to-end CIR. That is, for any $n \in \mathcal{N}$, if $\tilde{\mathbf{b}}_{l(n)}$ is the compact version of the vectorized beamforming matrix of the l-th relay which contributes to the n-th tap of the end-to-end CIR, then we define $\mathbf{a}_n \triangleq [\tilde{\mathbf{b}}_{1(n)}^T \ \ \tilde{\mathbf{b}}_{2(n)}^T \ \ \cdots \ \ \tilde{\mathbf{b}}_{K(n)}^T]^T$. Here, $k(n)$ is the index of the k-th relay which contributes to the n-th tap of the end-to-end CIR, and $K(n)$ is the number of the relays which contribute to the n-th tap of the end-to-end CIR. In Appendix 4.F, we show that for $\tilde{\mathbf{b}} \in \mathcal{C}_n$, one can write

$$|\zeta(\tilde{\mathbf{b}})|^2 = \mathbf{a}_n^H \mathbf{f}_n \mathbf{f}_n^H \mathbf{a}_n \tag{4.52}$$

where we define

$$\mathbf{f}_n = [(\mathbf{L}^H vec(\mathbf{q}_{1(n),2}\mathbf{q}_{1(n),1}^T))^T \ \ (\mathbf{L}^H vec(\mathbf{q}_{2(n),2}\mathbf{q}_{2(n),1}^T))^T \cdots (\mathbf{L}^H vec(\mathbf{q}_{K(n),2}\mathbf{q}_{K(n),1}^T)^T]^T. \tag{4.53}$$

Using (4.52), we can rewrite the minimization problem (4.51) as

$$\min_{n\in\mathcal{N}} \min_{\mathbf{a}_n} \ \frac{\sigma^2(\beta_{12}^{\text{opt}}+\beta_{21}^{\text{opt}})(1+\mathbf{a}_n^H\tilde{\mathbf{E}}_1^{(n)}\mathbf{a}_n)(1+\mathbf{a}_n^H\tilde{\mathbf{E}}_2^{(n)}\mathbf{a}_n)}{\mathbf{a}_n^H\mathbf{f}_n\,\mathbf{f}_n^H\mathbf{a}_n} + \sigma^2\mathbf{a}_n^H\mathbf{L}_n^H\mathbf{L}_n\mathbf{a}_n \tag{4.54}$$

where we define $\mathbf{L}_n = \mathbf{I}_{K(n)} \otimes \mathbf{T}$, and $\tilde{\mathbf{E}}_1^{(n)}$ and $\tilde{\mathbf{E}}_2^{(n)}$ are two block diagonal matrices whose diagonal blocks are subsets of those diagonal blocks of $\tilde{\mathbf{E}}_1$ and $\tilde{\mathbf{E}}_2$ corresponding to those relays which contribute to the n-th tap of the end-to-end CIR. More specifically, we define

$$\tilde{\mathbf{E}}_1^{(n)} \triangleq \text{blkdiag}\left(\{\mathbf{I}_2 \otimes \mathbf{q}_{l1}\mathbf{q}_{l1}^H\}_{l=1(n)}^{K(n)}\right), \ \tilde{\mathbf{E}}_2^{(n)} \triangleq \text{blkdiag}\left(\{\mathbf{q}_{l2}\,\mathbf{q}_{l2}^H \otimes \mathbf{I}_2\}_{l=1(n)}^{K(n)}\right). \tag{4.55}$$

For any $n \in \mathcal{N}$, the inner minimization problem in (4.54) amounts to solving the total power minimization problem for the synchronous sub-network which consists of those relays that contribute to the n-th tap of the end-to-end CIR [142], under the assumption that the relays employ symmetric beamforming matrices. As shown in

Chapter 3 (and also in [142]), the solution to the inner minimization of (4.54) can be written as

$$\mathbf{a}_n = \kappa_n \underbrace{(\sigma^2(\beta_{12}^{\text{opt}} + \beta_{21}^{\text{opt}})\tilde{\mathbf{E}}_2^{(n)} + \lambda_n(\rho_n\tilde{\mathbf{E}}_1^{(n)} + \sigma^2\mathbf{L}_n^H\mathbf{L}_n))^{-1}\mathbf{f}_n}_{\triangleq \mathbf{u}_n} \tag{4.56}$$

$$\kappa_n = \sqrt{\frac{\sigma^2(\beta_{12}^{\text{opt}} + \beta_{21}^{\text{opt}})}{\lambda_n\mathbf{u}_n^H(\rho_n\tilde{\mathbf{E}}_1^{(n)} + \sigma^2\mathbf{L}_n^H\mathbf{L}_n)\mathbf{u}_n}} \tag{4.57}$$

where the parameters ρ_n and λ_n are the solutions to the follwoing two nonlinear equations:

$$\sigma^2(\beta_{12}^{\text{opt}} + \beta_{21}^{\text{opt}})\frac{\rho_n^{-2} - \lambda_n\mathbf{u}_n^H\tilde{\mathbf{E}}_1^{(n)}\mathbf{u}_n}{\lambda_n^2\mathbf{u}_n^H(\rho_n\tilde{\mathbf{E}}_1^{(n)} + \sigma^2\mathbf{L}_n^T\mathbf{L}_n)\mathbf{u}_n} = 1 \tag{4.58}$$

$$\rho_n\mathbf{f}_n^H(\sigma^2(\beta_{12}^{\text{opt}} + \beta_{21}^{\text{opt}})\tilde{\mathbf{E}}_2^{(n)} + \lambda_n(\rho_n\tilde{\mathbf{E}}_1^{(n)} + \sigma^2\mathbf{L}_n^H\mathbf{L}_n))^{-1}\mathbf{f}_n = 1. \tag{4.59}$$

Here, $\rho_n \in \left(\frac{\sigma^2(\beta_{12}^{\text{opt}} + \beta_{21}^{\text{opt}})}{\mathfrak{q}_n^H\mathfrak{q}_n}, +\infty\right)$ must hold true, where we define

$$\mathfrak{q}_n \triangleq [\mathbf{q}_{1(n),1}^T \; \mathbf{q}_{2(n),1}^T \; \cdots \; \mathbf{q}_{K(n),1}^T]^T.$$

Note that for any value of $\rho_n \in \left(\frac{\sigma^2(\beta_{12}^{\text{opt}} + \beta_{21}^{\text{opt}})}{\mathfrak{q}_n^H\mathfrak{q}_n}, +\infty\right)$, the nonlinear equation (4.59) has a unique solution for λ_n. As such, λ_n can be viewed as a function of ρ_n, and hence, the non-linear equation (4.58) can be viewed as an equation only in terms of ρ_n. Based on this point of view, it is shown in [140] that (4.58) has a unique solution. As a result, to find ρ_n, one can use a bisection method, where in each step of this method, another bisection algorithm is used to obtain λ_n for intermediate values of ρ_n in the outer bisection method. Once ρ_n and λ_n are obtained, the minimum total transmission power corresponding to the scenario where only those relays which contribute to the n-th tap of the end-to-end CIR are active, can be obtained as [140]

$$\rho_n + \frac{\sigma^2(\beta_{12}^{\text{opt}} + \beta_{21}^{\text{opt}})}{\lambda_n}. \tag{4.60}$$

Hence, the index of the optimal non-zero tap of the end-to-end CIR can be obtained as

$$n^{\text{o}} = \arg\min_{n\in\mathcal{N}} \rho_n + \frac{\sigma^2(\beta_{12}^{\text{opt}} + \beta_{21}^{\text{opt}})}{\lambda_n}. \tag{4.61}$$

Note that if no relay contributes to the n-th tap of the end-to-end CIR, the total transmit power corresponding to that tap will be $+\infty$ and such value of n cannot be optimal. Replacing n in (4.56)-(4.59) with $n^{\rm o}$, we can obtain the optimal vector $\mathbf{a}_{n^{\rm o}} \triangleq [\tilde{\mathbf{b}}^T_{1(n^{\rm o})}\ \tilde{\mathbf{b}}^T_{2(n^{\rm o})}\ \cdots\ \tilde{\mathbf{b}}^T_{K(n^{\rm o})}]^T$. Then the vectorized version of the effective beamforming matrix of the l-th relay which contributes to the $n^{\rm o}$-th tap of the end-to-end CIR can be obtained as $\mathbf{b}_{l(n^{\rm o})} = \mathbf{T}\tilde{\mathbf{b}}_{l(n^{\rm o})}$. Reshaping $\mathbf{b}_{l(n^{\rm o})}$ yields the optimal value of the effective beamforming matrix $\mathbf{B}_{l(n^{\rm o})}$ of the l-th relay which contributes to the $n^{\rm o}$-th tap of the end-to-end CIR, and finally, the optimal value of the beamforming matrix $\mathbf{A}_{l(n^{\rm o})}$ of the l-th relay which contributes to the $n^{\rm o}$-th tap of the end-to-end CIR, can be calculated as $\mathbf{A}_{l(n^{\rm o})} = \mathbf{U}^*_{l(n^{\rm o})}\mathbf{B}_{l(n^{\rm o})}\mathbf{U}^H_{l(n^{\rm o})}$. The beamforming matrix of all those relays which do not contribute to the $n^{\rm o}$-th tap of the end-to-end CIR will be zero. One can then use the so-obtained beamforming matrices to obtain the transceivers transmit powers in closed-forms as

$$p_1 = \frac{\sigma^2\beta_{12}^{\rm opt}\left(1+\sum\limits_{l=1(n^{\rm o})}^{K(n^{\rm o})}\|\mathbf{g}_{l2}^T\mathbf{A}_l\|^2\right)}{\left|\sum\limits_{l=1(n^{\rm o})}^{K(n^{\rm o})}\mathbf{g}_{l2}^T\mathbf{A}_l\ \mathbf{g}_{l1}\right|^2}, \quad p_2 = \frac{\sigma^2\beta_{21}^{\rm opt}\left(1+\sum\limits_{l=1(n^{\rm o})}^{K(n^{\rm o})}\|\mathbf{g}_{l1}^T\mathbf{A}_l\|^2\right)}{\left|\sum\limits_{l=1(n^{\rm o})}^{K(n^{\rm o})}\mathbf{g}_{l1}^T\mathbf{A}_l\ \mathbf{g}_{l2}\right|^2}. \quad (4.62)$$

4.3 Algorithm

To summarize, we proved rigorously that the solution to the total power minimization for an asynchronous two-way network with MIMO relays (which use symmetric beamforming matrices) turns out to be a relay selection scheme, where only those relays which contribute to one of the taps of the end-to-end CIR are active. That is, only a synchronous sub-network of the relays are to be selected. Hence, as proved in the previous section, the network design reduces to finding the best synchronous sub-network which consumes the least amount of power. Once such sub-network is identified, the solution to the network beamforming problem for synchronous two-way MIMO relay networks with symmetric beamforming matrices can be employed to obtain the beamforming matrices.

The following table summarizes the proposed algorithm.

1. Calculate $\beta_{21}^{\text{opt}} = 2^{\frac{b_1}{N_s}} - 1$ and $\beta_{12}^{\text{opt}} = 2^{\frac{b_2}{N_s}} - 1$.

2. For $l = 1, 2, \dots L$, obtain the $M_l \times 2$ matrix $\mathbf{U}_l$ such that its ortho-normal columns span the space spanned by $\mathbf{g}_{l1}$ and $\mathbf{g}_{l2}$. For example, based on Gram-Schmidt approach, choose $\mathbf{U}_l = [\frac{\mathbf{g}_{l1}}{\|\mathbf{g}_{l1}\|} \ \frac{(\mathbf{g}_{l2} - \frac{\mathbf{g}_{l1}^H \mathbf{g}_{l2}}{\|\mathbf{g}_{l1}\|^2}\mathbf{g}_{l1})}{\|(\mathbf{g}_{l2} - \frac{\mathbf{g}_{l1}^H \mathbf{g}_{l2}}{\|\mathbf{g}_{l1}\|^2}\mathbf{g}_{l1})\|}]$. Then calculate $\mathbf{q}_{l1} = \mathbf{U}_l^H \mathbf{g}_{l1}$ and $\mathbf{q}_{l2} = \mathbf{U}_l^H \mathbf{g}_{l2}$, for $l = 1, 2, \dots L$.

3. Set $n = 0$.

4. If no relay contributes to the n-th tap of the end-to-end CIR $h[\cdot]$, i.e., if $d_{l,n} = 0$, for $l = 1, 2, \dots, L$, go to Step 15.

5. Define $\mathbf{q}_n = [\mathbf{q}_{1(n),1}^T \ \mathbf{q}_{2(n),1}^T \ \cdots \ \mathbf{q}_{K(n),1}^T]^T$, where $\mathbf{q}_{l1} = \mathbf{U}_l^H \mathbf{g}_{l1}$ and $\mathbf{q}_{l2} = \mathbf{U}_l^H \mathbf{g}_{l2}$, for $l = 1(n), 2(n), \dots, K(n)$. Here, $k(n)$ is the index of the k-th relay which contributes to the n-th tap of the end-to-end CIR and $K(n)$ is the number of relays which contribute to the n-th tap of the end-to-end CIR.

6. Calculate $\mathbf{E}_1^{(n)} = \text{blkdiag}\left(\{\mathbf{I}_2 \otimes \mathbf{q}_{l1}\mathbf{q}_{l1}^H\}_{l=1(n)}^{K(n)}\right)$ and $\mathbf{E}_2^{(n)} = \text{blkdiag}\left(\{\mathbf{q}_{l2}\,\mathbf{q}_{l2}^H \otimes \mathbf{I}_2\}_{l=1(n)}^{K(n)}\right)$ as well as $\mathbf{L}_n = \mathbf{I}_{K(n)} \otimes \mathbf{T}$, where $\mathbf{T} = \begin{bmatrix} 1 & 0 & 0 \\ 0 & 1 & 0 \\ 0 & 1 & 0 \\ 0 & 0 & 1 \end{bmatrix}$.

7. Define
$$\mathbf{u}_n(\theta, z) \triangleq (\sigma^2(\beta_{12}^{\text{opt}} + \beta_{21}^{\text{opt}})\tilde{\mathbf{E}}_2^{(n)} + \theta(\tilde{\mathbf{E}}_1^{(n)} + \sigma^2 \mathbf{L}_n^H \mathbf{L}_n))^{-1}\mathbf{f}_n$$
where the vector $\mathbf{f}_n$ is obtained as
$$\mathbf{f}_n = [(\mathbf{L}^H vec(\mathbf{q}_{1(n),2}\mathbf{q}_{1(n),1}^T))^T \ \ (\mathbf{L}^H vec(\mathbf{q}_{2(n),2}\mathbf{q}_{2(n),1}^T))^T \ \ \cdots \ \ (\mathbf{L}^H vec(\mathbf{q}_{K(n),2}\mathbf{q}_{K(n),1}^T)^T]^T.$$

8. For any value of $z \in \left(\frac{\sigma^2(\beta_{12}^{\text{opt}} + \beta_{21}^{\text{opt}})}{\mathbf{q}_n^H \mathbf{q}_n}, +\infty\right)$, define function $g_n(\cdot)$ as
$$g_n(z) = 1 - \sigma^2(\beta_{12}^{\text{opt}} + \beta_{21}^{\text{opt}})\frac{z^{-2} - \lambda \mathbf{u}_n^H(\lambda, z)\tilde{\mathbf{E}}_1^{(n)}\mathbf{u}_n(\lambda, z)}{\lambda_n^2 \mathbf{u}_n^H(\lambda, z)(z\tilde{\mathbf{E}}_1^{(n)} + \sigma^2 \mathbf{L}_n^T \mathbf{L}_n)\mathbf{u}_n(\lambda, z)}$$
where for any value of $z \in \left(\frac{\sigma^2(\beta_{12}^{\text{opt}} + \beta_{21}^{\text{opt}})}{\mathbf{q}_n^H \mathbf{q}_n}, +\infty\right)$, the value of λ is obtained, using a bisection method, as the provably unique positive solution to the following non-linear equation:
$$z\mathbf{f}_n^H(\sigma^2(\beta_{12}^{\text{opt}} + \beta_{21}^{\text{opt}})\tilde{\mathbf{E}}_2^{(n)} + \lambda(z\tilde{\mathbf{E}}_1^{(n)} + \sigma^2 \mathbf{L}_n^H \mathbf{L}_n))^{-1}\mathbf{f}_n - 1 = 0.$$

9. To solve $g_n(z) = 0$ in the interval $z \in \left(\frac{\sigma^2(\beta_{12}^{\text{opt}} + \beta_{21}^{\text{opt}})}{\mathbf{q}_n^H \mathbf{q}_n}, +\infty \right)$ using a bisection method, choose z_l as

$$z_l = \frac{\sigma^2(\beta_{12}^{\text{opt}} + \beta_{21}^{\text{opt}})}{\mathbf{q}_n^H \mathbf{q}_n} + \epsilon_1 \tag{4.63}$$

where ϵ_1 is an arbitrarily small positive number such that $g_n(z_l) < 0$. Also, choose z_u large enough such that $g_n(z_u) > 0$.

10. Choose ϵ_2 to be an arbitrarily small positive number. The parameter ϵ_2 determines the precision of the bisection algorithm used to obtain the roots of $g_n(\cdot)$.

11. Choose $z = (z_l + z_u)/2$.

12. If $|g_n(z)| < \epsilon_2$, go to Step 13. If $g_n(z) < -\epsilon_2$, then $z_l = z$. If $g_n(z) > \epsilon_2$, then $z_u = z$. Go to Step 11.

13. Set ρ_n equal to z and use a bisection technique to obtain λ_n as the unique positive solution to the following non-linear equation:

$$\rho_n \mathbf{f}_n^H (\sigma^2(\beta_{12}^{\text{opt}} + \beta_{21}^{\text{opt}})\tilde{\mathbf{E}}_2^{(n)} + \lambda_n(\rho_n \tilde{\mathbf{E}}_1^{(n)} + \sigma^2 \mathbf{L}_n^H \mathbf{L}_n))^{-1} \mathbf{f}_n - 1 = 0.$$

14. Calculate the total transmit power, denoted as P_{T}^n, consumed by the synchronous sub-network, whose relay nodes contribute to the n-th tap of the end-to-end CIR, as

$$P_{\text{T}}^n = \rho_n + \frac{\sigma^2(\beta_{12}^{\text{opt}} + \beta_{21}^{\text{opt}})}{\lambda_n} \tag{4.64}$$

15. Set $n = n + 1$. If $n \geq N$, go to Step 16, otherwise go to Step 4.

16. Find the optimal value of the only non-zero tap index of the end-to-end CIR as

$$n^{\text{o}} = \arg \min_{n \in \mathcal{N}} P_{\text{T}}^n. \tag{4.65}$$

17. Obtain $\mathbf{a}_{n^{\text{o}}} = [\tilde{\mathbf{b}}_{1(n^{\text{o}})}^T \ \tilde{\mathbf{b}}_{2(n^{\text{o}})}^T \ \cdots \ \tilde{\mathbf{b}}_{K(n^{\text{o}})}^T]^T$ using

$$\mathbf{a}_{n^{\text{o}}} = \kappa_{n^{\text{o}}} \underbrace{(\sigma^2(\beta_{12}^{\text{opt}} + \beta_{21}^{\text{opt}})\tilde{\mathbf{E}}_2^{(n^{\text{o}})} + \lambda_{n^{\text{o}}}(\rho_{n^{\text{o}}} \tilde{\mathbf{E}}_1^{(n^{\text{o}})} + \sigma^2 \mathbf{L}_{n^{\text{o}}}^H \mathbf{L}_{n^{\text{o}}}))^{-1} \mathbf{f}_{n^{\text{o}}}}_{\triangleq \mathbf{u}_{n^{\text{o}}}}$$

where $\kappa_{n^{\text{o}}}$ is obtained as

$$\kappa_{n^{\text{o}}} = \sqrt{\frac{\sigma^2(\beta_{12}^{\text{opt}} + \beta_{21}^{\text{opt}})}{\lambda_{n^{\text{o}}} \mathbf{u}_{n^{\text{o}}}^H (\rho_{n^{\text{o}}} \tilde{\mathbf{E}}_1^{(n^{\text{o}})} + \sigma^2 \mathbf{L}_{n^{\text{o}}}^H \mathbf{L}_{n^{\text{o}}}) \mathbf{u}_{n^{\text{o}}}}}.$$

18. The vectorized version of the effective beamforming matrix of the l-th relay which contributes to the n^{o}-th tap of the end-to-end CIR can be obtained as $\mathbf{b}_{l(n^{\text{o}})} = \mathbf{T}\tilde{\mathbf{b}}_{l(n^{\text{o}})}$.

19. Reshape $\mathbf{b}_{l(n^{\mathrm{o}})}$ to obtain the optimal value of the effective beamforming matrix $\mathbf{B}_{l(n^{\mathrm{o}})}$ of the l-th relay which contributes to the n^{o}-th tap of the end-to-end CIR, and finally, obtain the optimal value of the beamforming matrix $\mathbf{A}_{l(n^{\mathrm{o}})}$ of the l-th relay which contributes to the n^{o}-th tap of the end-to-end CIR as $\mathbf{A}_{l(n^{\mathrm{o}})} = \mathbf{U}^{*}_{l(n^{\mathrm{o}})}\mathbf{B}_{l(n^{\mathrm{o}})}\mathbf{U}^{H}_{l(n^{\mathrm{o}})}$. The beamforming matrix of all those relays which do not contribute to the n^{o}-th tap of the end-to-end CIR will be zero.

20. Use the so-obtained beamforming matrices to obtain the transceivers' transmit powers in closed-forms as:

$$p_1 = \frac{\sigma^2\beta_{12}^{\mathrm{opt}}\left(1+\sum\limits_{l=1(n^{\mathrm{o}})}^{K(n^{\mathrm{o}})}\|\mathbf{g}_{l2}^T\mathbf{A}_l\|^2\right)}{\left|\sum\limits_{l=1(n^{\mathrm{o}})}^{K(n^{\mathrm{o}})}\mathbf{g}_{l2}^T\mathbf{A}_l\ \mathbf{g}_{l1}\right|^2},\quad p_2 = \frac{\sigma^2\beta_{21}^{\mathrm{opt}}\left(1+\sum\limits_{l=1(n^{\mathrm{o}})}^{K(n^{\mathrm{o}})}\|\mathbf{g}_{l1}^T\mathbf{A}_l\|^2\right)}{\left|\sum\limits_{l=1(n^{\mathrm{o}})}^{K(n^{\mathrm{o}})}\mathbf{g}_{l1}^T\mathbf{A}_l\ \mathbf{g}_{l2}\right|^2}. \tag{4.66}$$

Remark 1: To evaluate the computational complexity of the proposed method, let us assume that all relays have the same number of (say M) antennas. As the first step, one has to obtain $\mathbf{U}_l$ from $[\mathbf{g}_{l1}\quad \mathbf{g}_{l2}]$ as $\mathbf{U}_l = [\mathbf{g}_{l1}\quad (\mathbf{g}_{l2} - \frac{\mathbf{g}_{l1}^T\mathbf{g}_{l2}}{\|\mathbf{g}_{l1}\|^2}\mathbf{g}_{l1})]$. As a result, the complexity of calculating $\mathbf{U}_l$ is $\mathcal{O}(M)$, and hence, the complexity of calculating $\{\mathbf{U}_l\}_{l=1}^{L}$ is $\mathcal{O}(LM)$. Also, the computational complexity of $\{\mathbf{q}_{l1}\}_{l=1}^{L}$ and $\{\mathbf{q}_{l2}\}_{l=1}^{L}$ is $\mathcal{O}(LM)$. Then, in Steps 4 to 15, one has to obtain the values of ρ_n and λ_n for all possible values of n between 0 and $N-1$, (see (4.61)). For any possible value of n, the proposed symmetric beamforming technique involves finding ρ_n, as the unique root of (4.58), using a simple bisection technique. In each iteration of this bisection technique, one has to find the unique positive root of (4.59) for a given value of ρ_n using another simple bisection technique, thereby obtaining λ_n. Both bisection methods converge very fast [128]. The number of iterations in these two bisection methods is insensitive to the problem under consideration [128]. As a result, the main computational complexity of the proposed algorithm resides in evaluating the left-hand sides of (4.58) and (4.59). Since the size of $\mathbf{u}_n$ is $3K(n)\times 1$ and $\tilde{\mathbf{E}}_1^{(n)}$ and $\mathbf{L}_n^T\mathbf{L}_n$ are $3K(n)\times 3K(n)$ block diagonal matrices, the complexity of computing the quadratic terms in (4.58) is $\mathcal{O}(K(n))$. The complexity of finding λ_n using (4.59) is also $\mathcal{O}(K(n))$ as $\tilde{\mathbf{E}}_1^{(n)}$, $\tilde{\mathbf{E}}_2^{(n)}$, and $\mathbf{L}_n^T\mathbf{L}_n$ are $3K(n)\times 3K(n)$ block diagonal matrices. Hence, evaluating ρ_n requires a computational complexity of order $K(n)$. Given that complexity of calculating λ_n is also $\mathcal{O}(K(n))$, we conclude that for any value of n, evaluating the cost function of (4.61) has a computational complexity of order $K(n)$. Therefore, the worst-case computational complexity of Steps 4 to 15 of the proposed algorithm is $\max_{0 \leq n \leq N-1} \mathcal{O}(K(n))$. Given the fact that a maximum of L relays can contribute to the tap n of the end-to-end CIR (i.e., $K(n) \leq L$), we conclude that the worst-case computational complexity of these steps of the proposed algorithm is $\mathcal{O}(L)$. It is worth mentioning that the maximum number of possible values of n is equal to the number of the relays L. Indeed, when each relay contributes to a distinct tap of the end-to-end CIR (i.e., when no two relays contribute to the same tap), then number of possible values of n is equal to L. If, on the other hand, all relays contribute to one tap of the end-to-end CIR, then the number of possible values of n is equal to 1. Hence, number of points in the search space of the minimization problem (4.61) ranges from 1 to L.

Once the index of the optimal non-zero tap of the end-to-end CIR is obtained, the corresponding vector $\mathbf{a}_{n^{\mathrm{o}}}$, can be determined using (4.56)-(4.57) with a computational complexity $\mathcal{O}(K(n^{\mathrm{o}}))$. Then one can use the reshaping operations and obtain the vectors $\{\tilde{\mathbf{b}}_{l(n^{\mathrm{o}})}\}_{l(n^{\mathrm{o}})=1(n^{\mathrm{o}})}^{K(n^{\mathrm{o}})}$ from the vector $\mathbf{a}_{(n^{\mathrm{o}})}$, the vectors $\{\mathbf{b}_{l(n^{\mathrm{o}})}\}_{l(n^{\mathrm{o}})=1(n^{\mathrm{o}})}^{K(n^{\mathrm{o}})}$ from the vectors $\{\tilde{\mathbf{b}}_{l(n^{\mathrm{o}})}\}_{l(n^{\mathrm{o}})=1(n^{\mathrm{o}})}^{K(n^{\mathrm{o}})}$, and the effective beamforming matrices $\{\mathbf{B}_l\}_{l=1(n^{\mathrm{o}})}^{K(n^{\mathrm{o}})}$ from the vectors $\{\mathbf{b}_{l(n^{\mathrm{o}})}\}_{l(n^{\mathrm{o}})=1(n^{\mathrm{o}})}^{K(n^{\mathrm{o}})}$, respectively. Since reshaping can be done by changing the indices, determining the matrices $\{\mathbf{B}_l\}_{l=1(n^{\mathrm{o}})}^{K(n^{\mathrm{o}})}$ from the vector $\mathbf{a}_{(n^{\mathrm{o}})}$ does not require any computation. The computational complexity of obtaining each of the beamforming matrices $\mathbf{A}_{l(n^{\mathrm{o}})} = \mathbf{U}_{l(n^{\mathrm{o}})}^{*} \mathbf{B}_{l(n^{\mathrm{o}})} \mathbf{U}_{l(n^{\mathrm{o}})}^{H}$ for $l(n^{\mathrm{o}}) \in \{1(n^{\mathrm{o}}), \ldots, K(n^{\mathrm{o}})\}$ is $\mathcal{O}(M)$. As a results, obtaining $\{\mathbf{A}_{l(n^{\mathrm{o}})}\}_{l(n^{\mathrm{o}})=1(n^{\mathrm{o}})}^{K(n^{\mathrm{o}})}$ has a computational complexity $\mathcal{O}(MK(n^{\mathrm{o}}))$. Once, the beamforming matrices are obtained, one can obtain the transceiver powers as in (4.62). The complexity of calculating the transceiver powers using (4.62) is $\mathcal{O}(MK(n^{\mathrm{o}}))$. Therefore, the worst-case computational complexity of Steps 16 to 20 of the proposed algorithm is $\mathcal{O}(ML)$. This worst-case computational complexity corresponds to the case when each relay contributes to a distinct tap of the end-to-end CIR. To summarize, we conclude that the worst-case computational complexity of the proposed algorithm is $\mathcal{O}(ML)$.

Remark 2 : It is worth mentioning that in asynchronous two-way relay networks, minimizing the total relay power is an interesting problem. Our result is however not applicable to the problem of total relay power minimization. Note also that minimizing the total relay power may lead to high power consumption at the transceivers, and in turn, could result in high total power consumption in the network.

Remark 3: It is worth emphasizing that the proposed method is amenable to a distributed implementation where the selected (activated) relays require only their local channel estimation along with a few common parameters that they all receive from the two transceivers. Indeed, as the proposed solution ends up being the selection of the most power-optimal synchronous sub-network, the distributed implementation presented in [140], which is applicable to any synchronous network, can be used to implement the proposed method in a distributed manner. We refer our reader to [140] for the details of this distributed implementation. In [140], two different approaches are presented for acquisition of channel state information. These approaches can also be used for the method which is developed herein for asynchronous networks.

4.4 Numerical Simulations

Considering the average value of the total transmission power consumed in the entire network as the measure of performance, we aim to evaluate the performance of an asynchronous two-way network consisting of two single-antenna transceivers which wish to exchange information with the help of L relays. In our simulations, each of the assisting relays is assumed to be equipped with M antennas and the relays' beamforming matrices are assumed to be symmetric.

Considering two fixed geographical points for transceivers positions at $(-5000\ m, 0\ m)$ and $(5000\ m, 0\ m)$, we assume that relays are randomly distributed in an area with dimension $5000\ m \times 5000\ m$ and centered around the middle point $(0\ m, 0\ m)$ of the line connecting the two transceivers. The path-loss exponent is considered to be 3.8 and the standard deviation of the shadowing effect is

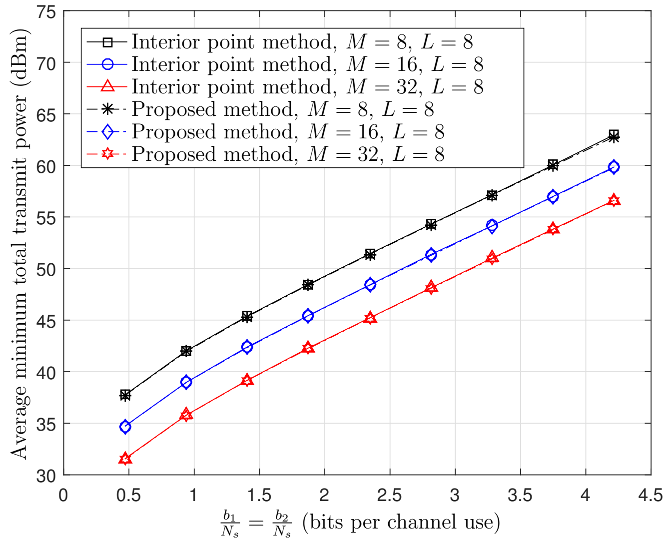

Figure 4.2: Comparison of the proposed method with the interior point method used to solve (4.27), without symmetric beamforming matrix assumption.

assumed to be 8 dB. The coefficients of the channels corresponding to the small-scale fading are modeled as complex Gaussian random variables with zero mean and unit variance. The noises received at the relays and at the transceivers are zero-mean spatially and temporally white Gaussian random processes with variance $\sigma^2 = -130$ dBm.

In Fig. 4.2, we compare the performance of the proposed method (which relies on symmetric beamforming matrix assumption) with a technique which relies on interior point method to solve (4.27), without symmetric beamforming matrix assumption[6]. As can be seen from this figure, the two methods perform very close to each other. In Fig. 4.3, we compare the performance of the proposed scheme with that of the interior point method for an arbitrarily chosen channel realization, but for 100 different random initialization points. In this figure, we choose $M = 8$ and $L = 8$ and plot the performance curves for three different values of $b_1 = b_2$. This figure shows that in these examples, for any of the 100 random initialization points, the interior point method performs very close to the proposed technique. These observations lead us to conjecture that the proposed method yields the optimal solution. Proving or

[6]Note that the latter method uses random initial point for each simulation run and it can trap in local optimal points.

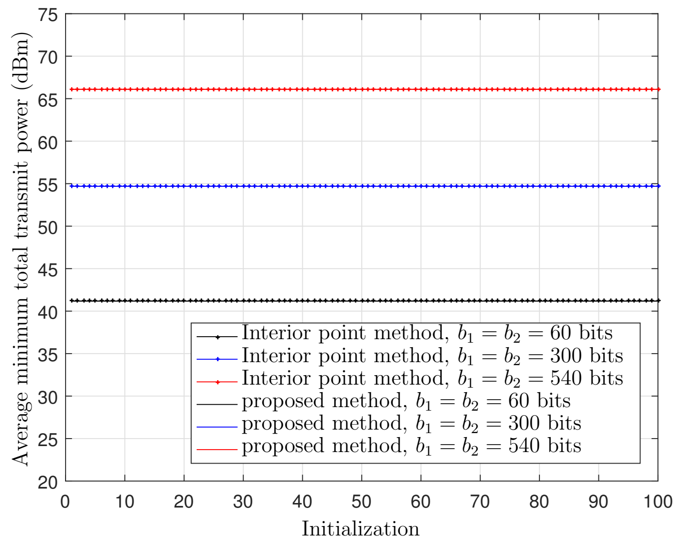

Figure 4.3: The average minimum total transmit power for the proposed method and that for interior point method for 100 different initialization, for $L = 8$ and $M = 8$ and different values of $b_1 = b_2$.

disproving this conjecture does not fit in the scope of this study.

Fig. 4.4 shows the average minimum total transmit power required for satisfying a range of data rate thresholds for networks with different numbers of relays. Each relay is assumed to be equipped with $M = 8$ antennas. Fig. 4.5 depicts the average minimum total transmit power versus data rate thresholds for networks with the same number of relays ($L = 8$), but with different numbers of antennas per relay (i.e., $M = 8, 16, 32, 64$). As can be seen from Fig. 4.4, for fixed number of antennas per relay, doubling the number of relays reduces the average minimum total transmit power by 1.96 to 2.31 dB over the considered range of rate thresholds. On the other hand, Fig. 4.5 shows that in networks with fixed number of relays, doubling the number of antennas per relay reduces the minimum total transmit power by 3.03 to 3.13 dB over the same range of rate thresholds.

In Fig. 4.6, we consider four asynchronous networks with $L = 8$ relays, but with different numbers of antennas per relay (i.e., $M = 8, 16, 32, 64$) and compare the performance of each of such asynchronous networks with that of a synchronous network which has the same number of relays as the corresponding asynchronous network se-

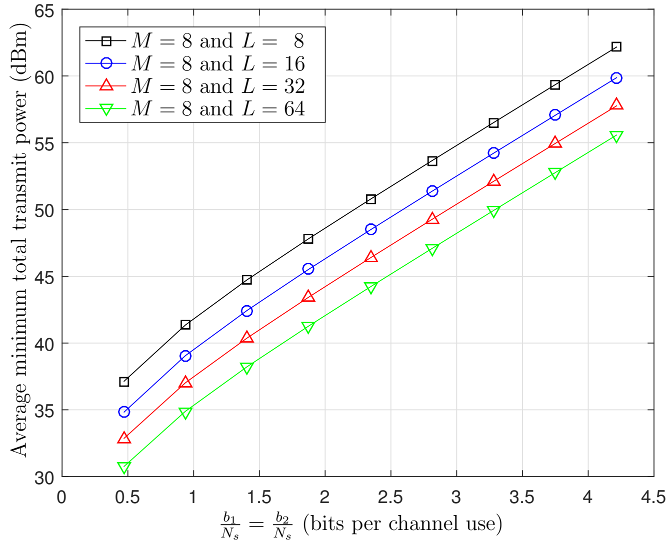

Figure 4.4: The average minimum total transmit power versus equal rate thresholds, for $L \in \{8, 16, 32, 64\}$ and $M = 8$.

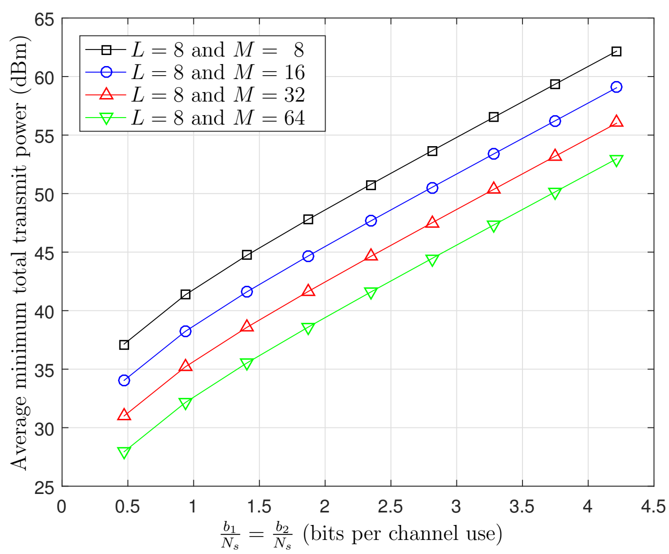

Figure 4.5: The average minimum total transmit power, versus $b_1/N = b_2/N$, for networks with $L = 8$, $M \in \{8, 16, 32, 64\}$.

lects. More specifically, once the solution to the asynchronous network is obtained for a given channel realization, we obtain the solution to a synchronous network which has the same number of relays as the asynchronous network activates, while assuming that those relays are causing minimal propagation delay. In order for relays employed in the synchronous network to be able to transfer symbols synchronously, i.e., without time misalignment, we assume that those relays are randomly distributed in an area with dimension of 540 $m \times 540$ m centered at the middle point $(0\ m, 0\ m)$ between the two transceivers. Fig. 4.6 shows that the total transmit power required for the asynchronous network to achieve a certain rate threshold is less than that for the corresponding synchronous network. we can also observe that with increasing the number of antennas per relay from $M = 8$ to $M = 16$, to $M = 32$, and then to $M = 64$, the performance gap between the two networks remains around 11 dB. This superior performance of the asynchronous networks in comparison with their synchronous counterparts can be explained by the fact that in each asynchronous scheme, the proposed algorithm chooses the best set of synchronous relays which results in the lowest power consumption, and hence, this algorithm exploits the spatial diversity of the relays. In the synchronous networks such spatial diversity does not exist.

Fig. 4.7 illustrates the comparison of the performance of our proposed scheme/method (for $M = 8, 32$, and $L = 8$), with that of the asynchronous two-way network of [1] with ML single-antenna relays. The latter network can be viewed as a special case of the proposed scheme when the relay beamforming matrices are restricted to be diagonal. As can be seen from this figure, the proposed scheme can outperform the scheme of [1] by 1.6 to 6.5 dB depending on the required data rates and the total number of available antennas, i.e., ML. The superior performance of the proposed scheme is due to the advantages offered by local beamforming at the relays. Note that based on Remark 1, the computational complexity of the method of [1] for an asynchronous network with ML single-antenna relays is the same as that of the proposed method.

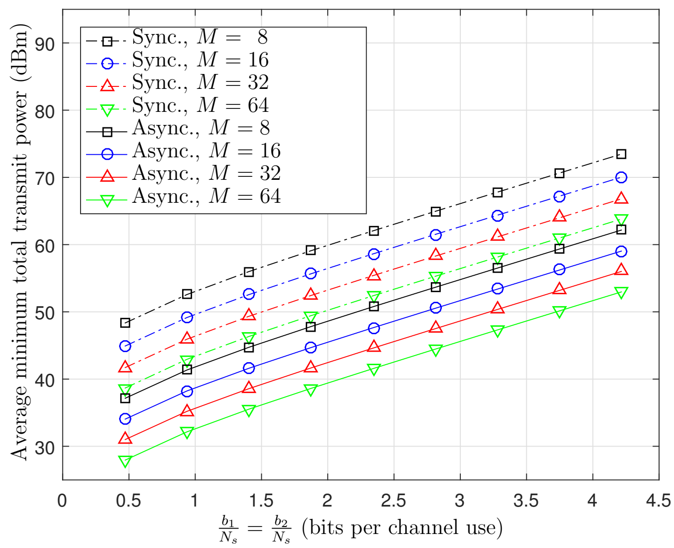

Figure 4.6: A comparison between synchronous and asynchronous networks: The average minimum total transmit power versus equal rate thresholds for $M \in \{8, 16, 32, 64\}$.

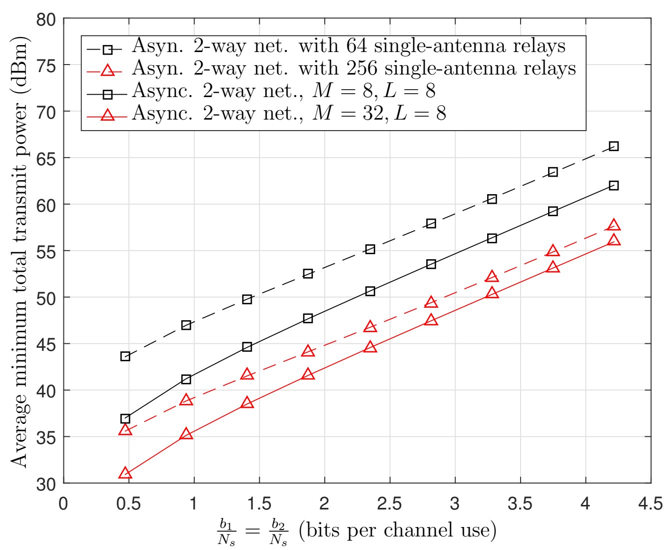

Figure 4.7: The comparison between the proposed scheme and the multiple single-antenna scheme of [1]: the average minimum total transmit power obtained vs. rate.

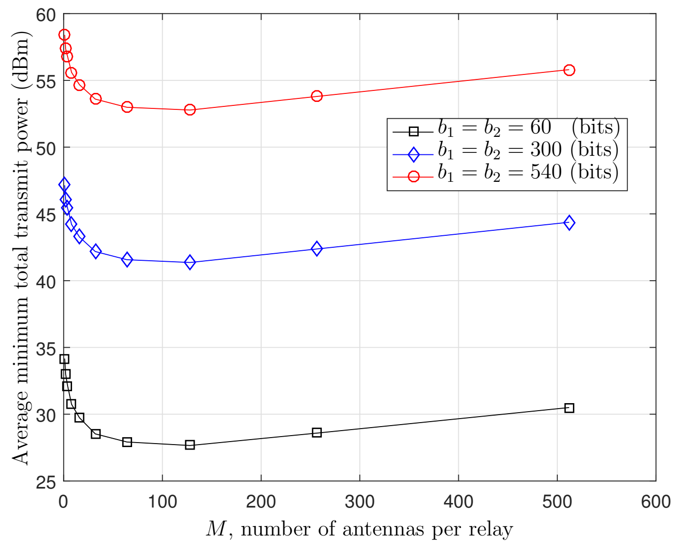

Figure 4.8: The average minimum total transmit power versus total number of antennas per relay, for $ML = 512$.

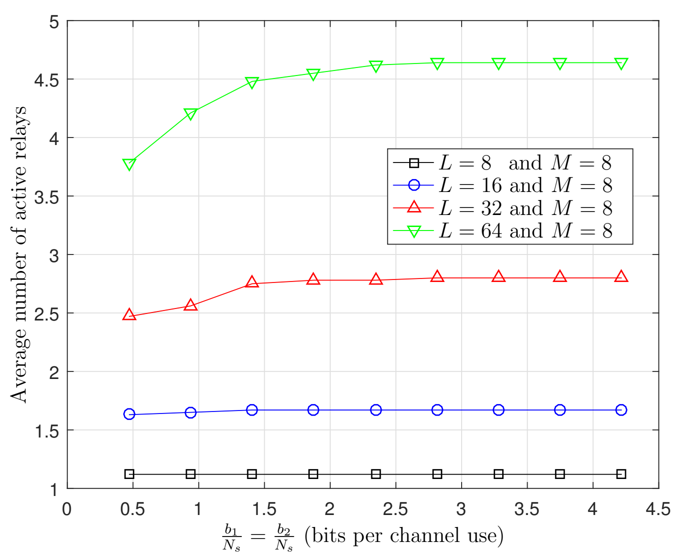

Figure 4.9: The average number of active relays versus rate threshold, for $M = 8$ and $L \in \{8, 16, 32, 64\}$.

In Fig. 4.8, assuming a fixed number of total antennas employed in the entire network, i.e., $ML = 512$, we plot the average minimum total transmit power versus the number of antennas per relay. Interestingly, this figure shows that there is an optimal number of antennas per relay which results in the minimum power consumption for the given required rates. This phenomenon can be explained as the result of two factors which affect the power performance of the network. When M is low, the network will benefit from the fact that a relatively large number of relays are distributed in the coverage area, and hence, on average, the distance of the transceivers from the closest relay will be relatively smaller. On the other hand, when M is low, the degrees of freedom for local beamforming at each relay is rather small. When M is large, such degrees of freedom will be relatively large while the number of relays will be small leading to an increase in the average distance of the transceivers from the relays. When M is increased, the degrees of freedom available for local beamforming increases, and at the same time, the average distances of the two transceivers form relays also increase. These two conflicting factors, i.e., the degrees of freedom available for local beamforming at the relays and the average distance of the two transceivers form the relays result in the performance trade-off shown in Fig. 4.8. That is, there appears to be an optimal number of antennas per relay which leads to the best power performance among all possible configurations of the available antennas. As shown in Fig. 4.8, for the given rates, the optimal value of M is 128 antennas and the number of relays is 4. Note that since the total number of antennas is fixed i.e., $ML = 512$, when $M = 512$ is chosen, the number of relays will be only 1 and the proposed algorithm calculates the power-optimal beamforming matrix (with the size 512×512) for this relay. When $M = 128$ is chosen, then the number of available relays is 4, and the proposed algorithm benefits form the spatial diversity offered by selecting the best subset of relays which leads to the least amount of power consumption. However, when $M = 512$ is chosen, such spatial diversity does not exist, as there is only one relay in the network. It is worth mentioning that as Fig. 4.8 shows, when reducing M from 512 to 128, exploiting this spatial diversity overcomes the loss in the number of degrees of freedom available for local beamforming. Fig. 4.8 also shows that as M is further reduced (and thus the number of available relays is increased), although the spatial diversity increases, the gain achieved by exploiting the spatial diversity cannot compensate for the loss in the number of degrees of freedom available for local beamforming.

In Fig. 4.9, we show the average number of active relays (which contribute to the optimal tap of the end-to-end CIR) versus the equal rate thresholds. As shown in this figure, for fixed M, for the scenario considered here, a small portion of the relays are selected and this portion does not change significantly with the rate thresholds.

Appendices

4.A Derivation of (4.18)

To derive (4.18), we can write

$$
\begin{aligned}
P_l \triangleq & \frac{1}{N_t} E\{\mathbf{1}^T \mathbf{T}_l^H(i) \mathbf{T}_l(i) \mathbf{1})\} = \frac{1}{N_t} E\{\mathbf{1}^T \mathbf{X}_l^H(i) \mathbf{A}_l^H \mathbf{A}_l \mathbf{X}_l(i) \mathbf{1}\} \\
= & \frac{1}{N_t} E\left\{\mathbf{1}^T (\sqrt{p_1}\, \bar{\mathbf{s}}_1^*\, \mathbf{g}_{l1}^H + \sqrt{p_2}\, \bar{\mathbf{s}}_2^*\, \mathbf{g}_{l2}^H + \mathbf{\Gamma}_l^H) \mathbf{A}_l^H \mathbf{A}_l (\sqrt{p_1}\, \mathbf{g}_{l1} \bar{\mathbf{s}}_1^T + \sqrt{p_2}\, \mathbf{g}_{l2} \bar{\mathbf{s}}_2^T + \mathbf{\Gamma}_l) \mathbf{1}\right\} \\
= & \frac{p_1}{N_t} E\{\mathbf{1}^T \bar{\mathbf{s}}_1^*\, \mathbf{g}_{l1}^H \mathbf{A}_l^H \mathbf{A}_l \mathbf{g}_{l1} \bar{\mathbf{s}}_1^T \mathbf{1}\} + \frac{p_2}{N_t} E\{\mathbf{1}^T \bar{\mathbf{s}}_2^*\, \mathbf{g}_{l2}^H \mathbf{A}_l^H \mathbf{A}_l \mathbf{g}_{l2} \bar{\mathbf{s}}_2^T \mathbf{1}\} + \frac{1}{N_t} E\{\mathbf{1}^T \mathbf{\Gamma}_l^H \mathbf{A}_l^H \mathbf{A}_l \mathbf{\Gamma}_l \mathbf{1}\} \\
= & \frac{p_1}{N_t} \mathbf{g}_{l1}^H \mathbf{A}_l^H \mathbf{A}_l \mathbf{g}_{l1} E\{\mathbf{1}^T \bar{\mathbf{s}}_1^*\, \bar{\mathbf{s}}_1^T \mathbf{1}\} + \frac{p_2}{N_t} \mathbf{g}_{l2}^H \mathbf{A}_l^H \mathbf{A}_l \mathbf{g}_{l2} E\{\mathbf{1}^T \bar{\mathbf{s}}_2^*\, \bar{\mathbf{s}}_2^T \mathbf{1}\} + \frac{1}{N_t} E\{\mathbf{1}^T \mathbf{\Gamma}_l^H \mathbf{A}_l^H \mathbf{A}_l \mathbf{\Gamma}_l \mathbf{1}\} \\
= & p_1 \mathbf{g}_{l1}^H \mathbf{A}_l^H \mathbf{A}_l \mathbf{g}_{l1} + p_2 \mathbf{g}_{l2}^H \mathbf{A}_l^H \mathbf{A}_l \mathbf{g}_{l2} + \sigma^2 tr(\mathbf{A}_l \mathbf{A}_l^H) \\
= & p_1 \|\mathbf{A}_l \mathbf{g}_{l1}\|^2 + p_2 \|\mathbf{A}_l \mathbf{g}_{l2}\|^2 + \sigma^2 tr(\mathbf{A}_l \mathbf{A}_l^H). \qquad (4.A.1)
\end{aligned}
$$

4.B Calculation of the noise correlation matrix at Transceiver q

To calculate $\mathbf{C}_q$, we write

$$\begin{aligned}
\mathbf{C}_q &\triangleq E\{\tilde{\boldsymbol{\eta}}_q\tilde{\boldsymbol{\eta}}_q^H\} = \mathbf{R}_{\mathrm{cp}}E\{\boldsymbol{\eta}_q\boldsymbol{\eta}_q^H\}\mathbf{R}_{\mathrm{cp}}^H \\
&= \mathbf{R}_{\mathrm{cp}}E\left\{\left(\sum_{l=1}^{L}\boldsymbol{\Gamma}_l^T\mathbf{A}_l^T\mathbf{g}_{lq} + \boldsymbol{\eta}'_q\right)\left(\sum_{l=1}^{L}\boldsymbol{\Gamma}_l^T\mathbf{A}_l^T\mathbf{g}_{lq} + \boldsymbol{\eta}'_q\right)^H\right\}\mathbf{R}_{\mathrm{cp}}^H \\
&= \mathbf{R}_{\mathrm{cp}}\left(E\left\{\sum_{l=1}^{L}\boldsymbol{\Gamma}_l^T\mathbf{A}_l^T\mathbf{g}_{lq}\mathbf{g}_{lq}^H\mathbf{A}_l^*\boldsymbol{\Gamma}_l^*\right\} + E\left\{\boldsymbol{\eta}'_q{\boldsymbol{\eta}'_q}^H\right\}\right)\mathbf{R}_{\mathrm{cp}}^H \\
&= \mathbf{R}_{\mathrm{cp}}\left(E\left\{\sum_{l=1}^{L}\boldsymbol{\Gamma}_l^T\mathbf{A}_l^T\mathbf{g}_{lq}\mathbf{g}_{lq}^H\mathbf{A}_l^*\boldsymbol{\Gamma}_l^*\right\} + \sigma^2\mathbf{I}_{N_t}\right)\mathbf{R}_{\mathrm{cp}}^H \\
&= \mathbf{R}_{\mathrm{cp}}\left(\left(\sum_{l=1}^{L}\mathbf{g}_{lq}^H\mathbf{A}_l^*\mathbf{A}_l^T\mathbf{g}_{lq} + 1\right)\sigma^2\mathbf{I}_{N_t}\right)\mathbf{R}_{\mathrm{cp}}^H \\
&= \sigma^2\left(\sum_{l=1}^{L}\|\mathbf{A}_l^T\mathbf{g}_{lq}\|^2 + 1\right)\mathbf{I}_{N_s} \qquad (4.B.1)
\end{aligned}$$

where we used the fact that $\mathbf{R}_{\mathrm{cp}} = [\mathbf{0}_{N_s\times N}\ \mathbf{I}_{N_s}]$, and $\mathbf{R}_{\mathrm{cp}}\mathbf{R}_{\mathrm{cp}}^H = \mathbf{I}_{N_s}$. Note that in the sixth equality, we have omitted straightforward derivations.

4.C Derivation of (4.23)

To derive (4.23), we note that the circulant matrix $\tilde{\mathbf{H}}_{\bar{q}q}(\mathcal{A})$ can be decomposed using a DFT matrix [139], denoted by $\mathbf{F}$, i.e.,

$$\tilde{\mathbf{H}}_{\bar{q}q}(\mathcal{A}) = \mathbf{F}^H \mathbf{D}_{\bar{q}q}(\mathcal{A}) \mathbf{F} \tag{4.C.1}$$

where $[\mathbf{F}]_{k,k'} = \frac{1}{\sqrt{N_s}} e^{-j2\pi(k-1)(k'-1)/N_s}$, and $\mathbf{D}_{\bar{q}q}(\mathcal{A}) \triangleq \text{diag}\{H_{\bar{q}q}(e^{j0}), H_{\bar{q}q}(e^{j2\pi/N_s}), \ldots, H_{\bar{q}q}(e^{j2\pi(N_s-1)/N_s})\}$ is defined as an $N_s \times N_s$ diagonal matrix of the frequency response of the end-to-end CIR, $h_{\bar{q}q}[\cdot]$ at integer multiples of $\frac{1}{N_s}$, that is, $H_{\bar{q}q}(e^{j2\pi f}) = \sum_{n=0}^{N-1} h_{\bar{q}q}(n) e^{-j2\pi f n}$. By substituting (4.C.1) and (4.22) in (4.21), $R_q(\mathcal{A}, p_{\bar{q}})$ can be recast as

$$\begin{aligned}
R_q(\mathcal{A}, p_{\bar{q}}) &= \log\det\left(\mathbf{I}_{N_s} + p_{\bar{q}} \mathbf{C}_q^{-\frac{1}{2}} \tilde{\mathbf{H}}_{\bar{q}q}(\mathcal{A}) \tilde{\mathbf{H}}_{\bar{q}q}^H(\mathcal{A}) \mathbf{C}_q^{-\frac{1}{2}}\right) \\
&= \log\det\left(\mathbf{I}_{N_s} + \frac{p_{\bar{q}}}{\sigma^2\left(\sum_{l=1}^{L} \|\mathbf{A}_l^T \mathbf{g}_{lq}\|^2 + 1\right)} \mathbf{F}^H \mathbf{D}_{\bar{q}q}(\mathcal{A}) \mathbf{F} \mathbf{F}^H \mathbf{D}_{\bar{q}q}^H(\mathcal{A}) \mathbf{F}\right) \\
&= \log\det\left(\mathbf{I}_{N_s} + \frac{p_{\bar{q}}}{\sigma^2\left(\sum_{l=1}^{L} \|\mathbf{A}_l^T \mathbf{g}_{lq}\|^2 + 1\right)} \mathbf{D}_{\bar{q}q}^H(\mathcal{A}) \mathbf{D}_{\bar{q}q}(\mathcal{A})\right)
\end{aligned} \tag{4.C.2}$$

where in the last equality, we have used the fact that $\mathbf{F}^H\mathbf{F} = \mathbf{F}\mathbf{F}^H = \mathbf{I}_{N_s}$, along with that for two arbitrary square matrices $\mathbf{U}$ and $\mathbf{V}$, the identity $\det(\mathbf{U}\mathbf{V}) = \det(\mathbf{V}\mathbf{U})$ holds true. As matrix $\mathbf{D}_{q\bar{q}}(\mathcal{A})$ is a diagonal matrix, we can rewrite (4.C.2) as

$$R_q(\mathcal{A}, p_{\bar{q}}) = \frac{1}{2} \log \prod_{k=1}^{N_s} \left(1 + \frac{p_{\bar{q}} |\psi_{\bar{q}q}^k(\mathcal{A})|^2}{\sigma^2\left(\sum_{l=1}^{L} \|\mathbf{A}_l^T \mathbf{g}_{lq}\|^2 + 1\right)}\right) \tag{4.C.3}$$

where $\psi_{\bar{q}q}^k(\mathcal{A})$ is the k-th diagonal entry of the diagonal matrix $\mathbf{D}_{\bar{q}q}(\mathcal{A})$, and is given as $\psi_{\bar{q}q}^k(\mathcal{A}) = H_{\bar{q}q}(e^{j2\pi(k-1)/N_s}) = \sum_{n=0}^{N-1} h_{\bar{q}q}(n) e^{-j2\pi n(k-1)/N_s}$. Using the definition of $\mathbf{D}_{\bar{q}q}(\mathcal{A})$, we can write

$$\mathbf{D}_{\bar{q}q}(\mathcal{A}) \triangleq \sqrt{N_s}\, \text{diag}\{\boldsymbol{\phi}_1^H \tilde{\mathbf{h}}_{\bar{q}q}, \boldsymbol{\phi}_2^H \tilde{\mathbf{h}}_{\bar{q}q}, \cdots, \boldsymbol{\phi}_{N_s}^H \tilde{\mathbf{h}}_{\bar{q}q}\} \tag{4.C.4}$$

where we use the following definition for $\boldsymbol{\phi}_k$

$$\boldsymbol{\phi}_k \triangleq \frac{1}{\sqrt{N_s}} [1 \;\; e^{\frac{j2\pi(k-1)}{N_s}} \;\; \cdots \;\; e^{\frac{j2\pi(N_s-1)(k-1)}{N_s}}]^T, \quad \text{for } k = 1, 2, \ldots, N_s, \tag{4.C.5}$$

and $\tilde{\mathbf{h}}_{\bar{q}q} \triangleq [\mathbf{h}_{\bar{q}q}^T \quad \mathbf{0}_{1\times(N_s-N)}]^T$ is defined as the zero-padded version of the channel vector $\mathbf{h}_{\bar{q}q}$. Using (4.C.4) and (4.C.5), we can recast $\psi_{\bar{q}q}^k(\mathcal{A})$ as $\psi_{\bar{q}q}^k(\mathcal{A}) = \sqrt{N_s}\boldsymbol{\phi}_k^H\tilde{\mathbf{h}}_{\bar{q}q}$. The derivation of (4.23) is now complete.

4.D Derivation of (4.37)

To derive (4.37), we can write

$$\begin{aligned}
\zeta^k_{\bar{q}q}(\mathcal{B}) &\triangleq \psi^k_{\bar{q}q}(\mathcal{A})\Big|_{\{\mathbf{A}_l=\mathbf{U}_l^*\mathbf{B}_l\mathbf{U}_l^H\}_{l=1}^L} \\
&= \sqrt{N_s}\boldsymbol{\phi}_k^H\tilde{\mathbf{h}}_{\bar{q}q}\Big|_{\{\mathbf{A}_l=\mathbf{U}_l^*\mathbf{B}_l\mathbf{U}_l^H\}_{l=1}^L} \\
&= \sqrt{N_s}\boldsymbol{\phi}_k^H\left[\begin{array}{c} \sum_{l=1}^L \mathbf{d}_l\, \mathbf{g}_{lq}^T\mathbf{A}_l\mathbf{g}_{l\bar{q}} \\ \mathbf{0}_{(N_s-N)\times 1}\end{array}\right]\Bigg|_{\{\mathbf{A}_l=\mathbf{U}_l^*\mathbf{B}_l\mathbf{U}_l^H\}_{l=1}^L} \\
&= \sqrt{N_s}\boldsymbol{\phi}_k^H\left[\begin{array}{c} \sum_{l=1}^L \mathbf{d}_l\, \mathbf{q}_{lq}^T\mathbf{B}_l\mathbf{q}_{l\bar{q}} \\ \mathbf{0}_{(N_s-N)\times 1}\end{array}\right].
\end{aligned} \tag{4.D.1}$$

4.E Proof of lemma 3

Let $P_{\mathrm{T}}^{\min}$ denote the minimum value of the total transmit power consumed in the entire network obtained by solving (4.47) and the corresponding optimal value of the optimization variables by $(\boldsymbol{\beta}_1^{\mathrm{opt}}, \boldsymbol{\beta}_2^{\mathrm{opt}}, \tilde{\mathbf{b}}^{\mathrm{opt}})$. We now consider the following optimization problem:

$$\begin{aligned}
&\max_{\boldsymbol{\beta}_1, \boldsymbol{\beta}_2, \tilde{\mathbf{b}}}. \quad \sum_{k=1}^{N_s} \log(1+\beta_{21}^k) \\
&\text{subject to} \quad \sum_{k=1}^{N_s} \log(1+\beta_{12}^k) = b_2, \qquad \text{for } k \in \{1,2,\ldots,N_s\} \\
&\frac{\sigma^2}{N_s}\left(\sum_{k=1}^{N_s} \frac{\beta_{12}^k+\beta_{21}^k}{|\zeta^k(\tilde{\mathbf{b}})|^2}\right)\left(1+\tilde{\mathbf{b}}^H\tilde{\mathbf{E}}_1\tilde{\mathbf{b}}\right)\left(1+\tilde{\mathbf{b}}^H\tilde{\mathbf{E}}_2\tilde{\mathbf{b}}\right)+\sigma^2\tilde{\mathbf{b}}^H\mathbf{L}^H\mathbf{L}\tilde{\mathbf{b}} \le P_{\mathrm{T}}^{\min}.
\end{aligned} \tag{4.E.1}$$

Let us represent the solution to the optimization problem (4.E.1) as $(\widehat{\boldsymbol{\beta}}_1^{\mathrm{opt}}, \widehat{\boldsymbol{\beta}}_2^{\mathrm{opt}}, \hat{\mathbf{b}}^{\mathrm{opt}})$, and denote the maximum achievable rate at Transceiver 1 as $R_1^{\max}$, which is obtained by solving (4.E.1) for the given power budget $P_{\mathrm{T}}^{\min}$. We now argue that $R_1^{\max} = b_1$ holds true. To show this, we consider that if $R_1^{\max} < b_1$, then $(\boldsymbol{\beta}_1^{\mathrm{opt}}, \boldsymbol{\beta}_2^{\mathrm{opt}}, \tilde{\mathbf{b}}^{\mathrm{opt}})$ results in a higher value for the objective function of (4.E.1). Indeed, since $(\boldsymbol{\beta}_1^{\mathrm{opt}}, \boldsymbol{\beta}_2^{\mathrm{opt}}, \tilde{\mathbf{b}}^{\mathrm{opt}})$ is a solution to (4.47), this solution attains a higher value for $\sum_{k=1}^{N_s}\log(1+\beta_{21}^k) = b_1 > R_1^{\max}$, while $\sum_{k=1}^{N_s}\log(1+\beta_{12}^k) = b_2$, and at the same time, $P_{\mathrm{T}} = P_{\mathrm{T}}^{\min}$ which contradicts the optimality of $(\widehat{\boldsymbol{\beta}}_1^{\mathrm{opt}}, \widehat{\boldsymbol{\beta}}_2^{\mathrm{opt}}, \hat{\mathbf{b}}^{\mathrm{opt}})$ for (4.E.1). On the other hand, it is easy to show that $R_1^{\max}$ cannot be greater than r_1 as well. Otherwise, if $R_1^{\max} > b_1$, then one can scale down the optimal value $\widehat{\boldsymbol{\beta}}_1^{\mathrm{opt}}$ such that $\sum_{k=1}^{N_s}\log(1+\beta_{21}^k) = b_1$ holds true, while $P_{\mathrm{T}} < P_{\mathrm{T}}^{\min}$. This means that, $(\widehat{\boldsymbol{\beta}}_1^{\mathrm{opt}}, \widehat{\boldsymbol{\beta}}_2^{\mathrm{opt}}, \hat{\mathbf{b}}^{\mathrm{opt}})$ results in a lower P_{T} while satisfying the two constraints in (4.47). This contradicts the optimality of $(\boldsymbol{\beta}_1^{\mathrm{opt}}, \boldsymbol{\beta}_2^{\mathrm{opt}}, \tilde{\mathbf{b}}^{\mathrm{opt}})$ for (4.47). Therefore, we can conclude that $R_r^{\max} = b_1$ holds true, meaning that the solution to the power minimization problem in (4.47) is indeed a solution to the rate maximization problem (4.E.1). The maximization problem (4.E.1), however, is similar to the optimization problem (18) in [91]. It has been proven in [91] that at the optimum of (4.E.1), i) $|\zeta^k(\tilde{\mathbf{b}})| = |\zeta^{k'}(\tilde{\mathbf{b}})|$ holds true, for $k, k' \in \{1,2,\ldots,N_s\}$ and

ii) $\beta_{12}^{k} = \beta_{12}^{k'}$ and $\beta_{21}^{k} = \beta_{21}^{k'}$ hold true, for $k, k' \in \{1, 2, \ldots, N_s\}$. As a result, at the optimum of (4.47), $\beta_{12}^{k} = \beta_{12}^{k'}$, $\beta_{21}^{k} = \beta_{21}^{k'}$, and $|\zeta^{k}(\tilde{\mathbf{b}})| = |\zeta^{k'}(\tilde{\mathbf{b}})|$ also hold true, for $k, k' \in \{1, 2, \ldots, N_s\}$. The proof is complete.

4.F Derivation of (4.52)

For $\tilde{\mathbf{b}} \in \mathcal{C}_n$, we can write

$$|\zeta(\tilde{\mathbf{b}})|^2 = \frac{1}{N_s}\sum_{k=1}^{N_s}|\zeta^k(\tilde{\mathbf{b}})|^2 = \sum_{k=1}^{N_s}|\boldsymbol{\phi}_k^H\tilde{\mathbf{h}}_{12}|^2 = \|\tilde{\mathbf{h}}_{12}\|^2 = \|\mathbf{h}_{12}\|^2 = \|\mathbf{h}\|^2 = |h[n]|^2 \tag{4.F.1}$$

In (4.F.1), the first equality follows from the fact that for $\tilde{\mathbf{b}} \in \mathcal{C}_n$, one can write $\zeta(\tilde{\mathbf{b}}) = \zeta^k(\tilde{\mathbf{b}})$, for $k = 1, 2, \ldots, N_s$, the second equality follows from (4.37), the third equality follows from the Parseval's theorem, the forth equality follows from the following definition: $\tilde{\mathbf{h}}_{12} \triangleq [\mathbf{h}_{12}^T \; \mathbf{0}_{1\times(N_s-N)}^T]^T = [\mathbf{h}^T \; \mathbf{0}_{1\times(N_s-N)}^T]^T$, and the fifth equality follows from the fact that for $\tilde{\mathbf{b}} \in \mathcal{C}_n$, only the n-th of the end-to-end CIR, i.e., $h[\cdot]$ is non-zero. Note that using (4.8), we can write

$$\begin{aligned}
h[n] = h_{12}[n] &= \sum_{l=1}^{L} d_{l,n}\,\mathbf{g}_{l1}^T\mathbf{A}_l\mathbf{g}_{l2} = \sum_{l=1(n)}^{K(n)} \mathbf{g}_{l1}^T\mathbf{A}_l\mathbf{g}_{l2} = \sum_{l=1(n)}^{K(n)} \mathbf{q}_{l1}^T\mathbf{B}_l\mathbf{q}_{l2} \\
&= \sum_{l=1(n)}^{K(n)} vec^T(\mathbf{B}_l)vec(\mathbf{q}_{l2}\mathbf{q}_{l1}^T) = \sum_{l=1(n)}^{K(n)} vec^T(\mathbf{B}_l^T)vec(\mathbf{q}_{l2}\mathbf{q}_{l1}^T) \\
&= \sum_{l=1(n)}^{K(n)} \mathbf{b}_l^H vec(\mathbf{q}_{l2}\mathbf{q}_{l1}^T) = \sum_{l=1(n)}^{K(n)} \tilde{\mathbf{b}}_l^H\mathbf{L}^H vec(\mathbf{q}_{l2}\mathbf{q}_{l1}^T) = \mathbf{a}_n^H\mathbf{f}_n
\end{aligned} \tag{4.F.2}$$

where we define

$$\mathbf{f}_n \triangleq [(\mathbf{L}^H vec(\mathbf{q}_{1(n),2}\mathbf{q}_{1(n),1}^T))^T \;\; (\mathbf{L}^H vec(\mathbf{q}_{2(n),2}\mathbf{q}_{2(n),1}^T))^T \;\; \cdots \;\; (\mathbf{L}^H vec(\mathbf{q}_{K(n),2}\mathbf{q}_{K(n),1}^T)^T]^T$$

.

Chapter 5

Multipair Two-way Relay Networks with Massive MIMO Relaying

In this chapter, we consider two-way relay networks with multiple massive MIMO relays helping to establish multiple bidirectional peer-to-peer communications. We assume that relays employ linear beamforming techniques such as the maximum ratio transmitting/combining and the zero-forcing schemes to precess their received signals. Exploiting the approximate orthogonality among relay-transceiver channel vectors when number of relay antennas are very large, we provide a computationally efficient solution to the problem of minimizing the total transmit power when the transceivers' signal-to-noise ratios (SNRs) are to be above given thresholds.

The organization of this chapter is as follows. In Section 5.1, we model the system and signals corresponding to the multipair two-way relay networks with a number of multi-antenna relays. In Section 5.2 we propose an approximation based on the fact that when number of relay antennas are very large the small scale fading and noise are asymptotically averaged out. Indeed, under such assumption, the channel vectors between each relay and transceivers become asymptotically orthogonal. In Section 5.3, we present the structure of beamforming matrices for two linear techniques i.e., the MRT/MRC- and the ZF–based schemes. We also show that under the assumption that channel vectors between each relay and transceivers are orthogonal, the structure of the beamforming matrices for these two schemes can be obtained from one another. As such, in Section 5.4 we proceed only with the MRT/MRC-based scheme, and formulate the total transmit power and signal-to-noise-ratio (SNRs) at the receiver front-end of users for this scheme. We then solve the problem for the MRT/MRC-based scheme. Next we explain how solution for the ZF–based technique can be calculated from the solution obtained for the MRT/MRC-based scheme. In Section 5.5, we provide the problem statement for the MRT/MRC-based scheme, where we minimize the total transmit power consumed in the entire network while certain SNR thresholds are satisfied at the receiver front-end of the transceivers. In Section 5.6, we use numerical examples to evaluate the network performance for the MRT/MRC- and the ZF-based schemes.

5.1 System Model

We consider a two-way relay network consisting of K pairs of single-antenna transceivers which communicate in a pair-wise manner. The information exchange between transceiver pairs is performed with the help of n_r relay nodes. Each relay is equipped with M antennas, where M is very large. The signals arrived at the antennas of each relay form a very long vector with size $M \times 1$. Each entry of this vector is the superposition of the noise-contaminated, attenuated copies of signals transmitted by transceivers. Each relay then transforms the vector of its received signals, by multiplying it with a complex "beamforming" matrix, into a new $M \times 1$ vector whose different entries will be transmitted over different antennas of that relay. Considering the relay beamforming matrices and multipair transceivers' transmit powers as design parameters, we aim to minimize the total power consumed in the entire network while the quality-of-service at the receiver front-ends of the transceivers are maintained above a set of given thresholds. Here, we study two different processing techniques at the relays. In the first technique, each relay uses an MRT/MRC method to obtain the relay's vector of transmitted signals from the relay's vector of received signals. In the second scenario, a ZF method is used as the relaying protocol. It is herein assumed that a complete round of information exchange between all the transceiver pairs follows the two time-slot MABC relaying scheme. In the first time-slot of this scheme, all the transceivers transmit their signals simultaneously and in the second time-slot, each relay forwards to the transceivers, a linearly transformed version of that relay's received signal vector. Denoting $\mathbf{x}_i$ as the $M \times 1$ vector of the received signals at the i-th relay in the first time-slot, we can write

$$\mathbf{x}_i = \mathbf{H}_i \mathbf{P}^{1/2} \mathbf{s} + \mathbf{n}_i, \quad \text{for } i \in \{1, 2, \ldots, n_r\} \tag{5.1}$$

where $\mathbf{H}_i \triangleq [\mathbf{h}_{1i} \ \mathbf{h}_{2i} \ \cdots \ \mathbf{h}_{2K,i}]$ is the $M \times 2K$ channel matrix associated with the i-th relay. The l-th column of $\mathbf{H}_i$, denoted as $\mathbf{h}_{li}$, is the $M \times 1$ channel vector between the M antennas of the i-th relay and the l-th transceiver, for $l \in \{1, 2, \ldots, 2K\}$ and $i \in \{1, 2, \ldots, n_r\}$. The $2K \times 2K$ matrix $\mathbf{P} \triangleq \mathrm{diag}\{p_1, p_2, \ldots, p_{2K}\}$ is a diagonal matrix whose l-th diagonal entry, p_l, represents the transmit power of the l-th transceiver, the vector $\mathbf{s} \triangleq [s_1 \ s_2 \ \cdots \ s_{2K}]^T$ denotes the $2K \times 1$ vector of the signals transmitted by all the transceivers, and s_l represents the symbol transmitted by the l-th transceiver. Note that s_{2k-1} and s_{2k} are the symbols transmitted by the two transceivers in the k-th pair with p_{2k-1} and p_{2k} as the corresponding transmit powers. That is, s_{2k-1} (s_{2k}) is transmitted by Transceiver $2k-1$ ($2k$) and is meant to be received by Transceiver $2k$ ($2k-1$), for $k \in \{1, 2, \ldots, K\}$. The $M \times 1$ vector $\mathbf{n}_i$ denotes the vector of the noise processes received at the M antennas of the i-th relay. Here, each entry of $\mathbf{n}_i$ is assumed to be zero-mean spatially white Gaussian noise with variance σ^2.

At the i-th relay, the received vector $\mathbf{x}_i$ is multiplied by a beamforming matrix $\mathbf{A}_i$. Let the $M \times 1$ vector $\mathbf{t}_i$ represent the vector of the signals transmitted by the i-th relay. We can then write

$$\mathbf{t}_i = \mathbf{A}_i \mathbf{x}_i. \tag{5.2}$$

The received signal at Transceiver l, denoted as y_l, is the superposition of the relays' transmitted signals attenuated by the channel coefficients, and the noise at the receiver front-end of the l-th transceiver which is represented by η_l. Hence, one can write

$$y_l = \sum_{i=1}^{n_r} \mathbf{h}_{li}^T \mathbf{t}_i + \eta_l, \quad \text{for } l \in \{1, 2, \ldots, 2K\}. \tag{5.3}$$

Using (5.2) in (5.3), y_l can be expressed as

$$y_l = \sum_{i=1}^{n_r} \mathbf{h}_{li}^T \mathbf{A}_i \mathbf{H}_i \mathbf{P}^{1/2} \mathbf{s} + \sum_{i=1}^{n_r} \mathbf{h}_{li}^T \mathbf{A}_i \mathbf{n}_i + \eta_l. \tag{5.4}$$

Also, using (5.1) and (5.2), the total relay transmit power, denoted as $P_{\rm r}$, can be written as

$$P_{\rm r} = \sum_{i=1}^{n_r} E\{\mathbf{t}_i^H \mathbf{t}_i\} = \sum_{i=1}^{n_r} \|\mathbf{A}_i \mathbf{H}_i \mathbf{P}^{1/2}\|^2 + \sigma^2 \sum_{i=1}^{n_r} tr(\mathbf{A}_i \mathbf{A}_i^H) \tag{5.5}$$

and thus, the total transmit power consumed in the entire network, denoted as $P_{\rm T}$, is given by

$$P_{\rm T} = \sum_{l=1}^{2K} p_l + P_{\rm r} = \sum_{l=1}^{2K} p_l + \sum_{i=1}^{n_r} \|\mathbf{A}_i \mathbf{H}_i \mathbf{P}^{1/2}\|^2 + \sigma^2 \sum_{i=1}^{n_r} tr(\mathbf{A}_i \mathbf{A}_i^H) \tag{5.6}$$

which is defined as the sum of the transceivers' transmit powers and the total relay transmit power.

5.2 Very Large Number of Relay Antennas

The channel coefficient from the k-th transceiver to the m-th antenna of the i-th relay is herein modeled as the product of a complex small-scale fading coefficient and an amplitude factor that accounts for the shadowing effect and path-loss (attenuation). That is, we can write the channel coefficient matrix $\mathbf{H}_i$ as

$$\mathbf{H}_i = \mathbf{G}_i \mathbf{D}_i^{1/2} \tag{5.7}$$

where $\mathbf{G}_i$ denotes the small-scale fading matrix and $\mathbf{D}_i = \text{diag}\{d_{1,i}, d_{2,i}, \ldots, d_{2K,i}\}$ is a positive real-valued diagonal matrix representing path-loss and shadowing effects namely the large-scale fading effect. Here, $d_{l,i}$ represents the large-scale effect of the channel between the l-th transceiver and the i-th relay, for $l \in \{1, 2, \ldots, 2K\}$ and $i \in \{1, 2, \ldots, n_r\}$. Note that channel coefficient variations due to the large-scale effect can be observed over communication ranges proportional to the distances between network nodes and the size of the obstacles in the communication environment. These ranges are much larger than the orders of the signal wavelength whereas the distances between the antennas on the same relay are in the order of signal wavelength. Hence, it is assumed that the large-scale fading coefficients corresponding to the links between each transceiver and different antennas of a given relay are identical. On the other hand, small-scale fading occurs over distances in the order of the signal wavelength [143]. The fact that the small-scale fading coefficients for different transceivers can be independent renders the channel vectors from different transceivers asymptotically orthogonal when M, the number of relay antennas, is large [117, 144, 145]. This asymptotic orthogonality enables us to approximately write $\frac{1}{M}\mathbf{H}_i^H\mathbf{H}_i$ in the form of a diagonal matrix, that is

$$\frac{1}{M}\mathbf{H}_i^H\mathbf{H}_i = \frac{1}{M}\mathbf{D}_i^{1/2}\mathbf{G}_i^H\mathbf{G}_i\mathbf{D}_i^{1/2} \approx \mathbf{D}_i^{1/2}\mathbf{I}_{2K}\mathbf{D}_i^{1/2} = \mathbf{D}_i. \tag{5.8}$$

Note that the approximation $\frac{1}{M}\mathbf{G}_i^H\mathbf{G}_i \approx \mathbf{I}_{2K}$ holds true for large values of M that are no less than $2K$ (i.e., $M \gg 2K$).

5.3 Linear Relaying Techniques

In this section, the MRT/MRC- and ZF-based techniques are assumed to be used as linear relaying techniques at relays equipped with a very large number of antennas.

5.3.1 The MRT/MRC-based Scheme

Based on the MRT/MRC scheme used for signal processing at the relays, the relay beamforming matrix, $\mathbf{A}_i^{\text{MRTC}}$ can be written as

$$\mathbf{A}_i^{\text{MRTC}} = \mathbf{H}_i^*\mathbf{C}_i^{\text{MRTC}}\mathbf{H}_i^H. \tag{5.9}$$

Here, $\mathbf{C}_i^{\mathrm{MRTC}}$ is assumed to be a $2K \times 2K$ block-diagonal matrix which is formed by K blocks $\{\mathbf{B}_{ki}^{\mathrm{MRTC}}\}_{k=1}^{K}$, and can be written as

$$\mathbf{C}_i^{\mathrm{MRTC}} \triangleq \begin{bmatrix} \mathbf{B}_{1i}^{\mathrm{MRTC}} & \cdots & \mathbf{0} \\ \vdots & \ddots & \vdots \\ \mathbf{0} & \cdots & \mathbf{B}_{Ki}^{\mathrm{MRTC}} \end{bmatrix} \tag{5.10}$$

where each block, an anti-diagonal matrix with size 2×2, is associated with one of the transceiver pairs and is given as

$$\mathbf{B}_{ki}^{\mathrm{MRTC}} \triangleq \begin{bmatrix} 0 & \beta_{(2k-1),i} \\ \beta_{2k,i} & 0 \end{bmatrix}. \tag{5.11}$$

The parameters $\beta_{(2k-1),i}$ and $\beta_{2k,i}$ can be viewed as intermediate design parameters. Once the optimal values of these parameters are obtained, the optimum values of matrices $\mathbf{B}_{ki}^{\mathrm{MRTC}}$, for $k \in \{1, \ldots, K\}$, and their corresponding matrix $\mathbf{C}_i^{\mathrm{MRTC}}$ can be calculated in a straightforward manner. The optimal beamforming matrices $\{\mathbf{A}_i^{\mathrm{MRTC}}\}_{i=1}^{n_r}$ are then easily calculated using (5.9). As such, in the next section our goal is to obtain the optimal values of the matrices $\{\mathbf{C}_i^{\mathrm{MRTC}}\}_{i=1}^{n_r}$ (or equivalently the optimal values of the intermediate design parameters $\beta_{l,i}$ for $l \in \{1, 2, \ldots, 2K\}$ and $i \in \{1, 2, \ldots, n_r\}$).

Note that according to (5.2) and (5.9), the signal vector received at the i-th relay is first multiplied by $\mathbf{H}_i^H$ which plays the role of a matched filter. According to (5.8), when the number of relay antennas are very large, the columns of $\mathbf{H}_i$ are approximately orthogonal. Hence, using (5.9), implies that the signal vector received at relay i is first multiplied by $\mathbf{H}_i^H$ yielding a $2K \times 1$ vector $\hat{\mathbf{s}}_i = \mathbf{H}_i^H \mathbf{x}_i$ which is the linear estimate of the symbol vector $\mathbf{s}$ at the i-th relay. Note that the $(2k-1)$-th and $2k$-th elements of $\hat{\mathbf{s}}_i$ are respectively the estimates of the two symbols transmitted by Transceivers $2k-1$ and $2k$, for $k \in \{1, 2, \ldots, K\}$. Taking into account $\mathbf{H}_i^*$, the left-most term in $\mathbf{A}_i^{\mathrm{MRTC}}$ (see (5.9)), the role of the anti-diagonal matrix $\mathbf{B}_{ki}^{\mathrm{MRTC}}$ on the k-th diagonal block of $\mathbf{C}_i^{\mathrm{MRTC}}$ is to swap these two estimates so that the estimate of the symbol transmitted by Transceiver $2k$ can be forwarded to Transceiver $(2k-1)$ and the estimate of the symbol transmitted by Transceiver $(2k-1)$ can be forwarded to Transceiver $2k$. This goal is achieved by multiplying $\hat{\mathbf{s}}_i$ with $\mathbf{C}_i^{\mathrm{MRTC}}$, as (5.9) implies and then by $\mathbf{H}_i^*$. As $\mathbf{H}_i^H\mathbf{H}_i \approx M\mathbf{D}_i$ holds for a very large M (see (5.8)), the use of $\mathbf{H}_i^*$ as the left-most component in $\mathbf{A}_i^{\text{MRTC}}$ guarantees that the transmitted symbol estimates will not interfere with each other for $M \to \infty$, as these estimates will be transmitted over asymptotically orthogonal columns of $\mathbf{H}_i^*$. However, when M is a finite number, the MRT/MRC-based relaying scheme suffers from inter- and intra-pair interferences.

5.3.2 The ZF-based Method

Denoting $\mathbf{A}_i^{\text{ZF}}$ as the relay beamforming matrix corresponding to the ZF-based method, we can write

$$\mathbf{A}_i^{\text{ZF}} = \mathbf{H}_i^*(\mathbf{H}_i^T\mathbf{H}_i^*)^{-1}\mathbf{C}_i^{\text{ZF}}(\mathbf{H}_i^H\mathbf{H}_i)^{-1}\mathbf{H}_i^H. \tag{5.12}$$

where $\mathbf{C}_i^{\text{ZF}}$ has the same block-diagonal structure as $\mathbf{C}_i^{\text{MRTC}}$ in (5.10), and its corresponding blocks are denoted as $\{\mathbf{B}_{ki}^{\text{ZF}}\}_{k=1}^K$, i.e., $\mathbf{C}_i^{\text{ZF}} = \text{blkdiag}\{\mathbf{B}_{1i}^{\text{ZF}}, \mathbf{B}_{2i}^{\text{ZF}}, \ldots, \mathbf{B}_{Ki}^{\text{ZF}}\}$. The block $\mathbf{B}_{ki}^{\text{ZF}}$ is an anti-diagonal 2×2 matrix with the same structure as $\mathbf{B}_{ki}^{\text{MRTC}}$ in (5.11).

Note that using (5.12) in (5.2) implies that the signal vector received at the i-th relay is first multiplied by $(\mathbf{H}_i^H\mathbf{H}_i)^{-1}\mathbf{H}_i^H$ which yields a $2K \times 1$ vector $\breve{\mathbf{s}}_i = (\mathbf{H}_i^H\mathbf{H}_i)^{-1}\mathbf{H}_i^H\mathbf{x}_i$. In this ZF-based scheme, the l-th element of $\breve{\mathbf{s}}_i$ does not suffer from interference caused by signals transmitted by transceivers other than the l-th transceiver. The anti-diagonal matrix $\mathbf{B}_{ki}^{\text{ZF}}$ (i.e., the k-th diagonal block of $\mathbf{C}_i^{\text{ZF}}$), swaps the estimated signals for k-th transceiver pairs such that the estimate of the symbol transmitted by Transceiver $2k$ can be forwarded to Transceiver $(2k-1)$ and the estimate of the symbol transmitted by Transceiver $(2k-1)$ can be forwarded to Transceiver $2k$. The so-obtained signal $\mathbf{C}_i^{\text{ZF}}\breve{\mathbf{s}}_i$ is now multiplied by matrix $\mathbf{H}_i^*(\mathbf{H}_i^T\mathbf{H}_i^*)^{-1}$. Doing so, the signals received at Transceivers $2k-1$ and $2k$ are noise contaminated *interference-free* versions of the estimates of the signals transmitted respectively by Transceivers $2k$ and $2k-1$.

When the number of relay antennas are very large, we can use (5.8) and (5.12) and rewrite $\mathbf{A}_i^{\mathrm{ZF}}$ as

$$\mathbf{A}_i^{\mathrm{ZF}} = \mathbf{H}_i^* \underbrace{(M\mathbf{D}_i)^{-1}\mathbf{C}_i^{\mathrm{ZF}}(M\mathbf{D}_i)^{-1}}_{\text{block diagonal}} \mathbf{H}_i^H. \tag{5.13}$$

In this case, $\mathbf{A}_i^{\mathrm{ZF}}$ has the same structure as $\mathbf{A}_i^{\mathrm{MRTC}}$ in (5.9). Indeed, a close look at (5.13) reveals that the matrix $(M\mathbf{D}_i)^{-1}\mathbf{C}_i^{\mathrm{ZF}}(M\mathbf{D}_i)^{-1}$ is block diagonal and the role this matrix plays in $\mathbf{A}_i^{\mathrm{ZF}}$ is the same as the role the block-diagonal matrix $\mathbf{C}_i^{\mathrm{MRTC}}$ plays in $\mathbf{A}_i^{\mathrm{MRTC}}$. As a result, once $\mathbf{C}_i^{\mathrm{MRTC}}$ is obtained, we can use (5.9) and (5.13) to rewrite $\mathbf{C}_i^{\mathrm{ZF}}$ as

$$\mathbf{C}_i^{\mathrm{ZF}} = M^2\mathbf{D}_i\mathbf{C}_i{}^{\mathrm{MRTC}}\mathbf{D}_i. \tag{5.14}$$

Doing so, we can first use the forthcoming MRT/MRC-based method and optimally (in some sense) determine $\{\mathbf{C}_i^{\mathrm{MRTC}}\}_{i=1}^{n_r}$. Once the total transmit power minimization problem is solved for the MRT/MRC-based method, we can use $\{\mathbf{C}_i^{\mathrm{MRTC}}\}_{i=1}^{n_r}$ in (5.14) and obtain $\{\mathbf{C}_i^{\mathrm{ZF}}\}_{i=1}^{n_r}$. We can then use $\{\mathbf{C}_i^{\mathrm{ZF}}\}_{i=1}^{n_r}$ in (5.12) to obtain $\{\mathbf{A}_i^{\mathrm{ZF}}\}_{i=1}^{n_r}$.

5.4 Power-optimal MRT/MRC-based relaying

Given the relationship between the solutions for the two linear relaying protocols explained in the previous section, without any loss of generality, we herein opt to proceed based on the MRT/MRC principle. Later, we rely on the results for MRT/MRC-based method to determine solution to the power minimization problem based on the ZF technique.

Using (5.9)-(5.11) in (5.5), the total relay transmit power for the MRT/MRC-based scheme, denoted as $P_{\mathrm{r}}^{\mathrm{M}}$, can be derived as

$$\begin{aligned}
P_{\mathrm{r}}^{\mathrm{M}} &= \sum_{i=1}^{n_r}\left(tr(\mathbf{A}_i\mathbf{H}_i\mathbf{P}\mathbf{H}_i^H\mathbf{A}_i^H) + \sigma^2 tr(\mathbf{A}_i\mathbf{A}_i^H)\right) \\
&= \sum_{i=1}^{n_r}\left(tr(\underbrace{\mathbf{H}_i^*\mathbf{C}_i\mathbf{H}_i^H}_{\mathbf{A}_i}\mathbf{H}_i\mathbf{P}\mathbf{H}_i^H\underbrace{\mathbf{H}_i\mathbf{C}_i^H\mathbf{H}_i^T}_{\mathbf{A}_i^H}) + \sigma^2 tr(\underbrace{\mathbf{H}_i^*\mathbf{C}_i\mathbf{H}_i^H}_{\mathbf{A}_i}\underbrace{\mathbf{H}_i\mathbf{C}_i^H\mathbf{H}_i^T}_{\mathbf{A}_i^H})\right) \\
&= \sum_{i=1}^{n_r}\left(tr(\mathbf{P}\underbrace{\mathbf{H}_i^H\mathbf{H}_i}_{M\mathbf{D}_i}\mathbf{C}_i^H\underbrace{\mathbf{H}_i^T\mathbf{H}_i^*}_{M\mathbf{D}_i}\mathbf{C}_i\underbrace{\mathbf{H}_i^H\mathbf{H}_i}_{M\mathbf{D}_i}) + \sigma^2 tr(\mathbf{C}_i\underbrace{\mathbf{H}_i^H\mathbf{H}_i}_{M\mathbf{D}_i}\mathbf{C}_i^H\underbrace{\mathbf{H}_i^T\mathbf{H}_i^*}_{M\mathbf{D}_i})\right) \\
&= \sum_{i=1}^{n_r} tr\left(M^3\mathbf{P}\mathbf{D}_i\mathbf{C}_i^H\mathbf{D}_i\mathbf{C}_i\mathbf{D}_i + \sigma^2 M^2\mathbf{C}_i^H\mathbf{D}_i\mathbf{C}_i\mathbf{D}_i\right)
\end{aligned} \tag{5.15}$$

where in the last equality, we have used (5.8). Since $\mathbf{D}_i$ is a diagonal matrix and $\mathbf{C}_i$ is a block-diagonal matrix with blocks formed as anti-diagonal matrices, $\mathbf{C}_i^H\mathbf{D}_i\mathbf{C}_i\mathbf{D}_i$ becomes a diagonal matrix[1]. Hence, we can write

$$\mathbf{C}_i^H\mathbf{D}_i\mathbf{C}_i\mathbf{D}_i = \mathrm{diag}\left\{|\tilde{\beta}_{2,i}|^2, |\tilde{\beta}_{1,i}|^2, \ldots, |\tilde{\beta}_{2K,i}|^2, |\tilde{\beta}_{2K-1,i}|^2\right\} = \mathrm{diag}\{|\tilde{\beta}_{\bar{l},i}|^2\}_{l=1}^{2K} \tag{5.16}$$

where we define

$$\tilde{\beta}_{l,i} \triangleq \sqrt{d_{l,i}d_{\bar{l},i}}\beta_{\bar{l},i}, \quad \text{for } l \in \{1, 2, \ldots, 2K\} \tag{5.17}$$

and $\bar{l} \in \{1, 2, \ldots, 2K\}$ is defined as

$$\bar{l} \triangleq \begin{cases} l+1, & \text{if } l \in \{1, 3, \ldots, 2K-1\} \\ l-1, & \text{if } l \in \{2, 4, \ldots, 2K\} \end{cases}. \tag{5.18}$$

Using (5.15) and (5.16), $P_{\mathrm{r}}^{\mathrm{M}}$ can be rewritten as

$$P_{\mathrm{r}}^{\mathrm{M}} = \sum_{i=1}^{n_r} tr(\underbrace{\left(M^3\mathbf{P}\mathbf{D}_i + \sigma^2 M^2\mathbf{I}\right)}_{\text{diagonal matrix}}\underbrace{\mathbf{C}_i^H\mathbf{D}_i\mathbf{C}_i\mathbf{D}_i}_{\text{diagonal matrix}}) = \sum_{i=1}^{n_r}\sum_{l=1}^{2K}\left(M^3 p_{\bar{l}} d_{\bar{l},i} + M^2\sigma^2\right)|\tilde{\beta}_{l,i}|^2. \tag{5.19}$$

[1] The k-th block of the product $\mathbf{C}_i^H\mathbf{D}_i\mathbf{C}_i\mathbf{D}_i$ can be written as

$$\begin{bmatrix} 0 & \beta_{2k,i}^* \\ \beta_{2k-1,i}^* & 0 \end{bmatrix}\begin{bmatrix} d_{2k-1,i} & 0 \\ 0 & d_{2k,i} \end{bmatrix}\begin{bmatrix} 0 & \beta_{2k-1,i} \\ \beta_{2k,i} & 0 \end{bmatrix}\begin{bmatrix} d_{2k-1,i} & 0 \\ 0 & d_{2k,i} \end{bmatrix} = \begin{bmatrix} d_{2k-1,i}d_{2k,i}|\beta_{2k,i}|^2 & 0 \\ 0 & d_{2k-1,i}d_{2k,i}|\beta_{2k-1,i}|^2 \end{bmatrix}.$$

Defining $\mathbf{f}_l \triangleq [\sqrt{d_{l,1}}\ \sqrt{d_{l,2}}\ \cdots\ \sqrt{d_{l,n_r}}]^T$, $\tilde{\boldsymbol{\beta}}_l \triangleq [\tilde{\beta}_{l,1}\ \tilde{\beta}_{l,2}\ \cdots\ \tilde{\beta}_{l,n_r}]^T$, and $\mathbf{F}_l \triangleq \mathrm{diag}(\mathbf{f}_l \odot \mathbf{f}_l)$, we can rewrite $P_{\mathrm{r}}^{\mathrm{M}}$ in (5.19) as

$$P_{\mathrm{r}}^{\mathrm{M}} = \sum_{l=1}^{2K} M^2 \tilde{\boldsymbol{\beta}}_l^H \left(M p_{\bar{l}} \mathbf{F}_{\bar{l}} + \sigma^2 \mathbf{I}_{n_r} \right) \tilde{\boldsymbol{\beta}}_l. \tag{5.20}$$

Hence, using (5.6) and (5.20), the total transmit power, $P_{\mathrm{T}}^{\mathrm{M}}$ can be rewritten as

$$P_{\mathrm{T}}^{\mathrm{M}} = \sum_{l=1}^{2K} \left(p_{\bar{l}} + M^2 \tilde{\boldsymbol{\beta}}_l^H (M p_{\bar{l}} \mathbf{F}_{\bar{l}} + \sigma^2 \mathbf{I}_{n_r}) \tilde{\boldsymbol{\beta}}_l \right). \tag{5.21}$$

Let us define $\mathbf{e}_{l,i} \triangleq [0\ 0 \cdots 0\ 1\ 0 \cdots\ 0]^T$ as a $2K \times 1$ vector associated with the i-th relay which consists of all 0 entries except for the l-th entry which is 1. Using (5.8) and (5.9), one can write y_l^{M}, the signal received at Transceiver l, for $l \in \{1, 2, \cdots, 2K\}$, as

$$\begin{aligned}
y_l^{\mathrm{M}} &= \sum_{i=1}^{n_r} \underbrace{\mathbf{h}_{l,i}^T \mathbf{H}_i^*}_{M d_{l,i} \mathbf{e}_{l,i}^T} \mathbf{C}_i \underbrace{\mathbf{H}_i^H \mathbf{H}_i}_{M \mathbf{D}_i} \mathbf{P}^{1/2} \mathbf{s} + \sum_{i=1}^{n_r} \underbrace{\mathbf{h}_{l,i}^T \mathbf{H}_i^*}_{M d_{l,i} \mathbf{e}_{l,i}^T} \mathbf{C}_i \mathbf{H}_i^H \mathbf{n}_i + \eta_l \\
&= M^2 \sum_{i=1}^{n_r} d_{l,i} \underbrace{\mathbf{e}_{l,i}^T \mathbf{C}_i}_{\beta_{l,i} \mathbf{e}_{\bar{l},i}^T} \mathbf{D}_i \mathbf{P}^{1/2} \mathbf{s} + M \sum_{i=1}^{n_r} d_{l,i} \underbrace{\mathbf{e}_{l,i}^T \mathbf{C}_i}_{\beta_{l,i} \mathbf{e}_{\bar{l},i}^T} \mathbf{H}_i^H \mathbf{n}_i + \eta_l \\
&= M^2 \sum_{i=1}^{n_r} d_{l,i} \beta_{l,i} \underbrace{\mathbf{e}_{\bar{l},i}^T \mathbf{D}_i \mathbf{P}^{1/2} \mathbf{s}}_{d_{\bar{l},i} \sqrt{p_{\bar{l}}} s_{\bar{l}}} + M \sum_{i=1}^{n_r} d_{l,i} \beta_{l,i} \underbrace{\mathbf{e}_{\bar{l},i}^T \mathbf{H}_i^H}_{\mathbf{h}_{\bar{l},i}^H} \mathbf{n}_i + \eta_l \\
&= M^2 \sum_{i=1}^{n_r} d_{l,i} \beta_{l,i} d_{\bar{l},i} \sqrt{p_{\bar{l}}} s_{\bar{l}} + M \sum_{i=1}^{n_r} d_{l,i} \beta_{l,i} \mathbf{h}_{\bar{l},i}^H \mathbf{n}_i + \eta_l.
\end{aligned} \tag{5.22}$$

In light of (5.22), it is worth noting that under the assumption of the orthogonality of the channel vectors, the received signal y_l, does not contain the signal from other transceiver pairs. That is, as long as the orthogonality of channel vectors holds, implementing the MRT/MRC-based technique incurs no interference at the receiver front-end of the transceivers. Based on (5.22), the SNR at Transceivers l can now be written as

$$\mathrm{SNR}_l^{\mathrm{M}} = \frac{M^4 p_{\bar{l}} \left| \sum_{i=1}^{n_r} \sqrt{d_{l,i} d_{\bar{l},i}} \tilde{\beta}_{l,i} \right|^2}{M^3 \sigma^2 \sum_{i=1}^{n_r} \left| \sqrt{d_{l,i}} \tilde{\beta}_{l,i} \right|^2 + \sigma^2}, \qquad \text{for } l \in \{1, 2, \ldots, 2K\} \tag{5.23}$$

where we have used the fact that $E\{|\mathbf{h}_{\bar{l},i}^H \mathbf{h}_{\bar{l},i}|\} = M d_{\bar{l},i}$, which in turn follows from using the assumption that $E\{\mathbf{n}_i^H \mathbf{n}_i\} = \sigma^2 \mathbf{I}_M$, along with (5.8). Using the following definition:

$$\mathbf{g}_l \triangleq \mathbf{f}_l \odot \mathbf{f}_{\bar{l}}, \quad \text{for } \ l \in \{1, 2, \ldots, 2K\} \tag{5.24}$$

we can rewrite $\mathrm{SNR}_l^{\mathrm{M}}$ in (5.23) as

$$\mathrm{SNR}_l^{\mathrm{M}} = \frac{M^4 p_{\bar{l}} |\mathbf{g}_l^T \tilde{\boldsymbol{\beta}}_l|^2}{\sigma^2 (1 + M^3 \tilde{\boldsymbol{\beta}}_l^H \mathbf{F}_l \tilde{\boldsymbol{\beta}}_l)}, \quad \text{for } l \in \{1, 2, \ldots, 2K\}. \tag{5.25}$$

Note that these expressions are obtained under the assumption that the channel vectors are asymptotically orthogonal (see (5.8)).

5.5 Power Minimization

Assuming perfect (ideal) orthogonality of the transceiver-relay channel vectors, i.e., $\mathbf{G}_i^H \mathbf{G}_i = M \mathbf{I}_{2K}$, we now aim to find the beamforming matrices and transceivers transmit powers such that the total transmit power $P_{\mathrm{T}}^{\mathrm{M}}$ is minimized, while the SNR at Transceiver l is maintained above given threshold γ_l, for $l \in \{1, 2, \ldots, 2K\}$. This power minimization problem can be expressed as

$$\min_{\mathcal{P}, \mathcal{A}} . \quad P_{\mathrm{T}}^{\mathrm{M}} \qquad \text{subject to} \quad \mathrm{SNR}_l^{\mathrm{M}} \geq \gamma_l, \quad \text{for } \ l \in \{1, 2, \ldots, 2K\} \tag{5.26}$$

where $\mathcal{P} \triangleq \{p_l\}_{l=1}^{2K}$ is the set of transceivers transmit powers and $\mathcal{A} \triangleq \{\mathbf{A}_i\}_{i=1}^{n_r}$ is the set of relay beamforming matrices. Using (5.21) and (5.25), the power minimization problem for the MRT/MRC-based scheme in (5.26) can be recast as

$$\begin{aligned} \min_{\mathcal{P}, \mathcal{B}} . \quad & \sum_{l=1}^{2K} \Big(p_{\bar{l}} + M^2 \tilde{\boldsymbol{\beta}}_l^H (M p_{\bar{l}} \mathbf{F}_{\bar{l}} + \sigma^2 \mathbf{I}_{n_r}) \tilde{\boldsymbol{\beta}}_l \Big) \\ \text{subject to} \quad & \frac{M^4 p_{\bar{l}} |\mathbf{g}_l^T \tilde{\boldsymbol{\beta}}_l|^2}{\sigma^2 (1 + M^3 \tilde{\boldsymbol{\beta}}_l^H \mathbf{F}_l \tilde{\boldsymbol{\beta}}_l)} \geq \gamma_l, \quad \text{for } \ l \in \{1, 2, \ldots, 2K\} \end{aligned} \tag{5.27}$$

where $\mathcal{B} \triangleq \{\tilde{\boldsymbol{\beta}}_l\}_{l=1}^{2K}$ is the set of vectors $\tilde{\boldsymbol{\beta}}_l$ each with size $n_r \times 1$. A closer look at (5.27) shows that the total transmit power minimization problem can be decoupled into a set of $2K$ total power minimization problems each of which written as

$$\min_{\tilde{\boldsymbol{\beta}}_l, p_{\bar{l}}} \; p_{\bar{l}} + M^2 \tilde{\boldsymbol{\beta}}_l^H (M p_{\bar{l}} \mathbf{F}_{\bar{l}} + \sigma^2 \mathbf{I}_{n_r}) \tilde{\boldsymbol{\beta}}_l \quad \text{subject to} \quad \frac{M^4 p_{\bar{l}} |\mathbf{g}_l^T \tilde{\boldsymbol{\beta}}_l|^2}{\sigma^2 (1 + M^3 \tilde{\boldsymbol{\beta}}_l^H \mathbf{F}_l \tilde{\boldsymbol{\beta}}_l)} \geq \gamma_l. \tag{5.28}$$

Indeed, the minimization problem (5.28) amounts to minimizing the total power consumed to guarantee a received SNR at Transceiver l. We can rewrite the optimization problem in (5.28) as

$$\begin{aligned} \min_{p_{\bar{l}}} \quad & p_{\bar{l}} + \min_{\tilde{\boldsymbol{\beta}}_l} M^2 \tilde{\boldsymbol{\beta}}_l^H (M p_{\bar{l}} \mathbf{F}_{\bar{l}} + \sigma^2 \mathbf{I}_{n_r}) \tilde{\boldsymbol{\beta}}_l \\ \text{subject to} \quad & M^3 \tilde{\boldsymbol{\beta}}_l^H (M p_{\bar{l}} \mathbf{g}_l^* \mathbf{g}_l^T - \sigma^2 \gamma_l \mathbf{F}_l) \tilde{\boldsymbol{\beta}}_l \geq \sigma^2 \gamma_l. \end{aligned} \tag{5.29}$$

To solve (5.29), we can first fix $p_{\bar{l}}$ and solve the inner minimization problem over $\tilde{\boldsymbol{\beta}}_l$. It can be shown[2] that the inner problem in (5.29) is feasible if and only if $p_{\bar{l}} > \frac{\sigma^2 \gamma_l}{M \|\mathbf{f}_l\|^2}$, and that the solution to the inner minimization problem can be written as

$$\tilde{\boldsymbol{\beta}}_l^{\text{opt}} = \mu_l \underbrace{(\sigma^2 \gamma_l M \mathbf{F}_l + \lambda_l (M p_{\bar{l}} \mathbf{F}_{\bar{l}} + \sigma^2 \mathbf{I}_{n_r}))^{-1} \mathbf{g}_l}_{\triangleq \mathbf{u}_l} \tag{5.30}$$

$$\mu_l = \sqrt{\frac{\sigma^2 \gamma_l}{\lambda_l M^2 \mathbf{u}_l^H (M p_{\bar{l}} \mathbf{F}_{\bar{l}} + \sigma^2 \mathbf{I}_{n_r}) \mathbf{u}_l}}. \tag{5.31}$$

Here, $\tilde{\boldsymbol{\beta}}_l^{\text{opt}}$ is the optimal value of $\tilde{\boldsymbol{\beta}}_l$ while $p_{\bar{l}}$ and λ_l, are required to satisfy the following two nonlinear equations:

$$\sigma^2 \gamma_l \frac{p_{\bar{l}}^{-2} - \lambda_l M^3 \mathbf{u}_l^H \mathbf{F}_{\bar{l}} \mathbf{u}_l}{\lambda_l^2 \mathbf{u}_l^H (M^3 p_{\bar{l}} \mathbf{F}_{\bar{l}} + M^2 \sigma^2 \mathbf{I}_{n_r}) \mathbf{u}_l} = 1 \tag{5.32}$$

$$p_{\bar{l}} M^2 \mathbf{g}_l^H (M \sigma^2 \gamma_l \mathbf{F}_l + \lambda_l (M p_{\bar{l}} \mathbf{F}_{\bar{l}} + \sigma^2 \mathbf{I}_{n_r}))^{-1} \mathbf{g}_l = 1 \tag{5.33}$$

and $p_{\bar{l}} \in \left(\frac{\sigma^2 \gamma_l}{M \|\mathbf{f}_l\|^2}, +\infty \right)$ must hold true. Note that for any given value of $z \in \left(\frac{\sigma^2 \gamma_l}{M \|\mathbf{f}_l\|^2}, +\infty \right)$, the following nonlinear equality

$$z M^2 \mathbf{g}_l^H (M \sigma^2 \gamma_l \mathbf{F}_l + \lambda (M z \mathbf{F}_{\bar{l}} + \sigma^2 \mathbf{I}_{n_r}))^{-1} \mathbf{g}_l = 1 \tag{5.34}$$

has a unique positive solution for parameter λ. That is, in (5.34), the parameter λ can be viewed as a function of z. As such, the function

$$\sigma^2 \gamma_l \frac{z^{-2} - \lambda M^3 \mathbf{u}_l^H \mathbf{F}_{\bar{l}} \mathbf{u}_l}{\lambda^2 \mathbf{u}_l^H (z M^3 \mathbf{F}_{\bar{l}} + \sigma^2 M^2 \mathbf{I}_{n_r}) \mathbf{u}_l} - 1 \tag{5.35}$$

[2]The same optimization problem has been solved in [146], see eq. (13) in this reference paper.

can be considered as a function of z, where λ is obtained, for any value of $z \in \left(\frac{\sigma^2\gamma_l}{M\|\mathbf{f}_l\|^2}, +\infty\right)$, via solving (5.34). As it has been proven in [146] and from (5.32), the parameter $p_{\bar{l}}$ is indeed the provably unique root of (5.35), and one can use a bisection method to find this root. Note that in this bisection method, the function in (5.35) has to be evaluated for intermediate values of z. As such, to obtain a value of λ corresponding to an intermediate value of z, one has to solve (5.34) using another bisection technique. Once $p_{\bar{l}}$, the root of (5.35), is obtained, the corresponding value of λ is indeed λ_l. Once $p_{\bar{l}}$ and λ_l are obtained, the value of the objective function in (5.29) is given by $(p_{\bar{l}} + \frac{\sigma^2\gamma_l}{\lambda_l})$, which is a portion of the minimum total transmit power being used to deliver information symbols to Transceiver l from its peer transceiver. Based on (5.27)-(5.29), the minimum value of the total transmit power can be obtained as

$$P_{\mathrm{T}}^{\mathrm{M}} = \sum_{l=1}^{2K}(p_{\bar{l}} + \frac{\sigma^2\gamma_l}{\lambda_l}). \tag{5.36}$$

Exploiting the optimal values of $p_{\bar{l}}$ and λ_l, we can obtain the optimal beamforming matrices using the following steps. Using $p_{\bar{l}}$ and λ_l, we first obtain the optimal vector $\tilde{\boldsymbol{\beta}}_l^{\mathrm{opt}}$ from (5.30) and (5.31)[3]. Once $\tilde{\boldsymbol{\beta}}_l^{\mathrm{opt}} \triangleq [\tilde{\beta}_{l,1}^{\mathrm{opt}}\ \tilde{\beta}_{l,2}^{\mathrm{opt}}\ \cdots\ \tilde{\beta}_{l,n_r}^{\mathrm{opt}}]^T$ is obtained, the optimal values of $\beta_{l,i}^{\mathrm{opt}}$ can be calculated from (5.17) as $\beta_{l,i}^{\mathrm{opt}} = \tilde{\beta}_{\bar{l},i}^{\mathrm{opt}}/\sqrt{d_{l,i}d_{\bar{l},i}}$, for $i \in \{1, 2, \ldots, n_r\}$. Using the so-obtained values of $\beta_{l,i}^{\mathrm{opt}}$ along with the definition of $\bar{l}$ in (5.18), the optimal values of $\beta_{2k-1,i}^{\mathrm{opt}}$ and $\beta_{2k,i}^{\mathrm{opt}}$ are determined for $k \in \{1, 2, \ldots, K\}$. Replacing $\beta_{2k-1,i}$ and $\beta_{2k,i}$ in (5.11), respectively with $\beta_{2k-1,i}^{\mathrm{opt}}$ and $\beta_{2k,i}^{\mathrm{opt}}$, the optimal anti-diagonal block of the i-th relay corresponding to the k-th pair of transceivers, denoted as $\mathbf{B}_{ki}^{\mathrm{MRTC,\,opt}}$, can be obtained. Replacing blocks $\mathbf{B}_{ki}^{\mathrm{MRTC}}$ for $k \in \{1, 2, \ldots, K\}$ in (5.10), with the so-obtained set of blocks $\{\mathbf{B}_{ki}^{\mathrm{MRTC,\,opt}}\}_{k=1}^{K}$, the effective beamforming matrix of i-th relay, denoted as $\mathbf{C}_i^{\mathrm{MRTC,\,opt}}$, can be formed. Finally, the optimal beamforming matrix of the i-th relay for the MRT/MRC-based scheme, denoted as $\mathbf{A}_i^{\mathrm{MRTC,\,opt}}$, can be calculated as $\mathbf{A}_i^{\mathrm{MRTC,\,opt}} = \mathbf{H}_i^*\mathbf{C}_i^{\mathrm{MRTC,\,opt}}\mathbf{H}_i^H$.

It is worth noting that when channel vectors between each relay and different

[3]Note that all diagonal matrices, vectors and scalar values of the right-hand side of (5.30) and (5.31) are positive real valued which renders $\tilde{\boldsymbol{\beta}}_l^{\mathrm{opt}}$ a vector with all positive real valued entries.

transceivers are asymptotically orthogonal as in (5.8), the relay beamforming matrices obtained using the MRT/MRC- and the ZF-based methods are the same. We can see this via comparing (5.9) and (5.13), where $\mathbf{A}_i$ is constructed from $\mathbf{H}_i^*$ as the left-most term multiplied by a block-diagonal matrix in the middle and then multiplied by $\mathbf{H}_i^H$ as the right-most term. Note that under the assumption that (5.8) holds true, the block-diagonal matrix between $\mathbf{H}_i^*$ and $\mathbf{H}_i^H$ will be the same for these two schemes. As such, once the optimal beamforming matrices are obtained using the MRT/MRC-based scheme (i.e., $\mathbf{A}_i^{\mathrm{MRTC}}$), the beamforming matrices pertinent to the ZF-based method are also at hand (i.e., $\mathbf{A}_i^{\mathrm{ZF}}\big|_{\mathbf{G}_i^H\mathbf{G}_i=M\mathbf{I}_{2K}} = \mathbf{A}_i^{\mathrm{MRTC}}\big|_{\mathbf{G}_i^H\mathbf{G}_i=M\mathbf{I}_{2K}}$). In reality, with a large but finite number of relay antennas, channel vectors between each relay and different transceivers are not perfectly orthogonal. When the columns of $\mathbf{G}_i$ are only asymptotically orthogonal, then, after solving the power minimization problem $\mathbf{A}_i^{\mathrm{MRTC}}$ and $\mathbf{A}_i^{\mathrm{ZF}}$ (given respectively in (5.9) and (5.12)) are no longer the same. As a result, these schemes will perform differently in terms of the total transmit power and quality of service. For example, when the MRT/MRC-based scheme is used, the transceivers suffer from the interference caused by signals transmitted by other transceivers. To the contrary, when the ZF-based scheme is employed transceivers do not suffer from interference.

In what follows, we describe how each of the proposed schemes perform in the presence of noise and interference, i.e., when the columns of $\mathbf{G}_i$ are only asymptotically orthogonal. A closer look at (5.9) reveals that the structure of $\mathbf{A}_i^{\mathrm{MRTC}}$ ignores interference. As such, when channel vectors between each relay and different transceivers are not perfectly orthogonal, the signal received at Transceiver l is not the same as the interference-free signal that the last equality in (5.22) suggests. The fact that the signal received at each transceiver is contaminated with the interference from other transceivers implies that the MRT/MRC-based scheme cannot satisfy the SNR thresholds, particularly in high-interference regimes. However, the MRT/MRC-based method is practically appealing in the sense that it does not suffer from the computational burden of matrix inversion. The structure of $\mathbf{A}_i^{\mathrm{ZF}}$ in (5.12) shows that the ZF-based method can eliminate the interference while noise is disregarded. That is, with ZF-based method being employed at relays, even if channel vectors between each relay and different transceivers are not perfectly orthogonal, the signals received at transceivers are interference-free. However, implementing the ZF-based scheme requires matrix inversion which can result in prohibitive computations.

The following Theorem reveals an interesting property of the total transmit power as well as the transceivers transmit powers obtained using the proposed methods.

Theorem 1 *The minimum total transmit power,* $P_{\mathrm{T}}^{\mathrm{M}}$ *in* (5.36)*, and the transceivers transmit powers,* p_l*, for* $l \in \{1, 2, \ldots, 2K\}$*, are inversely proportional to the number of relay antennas,* M*.*

$$P_{\mathrm{T}}^{\mathrm{M}} = \frac{c}{M} \quad \text{and} \quad p_l = \frac{z_l}{M} \text{ for } l \in \{1, 2, \ldots, 2K\}. \tag{5.37}$$

Here c *and* z_l *are scalar values which are independent of the number of relay antennas,* M*.*

Proof See Appendix 5.A. ■

In the next section, we evaluate the performance of the proposed methods and verify the result of Theorem 1 via numerical examples.

5.6 Numerical Results

Considering multipair two-way relay networks, we herein examine the total transmit power consumed in the entire network while a certain set of SNR thresholds are to be satisfied at the transceivers. To do so, we consider a two-way relay network consisting of $K = 4$ pairs of single-antenna transceivers which aim to exchange information with the help of $n_r = 4$ relays, each equipped with M antennas. In the different scenarios we herein evaluate, different numbers of relay antennas are considered (i.e., $M = 50, 100, 200, 1000$). We use the combined path-loss and shadowing model introduced in [143], where channel models for path-loss and shadowing are superimposed. As such, we assume that the path-loss exponent is 3.8 and the standard deviation of the shadowing effect is 8 dB. The channel coefficients corresponding to the small-scale fading are here modeled as complex Gaussian random variables with zero mean and unit variance. The noises received at the relays and transceivers are assumed to be zero-mean spatially white Gaussian random processes with variance $\sigma^2 = -130$ dBm.

The results we analytically derived for the MRT/MRC- and the ZF–based schemes were obtained under the assumption that (5.8) holds true which means that the channel vectors between each relay and different transceivers are asymptotically orthogonal. However, with a finite number of relay antennas, these channel vectors are not perfectly orthogonal. The question worth answering via simulations is how network performance is affected when the optimization parameters are calculated under the assumption that the channel vectors are orthogonal (here called the ideal condition) while in reality these vectors are not orthogonal (here referred to as the actual condition). To elaborate more on the definitions of the ideal and actual conditions, we now explain how the total transmit power and the quality-of-service at the transceivers are calculated under the ideal and the actual conditions. Under the ideal condition, we use (5.21) to calculate the total transmit power. To do so, we use $\tilde{\boldsymbol{\beta}}_l$ and μ_l obtained from (5.30) and (5.31), where $p_{\bar{l}}$ and λ_l are calculated by solving (5.32) and (5.33)[4].

Under the actual condition, we first use the optimal values of $\{\mathbf{C}_i^{\text{MRTC}}\}_{i=1}^{n_r}$, obtained under the ideal condition, in (5.14) to obtain the optimal values of $\{\mathbf{C}_i^{\text{ZF}}\}_{i=1}^{n_r}$. We then use the optimal values of $\{\mathbf{C}_i^{\text{MRTC}}\}_{i=1}^{n_r}$ and $\{\mathbf{C}_i^{\text{ZF}}\}_{i=1}^{n_r}$ in (5.9) and (5.12) to obtain the actual values of the beamforming matrices $\{\mathbf{A}_i^{\text{MRTC}}\}_{i=1}^{n_r}$ and $\{\mathbf{A}_i^{\text{ZF}}\}_{i=1}^{n_r}$, respectively. Next, we use these actual values of beamforming matrices along with the optimal values of $\{p_l\}_{l=1}^{2K}$ (obtained under the ideal condition) in (5.6) to calculate the total transmit power consumed under the actual condition for each of these schemes.

Taking into account the lack of perfect orthogonality between any two columns of $\mathbf{H}_i$, interference may not be perfectly canceled at the transceivers. As a result, we

[4]Under the ideal condition, we can also calculate the total transmit power from (5.36), where $p_{\bar{l}}$ and λ_l are found to satisfy (5.32) and (5.33).

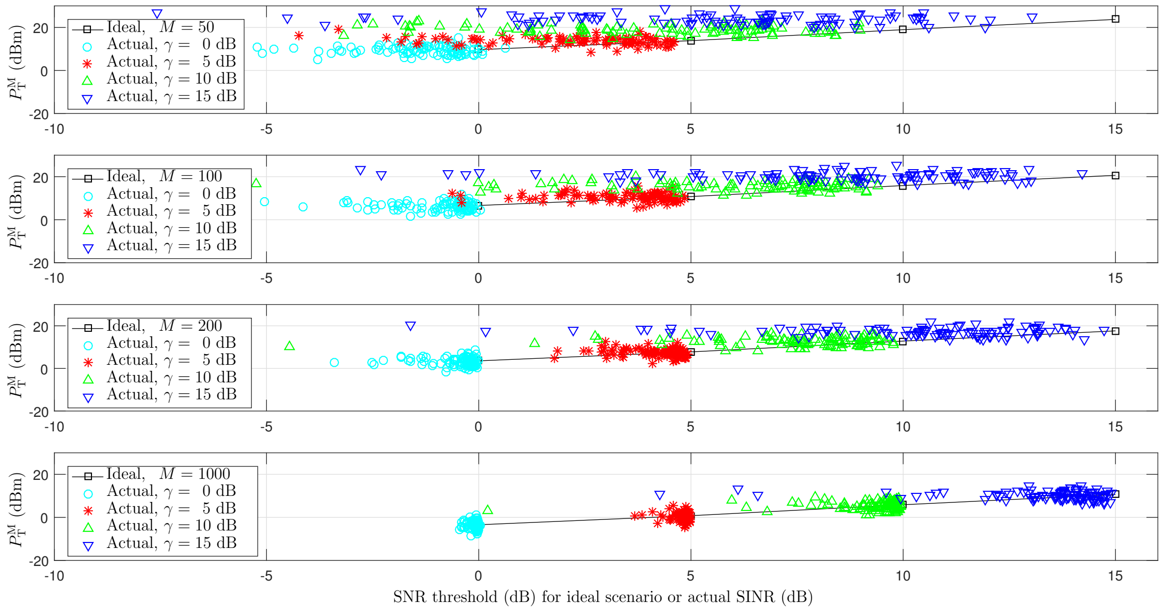

Figure 5.1: The average of the minimum total transmit power vs. the SNR threshold for ideal scenario and the actual minimum total transmit power vs. actual SINR, for MRT/MRC-based scheme when $K = 4$ and $n_r = 4$.

use SINR to evaluate the actual quality-of-signal at the transceivers. Using (5.4), we can write SINR at the receiver front-end of Transceiver l as

$$\mathrm{SINR}_l = \frac{p_{\bar{l}} \left| \sum_{i=1}^{n_r} \mathbf{h}_{l,i}^T \mathbf{A}_i \mathbf{h}_{\bar{l},i} \right|^2}{\sum_{\substack{r=1 \\ r \neq \bar{l}}}^{2K} p_l \left| \sum_{i=1}^{n_r} \mathbf{h}_{r,i}^T \mathbf{A}_i \mathbf{h}_{l,i} \right|^2 + \sigma^2 \left(\sum_{i=1}^{n_r} \left\| \mathbf{h}_{l,i}^T \mathbf{A}_i \right\|^2 + 1 \right)}, \quad \text{for } l \in \{1, 2, \cdots, 2K\}. \tag{5.38}$$

In light of (5.38), it is worth noting that under the actual condition, channel vectors between each relay and different transceivers are not perfectly orthogonal. As a result, when relays employ the MRT/MRC–based scheme, the interference power term $\sum_{\substack{r=1 \\ r \neq \bar{l}}}^{2K} p_l \left| \sum_{i=1}^{n_r} \mathbf{h}_{r,i}^T \mathbf{A}_i \mathbf{h}_{l,i} \right|^2$ in (5.38) is not zero. For the ZF-based scheme, however, this term is zero.

5.6.1 Numerical results for the MRT/MRC-based technique

In what follows, we present our numerical results obtained under the assumption that relays process their received signals using the MRT/MRC-based scheme. In Fig. 5.1, we show the performance of networks with different numbers of relay antennas (i.e., $M = 50, 100, 200, 1000$) under both the ideal and the actual conditions. For results obtained under the ideal condition, we show the average of the minimum total transmit powers versus the equal SNR thresholds denoted as γ (where $\gamma = \gamma_l$ for $l = 1, 2, \ldots, 2K$). This figure shows that under the actual condition, i.e., when a finite number of relay antennas are employed, the SINR values are smaller than the SNR threshold targeted. We can observe that when the power minimization problems are solved for 100 channel realizations but for the same SNR threshold, we arrive at 100 different values for the total transmit power each resulting in a different SINR value. A closer look at Fig. 5.1 reveals that for a given SNR threshold γ, increasing the number of relay antennas from $M = 50$ to $M = 1000$, renders the SINR values less scattered and closer to the SNR threshold. This observation is consistent with the fact that as the number of relay antennas is increased, the approximation to the channel vectors orthogonality (i.e., (5.8)) becomes more accurate. This figure also shows that for a fixed number of relay antennas, increasing the SNR threshold from $\gamma = 0$ dB to $\gamma = 15$ dB renders the achieved SINR values more scattered. Indeed, aiming to satisfy higher SNR thresholds, transceivers tend to transmit their signals with higher amounts of transmit powers which lead to an increase in the interference at the receiver front-end of transceivers. As the power of interference increases, the performance of the MRT/MRC-based method is expected to deteriorate further due to the fact that this method ignores interference and only aims to suppress noise.

In Fig. 5.2, we show the total transmit power, averaged over all simulation runs for the MRT/MRC-based scheme, under both the ideal and the actual conditions. This figure shows that as the number of relay antennas is increased, the total transmit power consumed under the ideal condition, is reducing by a factor of M. As an

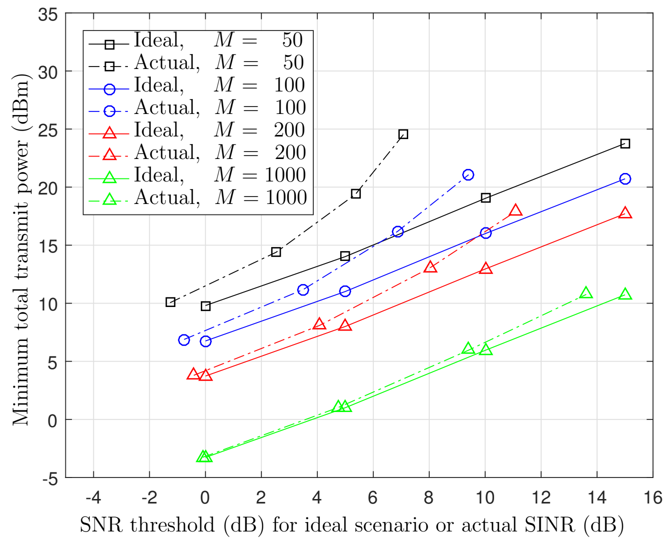

Figure 5.2: The minimum total transmit power vs. the minimum required SNR at the transceivers for ideal scenario and the actual minimum total transmit power vs. actual SINR, for MRT/MRC-based scheme when $K = 4$ and $n_r = 4$.

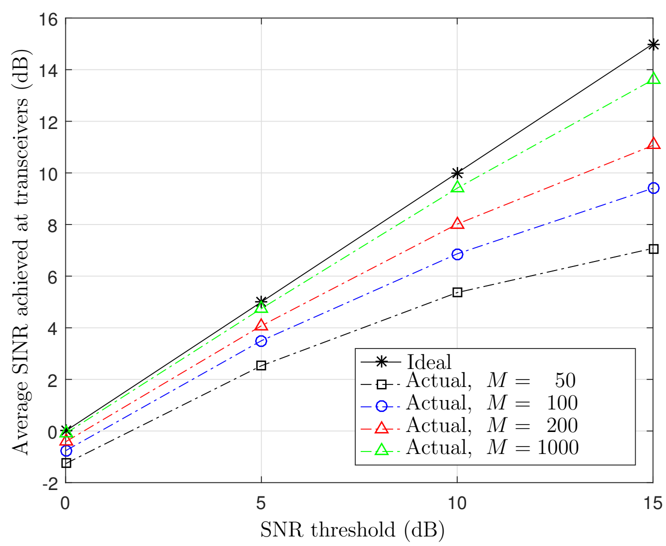

Figure 5.3: Average SINR achieved at the transceivers versus SNR thresholds for MRT/MRC-based scheme under the ideal and actual conditions.

example, for a fixed SNR threshold $\gamma = 15$ dB, a ten-fold increase in the number of relay antennas, from $M = 100$ to $M = 1000$, leads to a ten-fold decrease (i.e., 10 dB) in the total transmit power. This observation complies with the results of Theorem 1, which states that the minimum total transmit power is inversely proportional to the number of relay antennas. Fig. 5.2 also shows that the average total transmit power required for satisfying a certain SNR threshold under the actual condition, is higher than that under the ideal condition. However, we observe that for a fixed SNR threshold, for example $\gamma = 6$ dB, doubling the number of relay antennas from $M = 50$ to $M = 100$, can reduce the gap between the total transmit powers consumed under the ideal and the actual conditions from 6.28 dB to 2.97 dB. Further doubling the number of relay antennas to $M = 200$, can reduce this gap to 1.51 dB. Eventually, with a very large number of relay antennas, i.e., $M = 1000$, the difference between the total transmit powers under the ideal and the actual conditions reduces to 0.34 dB. This observation can be explained by the fact that as the number of relay antennas is increased the approximation to the channel vectors orthogonality (i.e., (5.8)) is *expected* to become more and more accurate. As a result, the network performances under the actual and the ideal conditions are *expected* to become closer.

Fig. 5.3 shows the average SINR achieved using the MRT/MRC-based scheme versus the SNR thresholds. In this figure, we examine how increasing the number of relay antennas can affect the SINR values. We also plot the average SINR achieved under the ideal condition as an upper bound to the achievable values of the SINR under the actual condition. We observe from this figure that SINR values achieved under the actual condition are less than those achieved under the ideal condition. This observation can be explained by the fact that, the MRT/MRC-based scheme ignores interference. As a result, unlike the ideal condition, under the actual condition the interference power term $\sum_{\substack{r=1 \\ r\neq \bar{l}}}^{2K} p_l \left| \sum_{i=1}^{n_r} \mathbf{h}_{r,i}^T \mathbf{A}_i \mathbf{h}_{l,i} \right|^2$ in (5.38) is not zero. As such, under the actual condition, the SINR values achieved using this method are expected to be less than the SNR thresholds. However, as can be seen from this figure, for a fixed SNR

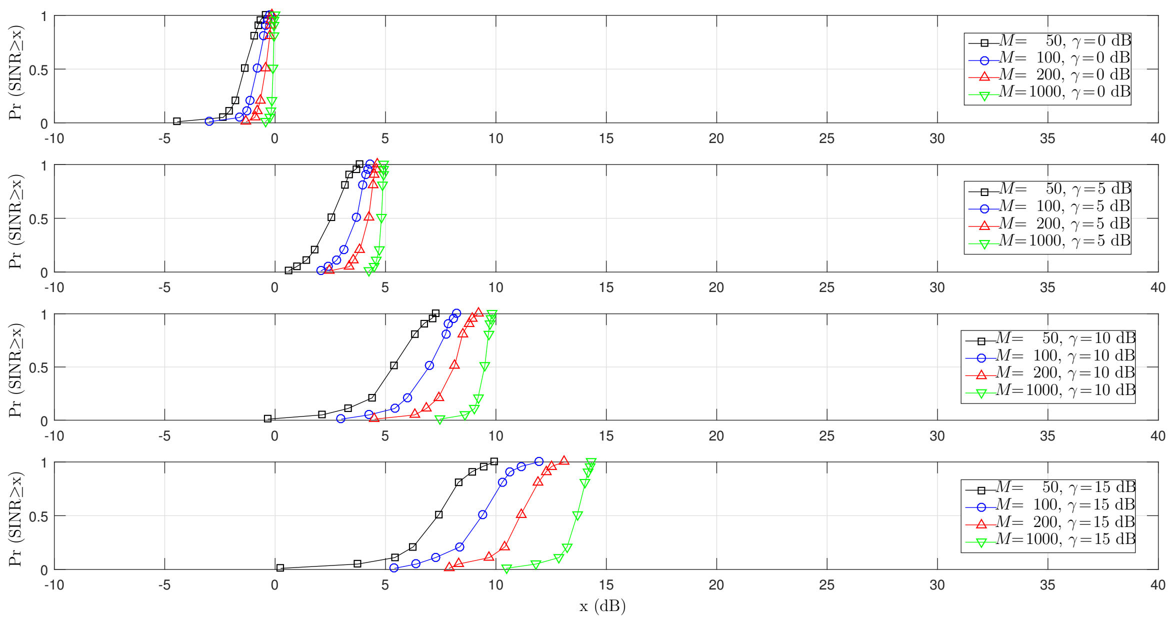

Figure 5.4: The CDF of the achievable SINR values versus SNR thresholds, for MRT/MRC-based scheme when $K = 4$, $n_r = 4$, and $M = 50, 100, 200, 1000$.

threshold, increasing the number of relay antennas can reduce the gap between the values of the SINR and SNR. For example, for a 15 dB SNR threshold, doubling the number of relay antennas from $M = 50$ to $M = 100$ reduces the gap between the values of the SINR and SNR from 7.6 to 5.6 dB. Further doubling the number of relay antennas, we observe that for $M = 200$, the gap is reduced to 3.9 dB. Eventually, for $M = 1000$ relay antennas, the gap between the values of the SINR and SNR is reduced to 1.4 dB. This observation complies with the fact that as the number of relay antennas is increased the approximation to the channel vectors orthogonality (i.e., (5.8)) becomes more accurate and the interference power term $\sum_{\substack{r=1 \\ r\neq \bar{l}}}^{2K} p_l \left| \sum_{i=1}^{n_r} \mathbf{h}_{r,i}^T \mathbf{A}_i \mathbf{h}_{l,i} \right|^2$ in (5.38) is further reduced. This reduction in the power of interference results in SINR values closer to the SNR thresholds.

In Fig. 5.4, we plot the cumulative distribution function (CDF) of the SINR values achieved using the MRT/MRC-based scheme versus the SNR thresholds for networks with different numbers of relay antennas (i.e., $M = 50, 100, 200, 1000$). This figure

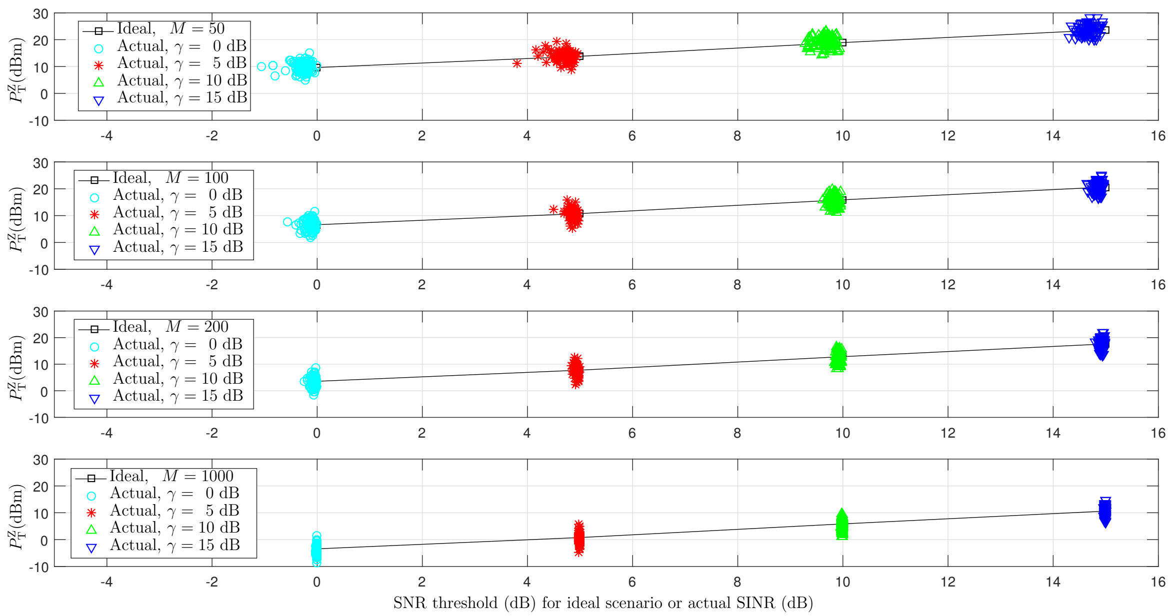

Figure 5.5: The average of the minimum total transmit power vs. the SNR threshold for ideal scenario and the actual minimum total transmit power vs. actual SINR, for ZF-based scheme when $K = 4$ and $n_r = 4$.

shows that for an SNR threshold of $\gamma = 0$ dB, increasing the number of relay antennas from $M = 50$ to $M = 1000$ leads to a decrease in the spread of the SINR values. This observation is in agreement with the fact that as the number of relay antennas is increased, the approximation to the channel vectors orthogonality (i.e., (5.8)) becomes more and more accurate. On the other hand, when the SNR threshold is increased from $\gamma = 0$ dB to $\gamma = 15$ dB, the spread of SINR values is increased. This observation is explained by the fact that when the SNR threshold is increased, transceivers have to increase their transmit powers to satisfy higher SNR thresholds. However, these increases in the transceiver transmit powers lead to an increase in the interference at the receiver front-end of transceivers. As the level of interference is increased, it becomes increasingly more probable that the MRT/MRC-based method suffer from the fact that it ignores interference.

5.6.2 Numerical results for the ZF-based Technique

We now present our numerical results obtained under the assumption that relays process their received signals using the ZF-based scheme. In Fig. 5.5, we show the performance of networks with different numbers of relay antennas (i.e., $M = 50, 100, 200, 1000$) both under the ideal and the actual conditions. For numerical results under the ideal condition, we plot the average of the minimum total transmit power versus equal SNR thresholds denoted as γ (where $\gamma = \gamma_l$ for $l = 1, 2, \ldots, 2K$). We observe that under the actual condition, when a finite number of relay antennas are employed, the SINR values are slightly smaller than the targeted SNR threshold, However, even for a small number of relay antennas, the SINR values achieved for the ZF-based method are not as scattered as those achieved for the MRT/MRC-based scheme in Fig. 5.1. This observation is partly explained by the fact that while the MRT/MRC-based scheme ignores interference, the ZF-based method completely eliminates interference. As such, even with a finite number of relay antennas, the ZF-based method does not suffer from inter-transceiver interference. On the other hand, it seems that when ZF-based method is employed at relays, the powers of the received signal and the noise at the l-th transceiver (given respectively as $p_{\bar{l}} \left| \sum_{i=1}^{n_r} \mathbf{h}_{l,i}^T \mathbf{A}_i \mathbf{h}_{\bar{l},i} \right|^2$ and $\sigma^2 \left(\sum_{i=1}^{n_r} \left\| \mathbf{h}_{l,i}^T \mathbf{A}_i \right\|^2 + 1 \right)$ in (5.38)) do not significantly differ under the ideal and the actual conditions.

Taking a closer look at Fig. 5.5, we observe that for a fixed SNR threshold γ, increasing the number of relay antennas from $M = 50$ to $M = 1000$, reduces the spread of SINR values achieved. The reduction in the SINR spread, when M is increased, can be attributed to the fact that as the number of relay antennas is increased, the powers of the received signal and the noise at the l-th transceiver (given respectively as $p_{\bar{l}} \left| \sum_{i=1}^{n_r} \mathbf{h}_{l,i}^T \mathbf{A}_i \mathbf{h}_{\bar{l},i} \right|^2$ and $\sigma^2 \left(\sum_{i=1}^{n_r} \left\| \mathbf{h}_{l,i}^T \mathbf{A}_i \right\|^2 + 1 \right)$ in (5.38)) further approach those under the ideal condition. As a result, as the number of relay antennas is increased, the performance under the actual condition further improves and becomes closer to that under the ideal condition.

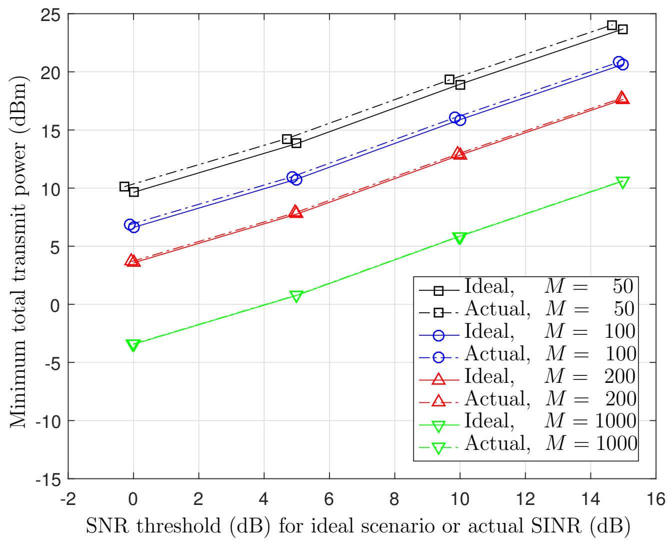

Figure 5.6: The minimum total transmit power vs. the minimum required SNR at the transceivers for ideal scenario and the actual minimum total transmit power vs. actual SINR, for ZF-based scheme when $K = 4$ and $n_r = 4$.

Fig. 5.5 also reveals that for a fixed number of relay antennas, the spread of the SINR values achieved using the ZF-based scheme, is only slightly sensitive to the increase in the SNR threshold from 0 dB to 15 dB (unlike the MRT/MRC-based scheme which ignores interference). This slight sensitivity of the performance under the actual condition reveals that when the ZF-based scheme is employed at relays, the lack of perfect orthogonality of the relay-transceiver channel vectors only slightly affects the powers of noise and desired signal at the transceivers.

In Fig. 5.6, we show the average of the total transmit power obtained using the ZF-based scheme under both the ideal and the actual conditions. This figure shows that for a fixed SNR threshold, the average of the total transmit powers under the actual condition is higher than that under the ideal condition. However, it is observed that for $M = 100$, $M = 200$, and $M = 1000$, the differences between the performances under the ideal and the actual conditions are very small. As can be seen from this figure, as the number of relay antennas is increased, the total transmit power consumed, under the actual conditions, is reduced by a factor of M. As an example, for a fixed SNR threshold $\gamma = 15$ dB, a ten-fold increase in the number of relay antennas,

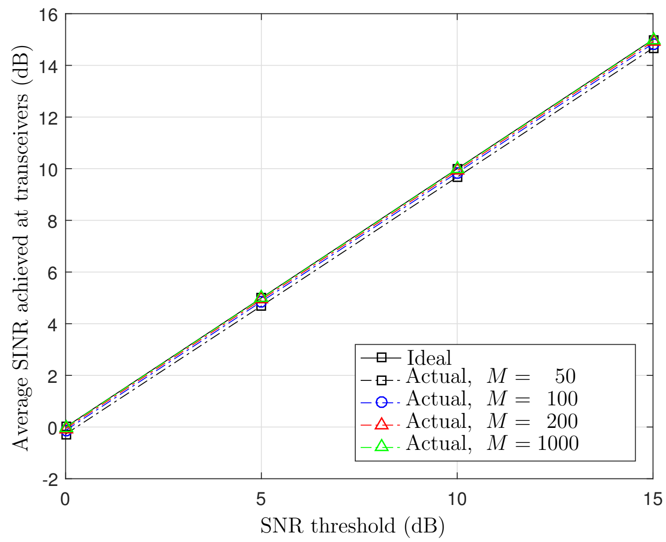

Figure 5.7: Average SINR achieved at the transceivers versus SNR thresholds for ZF-based scheme under the ideal and actual conditions.

from $M = 100$ to $M = 1000$, leads to approximately a ten-fold decrease (i.e., 10 dB) in the total transmit power. This observation implies that the minimum total transmit power consumed under the actual condition follows the same behaviour as that under the ideal condition (as proved in Theorem 1). The close performance of the ZF-based scheme under the ideal and the actual conditions observed in this figure can be attributed to the fact that this scheme eliminates the interference. As such, the performance of the ZF-based scheme is only slightly affected by the difference in the powers of signal and noise under the ideal and actual conditions. As the number of relay antennas is increased, the approximation to the channel vectors orthogonality (i.e., (5.8)) becomes more accurate. As a result, the network performances under the actual and the ideal conditions are expected to become more and more close.

Fig. 5.7 displays the average SINR achieved using the ZF-based scheme versus the SNR thresholds. This figure shows how increasing the number of relay antennas can affect the SINR values. The average SINR (SNR) value achieved under the ideal condition is also plotted as an upper bound to the achievable SINR values under the actual condition. As can be seen from this figure, for an SNR threshold of $\gamma = 15$ dB, doubling the number of relay antennas from $M = 50$ to $M = 100$, reduces the

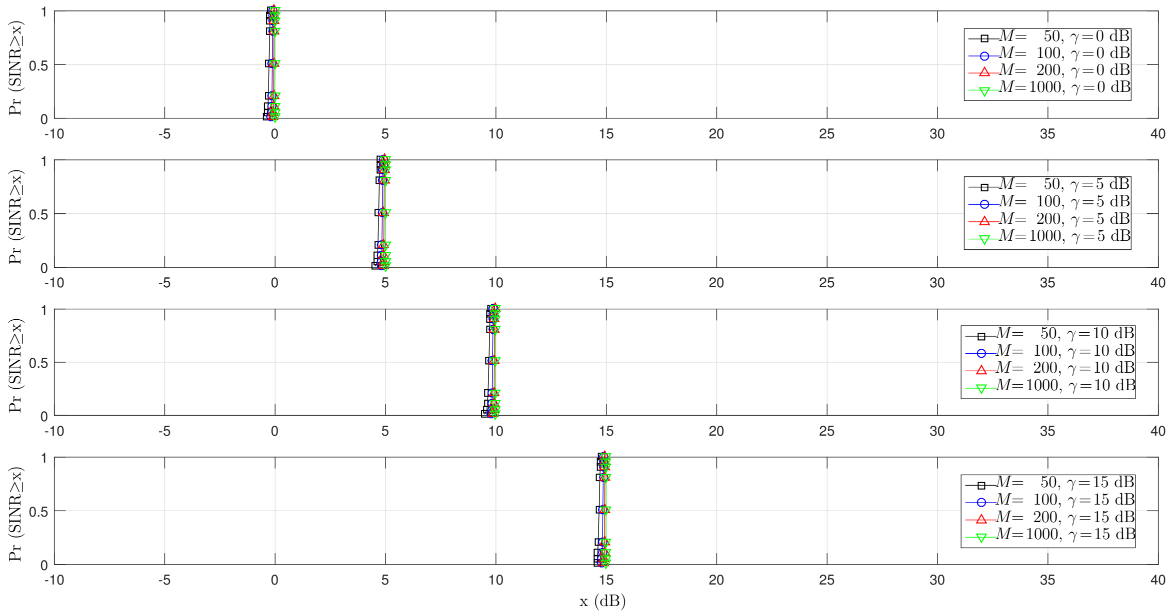

Figure 5.8: The CDF of the achievable SINR values versus SNR thresholds, for ZF-based scheme when $K = 4$, $n_r = 4$, and $M = 50, 100, 200, 1000$.

gap between the values of the SINR and SNR from 0.33 to 0.16 dB. Further doubling the number of antennas, we observe that for $M = 200$, the gap is reduced to 0.08 dB. Eventually, for $M = 1000$ relay antennas, the gap between the values of the SINR and SNR is reduced to 0.02 dB. These observations can be explained by the fact that the ZF-based method is designed to eliminate interference. As a result, even under the actual condition, the interference power term $\sum_{\substack{r=1 \\ r\neq \bar{l}}}^{2K} p_l \left| \sum_{i=1}^{n_r} \mathbf{h}_{r,i}^T \mathbf{A}_i \mathbf{h}_{l,i} \right|^2$ in (5.38) is zero. As such, the performance of this method can be only affected by the powers of received signal and noise (given respectively at the l-th transceiver as $p_{\bar{l}} \left| \sum_{i=1}^{n_r} \mathbf{h}_{l,i}^T \mathbf{A}_i \mathbf{h}_{\bar{l},i} \right|^2$ and $\sigma^2 \left(\sum_{i=1}^{n_r} \left\| \mathbf{h}_{l,i}^T \mathbf{A}_i \right\|^2 + 1 \right)$ in (5.38)). As can be seen from this figure, the close performance of the ZF-based scheme under the ideal and the actual conditions implies that the powers of signal and noise are only slightly different under the ideal and the actual conditions.

In Fig. 5.8, the CDF of the SINR values achieved using the ZF-based method under the actual condition are plotted versus the SNR thresholds for networks with different

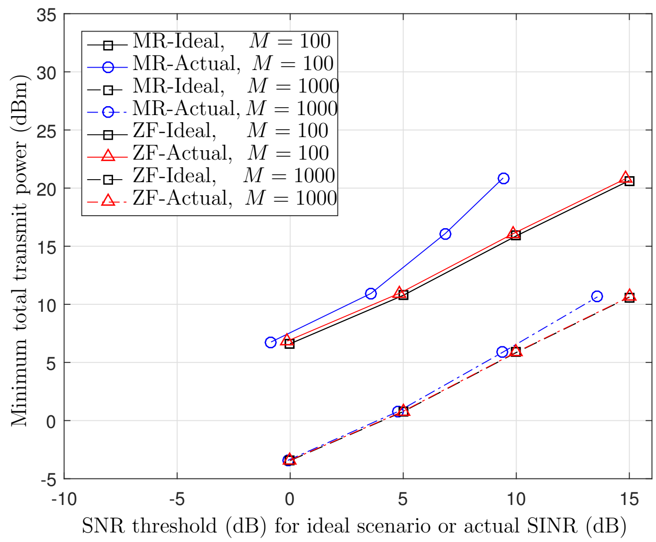

Figure 5.9: The minimum total transmit power vs. the minimum required SNR at the transceivers for ideal scenario and the actual minimum total transmit power vs. actual SINR, for MRT/MRC- and ZF-based schemes, when $K = 4$, $n_r = 4$, and $M = 100, 1000$.

numbers of relay antennas (i.e., $M = 50, 100, 200, 1000$). This figure shows that for a fixed SNR threshold γ, increasing the number of relay antennas from $M = 50$ to $M = 1000$, slightly reduces the spread of SINR values achieved. As can be seen from this figure, even for a small number of relay antennas, increasing the SNR threshold does not severely scatter the SINR values. Note that when the SNR threshold is increased, transceivers have to increase their transmit powers to satisfy higher SNR thresholds. As the ZF-based method completely eliminates interference, this increase in the transmit power (unlike the MRT/MRC-based method) does not lead to any interference at the receiver front-end of transceivers. As such, for a fixed number of relay antennas (even small numbers such as $M = 50$), the spread of the SINR values achieved using the ZF-based scheme (unlike the MRT/MRC-based scheme) is only slightly sensitive to the increase in the SNR threshold. This slight sensitivity of the performance under the actual condition can be attributed to the lack of perfect orthogonality in (5.8) (when the number of relay antennas are finite) which only affects the powers of noise and desired signal at the transceivers.

5.6.3 Performance comparison for the MRT/MRC- and the ZF-based relaying schemes

In Fig. 5.9, we compare performances of the MRT/MRC- and the ZF–based schemes under both the ideal and the actual conditions. In this figure, we illustrate the average total transmit power required for satisfying a certain SNR threshold. The performance is compared for networks with two different numbers of relay antennas, i.e., $M = 100, 1000$.

This figure shows that the performances of these two schemes under the ideal condition are the same. For example, under the ideal condition, regardless of the scheme being employed at relays, for a fixed SNR threshold $\gamma = 15$ dB, a ten-fold increase in the number of relay antennas, from $M = 100$ to $M = 1000$, leads to a ten-fold decrease (i.e., 10 dB) in the total transmit power. This observation is in agreement with the results of Theorem 1, which states that the minimum total transmit power is inversely proportional to the number of relay antennas. On the other hand, under the actual condition, we observe that the performance of the ZF-based scheme for $M = 100$ and $M = 1000$ is superior to that of the MRT/MRC-based scheme. A close look at results in this figure and the structures of beamforming matrices of the MRT/MRC- and the ZF-based schemes offers a trade-off between the performance and the computational complexity of these schemes. The performance superiority of the ZF-based scheme can be explained by the fact that the MRT/MRC-based scheme ignores interference, while the ZF-based scheme is designed to completely eliminate interference. However, such performance superiority comes with a cost. More specifically, the MRT/MRC-based method does not suffer from the computational burden of matrix inversion (see the structure of $\mathbf{A}_i^{\mathrm{MRTC}}$ in (5.9)), while implementing the ZF-based scheme requires the calculation of the matrix $\mathbf{H}^T\mathbf{H}$ (which is $\mathcal{O}(k^2M)$) followed by finding the inverse of this matrix (which is $\mathcal{O}(k^3)$), (see the structure of $\mathbf{A}_i^{\mathrm{ZF}}$ in (5.12)). As a result, the ZF-based scheme eliminates interference at the expense of adding computational burden. On the other hand, while the MRT/MRC-based

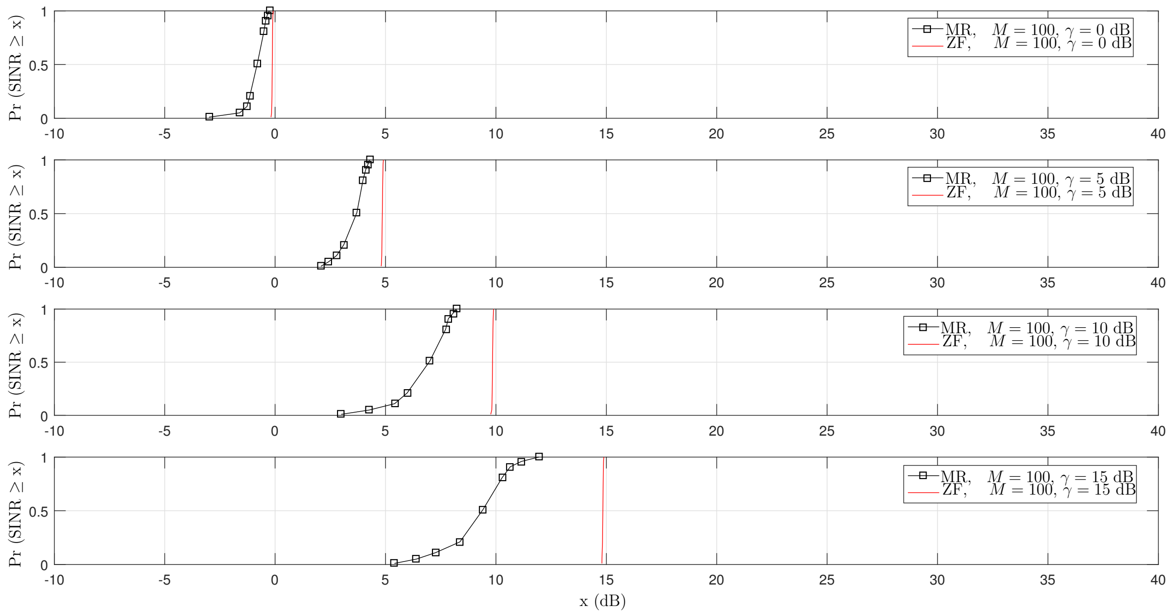

Figure 5.10: The CDF of the achievable SINR values versus SNR thresholds, for MRT/MRC- and ZF-based schemes, when $K = 4$, $n_r = 4$, and $M = 100$.

scheme does not require prohibitive computations, it suffers from ignoring interference, specially in high interference regimes or when the number of relay antennas are relatively low. Hence, one can recommend the MRT/MRC-based scheme to be used when SNR thresholds are relatively low or when the number of relay antennas is very large or when the number of transceiver pairs is high. The ZF-based method, on the other hand, can be recommended when the number of relay antennas is low and when SNR requirements are stringent and when the number of transceiver pairs is not too large.

In Figs. 5.10 and 5.11, we plot the CDF of the SINR values achieved using the MRT/MRC-and the ZF–based schemes, for networks with $M = 100$ and $M = 1000$ relay antennas, respectively. As can be seen from these two figures, in terms of the spread of the SINR values, the ZF-based scheme performs better than the MRT/MRC-based schemes. Moreover, we observe that for low SINR values (low-interference conditions), the MRT/MRC-based scheme performs close to the ZF-based scheme. However, as SINR threshold is increased (i.e., as transceivers transmit pow-

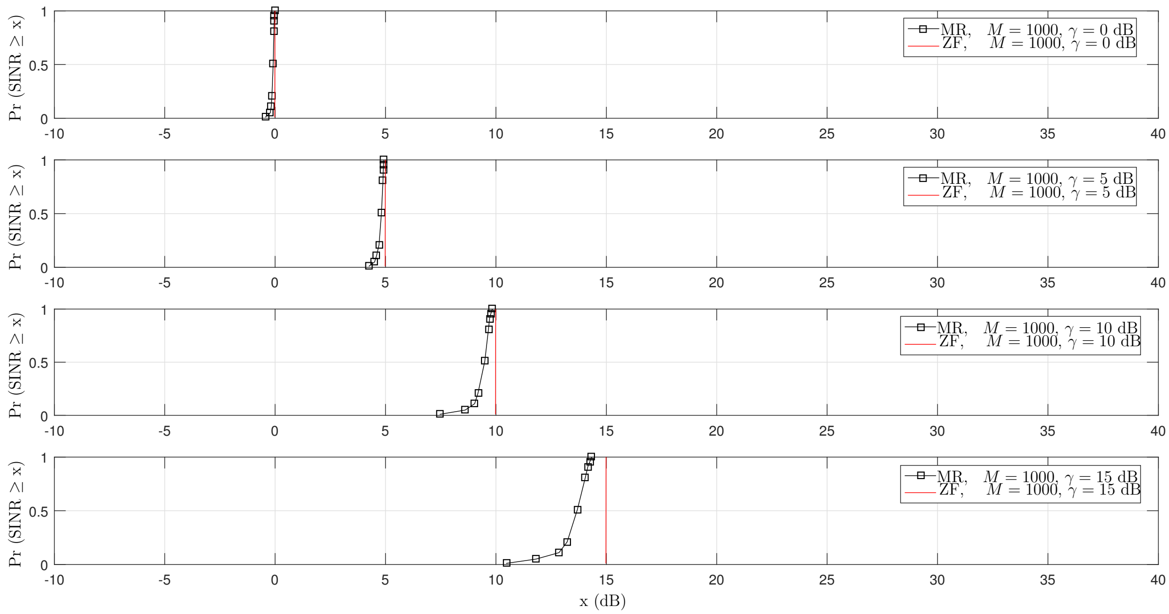

Figure 5.11: The CDF of the achievable SINR values versus SNR thresholds, for MRT/MRC- and ZF–based schemes, when $K = 4$, $n_r = 4$, and $M = 1000$.

ers, and as a result, interference are increased), the spread of the SINR values achieved using the MRT/MRC-based scheme moves away from the spread of the SINR values achieved using the ZF-based scheme. These observations can be explained by the fact that the MRT/MRC-based scheme ignores interference while ZF-based scheme eliminates interference. As such, while in low-interference conditions, the MRT/MRC-based scheme can afford a satisfactory performance, in high-interference conditions only the ZF-based scheme is able to do so.

Appendices

5.A Proof of Theorem 1

Defining new variables $z_l \triangleq Mp_l$ and $\zeta_l \triangleq \frac{\lambda_l}{M}$, we can rewrite vector $\mathbf{u}_l$ in (5.30) as

$$\mathbf{u}_l = \frac{1}{M} \underbrace{(\sigma^2 \gamma_l \mathbf{F}_l + \zeta_l (z_{\bar{l}} \mathbf{F}_{\bar{l}} + \sigma^2 \mathbf{I}_{n_r}))^{-1} \mathbf{g}_{\bar{l}}}_{\triangleq \mathbf{v}_l} = \frac{1}{M} \mathbf{v}_l \tag{5.A.1}$$

where, given z_l and ζ_l, the vector $\mathbf{v}_l$ is defined as a vector invariant with respect to (w.r.t.) M, and is in the same direction as $\mathbf{u}_l$. Using (5.A.1), we can rewrite (5.32) and (5.33), respectively as

$$\sigma^2 \gamma_l \frac{z_{\bar{l}}^{-2} - \zeta_l \mathbf{v}_l^H \mathbf{F}_{\bar{l}} \mathbf{v}_l}{\zeta_l^2 \mathbf{v}_l^H (z_{\bar{l}} \mathbf{F}_{\bar{l}} + \sigma^2 \mathbf{I}_{n_r}) \mathbf{v}_l} = 1 \tag{5.A.2}$$

$$z_{\bar{l}} \mathbf{g}_l^H \mathbf{v}_l = 1 \tag{5.A.3}$$

Interestingly enough, we observe that the optimal values of $z_{\bar{l}}$ and ζ_l, which are obtained via solving (5.A.2) and (5.A.3), do not depend on the number of relay antennas, i.e., M. This observation states that the optimal values of $z_{\bar{l}}$ and ζ_l, denoted respectively as z_l^{opt} and ζ_l^{opt}, remain unchanged for different numbers of relay antennas. As a result, at the optimum, equalities $p_l = \frac{z_l^{\text{opt}}}{M}$ and $\lambda_l = \frac{M}{\zeta_l^{\text{opt}}}$ hold true. As such, we can rewrite the minimum total transmit power in (5.36) as

$$P_{\mathrm{T}}^{\mathrm{M}} = \sum_{l=1}^{2K} (p_{\bar{l}} + \frac{\sigma^2 \gamma_l}{\lambda_l}) = \sum_{l=1}^{2K} (\frac{z_{\bar{l}}^{\text{opt}}}{M} + \frac{\sigma^2 \gamma_l}{M \zeta_l^{\text{opt}}}) = \frac{1}{M} \sum_{l=1}^{2K} (z_{\bar{l}}^{\text{opt}} + \frac{1}{\zeta_l^{\text{opt}}}) = \frac{c}{M} \tag{5.A.4}$$

where c is a scalar value invariant w.r.t. M. The proof is complete.

Chapter 6

Conclusions and Future Work

6.1 Conclusions

In Chapter 3 of this dissertation, we studied the total transmit power minimization problem for a two-way relay network under two constraints on the transceivers' received signal-to-noise-ratios. The network we considered in this chapter consists of multiple multi-antenna relay nodes and two single-antenna transceivers. Each relay linearly transforms the vector of its received signals (by multiplying this vector with a complex "beamforming" matrix), thereby obtaining a new vector whose entries are transmitted over different antennas of that relay. Assuming the relay beamforming matrices and the transceivers' transceiver powers as the design parameters, we first considered the problem of total power minimization under the assumption that the relay beamforming matrices are symmetric. Under such an assumption, we showed that the total power minimization problem is amenable to a semi-closed-form solution, and thus, can be solved efficiently. We then considered the case where the relay beamforming matrices may not be symmetric and showed that in this case, the total power minimization problem can be solved using a computationally prohibitive algorithm which involves a two-dimensional search over a grid in the space of the transceivers' powers and semi-definite programming at each vertex of this grid. Our numerical results showed that the symmetric assumption on the relay beamforming matrices incurs only insignificant loss, while this assumption allows us to significantly reduce the computational burden of solving the total power minimization problem.

In Chapter 4, we considered a single-carrier asynchronous relay network, where two transceivers exchange information with the help of multiple multi-antenna relays. The network is assumed to be asynchronous meaning that the signal transmitted by any of the two transceivers arrives at different relays with different delays and also signals transmitted by different relays arrive at any of the two transceivers with different delays. The network asynchronism renders the end-to-end channel frequency selective. We further assumed that each relay uses a *beamforming matrix* to transform the vector of the relay received signals into a new vector whose different entries will be transmitted over different antennas of that relay. Assuming the relay beamforming matrices as well as the transceivers' transmit powers as design parameters, we studied the problem of minimizing the total power consumed in the entire network while guaranteeing given data rates at the two transceivers. To this end, we developed a model for the end-to-end channel and used this model to solve the total power minimization problem. By restricting the relay beamforming matrices to be symmetric, we presented a computationally efficient solution to this problem. Our simulation results suggest that *for a given total number of antennas* to be employed in the network, there appears to be an optimal number of antennas per relay (and thus an optimal number of relays) which results in the lowest power consumption in the network.

In Chapter 5, we studied a two-way network of multiple multi-antennas relays which enable multiple pairs of transceivers to establish pairwise communications. Each relay is equipped with a very large number of antennas leading to the transceiver-relay channel vectors being approximately orthogonal. As a result, intra- and inter-pair interference will be negligible. Aiming to maintain the signal-to–noise ratio (SNR) at the receiver front-end of each transceiver above a certain threshold, we developed an algorithm to obtain the relay beamforming matrices and the transceiver powers such that the total transmit power consumed in the entire network is minimized. To do so, we assumed that the channel vectors between each relay and different transceivers are asymptotically orthogonal. For such power minimization problem, we derive computationally efficient solutions for the MRT/MRC- and the ZF-based techniques. Furthermore, we proved that when number of relay antennas are very large, at the optimum, both the minimum total transmit power and the transceivers transmit powers are inversely proportional to the number of relay antennas.

Our numerical results show that a trade-off holds between the performance and the computational complexity of the MRT/MRC- and the ZF-based schemes. The ZF-based scheme provides a superior performance in comparison to that provided by the MRT/MRC-based scheme. This superiority in performance is due to the fact that the MRT/MRC-based scheme ignores interference, while the ZF-based scheme completely eliminates interference. However, the superior performance of the ZF-based scheme is achieved at the expense of additional computational burden. On the other hand, while the computational complexity of implementing the MRT/MRC-based scheme is not prohibitive, this scheme suffers from ignoring interference, specially in high interference regimes or when the number of relay antennas are relatively low. Hence, the MRT/MRC-based scheme can be recommended for use when the SNR thresholds are relatively low or when the number of relay antennas is very large or when the number of transceiver pairs is high. On the other hand, one can recommend the ZF-based method when the number of relay antennas is low and when the SNR requirements are stringent and when the number of transceiver pairs is not too large.

6.2 Future Work

Some of the possible extensions to the work presented in the dissertation are listed below:

- Throughout this dissertation, we considered two-way relay networks with multiple multi-antenna relays and assumed that the channels between transceivers and relay antennas are frequency flat. A possible extension to our work in Chapters 3, 4, and 5 is to investigate these networks under the assumption that the channels between transceivers and relay antennas are frequency selective.

Addressing such networks in single-carrier mode, one can assume that some type of equalizers are implemented at the transceivers and/or at the relays. On the other hand, one can deal with the frequency selectivity of the channels between relays and transceivers via using OFDM technique both at the transceivers and at the relays. Addressing each of these extended cases of the networks we considered in this dissertation are interesting directions for future work.

- In this dissertation, we also assumed that all communications are performed in a single-carrier mode. However, one can solve the total power minimization problems for the case when communications are established in a multi-carrier mode or when the orthogonal frequency division multiplexing (OFDM) technique is employed.

- The analytical results in this dissertation are derived under the assumption that the channel vectors are fully known at the network nodes. Due to the fact that CSI can be acquired via traditional training procedures, using this assumption is a common practice in studies aimed at optimizing network parameters. However, as a future work, one can investigate how practical transceivers and relays have to operate under uncertain CSI or when CSI is only partially known at the transceivers and/or relays.

- In Chapter 4, we consider asynchronous two-way relay networks with multi-antenna relays and we obtained the minimal power consumption required to satisfy given data rate constraints at the two transceivers. While answering this question, we assumed no equalizer(s) at the transceivers and/or at the relays. However, as a future work, one can investigate this problem for the case that some type of equalizers (i.e., linear or otherwise) are implemented at transceivers and/or at relays (i.e., pre-channel equalization, post-channel equalization, or joint pre- and post-channel equalization). As an interesting approach, one can use the filter-and-forward (FF) relaying scheme, where relays employ finite-impulse-response (FIR) filters to equalize the propagation delays of different paths such that ISI is minimized at the receiver front-end of the transceivers.

- In Chapter 5, we considered multipair two-way relay networks with massive MIMO relays and assumed that the network is synchronous. As a future work, one can study this network under the assumption that the network is asynchronous. Based on the results we obtained for asynchronous networks serving a single pair of transceivers in Chapter 4, we conjecture that the solution to the total power minimization for asynchronous multipair two-way network with massive MIMO relays can also reduce down to a relay selection scheme. In such scheme, only those relays which contribute to the power-optimal tap of the end-to-end CIR are activated. Proving or disproving this conjecture is an interesting direction that can be pursued in the continuation of this dissertation.

- In this dissertation, we aimed to minimize the total power consumed in the entire network while some level of quality of services are satisfied at the transceivers. To do so, we assumed the relays beamforming matrices and the transceivers' transmit powers as the problem design parameters. However, while studying the same networks we studied in this dissertation, one can address different objective functions and or different design parameters to be optimized. For example, maximizing the network sum-rate or minimizing the minimum mean square error can be interesting problems to be considered in the continuation of this dissertation.

Bibliography

[1] S. Bastanirad, S. Shahbazpanahi, and A. Grami, "A total power minimization approach to optimal network beamforming and power allocation in single-carrier asynchronous two-way relay networks," vol. submitted, pp. xxxx–xxxx, August 2015.

[2] M. Iwamura, "NGMN view on 5G architecture," in *2015 IEEE 81st Veh. Technol. Conf. (VTC Spring)*, May 2015, pp. 1–5.

[3] E. Hossain, D. I. Kim, and V. K. Bhargava, *Cooperative cellular wireless networks.* Cambridge University Press, 2011.

[4] J. Furthmller and O. P. Waldhorst, "Energy-aware resource sharing with mobile devices," in *2011 8th Int. Conf. Wireless On-Demand Netw. Syst. Serv.*, Jan. 2011, pp. 52–59.

[5] A. F. Molisch, *Wireless communications.* John Wiley & Sons, 2007.

[6] D. Tse and P. Viswanath, *Fundamentals of wireless communication.* Cambridge university press, 2005.

[7] A. Goldsmith, *Wireless Communications.* Cambridge University Press, 2005.

[8] S. Ma, Y. Yang, and H. Sharif, "Distributed MIMO technologies in cooperative wireless networks," *IEEE Commun. Mag.*, vol. 49, pp. 78–82, May 2011.

[9] L. Zheng and D. N. C. Tse, "Diversity and multiplexing: a fundamental tradeoff in multiple-antenna channels," *IEEE Trans. Inf. Theory*, vol. 49, pp. 1073–1096, May 2003.

[10] X. Tang and Y. Hua, "Optimal design of non-regenerative MIMO wireless relays," *IEEE Trans. Wireless Commun.*, vol. 6, pp. 1398–1407, Apr. 2007.

[11] Y. Yang, H. Hu, J. Xu, and G. Mao, "Relay technologies for WiMax and LTE-advanced mobile systems," *IEEE Commun. Mag.*, vol. 47, pp. 100–105, October 2009.

[12] R. H. Y. Louie, Y. Li, and B. Vucetic, "Practical physical layer network coding for two-way relay channels: performance analysis and comparison," *IEEE Trans. Wireless Commun.*, vol. 9, pp. 764–777, Feb. 2010.

[13] P. Zhong and M. Vu, "Decode-forward and compute-forward coding schemes for the two-way relay channel," in *2011 IEEE Inf. Theory Workshop (ITW)*, Oct 2011, pp. 115–119.

[14] X. Wu and L. L. Xie, "On the optimal compressions in the compress-and-forward relay schemes," *IEEE Trans. Inf. Theory*, vol. 59, pp. 2613–2628, May 2013.

[15] A. Raja and P. Viswanath, "Compress-and-forward scheme for a relay network: Approximate optimality and connection to algebraic flows," in *2011 IEEE Int. Symp. Inf. Theory (ISIT)*, July 2011, pp. 1698–1702.

[16] J. Jiang, J. S. Thompson, P. M. Grant, and N. Goertz, "Practical compress-and-forward cooperation for the classical relay network," in *2009 17th Eur. Signal Process. Conf.*, Aug. 2009, pp. 2421–2425.

[17] K. Luo, R. H. Gohary, and H. Yanikomeroglu, "A decoding procedure for compress-and-forward and quantize-and-forward relaying," in *2012 50th Annu. Allerton Conf. Commun. Control Comput.*, Oct. 2012, pp. 2112–2119.

[18] Y. Tan and X. Yuan, "Compute-compress-and-forward: Exploiting asymmetry of wireless relay networks," *IEEE Trans. Signal Process.*, vol. 64, pp. 511–524, Jan. 2016.

[19] B. Rankov and A. Wittneben, "Spectral efficient protocols for half-duplex fading relay channels," *IEEE J. Sel. Areas Commun.*, vol. 25, pp. 379–389, Feb. 2007.

[20] Y. Wu, P. A. Chou, and S.-Y. Kung, "Information exchange in wireless networks with network coding and physical-layer broadcast," in *39th Annu. Conf. Inf. Sci. Syst. (CISS'05)*, Mar. 2005.

[21] M. Zaeri-Amirani, S. Shahbazpanahi, T. Mirfakhraie, and K. Ozdemir, "Performance tradeoffs in amplify-and-forward bidirectional network beamforming," *IEEE Trans. Signal Process.*, vol. 60, pp. 4196 –4209, Aug. 2012.

[22] S. J. Kim, P. Mitran, and V. Tarokh, "Performance bounds for bi-directional coded cooperation protocols," in *27th Int. Conf. Distrib. Comput. Syst. Workshops (ICDCSW)*, June 2007, pp. 83–83.

[23] P. Popovski and H. Yomo, "Physical network coding in two-way wireless relay channels," in *2007 IEEE Int. Conf. Commun. (ICC)*, June 2007, pp. 707–712.

[24] I. Hammerstrom, M. Kuhn, C. Esli, J. Zhao, A. Wittneben, and G. Bauch, "MIMO two-way relaying with transmit CSI at the relay," in *IEEE 8th Workshop Signal Process. Advances Wireless Commun. (SPAWC)*, Helsinki, June 2007, pp. 1–5.

[25] C. Yuen, W. H. Chin, Y. L. Guan, W. Chen, and T. Tee, "Bi-directional multi-antenna relay communications with wireless network coding," in *2008 IEEE Veh. Technol. Conf., 2008. (VTC Spring)*, May 2008, pp. 1385–1388.

[26] T. Cui and J. Kliewer, "Memoryless relay strategies for two-way relay channels: Performance analysis and optimization," in *IEEE Int. Con. Commun. (ICC)*, Beijing, May 2008, pp. 1139–1143.

[27] V. Havary-Nassab, S. Shahbazpanahi, and A. Grami, "Optimal distributed beamforming for two-way relay networks," *IEEE Trans. Signal Process.*, vol. 58, pp. 1238–1250, Mar. 2010.

[28] S. J. Kim, N. Devroye, and V. Tarokh, "A class of bi-directional multi-relay protocols," in *2009 IEEE Int. Symp. Inf. Theory*, June 2009, pp. 349–353.

[29] R. Zhang, Y.-C. Liang, C. C. Chai, and S. Cui, "Optimal beamforming for two-way multi-antenna relay channel with analogue network coding," *IEEE J. Sel. Areas Commun.*, vol. 27, pp. 699–712, June 2009.

[30] A. Khabbazibasmenj, F. Roemer, S. Vorobyov, and M. Haardt, "Sum-rate maximization in two-way AF MIMO relaying: Polynomial time solutions to a class of DC programming problems," *IEEE Trans. Signal Process.*, vol. 60, pp. 5478–5493, Oct. 2012.

[31] G. Li, Y. Wang, and P. Zhang, "Optimal linear MMSE beamforming for two way multi-antenna relay systems," *IEEE Commun. Lett.*, vol. 15, pp. 533–535, May 2011.

[32] T. J. Oechtering, E. A. Jorswieck, R. F. Wyrembelski, and H. Boche, "On the optimal transmit strategy for the MIMO bidirectional broadcast channel," *IEEE Trans. Commun.*, vol. 57, pp. 3817–3826, Dec. 2009.

[33] C. Y. Leow, Z. Ding, and K. K. Leung, "Joint beamforming and power management for nonregenerative MIMO two-way relaying channels," *IEEE Trans. Veh. Technol.*, vol. 60, pp. 4374–4383, Nov. 2011.

[34] J. Gao, J. Zhang, S. A. Vorobyov, H. Jiang, and M. Haardt, "Power allocation/beamforming for DF MIMO two-way relaying: Relay and network optimization," in *2012 IEEE Global Commun. Conf. (GLOBECOM)*, Dec. 2012, pp. 5657–5662.

[35] V. T. Muralidharan and B. S. Rajan, "Wireless network coding for MIMO two-way relaying," *IEEE Trans. Wireless Commun.*, vol. 12, pp. 3566–3577, July 2013.

[36] R. Wang, M. Tao, and Z. Xiang, "Nonlinear precoding design for MIMO amplify-and-forward two-way relay systems," *IEEE Trans.Veh. Technol.*, vol. 61, pp. 3984–3995, Nov. 2012.

[37] G. Amarasuriya, C. Tellambura, and M. Ardakani, "Sum rate analysis of two-way MIMO AF relay networks with zero-forcing," *IEEE Trans. Wireless Commun.*, vol. 12, pp. 4456–4469, Sept. 2013.

[38] C. Li, L. Yang, and W. P. Zhu, "Two-way MIMO relay precoder design with channel state information," *IEEE Trans. Commun.*, vol. 58, pp. 3358–3363, Dec. 2010.

[39] K. J. Lee, H. Sung, E. Park, and I. Lee, "Joint optimization for one and two-way MIMO AF multiple-relay systems," *IEEE Trans. Wireless Commun.*, vol. 9, pp. 3671–3681, Dec. 2010.

[40] S. Xu and Y. Hua, "Optimal design of spatial source-and-relay matrices for a non-regenerative two-way MIMO relay system," *IEEE Trans. Wireless Commun.*, vol. 10, pp. 1645–1655, May 2011.

[41] Y. Rong, "Joint source and relay optimization for two-way linear non-regenerative MIMO relay communications," *IEEE Trans. Signal Process.*, vol. 60, pp. 6533–6546, Dec. 2012.

[42] F. Roemer and M. Haardt, "A low-complexity relay transmit strategy for two-way relaying with MIMO amplify and forward relays," in *2010 IEEE Int. Conf. Acoust. Speech Signal Process.*, Mar. 2010, pp. 3254–3257.

[43] R. Wang and M. Tao, "Joint source and relay precoding designs for MIMO two-way relaying based on MSE criterion," *IEEE Trans. Signal Process.*, vol. 60, pp. 1352–1365, Mar. 2012.

[44] H. Park, H. J. Yang, J. Chun, and R. Adve, "A closed-form power allocation and signal alignment for a diagonalized MIMO two-way relay channel with linear receivers," *IEEE Trans. Signal Process.*, vol. 60, pp. 5948–5962, Nov. 2012.

[45] W. C. Choi, S. Choi, A. Heo, and D. J. Park, "Joint optimization of source and relay for MIMO two-way relay networks using MSE duality," *IEEE Commun. Lett.*, vol. 18, pp. 1246–1249, July 2014.

[46] A. Heo, W. C. Choi, J. H. Park, and D. J. Park, "Sum rate maximization of an MIMO two-way relay system using MSE duality," *IEEE Commun. Lett.*, vol. 19, pp. 863–866, May 2015.

[47] J. Li, M. Matthaiou, and T. Svensson, "I/Q imbalance in two-way AF relaying," *IEEE Trans. Commun.*, vol. 62, pp. 2271–2285, July 2014.

[48] Y. Zhang, L. Ping, and Z. Zhang, "Low cost pre-coder design for MIMO AF two-way relay channel," *IEEE Signal Process. Lett.*, vol. 22, pp. 1369–1372, Sept. 2015.

[49] E. G. Larsson, "MIMO detection methods: How they work [lecture notes]," *IEEE Signal Process. Mag.*, vol. 26, pp. 91–95, May 2009.

[50] M. Eslamifar, C. Yuen, W. H. Chin, and Y. L. Guan, "Max-min antenna selection for bi-directional multi-antenna relaying," in *Proc. IEEE Veh. Technol. Conf.*, May 2010, pp. 1–5.

[51] E. Yilmaz, R. Zakhour, D. Gesbert, and R. Knopp, “Multi-pair two-way relay channel with multiple antenna relay station,” in *2010 IEEE Int. Conf. Commun. (ICC)*, May 2010, pp. 1–5.

[52] L. Sanguinetti, A. A. D’Amico, and Y. Rong, “A tutorial on the optimization of amplify-and-forward MIMO relay systems,” *IEEE J. Sel. Areas Commun.*, vol. 30, pp. 1331–1346, Sept. 2012.

[53] F. Roemer and M. Haardt, “Algebraic norm-maximizing (ANOMAX) transmit strategy for two-way relaying with MIMO amplify and forward relays,” *IEEE Signal Process. Lett.*, vol. 16, pp. 909–912, Oct 2009.

[54] R. Wang and M. Tao, “Joint source and relay precoding designs for MIMO two-way relaying based on MSE criterion,” *IEEE Trans. Signal Process.*, vol. 60, pp. 1352–1365, Mar. 2012.

[55] J. Zhang and M. Haardt, “Energy efficient two-way non-regenerative relaying for relays with multiple antennas,” *IEEE Signal Process. Lett.*, vol. 22, pp. 1079–1083, Aug. 2015.

[56] K. J. Lee, K. W. Lee, H. Sung, and I. Lee, “Sum-rate maximization for two-way MIMO amplify-and-forward relaying systems,” in *2009. IEEE 69th Veh. Technol. Conf. (VTC Spring)*, Apr. 2009, pp. 1–5.

[57] R. Vaze and R. W. Heath, “Capacity scaling for MIMO two-way relaying,” in *IEEE Int. Symp. Inf. Theory, (ISIT)*, Nice, June 2007, pp. 1451–1455.

[58] D. Gunduz, A. Goldsmith, and H. Poor, “MIMO two-way relay channel: Diversity-multiplexing tradeoff analysis,” in *Proc. Asilomar Conf. Signals Syst. Comput.*, Oct. 2008, pp. 1474–1478.

[59] H. Kha, H. Tuan, H. Nguyen, and H. Tam, “Joint design of user power allocation and relay beamforming in two-way MIMO relay networks,” in *Proc. Int. Conf. Signal Process. Commun. Syst.*, Dec. 2013, pp. 1–6.

[60] A. P. T. Lau and S. Cui, “Joint power minimization in wireless relay channels,” *IEEE Trans. Wireless Commun.*, vol. 6, pp. 2820–2824, Aug. 2007.

[61] L. P. Qian, Y. Wu, and Q. Chen, “Transmit power minimization for outage-constrained relay selection over rayleigh-fading channels,” *IEEE Commun. Lett.*, vol. 18, pp. 1383–1386, Aug 2014.

[62] T. Wang, Y. Fang, and L. Vandendorpe, “Power minimization for OFDM transmission with subcarrier-pair based opportunistic DF relaying,” *IEEE Commun. Lett.*, vol. 17, pp. 471–474, Mar. 2013.

[63] D. H. N. Nguyen and H. H. Nguyen, “Power allocation in wireless multiuser multi-relay networks with distributed beamforming,” *IET Commun.*, vol. 5, pp. 2040–2051, Sept. 2011.

[64] H. Chen, S. Shahbazpanahi, and A. B. Gershman, "Filter-and-forward distributed beamforming for two-way relay networks with frequency selective channels," *IEEE Trans. Signal Process.*, vol. 60, pp. 1927–1941, Apr. 2012.

[65] S. Shahbazpanahi, "A semi-closed-form solution to optimal decentralized beamforming for two-way relay networks," in *2009 3rd IEEE Int. Workshop Comput. Advances Multi-Sensor Adaptive Process. (CAMSAP)*, Dec. 2009, pp. 101–104.

[66] S. Talwar, Y. Jing, and S. Shahbazpanahi, "Joint relay selection and power allocation for two-way relay networks," *IEEE Signal Process. Lett.*, vol. 18, pp. 91–94, Feb. 2011.

[67] Z. Hasan, H. Boostanimehr, and V. K. Bhargava, "Green cellular networks: A survey, some research issues and challenges," *IEEE Commun. Surveys Tut.*, vol. 13, pp. 524–540, Apr. 2011.

[68] F. Han, Z. Safar, W. S. Lin, Y. Chen, and K. J. R. Liu, "Energy-efficient cellular network operation via base station cooperation," in *2012 IEEE Int. Conf. Commu. (ICC)*, June 2012, pp. 4374–4378.

[69] R. Vaze and R. W. Heath, "On the capacity and diversity-multiplexing tradeoff of the two-way relay channel," *IEEE Trans. Inf. Theory*, vol. 57, pp. 4219–4234, July 2011.

[70] R. AliHemmati, S. ShahbazPanahi, and M. Dong, "Joint spectrum sharing and power allocation for ofdm-based two-way relaying," *IEEE Transactions on Wireless Communications*, vol. 14, no. 6, pp. 3294–3308, June 2015.

[71] M. Chang, M. Dong, F. Zuo, and S. ShahbazPanahi, "Joint subchannel pairing and power allocation in multichannel mabc-based two-way relaying," vol. 15, pp. 620–632, Jan. 2016.

[72] M. Chang and M. Dong, "Snr-based channel pairing design in multichannel tdbc-based two-way relaying," in *2013 Asilomar Conference on Signals, Systems and Computers*, Nov 2013, pp. 220–224.

[73] T. J. Oechtering, R. F. Wyrembelski, and H. Boche, "Multiantenna bidirectional broadcast channels: Optimal transmit strategies," *IEEE Trans. Signal Process.*, vol. 57, pp. 1948–1958, May 2009.

[74] S. J. Kim, N. Devroye, P. Mitran, and V. Tarokh, "Achievable rate regions and performance comparison of half duplex bi-directional relaying protocols," *IEEE Trans. Inf. Theory*, vol. 57, pp. 6405–6418, Oct. 2011.

[75] A. S. Avestimehr, A. Sezgin, and D. N. C. Tse, "Approximate capacity of the two-way relay channel: A deterministic approach," in *2008 46th Annu. Allerton Conf. Commun. Control Comput.*, Sept. 2008, pp. 1582–1589.

[76] B. Rankov and A. Wittneben, "Achievable rate regions for the two-way relay channel," in *2006 IEEE Int. Symp. Inf. Theory*, July 2006, pp. 1668–1672.

[77] M. P. Wilson, K. Narayanan, H. D. Pfister, and A. Sprintson, “Joint physical layer coding and network coding for bidirectional relaying,” *IEEE Trans. Inf. Theory*, vol. 56, pp. 5641–5654, Nov. 2010.

[78] R. Wang, M. Tao, and Y. Huang, “Linear precoding designs for amplify-and-forward multiuser two-way relay systems,” *IEEE Trans. Wireless Commun.*, vol. 11, pp. 4457–4469, Dec. 2012.

[79] M. Pischella and D. L. Ruyet, “Optimal power allocation for the two-way relay channel with data rate fairness,” *IEEE Commun. Lett.*, vol. 15, pp. 959–961, Sept. 2011.

[80] I. Krikidis and S. T. John, “MIMO two-way relay channel with superposition coding and imperfect channel estimation,” in *2010 IEEE Globecom Workshops (GLOBECOM)*, Dec. 2010, pp. 84–88.

[81] F. Gao, R. Zhang, and Y.-C. Liang, “Channel estimation for OFDM modulated two-way relay networks,” *IEEE Trans. Signal Process.*, vol. 57, pp. 4443 –4455, Nov. 2009.

[82] A. Abdelkader, S. Shahbazpanahi, and A. Gershman, “Joint subcarrier power loading and distributed beamforming in OFDM-based asynchronous relay networks,” in *2009 3rd IEEE Int. Workshop Comput. Advances Multi-Sensor Adaptive Process. (CAMSAP)*, Dec. 2009, pp. 105–108.

[83] R. Vahidnia and S. Shahbazpanahi, “Multi-carrier asynchronous bi-directional relay networks: Joint subcarrier power allocation and network beamforming,” *IEEE Trans. Wireless Commun.*, vol. 12, pp. 3796–3812, Aug. 2013.

[84] M. Dong and S. Shahbazpanahi, “Optimal spectrum sharing and power allocation for OFDM-based two-way relaying,” in *2010 IEEE Int. Conf. Acoust. Speech Signal Process. (ICASSP)*, Mar. 2010, pp. 3310–3313.

[85] A. Schad, H. Chen, A. Gershman, and S. Shahbazpanahi, “Filter-and-forward multiple peer-to-peer beamforming in relay networks with frequency selective channels,” in *2010 EEE Int. Conf. Acoust. Speech Signal Process. (ICASSP)*, Mar. 2010, pp. 3246–3249.

[86] Y. Wen Liang, A. Ikhlef, W. Gerstacker, and R. Schober, “Cooperative filter-and-forward beamforming for frequency-selective channels with equalization,” *IEEE Trans. Wireless Commun.*, vol. 10, pp. 228 –239, Jan. 2011.

[87] H. Chen, A. Gershman, and S. Shahbazpanahi, “Filter-and-forward distributed beamforming in relay networks with frequency selective fading,” *IEEE Trans. Signal Process.*, vol. 58, no. 3, pp. 1251–1262, Mar. 2010.

[88] R. Vahidnia and S. ShahbazPanahi, “Single-carrier equalization for asynchronous two-way relay networks,” *IEEE Trans. Signal Process.*, vol. 62, pp. 5793– 5808, Nov. 2014.

[89] R. Vahidnia, S. Shahbazpanahi, and A. Minasian, "Pre-channel equalization and distributed beamforming in asynchronous single-carrier bi-directional relay networks," *IEEE Trans. Signal Process.*, vol. 64, pp. 3968–3983, Aug. 2016.

[90] J. Mirzaei and S. ShahbazPanahi, "On achievable SNR region for multi-user multi-carrier asynchronous bidirectional relay networks," *IEEE Trans. Wireless Commun.*, vol. 14, pp. 3219–3230, June 2015.

[91] R. AliHemmati and S. Shahbazpanahi, "Sum-rate optimal network beamforming and subcarrier power allocation for multi-carrier asynchronous two-way relay networks," *IEEE Trans. Signal Process.*, vol. 63, pp. 4129–4143, Aug. 2015.

[92] M. Askari and S. Shahbazpanahi, "On sum-rate maximization approach to network beamforming and power allocation for asynchronous single-carrier two-way relay networks," *IEEE Access*, vol. 5, pp. 13 699–13 711, 2017.

[93] F. E. Dorcheh and S. Shahbazpanahi, "Jointly optimal pre- and post-channel equalization and distributed beamforming in asynchronous bidirectional relay networks," *IEEE Trans. Signal Process.*, vol. 65, pp. 4593–4608, Sept. 2017.

[94] Q. Wang and Y. Jing, "Power allocation and sum-rate analysis for multi-user multi-relay networks," in *2013 IEEE 78th Veh. Technol. Conf. (VTC)*, Sept. 2013, pp. 1–5.

[95] H. Wang, J. Ding, J. Yang, X. Gao, and Z. Ding, "Spectral and energy efficiency for multi-pair massive MIMO two-way relaying networks with imperfect CSI," in *2015 IEEE 82nd Veh. Technol. Conf. (VTC)*, Sept. 2015, pp. 1–6.

[96] X. Wang, Y. Wang, and R. Sun, "Approximate sum rate for massive multiple-input multiple-output two-way relay with Ricean fading," *IET Commun.*, vol. 10, pp. 1493–1500, 2016.

[97] M. Tao and R. Wang, "Linear precoding for multi-pair two-way MIMO relay systems with max-min fairness," *IEEE Trans. Signal Process.*, vol. 60, pp. 5361–5370, Oct. 2012.

[98] H. Chung, N. Lee, B. Shim, and T. W. Oh, "Joint transceiver and relay beamforming design for multi-pair two-way relay systems," in *2012 IEEE Int. Conf. Commun. (ICC)*, June 2012, pp. 3795–3799.

[99] R. S. Ganesan, H. Al-Shatri, T. Weber, and A. Klein, "Relay-aided interference alignment for bidirectional communications in multi-pair multi-relay networks," in *2013 IEEE 14th Workshop Signal Process. Advances Wireless Commun. (SPAWC)*, June 2013, pp. 66–70.

[100] H. Mu and J. K. Tugnait, "Interference alignment-like precoder design in multi-pair two-way relay cognitive radio networks," in *2012 IEEE Global Commun. Conf. (GLOBECOM)*, Dec. 2012, pp. 1471–1476.

[101] J. Zhang, F. Roemer, M. Haardt, A. Khabbazibasmenj, and S. A. Vorobyov, “Sum rate maximization for multi-pair two-way relaying with single-antenna amplify and forward relays,” in *2012 IEEE Int. Conf. Acoust., Speech Signal Process. (ICASSP)*, Mar. 2012, pp. 2477–2480.

[102] Z. Fang, X. Wang, and X. Yuan, “Beamforming design for multiuser two-way relaying: A unified approach via max-min SINR,” *IEEE Trans. Signal Process.*, vol. 61, pp. 5841–5852, Dec. 2013.

[103] M. Chen and A. Yener, “Multiuser two-way relaying: detection and interference management strategies,” *IEEE Trans. Wireless Commun.*, vol. 8, pp. 4296–4305, Aug. 2009.

[104] K. Jitvanichphaibool, R. Zhang, and Y. C. Liang, “Optimal resource allocation for two-way relay-assisted OFDMA,” *IEEE Trans. Veh. Technol.*, vol. 58, pp. 3311–3321, Sept. 2009.

[105] C. Y. Leow, Z. Ding, K. K. Leung, and D. L. Goeckel, “On the study of analogue network coding for multi-pair, bidirectional relay channels,” *IEEE Trans. Wireless Commun.*, vol. 10, pp. 670–681, Feb. 2011.

[106] C. Esli and A. Wittneben, “One- and two-way decode-and-forward relaying for wireless multiuser MIMO networks,” in *2008 IEEE Global Commun. Conf. (GLOBECOM)*, Nov. 2008, pp. 1–6.

[107] J. Joung and A. Sayed, “Multiuser two-way amplify-and-forward relay processing and power control methods for beamforming systems,” *IEEE Trans. Signal Process.*, vol. 58, pp. 1833–1846, Mar. 2010.

[108] C. Esli and A. Wittneben, “Multiuser MIMO two-way relaying for cellular communications,” in *2008 IEEE 19th Int. Symp. Pers. Indoor and Mobile Radio Commun. (PIMRC)*, Sept. 2008, pp. 1–6.

[109] J. Joung and A. H. Sayed, “User selection methods for multiuser two-way relay communications using space division multiple access,” *IEEE Trans. Wireless Commun.*, vol. 9, pp. 2130–2136, July 2010.

[110] Z. Ding, I. Krikidis, J. Thompson, and K. K. Leung, “Physical layer network coding and precoding for the two-way relay channel in cellular systems,” *IEEE Trans. Signal Process.*, vol. 59, pp. 696–712, Feb. 2011.

[111] J. Sima and W. Chen, “Joint network and dirty-paper coding for multi-way relay networks with pairwise information exchange,” in *2014 IEEE Global Commun. Conf. (GLOBECOM)*, Dec. 2014, pp. 1565–1570.

[112] R. S. Ganesan, H. Al-Shatri, A. Kuehne, T. Weber, and A. Klein, “Pair-aware interference alignment in multi-user two-way relay networks,” *IEEE Trans. Wireless Commun.*, vol. 12, pp. 3662–3671, Aug. 2013.

[113] E. G. Larsson, O. Edfors, F. Tufvesson, and T. L. Marzetta, “Massive MIMO for next generation wireless systems,” *IEEE Commun. Mag.*, vol. 52, pp. 186–195, Feb. 2014.

[114] F. Rusek, D. Persson, B. K. Lau, E. G. Larsson, T. L. Marzetta, O. Edfors, and F. Tufvesson, “Scaling up MIMO: Opportunities and challenges with very large arrays,” *IEEE Signal Process. Mag.*, vol. 30, pp. 40–60, Jan. 2013.

[115] J. Hoydis, S. ten Brink, and M. Debbah, “Massive MIMO in the UL/DL of cellular networks: How many antennas do we need?” *IEEE J. Sel. Areas Commun.*, vol. 31, pp. 160–171, Feb. 2013.

[116] H. Q. Ngo, E. G. Larsson, and T. L. Marzetta, “Energy and spectral efficiency of very large multiuser MIMO systems,” *IEEE Trans. Commun.*, vol. 61, pp. 1436–1449, Apr. 2013.

[117] T. L. Marzetta, “Noncooperative cellular wireless with unlimited numbers of base station antennas,” *IEEE Trans. Wireless Commun.*, vol. 9, pp. 3590–3600, Nov. 2010.

[118] C. Kong, C. Zhong, A. K. Papazafeiropoulos, M. Matthaiou, and Z. Zhang, “Effect of channel aging on the sum rate of uplink massive MIMO systems,” in *2015 IEEE Int. Symp. Inf. Theory (ISIT)*, June 2015, pp. 1222–1226.

[119] Q. Zhang, S. Jin, K. K. Wong, H. Zhu, and M. Matthaiou, “Power scaling of uplink massive MIMO systems with arbitrary-rank channel means,” *IEEE J. Sel. Topics Signal Process.*, vol. 8, pp. 966–981, Oct. 2014.

[120] C. Kong, C. Zhong, A. K. Papazafeiropoulos, M. Matthaiou, and Z. Zhang, “Sum-rate and power scaling of massive MIMO systems with channel aging,” *IEEE Trans. Commun.*, vol. 63, pp. 4879–4893, Dec. 2015.

[121] S. Shahbazpanahi and M. Dong, “A semi-closed-form solution to optimal distributed beamforming for two-way relay networks,” *IEEE Trans. Signal Process.*, vol. 60, no. 3, pp. 1511–1516, Mar. 2012.

[122] A. Alsharoa, H. Ghazzai, and M. S. Alouini, “Energy efficient design for MIMO two-way AF multiple relay networks,” in *2014 IEEE Wireless Commun. Netw. Conf. (WCNC)*, Istanbul, Apr. 2014, pp. 1007–1011.

[123] S. Cui, A. J. Goldsmith, and A. Bahai, “Energy-constrained modulation optimization,” *IEEE Trans. Wireless Commun.*, vol. 4, pp. 2349–2360, Sept. 2005.

[124] M. Grant and S. Boyd, “CVX: Matlab software for disciplined convex programming, version 2.1,” http://cvxr.com/cvx, Mar. 2014.

[125] Z.-Q. Luo, N. D. Sidiropoulos, P. Tseng, and S. Zhang, “Approximation bounds for quadratic optimization with homogeneous quadratic constraints,” *SIAM Journal on Optimization*, vol. 18, no. 1, pp. 1–28, 2007. [Online]. Available: https://doi.org/10.1137/050642691

[126] W. Ai, Y. Huang, and S. Zhang, “New results on Hermitian matrix rank-one decomposition,” *Math. Prog., Series A*, vol. 128, pp. 253–283, June 2011.

[127] Y. Ye and S. Zhang, “New results on quadratic minimization,” *SIAM J. Opt.*, vol. 14, pp. 245–267, Jan. 2003.

[128] S. Boyd, *Convex Optimization.* Cambridge University Press, 2004.

[129] S. Zhang, F. Gao, C. Pei, and X. He, “Segment training based individual channel estimation in one-way relay network with power allocation,” *IEEE Trans. Wireless Commun.*, vol. 12, pp. 1300–1309, Mar. 2013.

[130] F. Gao, R. Zhang, and Y.-C. Liang, “Channel estimation for OFDM modulated two-way relay networks,” *IEEE Trans. Signal Process.*, vol. 57, pp. 4443–4455, Nov. 2009.

[131] F. Gao, T. Cui, and A. Nallanathan, “On channel estimation and optimal training design for amplify and forward relay networks,” *IEEE Trans. Wireless Commun.*, vol. 7, pp. 1907–1916, May 2008.

[132] F. Gao, B. Jiang, X. Gao, and X.-D. Zhang, “Superimposed training based channel estimation for OFDM modulated amplify-and-forward relay networks,” *IEEE Trans. Commun.*, vol. 59, pp. 2029–2039, July 2011.

[133] B. Jiang, F. Gao, X. Gao, and A. Nallanathan, “Channel estimation and training design for two-way relay networks with power allocation,” *IEEE Trans. Wireless Commun.*, vol. 9, pp. 2022–2032, June 2010.

[134] F. Gao, T. Cui, and A. Nallanathan, “Optimal training design for channel estimation in decode-and-forward relay networks with individual and total power constraints,” *IEEE Trans. Signal Process.*, vol. 56, pp. 5937–5949, Dec. 2008.

[135] G. Wang, F. Gao, Y.-C. Wu, and C. Tellambura, “Joint CFO and channel estimation for OFDM-based two-way relay networks,” *IEEE Trans. Wireless Commun.*, vol. 10, pp. 456–465, Feb. 2011.

[136] S. Zhang, F. Gao, and C.-X. Pei, “Optimal training design for individual channel estimation in two-way relay networks,” *IEEE Trans. Signal Process.*, vol. 60, pp. 4987–4991, Sept. 2012.

[137] F. Gao, R. Zhang, and Y.-C. Liang, “Optimal channel estimation and training design for two-way relay networks,” *IEEE Trans. Commun.*, vol. 57, pp. 3024–3033, Oct. 2009.

[138] G. Wang, F. Gao, W. Chen, and C. Tellambura, “Channel estimation and training design for two-way relay networks in time-selective fading environments,” *IEEE Trans. Commun.*, vol. 10, pp. 2681–2691, Aug. 2011.

[139] Z. Wang and G. Giannakis, “Wireless multicarrier communications,” *IEEE Signal Process. Mag.*, vol. 17, pp. 29 –48, May 2000.

[140] R. Rahimi and S. Shahbazpanahi, "A two-way network beamforming approach based on total power minimization with symmetric relay beamforming matrices," *IEEE Access*, vol. PP, no. 99, pp. 1–1, 2017.

[141] Y. Rong, "Joint source and relay optimization for two-way linear non-regenerative MIMO relay communications," *IEEE Trans. Signal. Process.*, vol. 60, pp. 6533–6546, Dec. 2012.

[142] R. Rahimi and S. Shahbazpanahi, "Symmetric beamforming for multi-antenna two-way relay networks," in *2015 49th Asilomar Conf. Signals Syst. Comput.*, Nov. 2015, pp. 802–806.

[143] A. Goldsmith, *Wireless Communications.* Cambridge University Press, 2005.

[144] L. Lu, G. Y. Li, A. L. Swindlehurst, A. Ashikhmin, and R. Zhang, "An overview of massive MIMO: Benefits and challenges," *IEEE J. Sel. Topics Signal Process.*, vol. 8, pp. 742–758, Oct. 2014.

[145] M. Matthaiou, M. R. Mckay, P. J. Smith, and J. A. Nossek, "On the condition number distribution of complex Wishart matrices," *IEEE Trans. Commun.*, vol. 58, pp. 1705–1717, June 2010.

[146] S. Shahbazpanahi and M. Dong, "A semi-closed-form solution to optimal distributed beamforming for two-way relay networks," *IEEE Trans. Signal Process.*, vol. 60, pp. 1511–1516, Mar. 2012.